

The Journal of Refractory Innovations

# bulletin

Steel & Industrial Edition

Autumn 2017  
ISSUE 1

- 31 SOC-H Safety Closing System
- 64 TUNFLOW CHEVRON Impact Pot
- 71 PROIL—Innovative Liquid Casting Powder



RHI MAGNESITA



## bulletin

The Journal of Refractory Innovations  
Steel and Industrial Edition

---

Issue 1  
Autumn 2017

<b>Published by</b>	RHI Feuerfest GmbH, Vienna, Austria
<b>Chief Editor</b>	Stefan Schriebl
<b>Executive Editors</b>	Markus Dietrich, Alexander Maranitsch, Alfred Spanring, Marcos Tomas
<b>Raw Materials Expert</b>	Gerald Gelbmann
<b>Lingual Proofreader</b>	Janine Pink
<b>Project Manager</b>	Ulla Kuttner
<b>Photography, Graphics and Production</b>	Markus Kohlbacher, Christoph Brandner
<b>Design and Typesetting</b>	Universal Druckerei GmbH, Leoben, Austria
<b>Contact</b>	Ulla Kuttner RHI Feuerfest GmbH, Technology Center Magnesitstrasse 2 8700 Leoben, Austria
<b>E-mail</b>	<a href="mailto:bulletin@rhimagnesita.com">bulletin@rhimagnesita.com</a>
<b>Phone</b>	+43 50213 5323
<b>Website</b>	<a href="http://rhimagnesita.com">rhimagnesita.com</a>

The products, processes, technologies, or tradenames in the bulletin may be the subject of intellectual property rights held by RHI Magnesita N.V. or its affiliated companies.

# RHI Magnesita Worldwide news

---

## Worldwide

### Creation of a leading refractory company

The strategic rationale is to join forces to complement one another's footprints and become a more competitive, vertically integrated global provider of products, systems, and services in the refractory industry. The greater scale, wider global distribution network, and resulting cost synergies arising from the acquisition position the Combined Group well to compete and grow further in this consolidating industry. Furthermore, the Combined Group will be geographically better diversified and able to provide a more extensive product portfolio on both a regional and global basis.

#### Enabling Strategic Growth

As a result of its extended geographical reach and product and services portfolio, the Combined Group will have access to the core markets, customer base and geographical regions of each of RHI and Magnesita, enabling it to better service customers through a significantly expanded network of production and sales locations.

#### Achieving Synergies

Complementary markets and enhanced customer service: The geographical footprints of RHI and

Magnesita are highly complementary. Almost three quarters of RHI's revenues come from EMEA and Asia. By contrast, Magnesita has a strong presence in its home market of the Americas. The Combined Group will become a leading global refractory supplier by revenue in each of EMEA, Asia, and the Americas. It will be in closer proximity to its customers in terms of both production facilities, leading to shorter lead times, faster delivery, and shorter transport distances, as well as ready access to on-site functional support.

Complementary product and services portfolios: RHI and Magnesita's product and service portfolios are also complementary. The Combined Group intends to offer all products of both companies in each of the individual companies' existing markets, and plans to develop and offer bespoke packages integrating products from both companies to the Combined Group's expanded customer base.

Balancing of production capacities and results: The Combined Group's extended geographical footprint will bring about a more diversified composition of revenues across geographies with a balancing effect on the Combined Group's results and create a natural hedge of foreign exchange rate risks to the extent that the locations of the Combined Group's production facilities are better aligned with the distribution of the Combined Group's sales across geographies.

#### Sharing and Securing Technology and Know-How

The Combined Group will be enabled to gain access to technologies and know-how that are currently held either by RHI or by Magnesita. Furthermore, the Combined Group will lead to a combination of the management and R&D teams of the two companies and will also benefit from the market and product specific skills, know-how and experience of both RHI and Magnesita management and employees.

Overall we are convinced that this merger is surely a major step for us but specifically for our customers as we will provide an even better service.

---

## Worldwide

### New BOF Purging Plugs for High Gas Flow Rates

Trends in the steel industry to apply raw materials with higher phosphorus at similar or increasing productivity quality levels and the target of higher converter lifetimes increases the need for reliable, safe and long-term available inert gas purging.

The Power Plug series was developed as an extension to the existing MHP standards in order to comply with the customer needs for high gas flow rates, e.g., for improved dephosphorization, for high purging plug availability, low risk of breakout, and low wear rates. The Power Plug series includes purging plugs with 46 pipes and 100 pipes, with lining-specific shapes.

The optimized design at high gas flow rates assures higher availability even during BOF operation with

# RHI Magnesita

## Worldwide

### news (continued)

increased slag splashing rates and lower wear rates. The new MHP design decreases the thermal stress in the purging plug for decreased wear rates and longer lifetime.

Top-quality MgO-C surrounding bricks are included in the set of the MHP46 and MHP100 purging plugs in order to assure minimum wear rates and maximum purging plug lifetime with minimum installation efforts.

Five different customer trials have been evaluated so far and the performance of the new Power Plugs was compared with standard multi hole plugs. In all cases purging plug availability, purging efficiency, and metallurgical benefits were increased, at similar or lower wear rates.

#### Worldwide

### 100000 Tonne Q Series

In January 2017, we celebrated the production of the one hundred thousandth tonne of the ANKRAL Q-series. Since the market introduction of this series in 2010 it has become an essential component of the product portfolio for cement rotary kilns, due to the innovative and outstanding product properties and the associated growing demand now also available from production sites in China and Mexico.

The one hundred thousandth tonne of the ANKRAL Q-series was delivered to LafargeHolcim plant Beckum, which has benefitted from the characteristics of ANKRAL QF for many years. This brick is used in the upper transition zone of the precalciner kiln (5.3 x 80 m, capacity 2600 t/d). Prior to the introduction of ANKRAL QF completing a full

campaign period was a challenge due to heavy mechanical and chemical load. The use of ANKRAL QF resulted in the successful completion of a full campaign despite rising alternative fuel rates (currently > 80%).

In addition to the top product ANKRAL QF, the Q Series also includes the products ANKRAL Q1, ANKRAL Q2, ANKRAL QC and ANKRAL QE, which have above all a high resistance to mechanical stress due to the innovative hybrid spinel technology. In the course of the development the positive influence on other wear factors has also been revealed. Since the infiltration by alkali salts also causes a densification of the microstructure, in addition to the corrosion of the binder phase and, as a result, a worsening of the mechanical properties and the formation of cracks, the novel flexibilization concept also improved the chemo-thermal resistance.

With the Q Series, we offer a range of products meeting the most diverse customer requirements. The portfolio ranges from the special product for highest requirements to ensure kiln availability to the cost-efficient solution to contribute to the reduction of refractory costs.

#### Worldwide

## ANKERTAP JET-VK3

### New ANKERTAP JET-VK3 Machinery – Optimized Solution for BOF Taphole Systems

**Our BOF taphole system is evolving continuously providing optimized and tailor-made solutions to meet highest demands in future. The taphole system has been enlarged by the implementation of the ANKERTAP JET-VK3 machinery. The new taphole ring gap gunning application, exclusively laid out for the premium mix RUBINIT VK3, ensures a proper mix consistence adjustment, based on a fully automated water dosage process step. The optimum consistency of the mix was determined in several gunning tests at customer sites and integrated into the software programming.**

**The ANKERTAP JET-VK3 is equipped with weighing cell, water dosage hardware and gunning software where date, gunning duration, flow rate, and mix consumption per converter are recorded. After each taphole change, the required**

**gunning process will be started and stopped by pushing a button only.**

**Summarized, a maximum performance of the ring gap mix will be obtained, eliminating unsuitable water levels in the mix and practical mistakes in the water adjustment, which affects the taphole lifetimes significantly.**

**Worldwide**

## **Durability Record:**

### Flooring and Wall Installation at 120 Tonne DC Furnace at Thuringia Steel Works

Our company has been engaged in an FLS project since 1995 and delivers 95% of the material and 100% of the performance demand for the fire-retardant cladding of the steel work's main and auxiliary systems.

On 24 April 2017, project "Wall 2000 batches" which was started on 13 June 2013 has come to a satisfactory end with the furnace campaign O1-2017. The furnace campaign returned a durability record of 1997 batches and the exposed prewear areas' thickness showed a potential of up to 2200 batches.

This result is even more remarkable considering that the ratio of batches with an oxygen content of approx. 1000 ppm has increased from 30 to 50% in the framework of the project phase. Thus, allowing SWT to plan with furnace campaigns of 12 to 14 weeks. Therefore, I would like to take this opportunity to thank all those involved in the project for their excellent performance.

**Worldwide**

## **New National and International Research Network**

By tradition we are part of the scientific network in the world of refractories. Beneath different universities also collaborations with other research organizations as well as industrial partners are actively driven and vivid.

As a new activity started from FIRE (Federation for International Refractory Research and Education) recently we are participating in an international project founded by the EU called ATHOR (Advanced Thermomechanical multiscale mOdeling of Refractory linings). This program with 8 industrial partners and 6 universities is mainly dedicated to

train Early Stage Researchers (ESRs) in multi engineering fields for a better understanding of thermomechanical behaviour of refractory linings. The 4 year European Training Network program will start in October 2017 within the frame of a Marie-Sklodowska-Curie action (MSCA). The ESRs will have the opportunity to collaborate with experts in various research groups and will take advantage of the most sophisticated numerical tools to model, design, and predict the life of refractory lining configurations in critical operation conditions. Being trained in such a way the ESRs selected in the program will be the next generation of highly employable scientists and engineers for the refractory industry and related areas. From the scientific point of view the project will cover all the main features of thermomechanical analysis of refractory linings from the micro scale, the structure of refractories, to the macro-scale, the thermo mechanical behaviour of linings in industrial vessels under operation conditions. New computational modelling and testing methods will be developed to address the scientific and technological challenges for these industrial applications and will help to develop better performing refractory materials and linings.

Through the ATHOR network and long term partnership, all partners are deeply committed to provide a combination of research and training activities which will support and enlarge the initiative of FIRE.

For more information, visit the ATHOR website at [www.etn-athor.eu](http://www.etn-athor.eu).

**Worldwide**

## **Big Improvements to Ultra Low Carbon Steel Production**

Modern ultra low carbon steels used for deep-drawing require a carbon content below 30 ppm. By using standard carbon bonded bricks in the ladle, during secondary metallurgy carbon may be picked up again from the refractory material. This makes it more difficult or even impossible to reach the target for ultra low carbon steel. As a solution we offer RESISTAL KSP95-1, a carbon-free high grade alumina spinel based brick. Depending on the metallurgy its performance in the steel bath area can exceed the standard material. RESISTAL KSP95-1 has been tested by a European steel mill in the sidewall and bottom of the ladle. The median carbon pickup was reduced to only 1 ppm (presumably from the slagzone bricks) and no pickup over 10 ppm carbon was detected. Additionally, the ladle lifetime was increased. Alternatively a second trial with a special alumina-magnesia-carbon brick was carried out. With this brick, carbon pickups exceeding 10 ppm were reduced by 84%. Ongoing trials with both grades are being carried out to find the solution with the best cost/performance ratio.

# RHI Magnesita Worldwide news (continued)

## Worldwide

### New Laboratory Test for Porous Plugs Used in Aluminium Applications

During the past years porous plugs have been facing serious challenges in numerous aluminium applications, especially where aggressive aluminium alloys are processed. Shortened production sequences and higher process temperatures have led to higher thermal shock loads. Reduced melt viscosities have raised the melts' potential ability to enter and block the plugs' pores. Until recently, the plug's supposed performance under operating conditions could only be estimated by summarizing test results for standard properties and performance in a water model. A clear statement on performance would only be given by field trials, where plug assemblies are finally exposed to flux gas, alloy melt, temperature changes, and hydrostatic pressure. Now, a small, laboratory scale test assembly has been engineered. It comprises a cast sample holding device containing a standard 5 cm sample cylinder equipped with a flux gas supply line. In the high frequency induction furnace, this "miniature plug" assembly is immersed in an aggressive aluminium melt, providing the opportunity to observe physical and chemical reactions caused by the combined influence of melt and flux gas. The connection of a vacuum pump to the plug assembly also allows for simulation of hydrostatic pressure. A small trial series has shown "realistic" corrosion and infiltration patterns similar to the ones observed with real live samples.

## Worldwide

### Clearer Pictures for More Detailed Information

#### —Glass Division Endoscopy Service Worldwide

In order to assess and diagnose the state of a glass furnace during operation endoscopic inspection has become a common but valuable service. With our partner Franke IndustrieOfen-Service we take known furnace endoscopy to a new level.

HD videos and photos based on a self-developed camera and lance technology, which is continuously maintained and further developed internally, offer the most detailed and sharpest pictures in the industry. The inspection procedure is designed to have a minimum influence on the furnace operations by using pre-assembled lenses and entering the furnace by using existing peep-holes or burner blocks. The combination of the endoscopy with visual inspection and thermography adds additional value for the glass furnace operators by offering a more complete understanding of the actual state of the furnace. The quality of the endoscopy videos and final evaluation of the inspection results by a refractory expert allow the customer and its service partners to plan furnace maintenance activities and changes in operations easily.

This service for container, flat, and fibre glass tanks is available worldwide. By storing endoscopy equipment in Germany, Russia, and most recently in the USA, we and our service partners can respond even faster and more flexibly to requests from customers. Established procedures for endoscopy and equipment maintenance ensure the same inspection and report quality anywhere and anytime.

## Worldwide

### Competence in Electric Boosting Systems

We hold to our commitment to offer expert knowledge and sophisticated services for each phase of a glass furnace campaign. The newest member of the comprehensive service network, Bock Energietechnik GmbH adds expertise in electrical boosting systems for glass furnaces and forehearth. Situated in Floß, Germany Bock Energietechnik is a "down to earth" family-owned company with 40 years of experience in the field of design, manufacturing and installation of these systems. Bock is active worldwide and has developed into a technology leader in its field. For us this partnership fits right into the approach of offering services to our customers that optimize their furnace operations and support a longer and safer furnace life time. The

service portfolio includes planning and installation of new electrical boosting systems as well as maintenance and re-design/optimization of existing installations. The new cooperation also adds to the hot repair portfolio of the service group with the ability to push and replace electrodes in furnaces or forehearth on the run.

---

### Worldwide

## New Test for Products Used in High-Alloyed Aluminium Applications

Growing demand for specialized alloys and changing, more aggressive operating conditions are challenging our mixes and bricks in the field of aluminium applications. In order to approach these new challenges, we have been constantly improving product properties. As we have seen in the past, available standard test methods, such as the ALCAN immersion test or crucible test arrangements, have shown limited resemblance of actual operating conditions at customer plants. Therefore, development of a new test method has been started. A rotary drum furnace has been lined with both standard mix and standard bricks for aluminium applications. Charged with a highly aggressive alloy and burner arrangement, fuel composition, atmosphere, and operating temperature very close to typical industrial operating conditions, the first trial run has been completed. Macroscopical examination has already shown characteristic wear phenomena usually encountered by customers after several months in operation. Removed lining and alloy charge are currently undergoing mineralogical and chemical investigation.

---

### Worldwide

## Innovative Bricks for Reducing Emissions During Ladle Heat-up

We proudly presents a new brand line of reduced emission bricks for ladle linings meeting higher environmental standards and improved occupational safety regulations.

Emissions during ladle heat up can be significantly reduced for magnesia-carbon, doloma-carbon and alumina-magnesia-carbon bricks representing the most important materials for ladle lining. Comparing emission rates of conventional bricks (270 ppm/min) an enormous improvement has been achieved with the new low emission brands with only up to 100 ppm/min. Peak emissions at 460 °C were even reduced up to 75%. The focused effort of our R&D team resulted in new brick qualities with a significantly lower outgassing of formaldehyde,

phenol, polycyclic aromatic hydrocarbons (PAHs), H<sub>2</sub>S and SO<sub>2</sub>.

The performance of these new bricks was on the same high level as expected for our conventional bricks. Patent protection for this innovation will be granted by the European Patent Office.

Within the last three years these brand lines have successfully been introduced into the market and have been established as standard linings at innovative customer's plants. Since environmental, health, and safety aspects become more and more important in the steel industry there is a significant trend towards greener refractory solutions.

With this new brand lines another important step towards environmental protection and improvement of health and safety has been taken.

---

### Worldwide

## New SOC-H Demonstration Stand for Customers and Technicians in Plant Veitsch

A brand new SOC-H demonstration stand has been setup in plant Veitsch/MTC. This stand allows testing and exercising the SOC-H system under cold conditions but close to reality. All related accessories and tools (e.g., small overhead crane, plug setting tool, plug extraction tool, replacement plug, and refractory mortar) are available and ready for use. This set-up provides a perfect way to show the working principle and all advantages of the SOC-H system. It is also an excellent opportunity to realize training with customers who have decided to use SOC-H as well as with our new employees. Due to a higher wear rate compared to the ladle bottom lining, plugs for gas purging are often used with closing systems to allow an exchange under hot conditions. To reduce safety risks in this critical area of the steel ladle, SOC-H (safety optimized closing system with hinged door) has been developed.

# A letter from our editor



## Welcome to the 2017 RHI Magnesita Bulletin.

This has been an exciting and monumental year for us, as the planned merger of the two companies became reality. For further details regarding the consolidation, please see the news item on page 3 in the Worldwide section.

This edition was created by RHI and it is one of the most comprehensive in the history of the publication. In the future we hope you will gain additional benefits, as the forthcoming Bulletin will comprise the combined knowledge and experience of two global players in the refractory industry. We will use these advantages to support our customers through both innovation and progression in every aspect of our business.

The first article in this edition focuses on how efficient and comprehensive refractory maintenance can be achieved in the EAF using various tools including Automated Process Optimization (APO), which is a step towards harnessing the wealth of steel plant data to achieve predictable and improved operations. The differences and similarities of resin and pitch bonding for basic refractories are discussed in the next paper, with particular emphasis on emissions and environmental issues. This is followed by a description of DIVASIL FP, a frost protected binder for the extensive portfolio of nonbasic Sol Mixes. These monolithics show outstanding performance in various applications and this new product simplifies the transport logistics and binder storage. In the fourth paper, various approaches to achieve efficient stirring in steel teeming ladles are described, including the use of CFD modelling, a plug functionality device, and the SOC-H closing system for high operational safety. In metallurgy an open eye is required for the addition of alloying elements; however, its formation should be avoided when soft bubbling is carried out. By means of a water modelling approach, the influence of purging plug design and size on slag opening was examined and the results are presented.

Experimental approaches used to examine the influence of different flexibilizers on basic cement rotary kiln brick properties are described in the next article, which identified hercynite as the most suitable flexibilizing additive. This is followed by a paper providing different examples of how modelling and simulation tools are applied to predict the behaviour and characterize the benefits of refractory products such as tapholes and purging plugs. A newly developed digital fibre optic pyrometer that enables accurate real-time measurement of metal bath temperatures is introduced in the next article, which provides many benefits including proactive process control.

The next three papers in this edition cover flow control topics for the steel industry and include a description of our new slide gate water modelling facility, the effect of impact pot parameter variations on steel fluid flow in the tundish, and an overview of the latest continuous casting solutions as an outcome of the cooperation with PROSIMET, a company developing and manufacturing tundish and mould powders. A calculation model to quantify the amount of slag carryover from primary metallurgical vessels is presented in the penultimate article and this is followed by a description of the work conducted to enable the development of a caustic calcined magnesia product with optimized properties for use in the cobalt and nickel hydrometallurgical extraction industry.

This edition of the Bulletin was only possible due to the dedication and professionalism of the authors and editorial team and in closing I would like to express my gratitude to all those involved.

Yours sincerely

**Stefan Schriebl**

Corporate research and development  
RHI Magnesita





“ This edition is one of the most comprehensive in the history of the publication. The forthcoming Bulletin will comprise the combined knowledge and experience of two global players in the refractory industry. ”



RHI MAGNESITA

Introducing...

# The driving force of the refractory industry

RHI and Magnesita.  
A new global leader in refractories.

Find out more at  
[rhimagnesita.com](http://rhimagnesita.com)

# Contents



**31**  
SOC-H  
Safety Closing  
System



**64**  
TUNFLOW  
CHEVRON  
Impact Pot



**71**  
PROIL—Innovative  
Liquid Casting Powder

- 12** [Digital Refractory Age](#)
- 22** [Avoidance of Hazardous Substances via Low Emission MgO-C Technology Shown with the Example of a Ladle Lining Refractory](#)
- 28** [DIVASIL FP—Frost Protected Binder for Sol Mixes](#)
- 31** [Holistic Approach for Gas Stirring Technology in a Steel Teeming Ladle](#)
- 37** [Open Eye Formation: Influences of Plug Design and Size Investigated in a Water Modelling Comparison of Hybrid, Porous, and Slot Purging Plugs](#)
- 43** [Influence of Flexibilisers on Basic Cement Rotary Kiln Brick Properties](#)
- 49** [Characterization and Improvement of Steelmaking Process Steps Influenced by Refractory Products Using Modelling and Simulation Tools](#)
- 55** [Continuous Online Temperature Measurement System](#)
- 60** [New Slide Gate Water Model Facility](#)
- 64** [Tundish Technology and Processes: Ladle to Mould Systems and Solutions \(Part II\)](#)
- 71** [New Casting Solutions: Value Innovation for RHI Customers](#)
- 76** [Calculation Model to Quantify the Amount of Carry—Over Slag From Primary Metallurgical Plants](#)
- 82** [Investigation of Caustic Calcined Magnesium Oxide Produced From Seawater for Hydrometallurgical Applications in Cobalt and Nickel Extraction Processes](#)

## Subscription service and contributions

We encourage you, our customers and interested readers, to relay your comments, feedback, and suggestions to improve the publication quality. Furthermore, to receive the Bulletin free of charge or contribute to future editions please e-mail your details (name, position, company name, and address) to the Subscription Service:

Email  
[bulletin@rhimaginesita.com](mailto:bulletin@rhimaginesita.com)

Phone  
**+43 50213 5323**

Gregor Lammer, Ronald Lanzenberger, Andreas Rom, Ashraf Hanna, Manuel Forrer, Markus Feuerstein, Franz Pernkopf and Nikolaus Mutsam

# Digital Refractory Age

## Introduction

The full digitization of industry promises significant efficiency gains. This development has started to have an impact on the operation in steel plants, when decisions are made based on traceable data.

This paper presents an approach to discover patterns in big data sets and applying methods of artificial intelligence (AI) for interpretation. The paper will present the use of AI to identify the main refractory wear mechanism in the hot spots and the use of AI to predict the refractory behaviour. Further, we applied this intelligent system to analyze and compare different maintenance philosophies.

As example of the impact on daily operations in steel plants, we present the Daily Report, which provides all necessary key information when a refractory related decision is to be made.

The paper also examines and discusses the operational impact and future applications.

## Industry 4.0

### Definition

The three industrial revolutions of the past were all triggered by technical innovations: the introduction of water and steam powered mechanical manufacturing at the end of the 18<sup>th</sup> century, the division of labour at the beginning of the 20<sup>th</sup> century and introduction of programmable logic controllers (PLC) for automation purposes in manufacturing in the 1970s [1].

Currently, Industry 4.0 is a popular term to describe the imminent changes of the industrial landscape, particularly in the production and manufacturing industry of the developed world. Yet the term is still used in different contexts and lacks an explicit definition. In this paper we define Industry 4.0 as fourth industrial revolution focusing on the establishment of intelligent production processes and products.

Nowadays decisions of process adaption are predominately made by humans on the basis of experience. In the future, the decision process will be increasingly assisted by self optimizing and knowledgeable manufacturing systems [2]. In future manufacturing, factories will have to cope with the need of rapid product development, flexible production as well as complex environments [1].

Within the steel plant of the future, also considered as a smart factory, CPS (cyber physical systems) will enable the communication between humans, machines, and products alike [3,4]. As they are able to acquire and process data, they can self control certain tasks and interact with humans via interfaces Figure 1.

Especially for companies in the steel industry it will be important to offer customized products that are superior in quality and competitive in price. This can be achieved by intelligent automation and reorganization of labour within the production system [5]. The resolution of the automation pyramid towards self controlling systems leads to an extreme amount of data, which can be extracted, analyzed, and visualized [6].

## Refractory Maintenance

Over the past years the EAF service life at many steel plants has increased successively. This achievement is based on modern production technologies, improved lining concepts, as well on the use of various techniques for refractory lining maintenance as standard gunning using a hand lance, semi and automated gunning by using a TERMINATOR, or the use of special hearth repair mixes.

In contrast to other practices it has been established that gunning repair is one of the most effective methods for prolonging the life of all kinds of steel making and steel refining vessels, because the mixes can be applied very accurately on specific preworn areas.

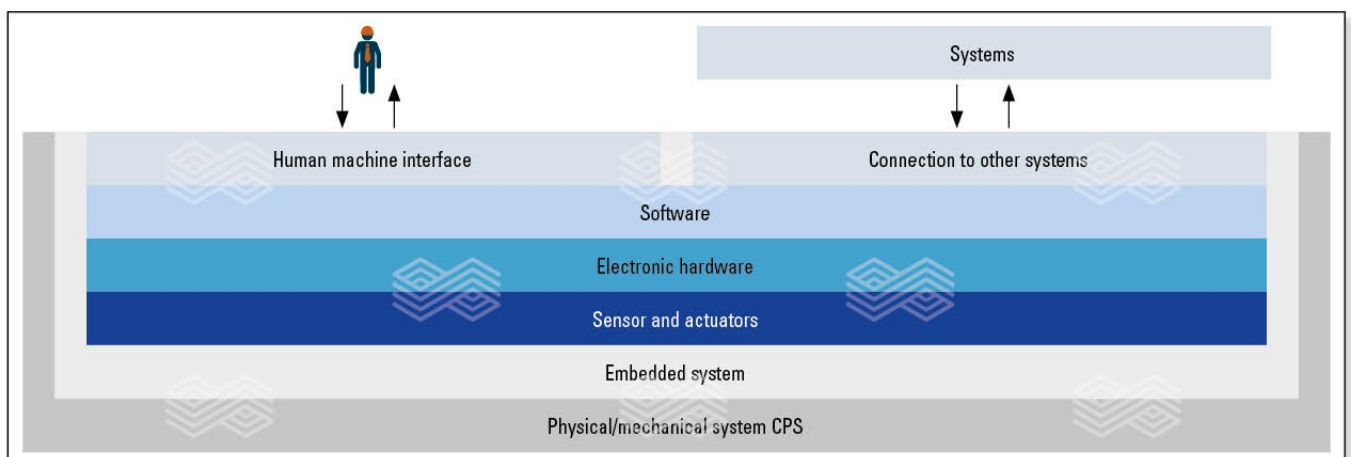


Figure 1. Interaction between humans and machines via Cyber Physical Systems [1].

An intelligent maintenance concept can help to improve refractory efficiency which results in higher service life, higher steel production and more flexibility for plant maintenance (plant logistic) at reasonable refractory costs. See Figure 2 for an example.

Often, refractory maintenance costs are rated as a minor cost factor, when only direct refractory costs are evaluated. In most cases, the influence of the maintenance method contributes far more to TCO [7] costs. The influence of the maintenance method becomes obvious when considering:

### Refractory Maintenance With Manipulator TERMINATOR XL

Reducing physical stress of operators, decreasing the required maintenance time, and limiting the influence of humans in refractory application were considered in the decision process for the TERMINATOR XL. Figure 3 shows an Terminator in operation. The system is equipped with a laser scanner to measure the residual lining thickness of the EAF (electric arc furnace) refractory. The system is pulpit operated and features a fully automated gunning mode. Based on laser measurement evaluation, the gunning map can be defined on the user interface. The TERMINATOR then automatically applies the correct repair material at the right place with the ideal amount. Modern TERMINATORS are established with an advanced water mixing. A new water fog injection system called binary nozzle was developed, whereby fine dispersed water is used for a more homogenous wetting of the mix with water which is an essential precondition for an effective gunning repair and is

strongly influenced by the nozzle design. To improve the moistening process the binary nozzle was developed in close cooperation with the Process Engineering department of the University Leoben. The initial idea behind this new system was to improve the wettability of the refractory particles by producing a fine spray of water. This secondary air additionally creates a higher driving force in a radial direction which leads to higher turbulences in the mixing zone. Benefits include less dust, a more defined jet shape, better first adherence. Further positive effects can be seen in the applied gunning layer. Due to the reduced rebound the gunning matrix contains more coarse grains which leads to higher wear resistance. With the impact of these coarse grains in the gunning bed the applied layer is compacted which increases the density and decreases the open porosity of the mix (Figure 4 and 5). This results in a higher erosion and infiltration resistance.

General advantages of the TERMINATOR compared to manual methods are:

- >> Precise gunning.
- >> Reduced rebound of material.
- >> Reduced physical stress on operating personnel.
- >> Minimal preparation time.
- >> High flow rate of repair material ensuring a short repair time.
- >> Application of two different mixes (one for gunning, one for bank repairs).
- >> Detailed information about the refractory condition (residual lining thickness).

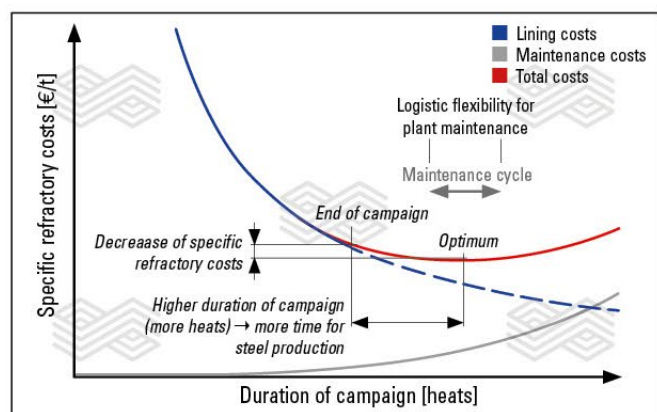


Figure 2. Example for an intelligent maintenance cycle.

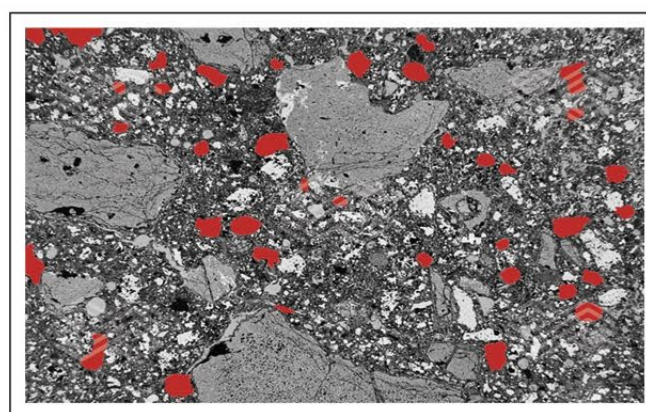


Figure 4. Microscopic detail of gunning mix applied with binary nozzle.



Figure 3. TERMINATOR in operation.

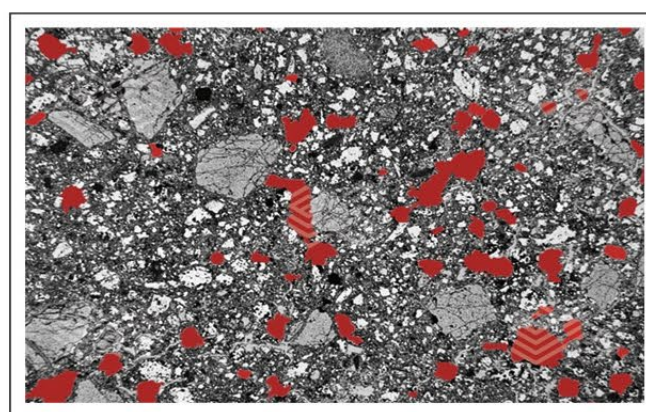


Figure 5. Microscopic detail of gunning mix applied with standard nozzle.

### Visualization

The visualization is the standard interface between the TERMINATOR and the laser measuring device. After scanning the furnace, the measurement data (residual thickness of the refractory lining) from the laser scanner will be displayed on the visualization screen in the operation room. (Figure 6).

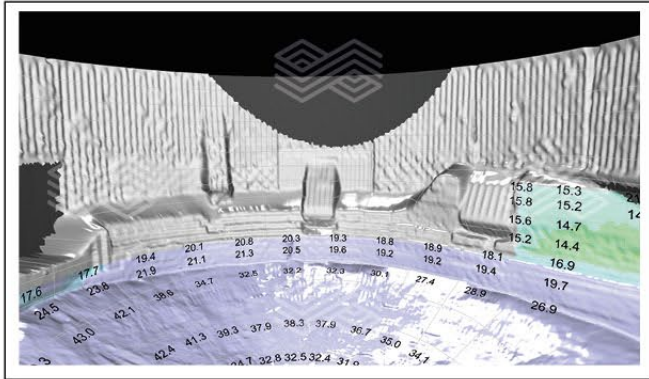


Figure 6. Laser scan representation on visualization.

The operator can easily identify pre-worn areas in the furnace and marks the areas requiring repair by using a pointing device (PC mouse). In addition, certain repetitive areas can be simply stored, which makes the further selection very easy. In the gunning data management specific areas can also be pre-defined for fettling and gunning manually. The repair mix consumption and gunning duration for the marked areas are calculated and displayed automatically. By pushing the start button, the TERMINATOR fully automatically repairs the worn refractory lining accordingly. Thereafter, the relevant current gunning data such as mix throughput, water consumption, etc. are displayed and further step, added to the data of the previous repairs. Thus, a complete traceability of the refractory maintenance is provided. As a further option the current laser measurement, and the furnace lining in the background in transparent appearance can be displayed in the gunning data management automatically (Figure 7)

On the visualization, a so-called gunning map showing the applied mix on a defined wall grid is available. Customer-specific predefined areas can provide an accurate overview of the maintenance behaviour in exposed areas (Figure 8).

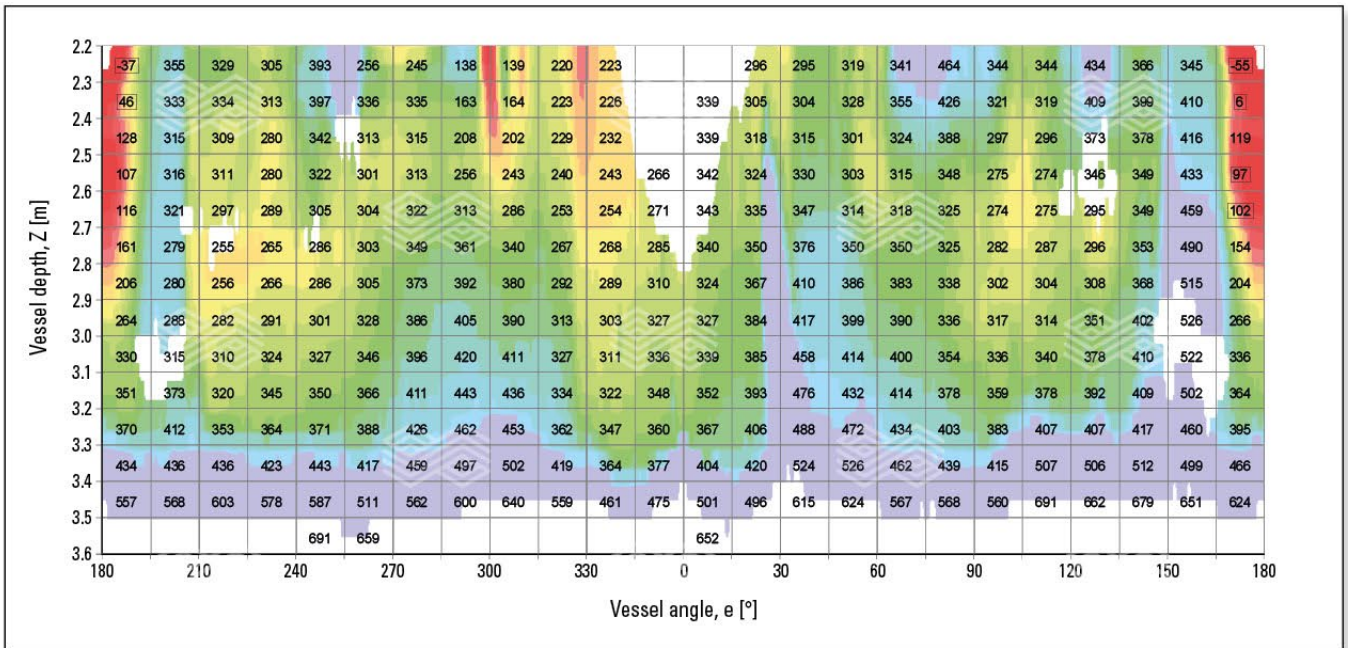


Figure 7. Gunning map.

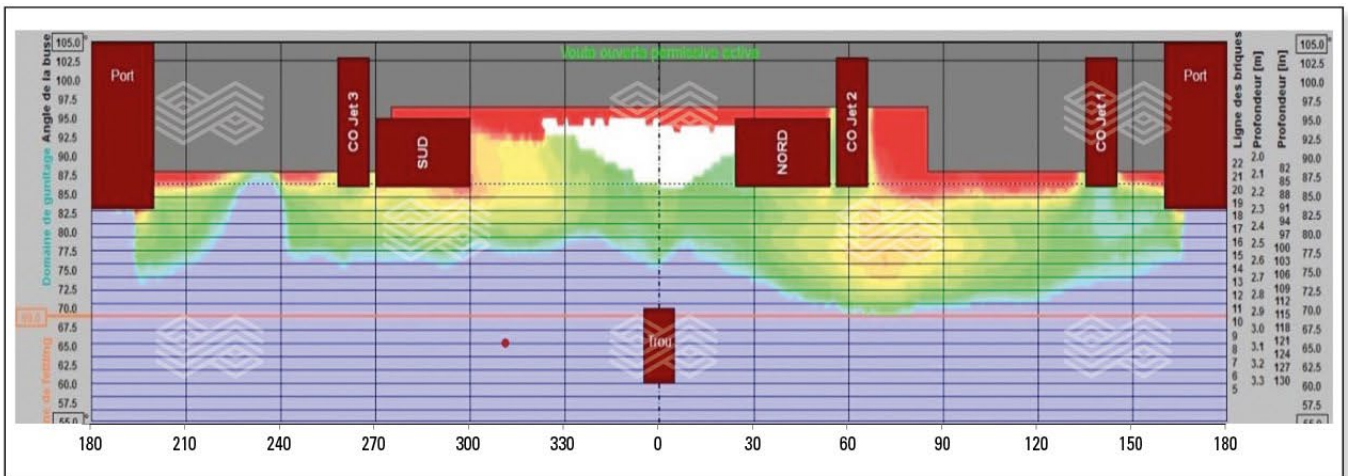


Figure 8. Gunning Data Management inclusive laser measurement.

The laser scan images give a very good understanding of the current state of the refractory lining and facilitate the definition of the short-term maintenance tasks. However laser scans do not give an easily accessible time-dependent wear progress for analysis. They also do not indicate the cause of specific refractory wear or allow predictions of future wear behaviour

### Lining Clustering

The refractory wear of different areas of the EAF's inner surface is influenced by the chosen refractory concept (mainly quality) and different production parameters. By applying a clustering framework we seek to identify areas where refractory wear characteristics show similar temporal evolution. This can be done by applying various clustering algorithms like k-means [8] or affinity propagation [10] to the laser measurement data. We also introduced different transformations, the so-called input generation schedules, and applied them to the laser data in order to construct multidimensional vectors that serve as input for the clustering algorithm.

For the analysis shown in Figure 9, we used more than 240 scans. One laser scan has more than 500.000 points. Areas in one colour show similar wear behaviour.

Based on such information, the zoning for different refractory material can be determined. High wear resistance bricks in the hot spots (green) and less performing bricks in the other areas. For each zone a refractory model can be trained and used for further analysis.

In the past this approach was used on the basis of experience rather than on traceable data for designing a balanced lining to even out the different wear speeds.

### Industry 4.0 Application for Refractory

Usually, the steel manager's decisions in selecting the maintenance method and related equipment depend on the general plant strategy, the budget, orders, production process

bottlenecks, and space conditions on site. Not all of this data is available and/or considered for the refractory concept all the time. Furthermore, the refractory behaviour during operation is also strongly influenced by operation conditions (Figure 10). Traditional refractory design and maintenance approaches may not integrate the whole data set.

What makes most Industry 4.0 applications more complex is that no single partner has all required data or knowledge. One hurdle is to find a way to share data and knowledge by preventing in the same time to give away company core knowledge. Figure 11 gives an impression of the data sources and interfaces between typical partners in Industry 4.0. projects.

### Automated Process Optimization (APO) [9]

APO is a development project started in 2011 and intended to foster greater understanding between steel production operation, maintenance, and refractory by analyzing data on a central master computer using artificial intelligence methods.

APO is a basic first step in linking furnace floor technologies and moving towards the goal of predictable operation. By establishing a central data pool, APO allows managers to analyze and understand vessel operation using a holistic approach, thus empowering them to make decisions aimed at providing more efficient operations, improved production optimization and increased productivity.

In a typical scenario APO helps to improve the refractory strategy by optimizing the following topics:

- >> Predictable lining lifetime.
- >> Reduction of specific refractory consumption.
- >> Targeted maintenance of premature wear areas.
- >> Increasing breakout safety.
- >> Steel plant logistics.
- >> Decreased vessel downtime (e.g., due to maintenance).

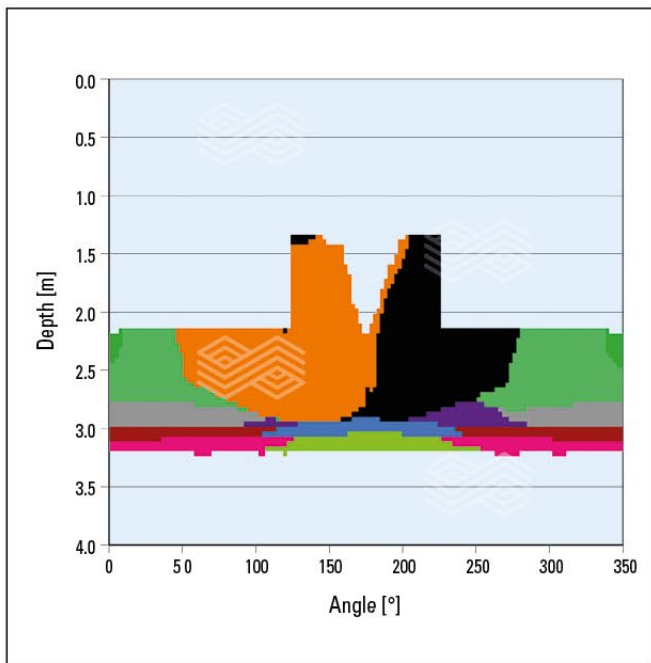


Figure 9. Example of refractory lining clustering. [8]

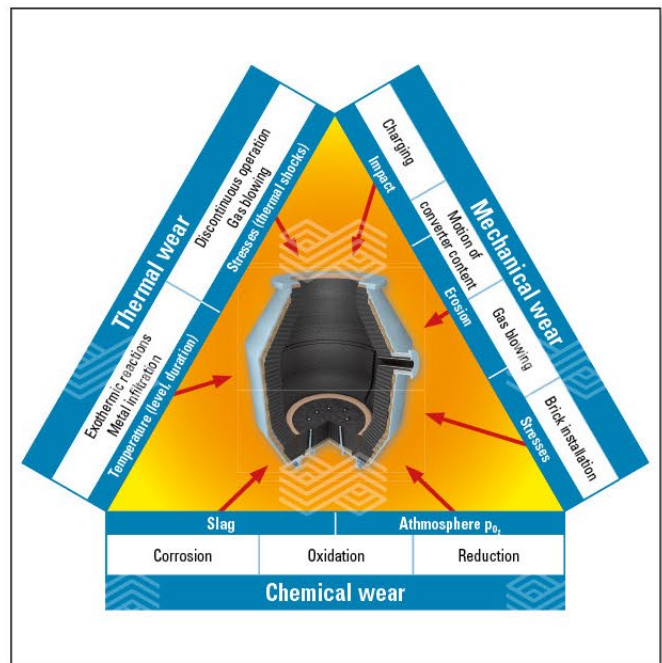


Figure 10. Refractory wear.

For APO customers it will be possible to manage their own refractory data in APO, to look at statistics and make a wide range of different evaluations. With the Wear Prognosis feature, APO is able to provide managers with online refractory data that increase planning security while providing a traceable common data base.

### Technical Approach

In data science, where the amount of available data has increased dramatically over the recent past, intelligent systems modelling complex dependencies are developed to support the supervision of hazardous production processes such as steel making. We are at the beginning of a decade's long trend toward data intensive, evidence based decision making across many aspects of science and commerce. Steadily increasing data volume impose new demands such as computationally tractable algorithms, sensitive data raise the need for protecting privacy issues, and large amounts of unlabeled data require machine learning methods to be fully utilised.

APO builds on methods from machine learning and artificial intelligence to determine the condition of the lining based on several data sources without any human interference. Moreover, APO predicts the refractory wear and the lining lifetime. Furthermore, the influence of the production parameters on the refractory wear lining can be determined, and the most influential parameters are ranked. In addition to the visualization of the steel making process statistics, APO infers a maintenance proposal for optimal exploitation of the maintenance resources and refractory lining treatment.

Figure 11 shows the APO data processing pipeline.

Currently, APO uses three main data sources, namely:

- >> Laser measurements: During a production campaign laser measurements are recorded to determine the remaining refractory lining thickness. These laser measurements are prone for optical insufficiencies such as dust which can lead to missing data values and insufficient measurement results. We introduced a pre-processing stage to remove outliers, fill measurement holes [10] and to de-noise the laser measurements based on statistics of the local spatial neighborhood, to compensate these erroneous measurements.

- >> Production parameters: During each heat several hundred production parameters are recorded such as temperatures, energies, durations, chemical ingredients, etc. A feature selection module, discussed further below, is introduced to determine a subset of production parameters which are useful for APO.
- >> Maintenance data: Occasionally maintenance (gunning, fettling) is performed to repair the lining in zones of large wear rates (hot spots) to increase the lining lifetime. Here gunning data such as time, gunning mix, gunning consumption, maintenance areas, gunning mix per area are delivered to APO.

Feature selection: In real-world prediction problems the relevant features (i.e., production parameters) are often unknown a priori. Thus, the most useful features (with the highest informative content) for APO have to be selected. Feature selection has become important for numerous pattern recognition and data analysis methods [11,12,13]. Many search heuristics have been proposed where an exhaustive search is usually computationally impractical. Even for a given cardinality of the final feature set, the total number of different subsets is too large for performing an exhaustive search, where  $D$  is the total number of production parameters. For this reason, many suboptimal deterministic and stochastic search heuristics have been proposed [11, 14]. Particularly interesting methods are based on genetic algorithms (GAs) [15,16]. GAs are optimization algorithms founded upon the principles of natural evolution discovered by Darwin. In nature, individuals have to adapt to their environment in order to survive in a process of further development. GAs turn out to be competitive for certain problems, e.g., large-scale search and optimization tasks.

$$q = \binom{D}{d} = \frac{D!}{(D-d)!d!}$$

APO Wear Prediction: To provide insights on APO we would like to focus on a simple wear approach. Laser measurements of the lining are not available for every heat due to the time needed to record a measurement. Between two consecutive laser measurements  $LM_t$  and  $LM_{t+1}$  we do not know the current lining thickness. Let us introduce this time span as a slot.

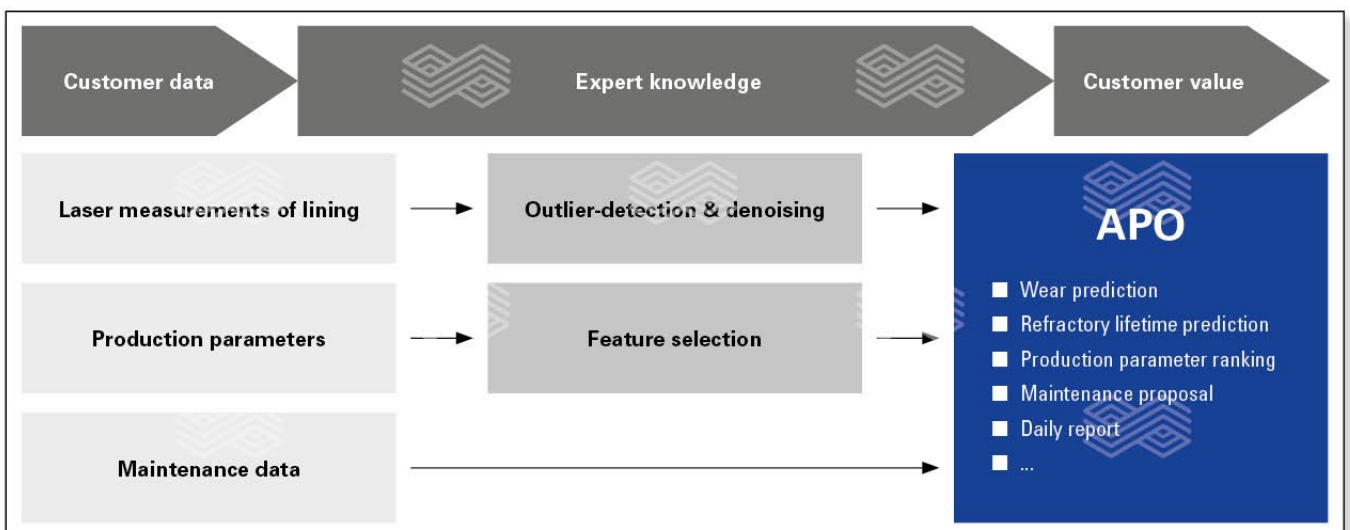


Figure 11. APO data processing pipeline.



Figure 12 shows a sketch of the refractory wear over the heats including steel grades and laser measurements. On the one hand, the slot sizes may vary, on the other hand, within a slot, it is possible that several different steel grades are produced. Moreover, several maintenance actions could have occurred in each slot (not visualized in Figure 12). The aim of this approach is to predict the refractory lining thickness based on produced steel grades, assuming that each steel grade has its individual wear on the lining.

**Least Squares Approach:**

Having the definitions above in mind a simple first linear approach can be postulated. For this wear prediction approach, least squares methods are used where the weights  $w_i$  model the wear per heat for each steel grade. The least squares solution for  $[w_1 \dots w_{n+1}]^T$  of the following system of equations

$$\begin{bmatrix} SG_{1,1} & \dots & SG_{1,n} & GC_1 \\ \vdots & \ddots & \vdots & \vdots \\ SG_{m,1} & \dots & SG_{m,n} & GC_m \end{bmatrix} \begin{bmatrix} w_1 \\ \vdots \\ w_{n+1} \end{bmatrix} = \begin{bmatrix} \Delta x_1 \\ \vdots \\ \Delta x_m \end{bmatrix}$$

can be determined, where  $\Delta x_i$  models the wear in a slot,  $GC_i$  models the gunning frequency count per slot,  $SG_{ij}$  is the frequency count of produced steel grade  $j$  between two laser measurements,  $n$  and  $m$  denote the number of steel grades and data samples, respectively. Each line of the system of equations corresponds to the recorded data per slot. As a result, this simple approach performs well as long as the data noise is low. The prediction accuracy is insufficient in the case of noisy data.

For this reason, this approach is currently extended in various directions. In doing so, a subset of selected production parameter is included in the model. Furthermore, this model is extended by a Kalman-Filter to account for parameter adaptation over the campaign [17]. Additionally, we introduced a hybrid optimization objective which increases the prediction accuracy [18]. Moreover, a Gaussian processes approach using selected production parameters instead of the steel grades is part of APO, too [10].

**Refractory Wear Profile for Specific Areas in General**

For some specific areas in the EAF, a continuous and close monitoring of the refractory wear provides important information, such as areas like hot spots. The knowledge about the residual lining thickness and the wear speed is essential input for steel plant managers when planning the duration of the campaign and the maintenance cycles. Figure 13 shows an example of different refractory wear speeds. The blue line represents a high, the red line a medium and the green line a zero maintenance scenario. The values can be calculated in APO based on a trained and validated refractory wear model. The model is influenced by the production parameters like produced steel quality, process times and process parameters.

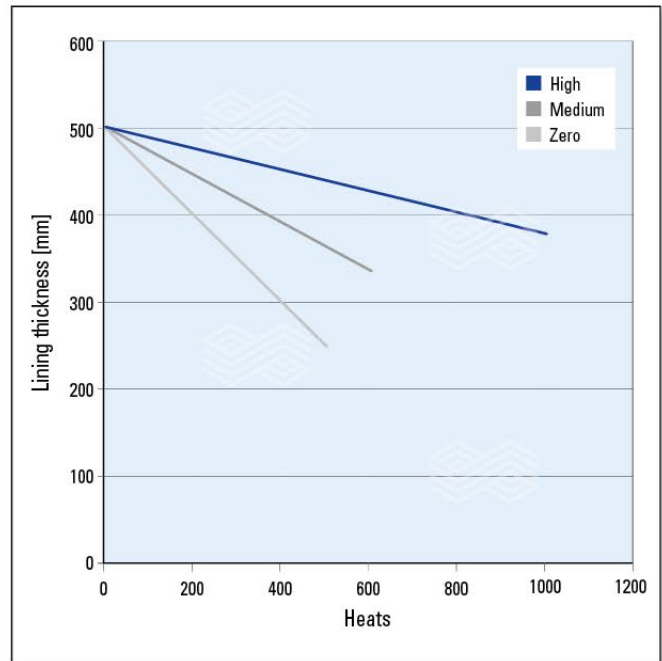


Figure 13. Wear speeds for different maintenance levels.

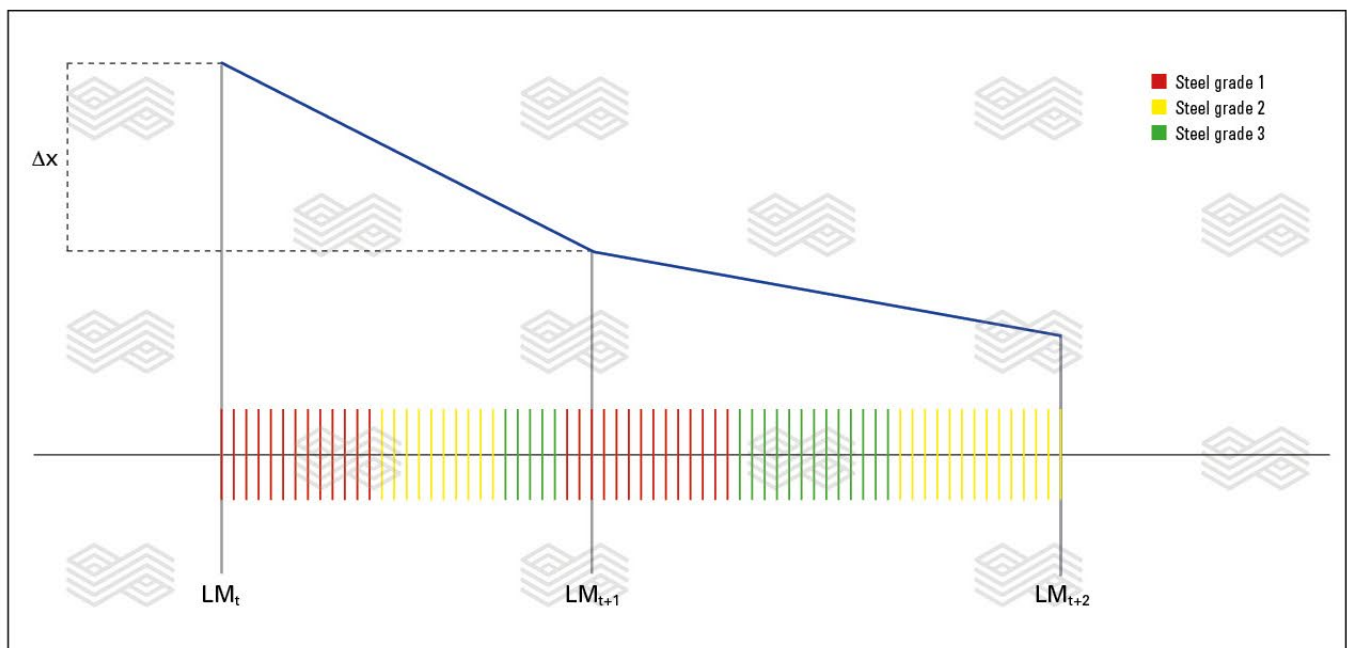


Figure 12. Refractory wear (blue line) over heats with different steel grades per slot.

## Condition Monitoring

Condition monitoring is the process of monitoring a parameter or condition (vibration, temperature etc.), in order to identify a significant change which is indicative of a developing fault. It is a major component of predictive maintenance. The use of condition monitoring allows maintenance to be scheduled, or other actions to be taken to prevent failure and avoid its consequences. Condition monitoring has a unique benefit in that conditions that would shorten normal lifespan can be addressed before they develop into a major failure. Condition monitoring techniques are normally used on rotating equipment and other machinery (pumps, electric motors, internal combustion engines, presses), while periodic inspection using non-destructive testing techniques and fit for service evaluation are used for stationary plant equipment such as steam boilers, piping and heat exchangers. In this paper we present condition monitoring for refractory lining. APO calculates the target wear areas based on historical data to reach a defined lining lifetime. In the example shown in Figure 14, a desired lifetime of 1000 heats was set. APO then calculates the target wear profile for specific areas in the furnace.

The upper yellow area indicates that the refractory condition state is as planned while the lower yellow area indicates that more refractory maintenance is required to reach the target lifetime. In the example given in Figure 14, the (mean) refractory wear of Hot Spot 1 (black line) remains in the upper yellow area indicating that no additional maintenance is required. APO also features refractory wear predictions to provide information on the future behaviour of the refractory wear. Additionally, APO shows a 3D brick model of the hot spots based on laser measurements. The blue line in the example figure below indicates the

predicted future lining thickness. APO can recalculate the refractory wear prediction after every heat. As soon as APO receives new laser measurements, the prediction model is validated and if required adapted.

## Daily Report

In data processing operational reporting is reporting about operational details that reflects current activity. Operational reporting is intended to support the day-to-day activities of the organization. "Examples of operational reporting include bank teller end-of-day window balancing reports, daily account audits and adjustments, daily production records, flight-by-flight traveler logs and transaction logs" [19]. In APO we generate a Daily Report (DR) giving the operation manager an easy accessible overview of the current state of the furnace lining. The DR shows the refractory thickness over time or heats for specific areas (black line in Figure 15). The red zone labeled 'Critical thickness area' indicates the minimum required lining thickness for that area. The light blue vertical lines represent laser measuring. The 3D model shown is based on the last laser measuring. Next to the 3D model is a scale indicating the condition of each brick. This makes the assessment very easy. The blue line starting right of the last laser scan is the refractory wear prediction and allows to evaluate if the targeted lifetime of the lining can be reached.

APO can also include maintenance data in the DR. In the example given in Figure 16 the gunning data are represented with green vertical bars. The height of the bars indicates the amount of gunning material applied in this area. Each bar stands for one maintenance intervention, in this case gunning with the TERMINATOR XL. The dotted blue line shows the cumulated gunning mix consumption from campaign start.

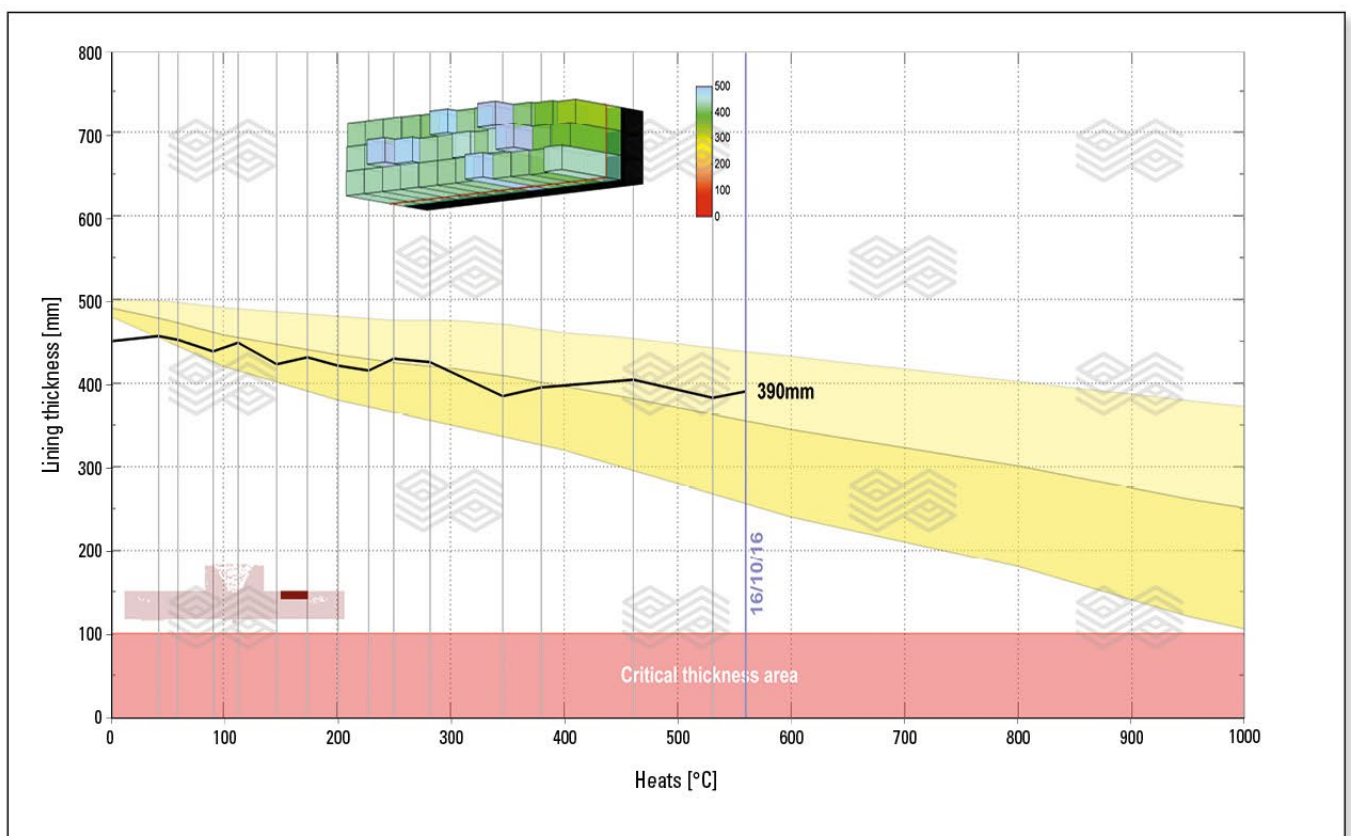


Figure 14. Example for lining monitoring (Hot Spot 2).

### Data Mining – Parameter Ranking

Data mining is the computational process of discovering patterns in large data sets involving methods at the intersection of artificial intelligence, machine learning, statistics, and database systems. It is an interdisciplinary

subfield of computer science. The overall goal of the data mining process is to extract information from a data set and transform it into an understandable structure for further use. In this case to identify and rank wear influencing parameters. Figure 17 shows an example of the ranking for one

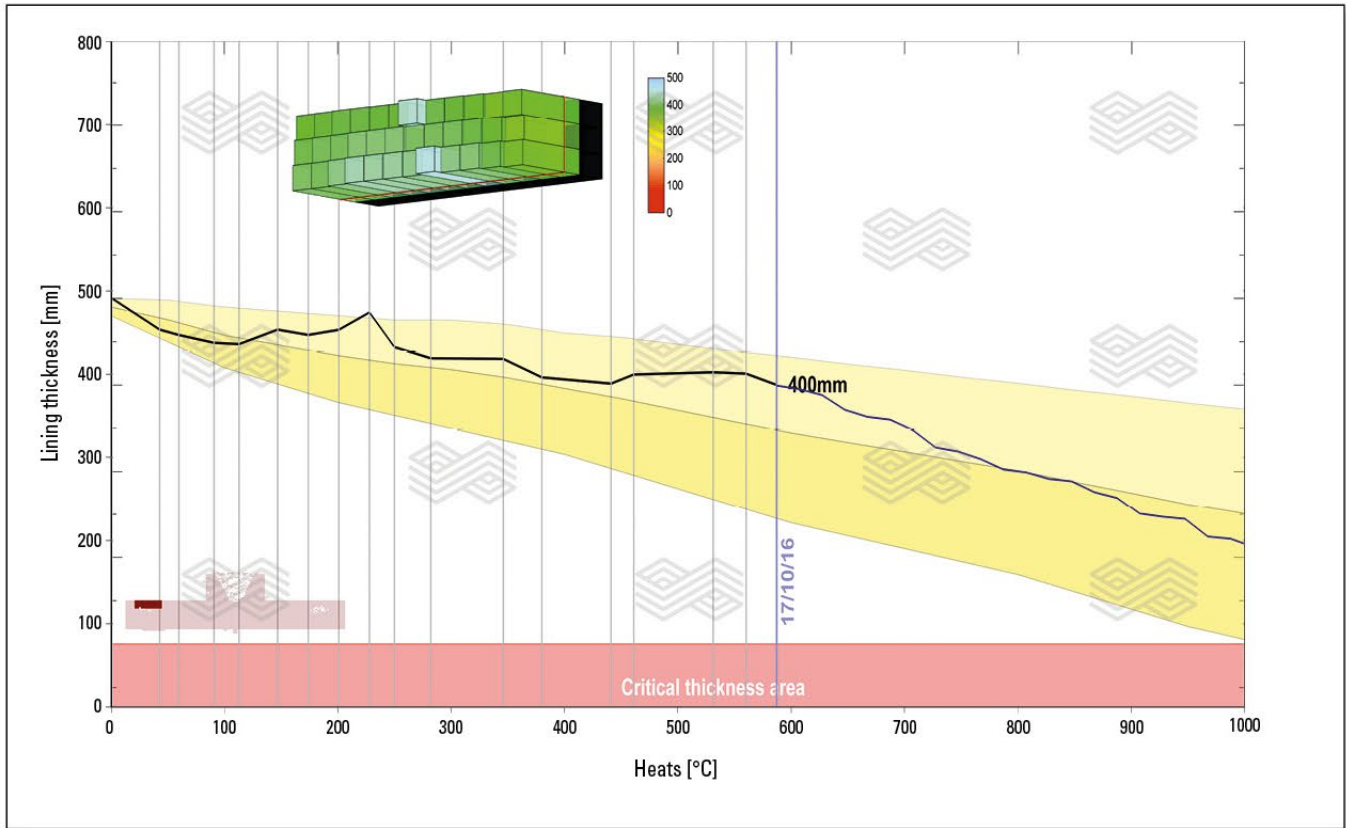


Figure 15. Example for refractory wear prediction (blue line).

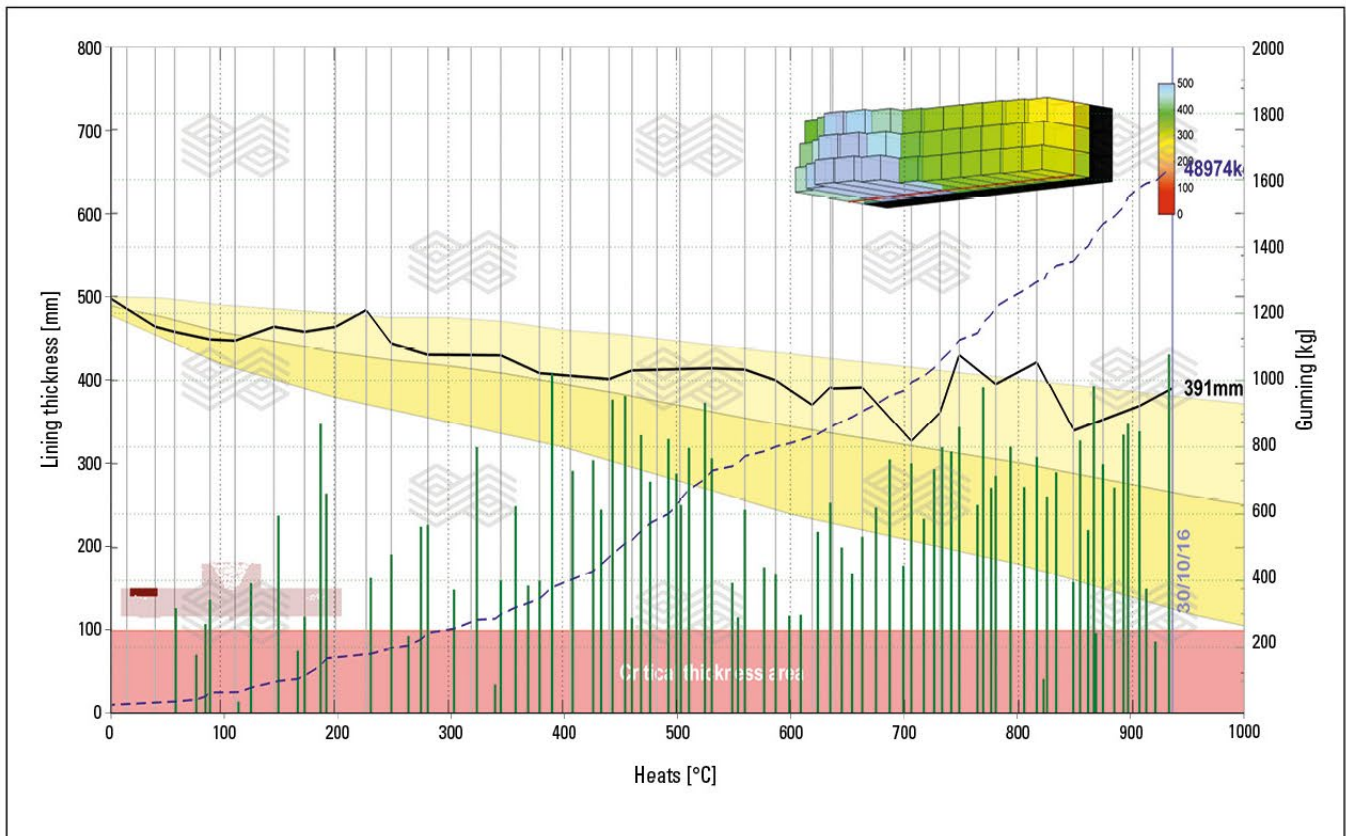


Figure 16. Example for Daily Report (excerpt).

specific campaign. When thinking about optimization of the furnace productivity the knowledge of the wear influencing parameters become obvious. Depending on process and product mix the ranking of the parameter can vary in a large scale.

## Outlook

In the near future APO plans to provide an online simulation tool to evaluate the impact of production parameters on the refractory performance. These features must be easily accessible and understandable. Allowing operators to execute their control on machineries is the goal of human-machine interfaces, and therefore their objective is also to interact with the productive process. The more intuitive the program, the easier and quicker the job, with consequent saving of resources and time. Hence, making their control easier is one key to improve productivity.

## Conclusions

Command and execution, thought and action: the balance between HMI devices and software in the Industry 4.0 is becoming more and more important. While laser measuring increases the capabilities of judging and controlling the refractory condition at a specific moment, APO predicts the

refractory wear enabling steel plant operation managers to base their decisions on a different level. The identification of the wear influencing parameters allows the generation of a trustworthy refractory model to simulate the impact of process changes on the refractory lifetime.

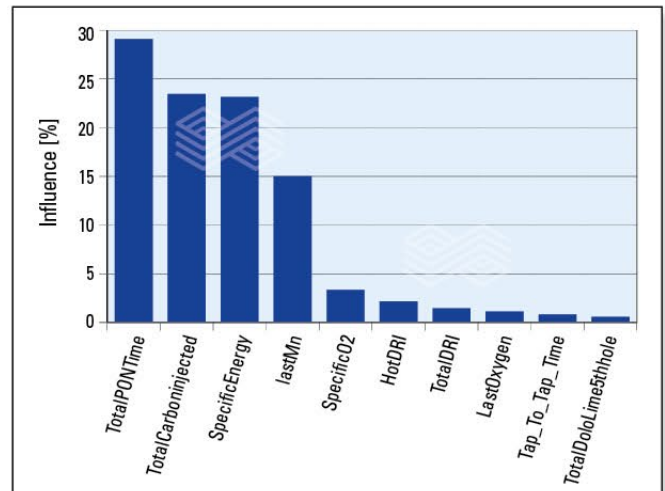


Figure 17. Example: wear influencing parameters.

## References

- [1] Industrie 4.0 Working Group, *Recommendations for implementing the strategic initiative Industrie 4.0*, 2013.
- [2] Yan, H. S. and Xue, C. G. *Decision-making in self-reconfiguration of a knowledgeable manufacturing system*, Jun. 2007, Int. J. Prod. Res., vol. 45, no. 12, pp. 2735–2758.
- [3] Brecher, C. et al., *Integrative Produktionstechnik für Hochlohnländer*, Heidelberg: Springer Berlin Heidelberg, 2011, pp. 17–81.
- [4] Womack, J. P., Jones, D. T. and Roos, D. *The Machine That Changed the World: The Story of Lean Production*, 1990.
- [5] Brettel, M., Friederichsen, N., Keller, M. and Rosenberg, M. *How Virtualization, Decentralization and Network Building Change the Manufacturing Landscape: An Industry 4.0 Perspective* World Academy of Science, Engineering and Technology International Journal of Mechanical, Aerospace, Industrial, Mechatronics and Manufacturing Engineering Vol:8, No:1, 2014, pp 43
- [6] Spath, D. et al., *Produktionsarbeit der Zukunft – Industrie 4.0*, Stuttgart, 2013.
- [7] Springer Gabler Verlag (Herausgeber), Gabler Wirtschaftslexikon, Stichwort: Total Cost of Ownership, <http://wirtschaftslexikon.gabler.de/Archiv/16735/total-cost-of-ownership-v6.html>, retrieved June 22, 2016
- [8] Bishop, C.M. *Pattern recognition and machine learning*, Springer, New York, 10. Edition 2009, pp 6,7,9,18.
- [9] Patent applications and patents pending.
- [10] Forrer, M. *Prediction of refractory wear with Machine Learning methods*, Master Thesis, Graz University of Technology, 2012, pp 126.
- [11] Jain, A.K. and Zongker, D. *Feature selection: Evaluation, application, and small sample performance*, IEEE Transactions on Pattern Analysis and Machine Intelligence, 1997, 19(2), pp 153–158.
- [12] Kohavi, R. and John, G.H. *Wrappers for feature subset selection*, Artificial Intelligence, 1997, pp 273–324.
- [13] Guyon, I. and Elisseeff, A. *An introduction to variable and feature selection*, Journal of Machine Learning Research, 2003, pp 1157–1182.
- [14] Pernkopf, F. and O’Leary, P. *Visual inspection of machined metallic high-precision surfaces*, Special Issue on Applied Visual Inspection, Eurasip Journal on Applied Signal Processing, 2002, pp 667–678.
- [15] Siedlecki, W. and Sklansky, J. *A note on genetic algorithms for large-scale feature selection*, Pattern Recognition Letters, 1989, pp 335–347.
- [16] Pernkopf, F. and O’Leary, P. *Feature Selection for Classification Using Genetic Algorithms with a novel Encoding*, International Conference on Computer Analysis of Images and Patterns, 2001, pp 161–168.
- [17] Feuerstein, M. *Refractory Wear Modeling using Statistical Methods*, Master Thesis, Graz University of Technology, 2016, pp 61.
- [18] Pernkopf, F. Forrer, M., Feuerstein, M. and Mutsam, N. *Wear Prediction @ SMP2 in Abu Dhabi*, Presentation at RHI, 2016.
- [19] Inmon, Bill (Jul 1, 2000), *Operational and Informational Reporting*, Information Management, 2013, Retrieved June 22, 2016.

Originally presented at AISTECH 2017, 8–11 May, Nashville, USA. Reprinted with permission from the Association for Iron and Steel Technology (AIST).

## Authors

Gregor Lammer, RHI Magnesita, Steel Division, Vienna, Austria.  
 Ronald Lanzenberger, RHI Magnesita, Technology Center, Leoben, Austria.  
 Andreas Rom, RHI Magnesita, Steel Division, Vienna, Austria.  
 Ashraf Hanna, RHI Magnesita, Steel Division, Burlington, Canada.  
 Manuel Forrer, ferrisol, Kalsdorf bei Graz, Austria.  
 Markus Feuerstein, mFeu Solutions, Graz, Austria.  
 Franz Pernkopf, Graz University of Technology, Graz, Austria.  
 Nikolaus Mutsam, Nikolaus Mutsam Consulting, Graz, Austria.  
**Corresponding author:** Gregor Lammer, [gregor.lammer@rhimaginesita.com](mailto:gregor.lammer@rhimaginesita.com)





RHI MAGNESITA

RHI Magnesita

# A new global leader

RHI Magnesita is the driving force of the refractory industry. Our 14,000 highly-skilled people are dedicated to delivering the best possible solutions for our customers, enhancing not only their operations but also their business performance.

Find out more at  
[rhimagnesita.com](http://rhimagnesita.com)



Clemens Ebner, Korey Skala, Laura Rechberger and Bernd Neubauer

# Avoidance of Hazardous Substances via Low Emission MgO-C Technology Shown With the Example of a Ladle Lining Refractory

## Introduction

With increasing focus on health and environmental issues associated with steel production, refractory material suppliers have been put to the challenge of improving ecological aspects of MgO-C bricks.

Over the last decades, magnesia carbon refractories have been used in steel producing aggregates with great success owing to their unique properties in terms of excellent slag corrosion and thermal shock resistance, high refractoriness as well as low thermal expansion [1–3]. Since the advent of MgO-C based refractories in the late 1970's and early 1980's there has been a debate on the principles of the two major bonding systems used for this kind of high temperature materials [4,5].

In those days, the development of pitch bonding technology was mainly based in Europe, while refractory production using synthetic phenol-formaldehyde resins predominantly goes back to the work of Japanese material scientists and product developers [5].

The general differences and similarities of resin and pitch bonding for basic refractories are discussed in terms of production and application; special emphasis is put on emission topics and environmental issues. Concerning the emission of organic and inorganic substances, a direct comparison between resin and pitch technology as well as recent developments in this field are presented and discussed under health, safety, environmental and economic aspects.

## Resin vs. Eco-Pitch Bonding for Unfired Ladle Lining Refractories

For the production of resin bonded refractories, various types of phenol-based materials are used with phenol-formaldehyde (PF) prepolymers being the most extensively used ones. Owing to the type of chemical synthesis, two different structures of these PF resins are available: Water based resoles are synthesized utilizing basic catalysis and an overstoichiometric ratio between phenol and formaldehyde while so-called novolacs are yielded by reacting an excess of phenol with formaldehyde under acidic conditions [6]. The low viscosity of PF resins at room temperature allows for mixing under ambient conditions. In resoles, the presence of reactive groups makes curing without the addition of any type of hardener possible; if novolacs are used, an additional hardening agent like hexamethylenetetramine is needed to complete hardening upon tempering at temperatures of around 200 °C [6]. During tempering, a hard and rigid so-called resite structure is formed yielding bricks with very high strength at room temperature and high strength after coking.

Eco-pitch, also called carbon bonding, on the other hand, owing to the high softening points of (synthetic) pitch, requires a more sophisticated production process in which mixing, pressing and tempering are carried out at elevated temperatures. Typical temperatures of 250–350 °C are employed to obtain products with sufficient cold crushing strength in the original state and high strength after coking.

## Technological Aspects of MgO-C Bonding Systems

Besides the production process, there are some quite pronounced differences in the technological features brought about by the different bonding systems such as (coked) carbon structure, micro structure flexibility and oxidation stability. A summary of the main differences between resin and carbon bonding is presented in Table I.

The main difference between the coke structure of resin and carbon bonded refractories is related to the processes taking place until the final bricks' structure is reached: Carbon binders tend to soften before the final coke structure is developed. This behavior is triggered by the formation of liquid crystal meso-phases that allow the organic binder molecules to rearrange during coking [7,8]. As a result the ordering on the molecular level of the final coke skeleton is higher than the one formed by the hard, rigid and infusible resin resite structure.

For carbon bonding, the term graphitic carbon is used while the resin coke structure is referred to as amorphous or glassy carbon [8,9]. The difference in the coke structure has significant influence on the mechanical properties and oxidation resistance. Examples for oxidation resistance of carbon and resin binders and flexibility of carbon and resin bonded refractory bricks are shown below (Figure 1).

Characteristic	Bonding system	
	Resin bonding	Carbon (eco-pitch) bonding
Degree of ordering in carbon structure	–	+
Oxidation stability of coke (need for AOX)	–	+
Strength at room temperature	+	–
Strength after coking	+	+
Linear expansion from room temperature to 1650 °C (application temperature)	– (higher)	+ (lower)
Flexibility of brick structure at elevated temperatures	–	+

**Table I.** Comparison of technological characteristics between resin and carbon bonding technology.

Higher oxidation resistance of carbon bonded refractories enables for using little or no antioxidants which can be an advantage for highly oxidative applications where brittleness is an additional concern. In spite of the differences pointed out in this section, it is worth mentioning that both, resin and carbon bonded refractories can have an equal performance in all steel-related applications if the choice of recipe and application area has been accurately taken with regard to the respective aggregate and process conditions.

## Health, Safety and Environmental Aspects

Owing to the totally different chemical nature of resin and carbon binders, assessment of health, safety and environmental (HSE) aspects is of crucial importance for refractory producers and steel mill operators. As stated above, phenol-formaldehyde resins used as refractory binders mainly consist of phenol, phenol derivatives, oligo- and polymeric phenol structures and very small amounts of free formaldehyde, normally in the range below 0.1 wt.%. During production, some phenol, minor amounts of formaldehyde and reaction water are emitted in the tempering step. As state-of-the-art tempering kilns are equipped with post combustion systems, these emissions are generally of no concern; about 40–50 wt.% of the overall emissions are removed. Another 40–50 wt.% of vaporizable structures stay in the product delivered to steel plants. The residual 40–50 wt.% of pyrolysis products are emitted during preheating and frequently also in the first heats. Consequently, expensive ladle preheating enclosures equipped with post combustion systems cannot guarantee complete avoidance of hazardous substance emissions during preheating and the first few heats.

Permissible exposure limits (PEL, weighted average for 8 hours/day, 40 hours/week) for phenol and its most prominent derivative cresol (all isomers) have been set to 19 and 22 mg/m<sup>3</sup> air by the Occupational Safety and Health Administration (OSHA), while for other phenolics like xylenols or trimethylphenol no limits have been defined. The OSHA PEL for formaldehyde is 0.75 mg/m<sup>3</sup> air; formaldehyde has been categorized as known carcinogenic to humans by the International Agency for Research of Cancer [10].

In case of carbon bonding the chemical composition of pyrolysis products is substantially different (Figure 2). Main

products derived from eco-pitch binder pyrolysis are aromatic structures such as toluene or benzene, in combination with larger polycyclic aromatic hydrocarbons (PAHs) and small molecules like H<sub>2</sub>S and SO<sub>2</sub>.

OSHA permissible exposure levels for BaP and other coal tar pitch-derived PAHs are 0.2 mg/m<sup>3</sup> air. Maximum allowed concentrations of SO<sub>2</sub> are around 13 mg/m<sup>3</sup> air, while no weighted average limit for H<sub>2</sub>S is applicable based on the acute adverse effects induced by this substance. The ceiling value (limit never to be exceeded) is 28 mg/m<sup>3</sup> air.

Over the past years, the discussion of the different pyrolysis products derived from resin and carbon bonded bricks has intensified and refractory producers were urged to take a closer look at the nature of ladle emissions and new methods to characterize product safety had to be established in the refractory business. In this context, pyrolysis gas chromatographic systems (Pyro-GC-MS), allowing for simulation of a heat up process at very small scale, has made significant contributions to the understanding of binder pyrolysis. Combination with weight loss experiments by means of thermogravimetric analysis (TGA) creates a powerful tool for estimation of amount and elucidation of organic structures formed in binder pyrolysis processes. Examples of such comparative Pyro-GC-MS experiments for carbon and resin bonded refractory products are illustrated (Figure 2).

These so-called pyrograms can be used to identify the chemical structure of emissions released under highly reproducible oxygen-deprived conditions allowing for estimation of potential hazards. As indicated before, the main pyrolysis products of resin bonded refractory products are phenol, phenol derivatives and small amounts of condensation products formed during binder coking. Another important pyrolysis product is not visible in this experiment due to the lack of oxygen: While phenol and its derivatives are still present in the residue structure and are vaporized by the thermal stress, formaldehyde is structurally incorporated into the polymer and can only be formed after thermal cracking and subsequent oxidation. As oxygen cannot be fully excluded during preheating of ladle linings, formaldehyde emissions can be an issue. Based on the present state of knowledge, phenol and its derivatives are not carcinogenic but acutely

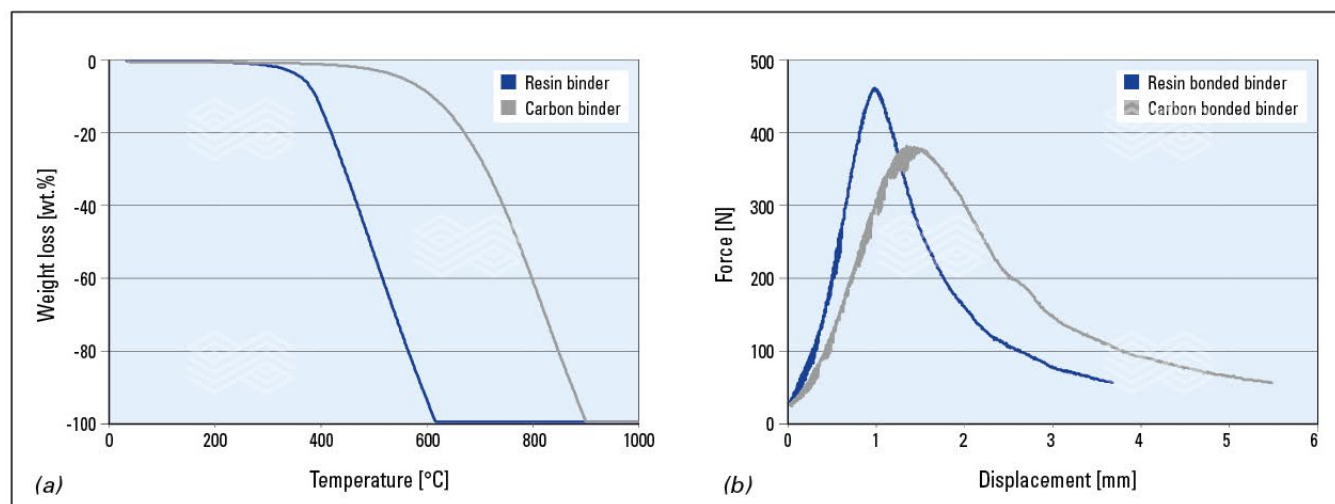


**Figure 1.** (a) Oxidation stability of resin and carbon binders. (b) Visualization of structure flexibility of resin and carbon bonded bricks shown in wedge splitting tests.

toxic in high concentrations and substantially smell active: Air concentrations of phenol and some of its derivatives far below the permissive exposure level may already provoke seriously negative smell impression.

Organic constituents formed in carbon binder pyrolysis, on the other hand have significantly higher boiling points and molecular weights. This renders them less volatile and emissions of these compounds are frequently not entirely gaseous but rather particulate. The subjective smell impression induced by PAHs and alike is much less negative and is sometimes even described as moderately pleasant. In contrast to phenolics, PAHs show much less acute toxicity to humans but some PAHs like benzo[a]pyrene (BaP) have already been proven to be carcinogenic to humans while others are still suspected to have severe negative long-term effects on the human health. Already in the 1980s, the US-American Environmental Protection Agency (EPA) has listed 16 substances, the monitoring of which in work places and the environment is recommended. Candidates on this list are referred to as EPA-16 PAHs and as a reference substance, BaP has been chosen due to its high hazard potential and relatively simple and accurate traceability. In 1995, a suggestion to indicate products containing more than 50 ppm BaP (0.005 wt.%) as carcinogenic has been made for refractory products in the German technical guideline TRGS-551.

## Reduction of Brick Emissions During Ladle Heat Up: Recent Developments

With respect to the above described health and safety concerns and by rising attention from authorities since the 80's and 90's of the past century, refractory and steel producers have been forced to improve the emission situation and a number of approaches has been developed and followed after ever since. The following section will deal with these approaches and will try to objectify them with regard to their effectiveness in HSE as well as economic aspects. Special focus is laid on the cost-benefit calculation of measures against refractory brick emission.

### Optimized Heat Up Procedure for Steel Ladles

Optimization of heating procedures includes the place of ladle preheating as well as heating time, temperature, oxygen supply and rate of temperature increase. Steel mills operating completely separated and sealed preheating stands equipped with modern post combustion systems generally do not face severe emission issues. Thorough preheating to reach at least 600 °C in the complete working lining is time-consuming and demands for highly sophisticated ladle park logistics. Ladles whose working lining has not fully reached the temperature needed to eliminate all organic substances from binder materials still can emit substantial amounts of malodorous and/or toxic substances.

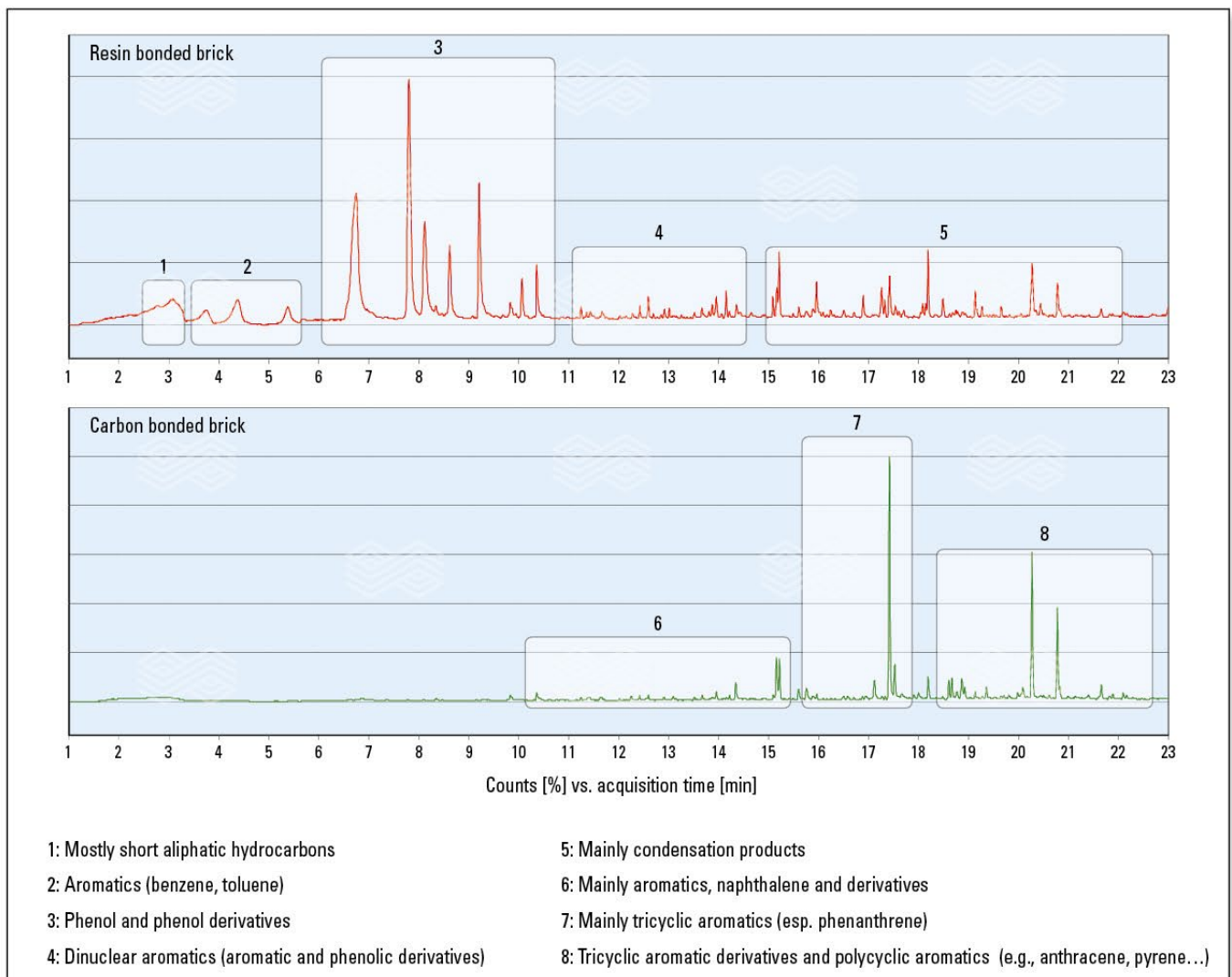


Figure 2. Emission patterns of resin and carbon bonded refractories (Pyro GC MS).



An easier but less effective way to reduce emissions is the choice of the preheating curve itself: Based on the steadily increasing demand for higher productivity, steel plants generally prefer rather short ladle preheating programs with steep temperature profiles that provide sufficient safety for a ladle going into operation but are not optimized for improving the emission situation. Examples for preheating curves recommended for standard applications and optimized heating procedure for emission avoidance are shown below (Figure 3).

Generally, a constant heating rate between 60 and 100 °C can be employed if no emission issues are foreseeable. For emission-optimized preheating, a heating rate of 95 °C/h up to 600 °C is recommended, followed by a switch to lower heating rate (75 °C/h) at 600 °C brick surface temperature. The temperature up to which the highest emission rate is expected is reached within shorter time and gaseous organic pollutants are more likely to be completely combusted and predominantly yield uncritical products. Subsequent reduction of heating rate aims at a more homogeneous temperature distribution throughout the entire working lining. This way, further pyrolysis induced by steady temperature increase can be retarded and high-boiling substances and emissions from the bricks' cold side are expected to be lowered. In addition to this recommendation, the preheating system's air or oxygen supply should be adapted with regard to temperature: Below 300 °C, air supply is kept slightly oxidizing at  $\lambda > 1$ , while between 300 and 800 °C, 15–25% of excess air is added to the burning gas ( $1.15 < \lambda < 1.25$ ). The emission rate of organic substances in this temperature range is at its highest level and oxygen excess can positively influence complete combustion. In the final heating stage between 800 and 1100 °C,  $\lambda$  again is reduced to equilibrium in order to minimize carbon burnout and lining damage. Due to the same reason, a ladle not being taken in operation right after preheating should be kept at 750 °C and fully (re-)heated to working temperature only shortly before use. The recommendations given in this section can surely help to prevent excessive pollutant loads, but given the magnitude of ladle sizes, designs and types of permanent linings as well as steel shells, the trickiness in choosing the right preheating procedure becomes obvious. A large variety of preheating and temperature monitoring systems in combination with different local

conditions in steel shop floors bring about additional imponderables. Hence, these general recommendations only represent guidance parameter levels. These need to be modified with respect to individual steel plant demands in order to be effective in handling potential emission hazards.

### **New Recipe Development for Reduced Emission MgO-C Bricks**

Given the fact that changes in the refractory product itself are not influenced by the surrounding conditions in steel mills, the right choice of high-quality bonding agents and binder additives can be a very useful tool for emission reduction. This is valid for both, resin and carbon bonded bricks, but with respect to binder availability and scope of influence, improvements in resin bonding technology seem to have higher chances to be effective. Consequently, the main focus here is put on optimization of resin bonding technology, additionally including improvements recently implemented for carbon bonding.

In the beginning of the third millennium, the first refractory producers started to substitute coal tar pitch binders by newly developed modified coal tar products and petroleum based raw materials. This way, a significant reduction of the EPA-16 lead substance BaP in tempered refractory bricks by a factor of 10–20 was achieved. Bricks produced with coal tar pitch in the 1990's were loaded with BaP levels of 150–200 ppm, while their modern successors reach BaP levels  $< 50$  ppm. With additional adjustments of dehydrogenation agents, combined with optimized tempering, current state-of-the-art carbon bonded MgO-C bricks typically contain less than 15 ppm and unfired doloma products typically rank below 40 ppm BaP. Furthermore, bad smell impression provoked during preheating of carbon bonded refractories could be effected by substitution of currently used carbon binder additives with alternative pitch polymerization agents. By implementing aforementioned measures the safety of carbon bonded refractory products was significantly improved.

Even more improvement could be realized by introducing low or reduced-emission resin bonding technology [11]: By careful selection of high-purity liquid-synthetic resins with excellent performance and supported by extensive improvements in the area of auxiliary carbon-based

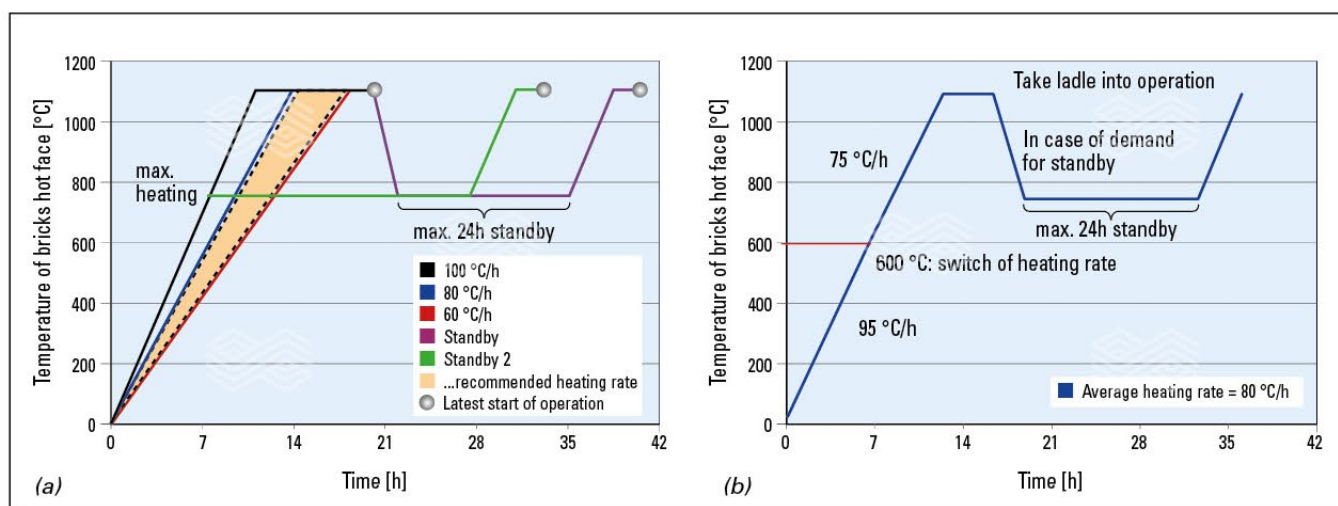


**Figure 3.** (a) General recommendation for heat up procedures with constant heating rate for a newly lined ladle. (b) Recommended heat up procedure optimized by temperature rate change for emission avoidance.

high-temperature binders, substantial improvements in emission characteristics were reached and proven for effectiveness by means of weight loss in TGA and structure elucidation in Pyro-GC-MS experiments (Figure 4 and 5).

Direct comparison of brick emission behavior as shown by the TGA plots quite impressively indicates the improvements brought about with the newly developed reduced emission (RE)-resin bonding system for MgO-C bricks. By simple calculation of the emission ratio between standard and RE bonding, a reduction of approx. 40 wt.% could be proven (Figure 4a). In addition, emission rate plots derived from TGA curves display a significantly improved emission rate. In this case, a reduction of peak intensity by a factor of about 3 was reached (Figure 4b). As organic molecular structures cannot be elucidated by simply recording the weight loss in TGA, brick samples were subjected to Pyro-GC-MS characterization (Figure 5).

Although Pyro-GC-MS measurements cannot be quantitatively interpreted, distinct improvement of RE resin over standard bonding can clearly be seen in the pyrograms by using the exact same sample mass in analysis.

Translating the recipe changes and characterizations in TGA and Pyro-GC-MS to absolute numbers, the emission of e.g. phenolics and formaldehyde from RE-brands is reduced by about 1/3 in comparison to standard state-of-the-art resin bonded MgO-C bricks. In addition to lab trials and recipe-related calculations, significant improvement in terms of emission behavior during ladle heat up in field application were found. By using RE resin bonded refractory linings, steel producers are able to produce effective measures for continuous improvement in HSE issues without significant cost increase or adverse effect on ladle lifetime and brick performance.

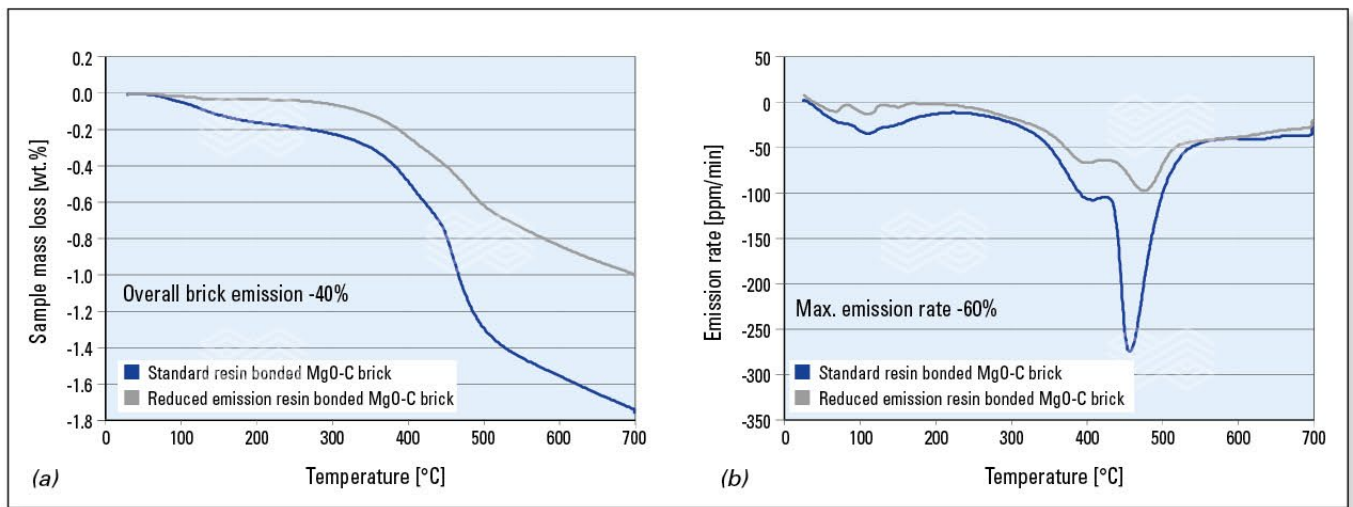


Figure 4. Thermogravimetric analyses of standard resin bonded MgO-C bricks conducted between RT and 700 °C under N<sub>2</sub> atmosphere. (a) Overall mass loss over temperature representative of overall brick emission with respect to sample weight and (b) Derived plot of emission rate over temperature.

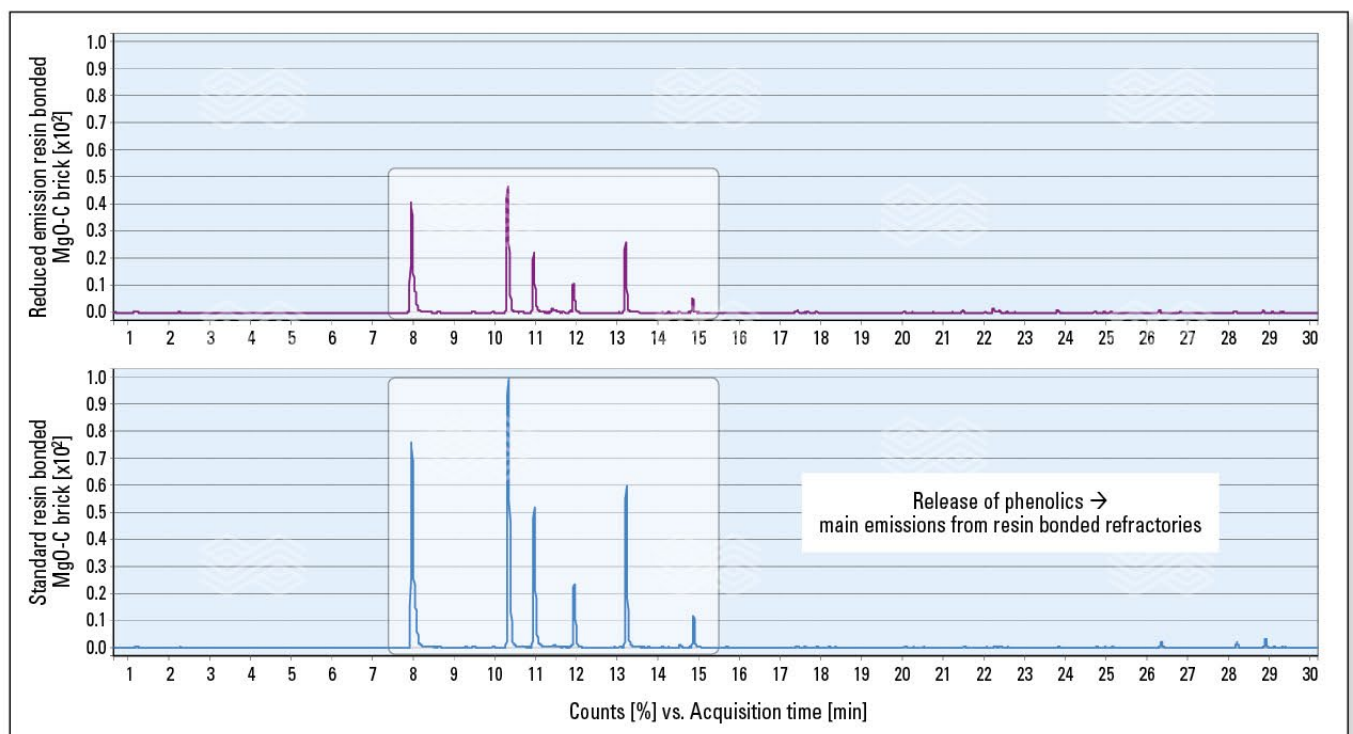


Figure 5. Comparative emission study of resin and carbon bonded refractory samples by Pyro GC MS (equal sample weight).

### Reduced Emission vs. Zero Emission Technology

In contrast to the aforementioned benefits of RE resin bonding technology, a discussion of possibilities to create zero emission bonding systems and other methods for producing refractory for complete emission avoidance has been started with respect to even more restrictive needs.

A convenient approach for zero emission MgO-C bricks is related to improved temperature treatment in production. The basic idea is to increase tempering kiln temperatures in order to get rid of all organic volatiles formed in the binder coking process [12]. This way, no recipe adaptations are necessary since all potentially harmful volatiles, independent of their origin are eliminated already under tempering, but higher tempering intensity can also have negative implications on production costs and resulting product quality. Tempering kilns currently used in refractory production are not equipped for such high temperatures and offer no options for oxygen exclusion necessary to prevent carbon burn out and severe quality issues. Hence, new aggregates constructed with special high-temperature resistant steel having the possibility to form a reducing (or non-oxidizing) atmosphere are needed for production.

Since higher tempering temperatures alter the amount and structure of the binder present in the delivered product, changes in porosity, bulk density and cold crushing strength have to be accepted. Higher porosity potentially renders MgO-C bricks more susceptible to hydration and can shorten the product's shelf life. In addition, carbon burnout on the lining's surface can be expected due to a surplus of oxygen. Regarding field application of such high-temperature-treated (HT) bricks, lower lining life in connection with increased structure brittleness and brick spalling after preheating, resulting in higher performance variations is possible. Together with an increase in manufacturing costs, these factors may have a negative impact on the cost-benefit-calculation and HT-tempered

lining concepts are only recommended if the goal of zero ladle emission has to be achieved under any circumstances.

### Conclusions

From the findings presented in this paper, some final remarks about ladle emission reduction and avoidance can be made: Both, unfired resin and carbon bonded refractory products can potentially compromise health and safety levels in steel plants due to emission of hazardous and/or irritating substances during ladle heat up. Depending on steel producer's internal safety standards and local environmental legislation, standard bonding systems can lead to higher than permitted exposure levels. Because of this and due to the regulatory claim for continuous improvements in HSE issues, several products with significantly improved emission characteristics have recently been rolled out on the refractory market. These products include carbon bonded bricks with reduced smell emission, reduced emission resin bonded bricks enabling for a reduction of e.g. phenol, phenol derivatives and formaldehyde emissions by about 1/3, and bricks exhibiting genuine zero emission behaviour effected by means of high temperature treatment.

In an effort to improve working conditions with minimal negative effect on the cost-benefit-calculation, steelmakers should consider the level of emission reduction that makes sense. If the target is a reduction of emissions because of regulatory actions or if continuous improvements in HSE issues are needed, the use of reduced emission resin bonded refractories is expected to have the best cost-benefit-ratio, also with regard to the similar performance of these bricks as compared to standard resin bonded products. Complete avoidance of ladle refractory lining emissions is normally not called for as exposure below the set values is not deemed as a health risk. Hence, the potential cost increase and performance issues by currently available zero-emission refractory solutions may not be compensated for by the benefits.

### References

- [1] Buchebner, G., Hanna, A. and Samm, V. Latest Developments in Magnesita Carbon Bricks. *Proc. AISTech 2012 Atlanta*, pp. 821-828.
- [2] Buchebner, G., Panthen, B., Pungerssek, R. and Samm, V. Advanced BOF-Lining Solutions. Presented at *UNITECR '07 Dresden*, Germany, Sept., 18-21, 2007; pp. 300-303.
- [3] de Silveira, W. and Falk, G. *Low Carbon Economy 2012*, 3, pp. 83-91.
- [4] Schulle, W. and Ulbricht, J. *Bol. Soc. Esp. Ceram. Vidr.* 1992, 31, 5, pp. 419-425.
- [5] Landy, R.A. *Refractories Handbook*, Schacht, C.A. (ed.), CRC Press, Taylor & Francis Group, Boca, Raton, 2004, pp. 109-149.
- [6] Gardziella, G., Pilato, L.A. and Knop, A. *Phenolic Resins, Chemistry, Applications, Standardization, Safety and Technology 2<sup>nd</sup> Edition*, Springer-Verlag, Berlin, Heidelberg, 2000, pp. 24-50.
- [7] McEnaney, B. and Rand, B. *Br. Ceram. Trans. J.* 1985, 84, pp. 157-164.
- [8] McEnaney, B. and Rand, B. *Br. Ceram. Trans. J.* 1985, 84, pp. 193-198.
- [9] Jenkins, G.M. and Kawamura, K. *Nature* 1971, 21, 175-176.
- [10] United States. OSHA Occupational Chemical Database. Washington, DC: U.S. Dept. of Labor, Occupational Safety & Health Administration, n.d. <<http://purl.access.gpo.gov/GPO/LPS86421>>.
- [11] Patent applications and patents pending.
- [12] Mendheim, J. The Heat Treatment of Organically Bonded and Impregnated Refractories. *Proc. Tehran International Conference on Refractories Tehran*, 4-6 May, 2004.

Originally presented at AISTECH 2017, 8-11 May, Nashville, USA. Reprinted with permission from the Association for Iron and Steel Technology (AIST).

### Authors:

Clemens Ebner, RHI Magnesita, Technology Center, Leoben, Austria.  
 Korey Skala, RHI Magnesita, Steel Division, Munster, USA.  
 Laura Rechberger, RHI Magnesita, Technology Center, Leoben, Austria.  
 Bernd Neubauer, RHI Magnesita, Technology Center, Leoben, Austria.

**Corresponding author:** Clemens Ebner, [clemens.ebner@rhimagnesita.com](mailto:clemens.ebner@rhimagnesita.com)



Gerald Reif, Roland Krischanitz, Rene von der Heyde and Stephan Ullly

# DIVASIL FP—Frost Protected Binder for Sol Mixes

The Sol mixes are an emerging, extraordinary successful, and steadily growing product group within the area of nonbasic monolithics. It has been shown that due to their unique properties the Sol mixes already set new standards in cement applications. In nonferrous metal and in environmental, energy and chemical (EEC) applications they also increasingly deliver very promising results and show superiority over conventional mixes. To date, the binder DIVASIL, a colloidal silica aqueous fluid that is used in combination with the Sol mixes had the disadvantage of being irreversibly destroyed when frozen. To overcome this drawback the frost protected binder DIVASIL FP was developed. The new blue colored binder freezes at  $-5\text{ }^{\circ}\text{C}$  and can be used after thawing.

## Introduction

Since the introduction of Sol Mixes to the market in 2010 [1] the portfolio has been steadily increased in terms of raw material base as well as concerning installation technique (Figure 1) [2,3]. Today there is a wide range of approximately 100 Sol bonded monolithics for different industries available and the portfolio is constantly further expanded. The broad range of base raw materials ranges from fireclay to alumina chromium oxide. Mixes for casting, dry gunning, and shotcreting application are available. The product availability has been globally harmonized, the most important Sol mixes are not only manufactured in Urmitz (Germany) but also in the RHI plants in Burlington (Canada), Tlalnepantla (Mexico), Vishakapatnam (India) and most recently in Santiago (Chile). These efforts have led to a continually growing sales volume of the Sol Mixes. In 2017, deliveries are expected to exceed 10000 tonnes. In addition to the advantages concerning easy installation and rapid heat up the Sol mixes have shown outstanding performance in the cement industry (outlet zone, cooler, pre-heater) in some applications the lifetime was at least tripled [4]. The Sol mixes have also delivered very promising results and show superiority over conventional and low cement mixes in growing application areas in nonferrous metal (e.g., Fe-Ni rotary kiln) and EEC (e.g., boiler) applications. Up to now the liquid binder DIVASIL, a colloidal aqueous silica solution that is used in combination with the dry delivered Sol mixes, had the disadvantage of being irreversibly destroyed when frozen (Figure 2). This has led to an increase in logistical requirements such as cost intensive thermal transport and temperature controlled storage at the customer sites.

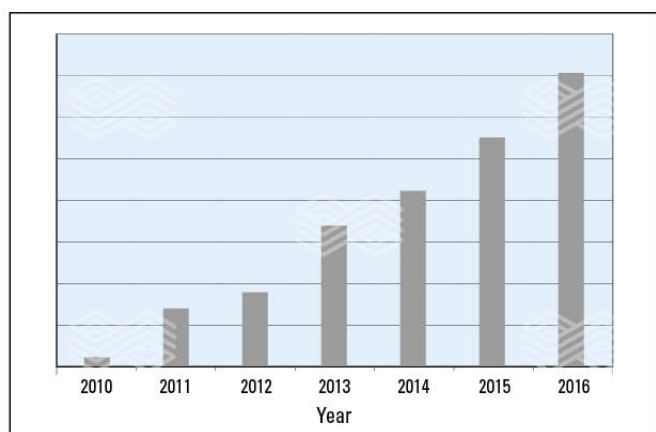


Figure 1. Sales volume of Sol mixes 2010 – 2016

These restrictions have retarded the utilisation of Sol mixes especially in regions where cold temperatures are common and during the winter season. To overcome this drawback and ensure the Sol bonded monolithics are accessible for all consumers and to simplify the logistics of the binder transport and storage, a R&D project was initiated at the end of 2015.

## Development and Technical Information

### DIVASIL FP Development

This R&D project was carried out in cooperation with a Sol supplier, so that expertise from both areas Sol technology and refractory materials could be combined. Intensive development led to the new product DIVASIL FP. DIVASIL FP has a lower freezing point ( $-5\text{ }^{\circ}\text{C}$ ) and most importantly is not destroyed through freezing, after thawing it returns to the stable colloidal silica aqueous fluid. It was established in numerous experiments that this behaviour is consistent for short term, long term, and cyclical freezing conditions at various temperatures ( $-5$ ,  $-15$ ,  $-35\text{ }^{\circ}\text{C}$ ). Additionally long term exposure of larger volumes at temperatures around the freezing point, maintaining the material in a semi frozen state did not result in harm to the product (Table I).

### DIVASIL FP as Binder for Sol Mixes

DIVASIL FP was tested with the whole range of Sol mixes. The amount of binder required and the workability concerning mixing, casting, and setting was not influenced. It should be noted that the binder must be in a liquid state when added during mixing. The standard recommendation



Figure 2. Showing the irreversible destruction of DIVASIL due to freezing.

to process mixes at temperatures above 5 °C applies also to Sol mixes used in combination with DIVASIL FP. In Table II the results of laboratory tests are shown. It can be seen that the properties of the Sol mixes with different raw material concepts are not influenced when using DIVASIL FP. Additional tests were carried out with DIVASIL FP that had been frozen 5 times at different temperatures to investigate possible influences due to freezing. As shown in Table III, it was demonstrated that multiple freezing cycles do not harm DIVASIL FP and final properties of mixes are unaffected. Figure 3 shows an example of hot properties of Sol mixes when using DIVASIL FP. Untreated and previously frozen DIVASIL FP samples were utilised. The results shown in the refractoriness under load curves (according DIN 51053/1) are almost identical which establishes the interchangeability of DIVASIL and DIVASIL FP and the tolerance of DIVASIL FP to freezing. To establish the behaviour of DIVASIL FP for dry and wet gunning applications a series of gunning trials were conducted at a gunning test rig. The results show that no difference in gunning behaviour between DIVASIL and DIVASIL FP could be detected (Figure 4). To simulate complex casting applications, a burner lance tip was cast using COMPAC SOL MB A100-6 in combination with DIVASIL FP. The trial was carried out at the Training Center Cement (TCC) in Leoben. The trial was successful, the cast segment could be easily demoulded and showed no optical defects (Figure 5).

Initial field-feedback has been obtained from customers. In addition to the reduced logistical requirements no differences in handling have been reported from customers or technical support staff when compared to the standard DIVASIL product. DIVASIL FP can therefore be used as a

Freezing test at -35 °C		DIVASIL FP
Experiment	Duration	Observation
One freeze cycle	24 h	OK
5 cycles freeze - thaw	5 x 24 h	OK
Long freeze cycle	4 w	OK

**Table I.** The results of a typical freezing experiment for DIVASIL FP.

	Divasil-Type	CCS [N/mm <sup>2</sup> ]		AR [cm <sup>3</sup> ]
		110 °C	1000 °C	
COMPAC SOL M64COR-6	Std	62	122	5.8
	FP	54	129	6.0
CARSIT SOL M10-6	Std	66	153	6.1
	FP	62	155	5.7
COMPAC SOL B88-6	Std	62	142	4.5
	FP	50	153	4.7

AR Abrasion resistance according ASTM C704 calibrated  
CCS Cold crushing strength according EN ISO 1927-6

**Table 2.** Physical properties of Sol bonded mixes: DIVASIL FP vs DIVASIL. Where CCS represents cold crushing strength according EN ISO 1927-6 and AR represents abrasion resistance according ASTM C704 calibrated.

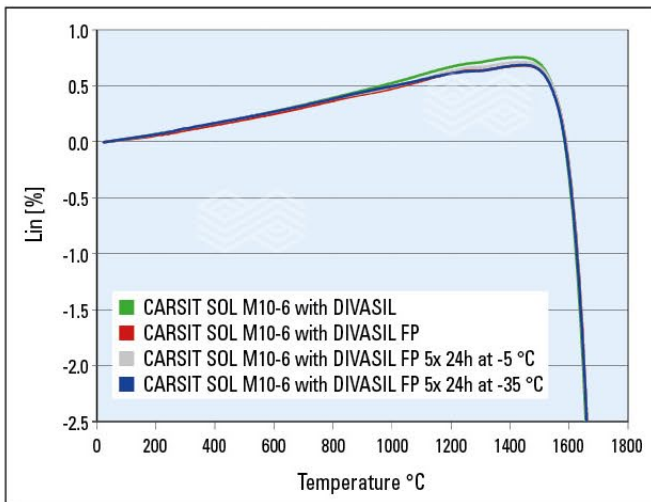


**Figure 3.** Refractoriness under load of CARSIT SOL M10 with DIVASIL and DIVASIL FP untreated and after multiple freezing/thawing cycles.

	Divasil-Type	Binder-treatment	CCS [N/mm <sup>2</sup> ]		AR [cm <sup>3</sup> ]
			110 °C	1000 °C	
CARSIT SOL M10-6	FP	untreated	62	155	5.7
	FP	5x 24h -5°C	58	156	6.3
	FP	5x 24h -35°C	59	151	6.1

AR Abrasion resistance according ASTM C704 calibrated  
CCS Cold crushing strength according EN ISO 1927-6

**Table 3.** DIVASIL FP untreated and after multiple freezing/thawing cycles with CARSIT SOL M10-6. Where CCS represents cold crushing strength according EN ISO 1927-6 and AR represents abrasion resistance according ASTM C704 calibrated.



**Figure 4.** Showing (a) dry gunning trial with COMPAC SOL F53G-6 and (b) shotcreting trial with COMPAC SHOT SB 64-6 and DIVASIL FP.

1:1 replacement for DIVASIL in all standard Sol mixes. In cases where COMPAC SOL MB and COMPAC ROX mixes are used in complex designs and frameworks, it is recommended to consult with RHI in advance. For better optical differentiation DIVASIL FP is dyed blue, the standard DIVASIL will continue to be available (Figure 6).

## Conclusion

The Sol mixes offer unique features in terms of ease of handling and rapid heat-up and show exceptional service life in many applications. To date, the binder DIVASIL that has been used in combination with the Sol mixes had the

disadvantage of being irreversibly destroyed when frozen. To overcome these drawbacks DIVASIL FP, a frost protected Sol binder was developed. DIVASIL FP has a freezing point of approximately  $-5\text{ }^{\circ}\text{C}$  and most significantly is not destroyed through freezing. After thawing it can be used without restriction. It was shown in a series of tests and experiments that workability and final product properties of the Sol mixes remain unchanged. With the launch of DIVASIL FP, RHI is now in the position to supply a Sol binder that does not require thermal transport and ensures easier handling at customer site. This product provides a significant improvement in terms of ease of application and further demonstrates RHI's role as technology leader in this field.

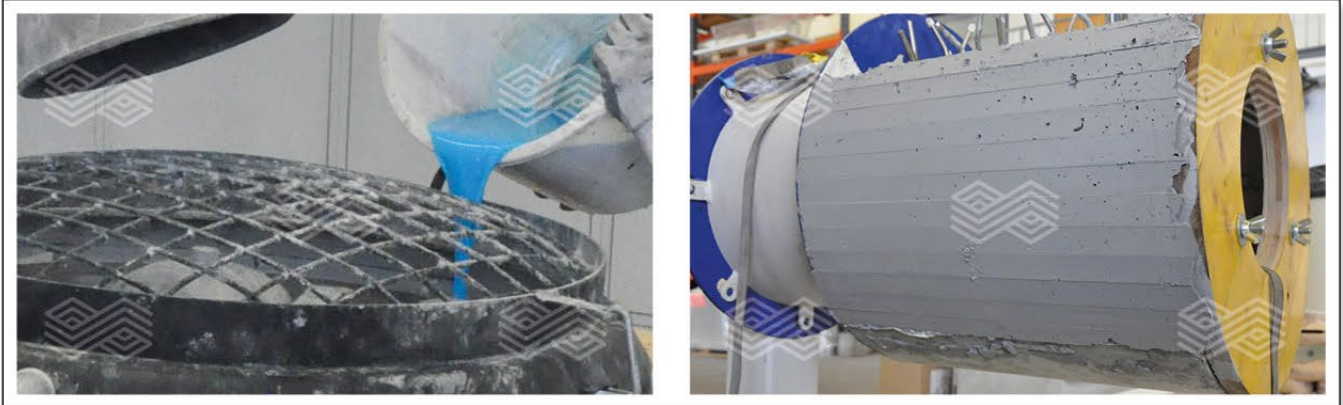


**Figure 5.** Casting of a burner lance tip with COMPAC SOL MB A100-6 and DIVASIL FP at TCC. Showing (a) initial mixing and (b) final cast burner lance tip.



**Figure 6.** DIVASIL FP and DIVASIL.

## References

- [1] Blajs, M., von der Heyde, R., Fritsch, P. and Krischanitz, R. COMPAC SOL- The New Generation of Easy, Safe and Fast Heat-Up No Cement Castables. *RHI Bulletin*. 2010, No. 1, 13–17.
- [2] von der Heyde, R., Krischanitz, R., Hall D. and Zingraf E. COMPAC SOL- The Success Story Continues With Gunning Mixes and New Product Developments. *RHI Bulletin*. 2012, No. 2, 12–16.
- [3] von der Heyde, R., Krischanitz, R. and Blajs, M. NEW Sol Bonded Product Members- Gunning Experiences and Shotcasting Applications. *RHI Bulletin*. 2013, No. 2, 13–16.
- [4] Schneider, U., Krischanitz R. and Fritsch, P. No-Cement Sol Mixes Achieve Service Life Records at Solnhofer Portland Zementwerke. *RHI Bulletin*. 2015, No. 2, 40–43.

## Authors

Gerald Reif, RHI Magnesita, Technology Center, Leoben, Austria.  
 Roland Krischanitz, RHI Magnesita, Industrial Division, Vienna, Austria.  
 Rene von der Heyde, RHI Magnesita, Industrial Division, Muelheim-Kaerlich, Germany.  
 Stephan Ullly, RHI Magnesita, Industrial Division, Leoben, Austria.

**Corresponding author:** Stephan Ullly, stephan.ully@rhimagnesita.com



Andreas Viertauer, Bernd Trummer, Leopold Kneis, Bernhard Spiess, Michael S. Pellegrino, Reinhard Ehrenguber and Gernot Hackl

# Holistic Approach for Gas Stirring Technology in a Steel Teeming Ladle

The paper describes a holistic approach and tasks for efficient stirring performance in a steel teeming ladle. For the processes in secondary metallurgy- which are mainly performed in the steel teeming ladle, the main focuses are homogenization, fine adjustment of steel and slag chemistry and temperature adjustment. A further aspect if required is steel desulphurization and removal of non-metallic inclusions (NMI). CFD (computational fluid dynamics) analyses demonstrate the advantages of installing a 2<sup>nd</sup> purging plug into a steel teeming ladle. Apart from the proper choice of the most suitable purging plug type purging performance can be strongly influenced by purging instrumentation, visualization, ladle logistics, closing, and auto coupling systems as well as standardized plug cleaning devices. All these components and processes have a major impact on availability and reproducibility for ladle stirring.

## Introduction

Bottom gas stirring is state-of-the-art in a steel teeming ladle. But nowadays high reliability, reproducibility and availability are essential for efficient gas stirring. These are the important key factors for secondary steel making [1]. The main purposes of ladle bottom gas stirring are homogenization of temperature and chemistry, high interaction with the ladle slag (e.g., for steel desulphurization) and the removal of NMI. The ideal number of plugs and their location can be efficiently described by means of CFD modelling [2]. Another important component is the gas control system [3]. Due to increasing demand for steel cleanliness soft stirring is becoming an important final step in ladle metallurgy [10, 11]. Ladle logistics and especially the waiting time for

treatment have a significant influence on the purging availability [5, 6]. The use of a plug functional device (PFD) will be described which is used to check the purging availability at the ladle maintenance stand after the end of casting [1]. An introduction of the safety optimised closing system with hinged door (SOC-H) [7] and an overview of the plug portfolio completes the subject [7, 8].

## Results and Discussion

A CFD investigation considering several plug configurations was performed to quantify the influence of a 2<sup>nd</sup> plug in a 120 t steel teeming ladle. Vector plots on vertical cross sections and the slag surface, as shown in Figure 1, give evidence of significant differences among the configurations.

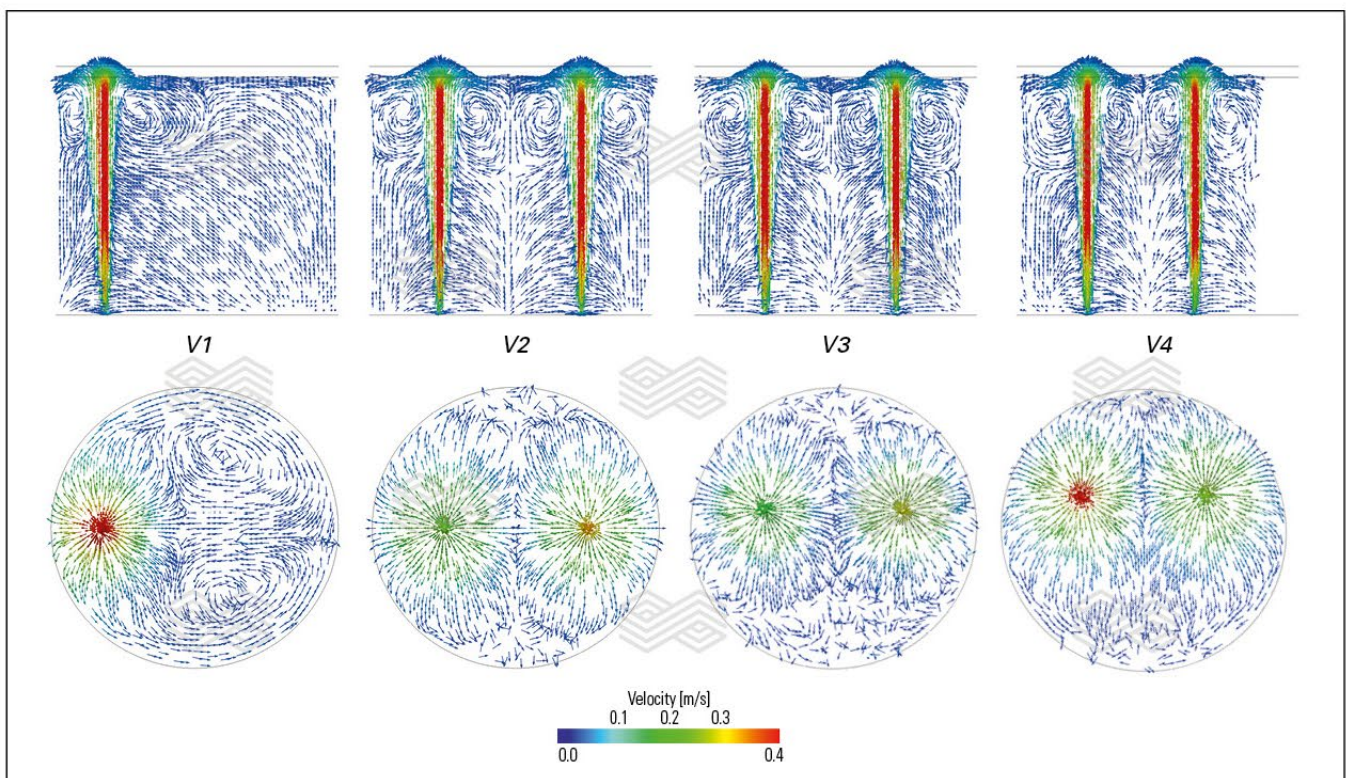


**Figure 1.** CFD simulation, cross section and top view of velocity vectors for one and two plugs with different positions at 24 Nm<sup>3</sup>/h for each plug.

The one plug configuration shows large areas of low velocities in top and cross section. In contrast the two plug configurations show a good distribution of the top and cross section flow vectors. A two plug configuration ensures that the whole slag volume is mixed which is essential for desulphurization. In comparison the one plug configuration moves the slag only partly around the open eye, resulting in large slag volumes not utilized in the desulphurization process. Some plants using a one plug configuration overcome this problem of immobilized slag by excessively using a type of slag liquefier such as fluorspar or pre-melted calcium aluminates. With this practice a sufficient desulphurization practice can be achieved. However, negative influences on the slag line wear needs to be considered.

A further investigated aspect was the duration of homogenization for alloying materials. Figure 2 describes the mixing time for all 4 different configurations. Again, the main differences were observed between one and two plug configurations. Through the use of a 2<sup>nd</sup> plug the homogenization step was shortened by approximately 40 seconds for the considered cases. The differences between various two plug configurations were negligible.

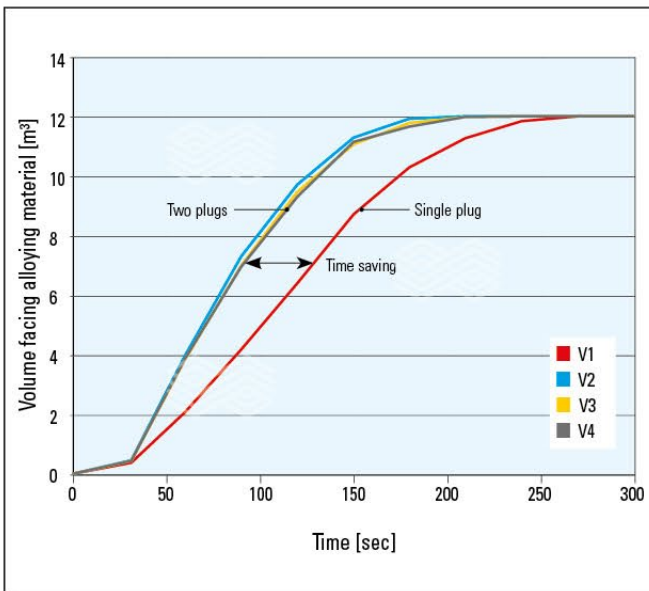


Figure 2. Comparison of homogenization for one and two plugs with different positions.

## Tapping and Secondary Metallurgical Processes

Secondary metallurgy starts with the tapping process. This is done as a standardized procedure. Depending on the steel grade the additional tasks during tapping are mostly deoxidation, pre-alloying and slag forming. The kinetic energy of the tapping stream and the duration of tapping are insufficient to liquefy and homogenize the alloying agents and slag formers (e.g., lime, dolomite, in some cases fluorspar and/or pre-melted calcium aluminates). This must be considered especially for heavy complex alloyed steel grades like X65 or API. By using bottom gas purging during tapping a strong additional kinetic force is applied. With this force the tasks described above can be fulfilled. Therefore, purging should begin immediately before tapping and should end some minutes after tapping is completed.

## Gas Control System

Modern steel making requires more than simple gas control boxes. The gas flow rates which are utilized for particular process steps are based on several parameters like steel grade and treatment steps (e.g., purging during heating, alloying, desulphurization, and finally soft stirring). Figure 3 shows a schematic view of the instrumentation of a modern gas purging control system which fulfils the requirements. The gas flow rate can reach up to 80 Nm<sup>3</sup>/h for intensive homogenization e.g., during alloying or desulphurization with the slag where as a flow rate of only approximately 1.5 Nm<sup>3</sup>/h is required for soft bubbling. This wide range has to be considered for the configuration of the flow controller.

For auto-mode procedures the actual gas flow rate is described in a recipe matrix. This purging recipe is one part of the process automation system (Level 2). The execution takes place at the basic automation (Level 1). These recipe flow rate set points are compared with the real achieved values and recorded in the data warehouse (Level 3). The data obtained regarding purging are stored and used as a basis for quality predictions for the steel cleanliness. Based on the stored data, feedback about instrumentation e.g., gas control unit (flow, back-pressure, duration), purging ceramics, piping, and the correlation with the steel cleanliness itself can be made. For steelmakers producing steel grades for special applications e.g., API grades and grades with high steel cleanliness, it is clear that purging efficiency and availability are the main sources of quality influence.

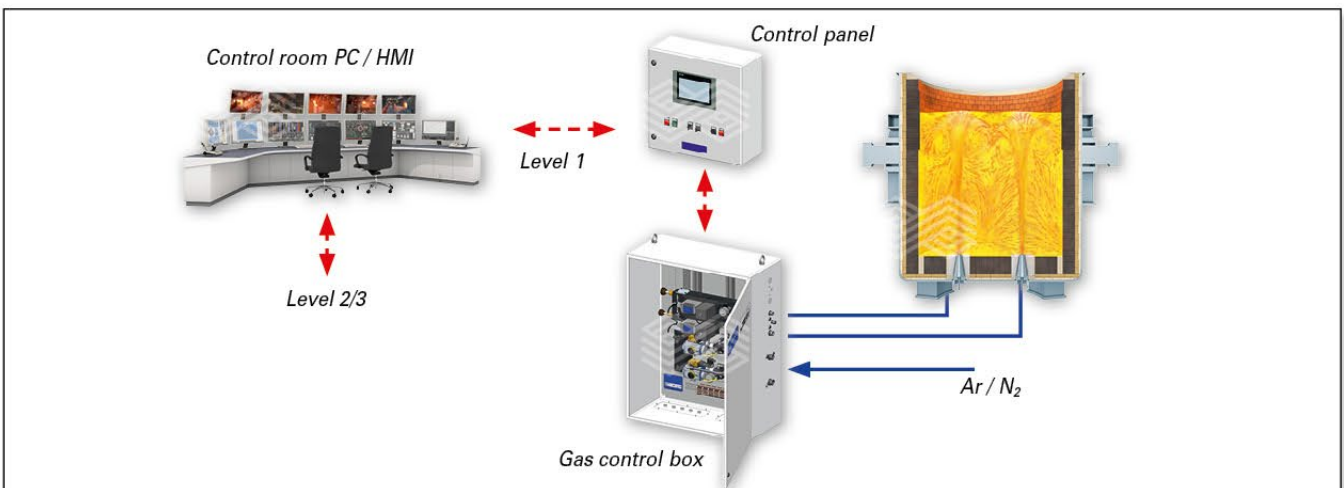


Figure 3. Layout and instrumentation of a purging system [3].



Figure 4 illustrates a regulation schema with two separately regulated lines. For both lines the optional bypass is installed but not in use. The set point for the argon flow rate is 33 Nm<sup>3</sup>/h for both gas lines. The actual flow rate for the upper line is 6.2 Nm<sup>3</sup>/h, the flow controller is 100 % open and the back pressure is 12.7 bar. This pressure value is close to the line pressure of 12.9 bar. This means that the flow set point value cannot be reached. The most likely reason for this is a partially blocked purging plug. Skull formation on the hot face of the plug (due to a cold steel temperature which is close to or below the liquidus temperature) or simply a partial steel and slag infiltration into the purging slits could lead to a blocked plug. The argon flow of the 2<sup>nd</sup> line is 32.4 Nm<sup>3</sup>/h which is close to the set point. The flow controller valve is 52 % open and the corresponding back pressure is 6.2 bar. This indicates ideal plug performance.

A typical purging trend of two purging plugs in operation is given in Figure 5. The line pressure for both plugs is approximately 13.8 bar (black line). The flow set point for each plug is 40 Nm<sup>3</sup>/h for the 1<sup>st</sup> treatment (dark blue line). Plug #1 reaches the flow set point after a short time (green line) and the back pressure comes down from 13 to 8 bar (pink line). The flow rate of plug #2 increases continuously up to 32 Nm<sup>3</sup>/h but does not reach the flow set point of 40 Nm<sup>3</sup>/h (light blue line). The back pressure is 12 bar during the entire treatment (orange line). This means that during the 1st treatment plug #1 was operating correctly and plug #2 had some partial blockages. For the 2<sup>nd</sup> treatment the flow set point is 18 Nm<sup>3</sup>/h for each plug. Both plugs reach the flow set point. The back pressure of plug #1 drops

down to 4.8 bar whereas the back pressure of plug #2 continuously decreases to 7 bar due to some persistent partial blockages. At the end of the 2<sup>nd</sup> treatment the set point of the flow rate is reduced to 9 Nm<sup>3</sup>/h and the back pressure of both plugs drop accordingly. Based upon the detailed knowledge on flow rate and back pressure further maintenance steps such as cleaning, plug exchange or leakage detection have to be decided.

**Preventing Deep Steel Infiltration Into the Purging Plug Slits:**

An automatic gas coupling connection between transfer car and ladle piping is state-of-the-art at new integrated steel mills. A revamping of existing steel mills, where the coupling is done manually by the operator is often not feasible due to economic reasons except when the existing coupling practice is regarded as a safety issue. For auto coupling, there are many different solutions available on the market [4] each requiring preventive maintenance in order to avoid malfunction. Insufficient tightness of the coupling device or leakages in the piping may generate an effect comparable to a water jet pump resulting in deep steel infiltrations into the purging plugs. In general, leakages and improper handling are frequent sources of deep infiltrations.

**Plug Functional Device (PFD)**

Usually the purging plug inspection is done during the slide gate maintenance at the ladle service area. This maintenance task is carried out after casting and removal of the remaining ladle slag. Standardized purging plug checking

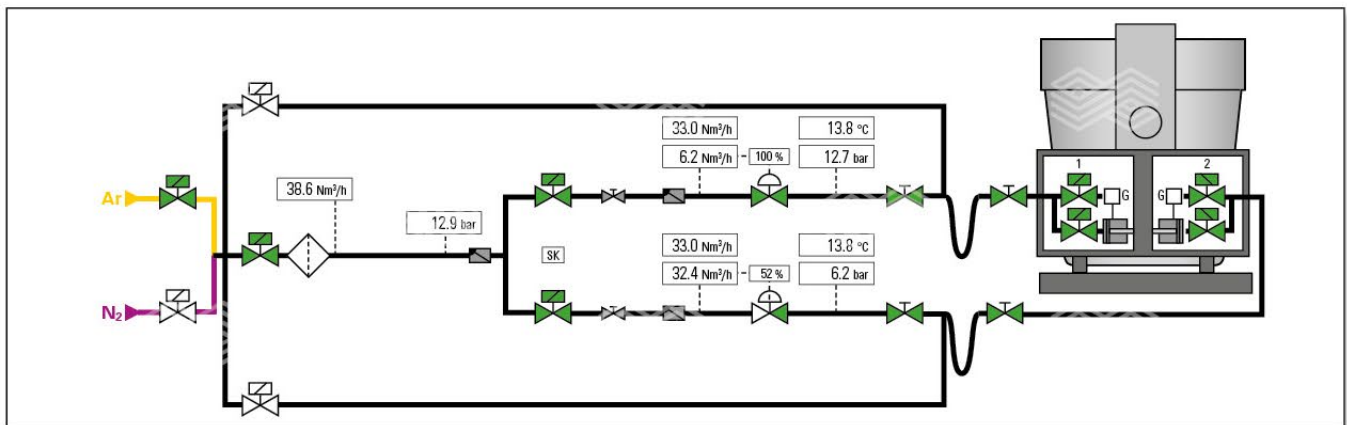


Figure 4. Purging instrumentation and visualization with bypass lines [1].

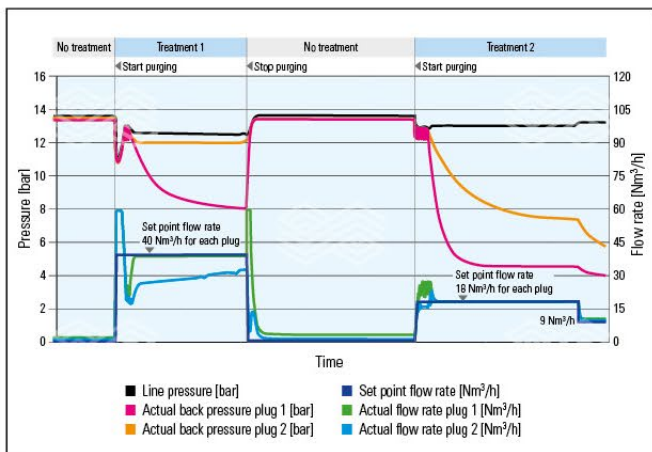


Figure 5. Purging trend of two purge plugs in operation.

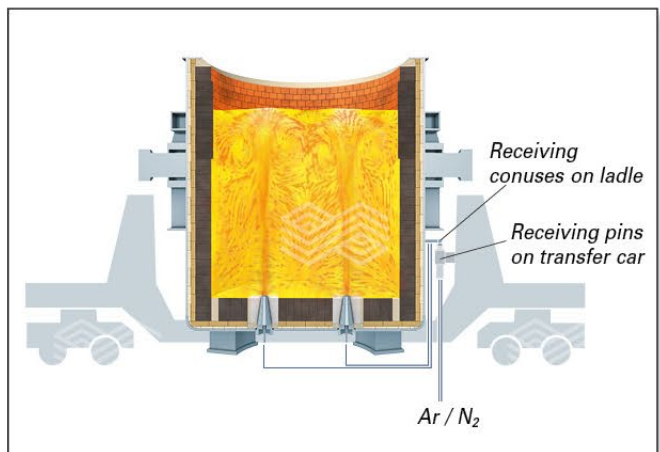


Figure 6. Ladle on transfer car connected with automatic purging coupling system.

procedures are used in some steel plants. The use of the PFD based on the decision chart (Figure 7) supports the operator to achieve a standardized cleaning procedure. Insufficient O<sub>2</sub> cleaning may result in no-stirs whereas over cleaning will even result in higher prewear of the purging ceramics. Both cases are frequent reasons for an unscheduled early exchange of the plugs.

The PFD (Figure 8) [1] has two main functions, the leakage and the plug test. The leakage test checks the tightness of the ladle piping and detects potential leaks. The plug test checks the gas flow through the plug. When the measured gas flow does not achieve a pre-set limit value the PFD sends a signal to the operator that the plug is blocked and oxygen cleaning is required. The operator receives a signal again when the gas flow reaches the specific limit to stop the plug cleaning. Flow and pressure values are stored together with information about the ladle history for further data analyses at the PFD or externally.

### Logistics

Ladle logistics have an important influence on bottom purging availability. Usually the first unit in the secondary metallurgy (e.g., LF or LT or CAS-OB) is the bottle neck preventing the tapped heat being treated as soon as possible. If the treatment unit is still utilized with the previous heat, the subsequent heat must wait for treatment. The duration of this delay can be more than 60 minutes [5].

Figure 9 demonstrates the waiting time and the corresponding decrease in steel temperature in a filled teeming ladle after tapping without stirring. The upper blue line is a theoretical line based on the specific thermal conductivity and describes a steady-state heat transfer. The lower gray line shows an unsteady heat transfer for a ladle which is preheated and filled with the first heat of a new ladle life campaign. It can be clearly seen that after a waiting time exceeding 50 minutes, the steel temperature in a filled

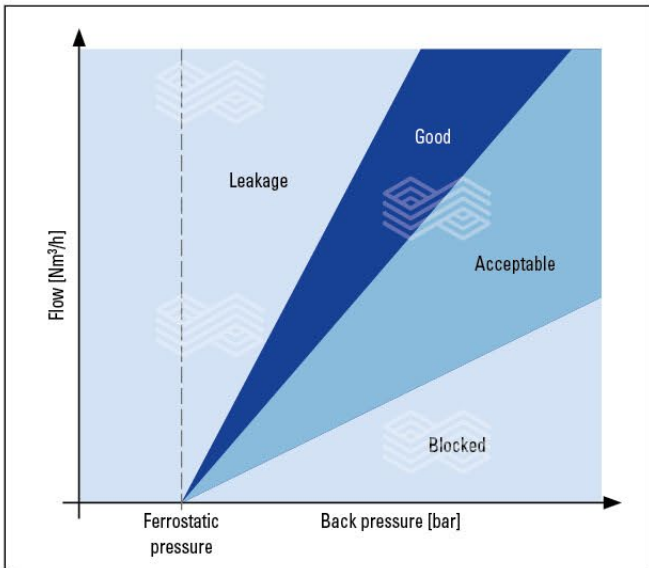


Figure 7. Decision chart, flow vs. back pressure [1].

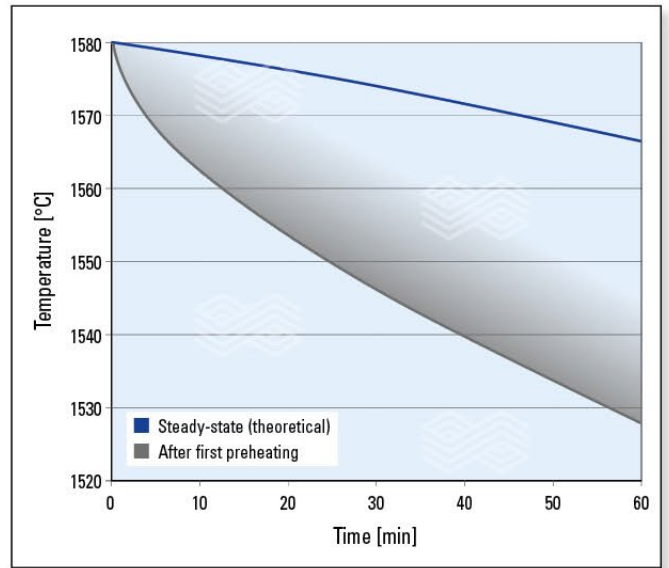


Figure 9. Steel temperature losses vs. waiting time in a ladle without purging.

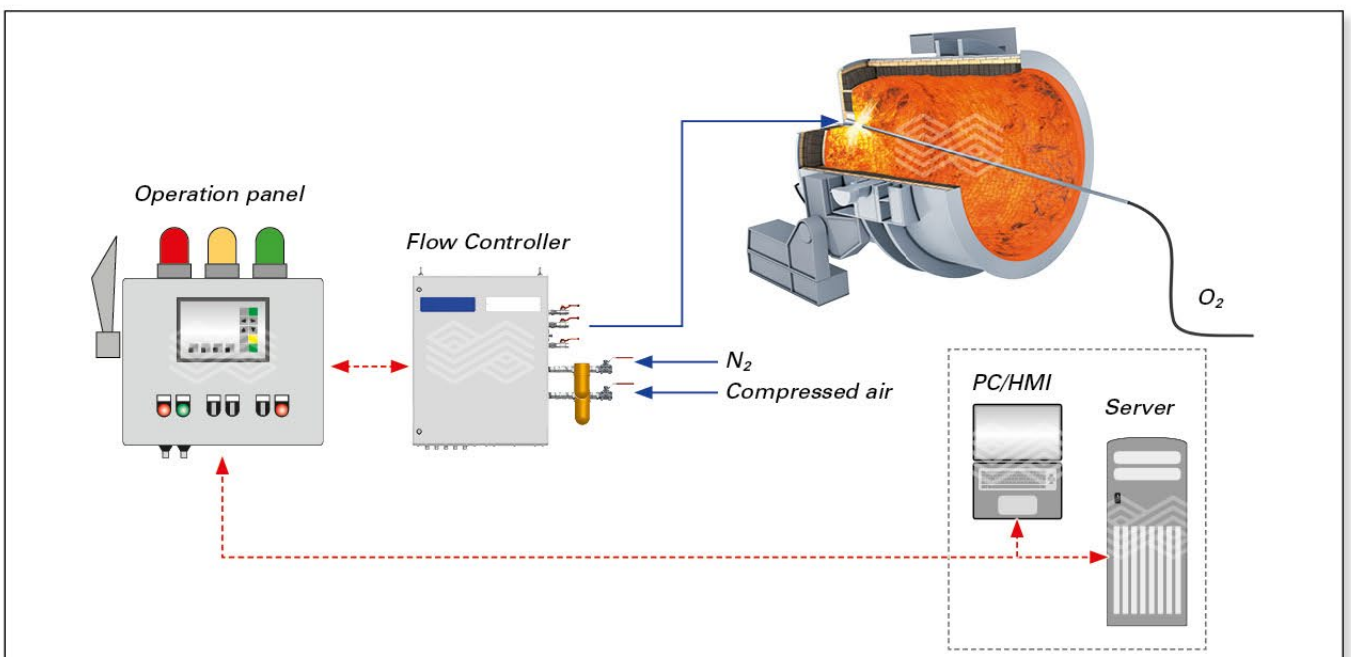


Figure 8. Plug functional device.

teeming ladle decreases to approx. 1535 °C which is in the range of the solidification temperature. Steel will freeze onto the ladle floor preventing a free gas flow through the plug into the melt. In order to start the treatment the purging plug needs to be reopened by additional intensive heating at a ladle furnace in combination with usage of an emergency stirring lance. In this case hot steel can be circulated to the bottom area where solidification took place and reopens the blocked plug surface. Additional heating without stirring is not efficient. The slag will be overheated leading to a high prewear, especially at the slag line. Under these adverse conditions, in most cases the treatment will be abandoned and the heat will be re-ladled or returned to the primary steel making unit. This leads to an unplanned sequence break and further cost intensive steps. To overcome the described issue a logistic planning model (e.g., heat tracking system) is used in some integrated steel plants [6].

The implementation of such a model helps to avoid too many ladles in hot operation and shortens the ladle waiting time.

### Safety: Prevention of Break Outs Through the Purge Plug

The plug lifetime is in most cases lower than the lifetime of the working lining. Therefore, the plugs will be changed on a regular basis during the hot ladle operation. To reduce safety risks (e.g., breakout in the purging area) a closing system with best available technology is required. The safety operating closing system with hinged door (SOC-H) provides a high level of operational safety and simple handling for the operator. It is able to stop a breakout in the event of penetration with liquid steel passing through the plug. The steel will be guided into the copper spiral or into the non return valve (NRV). Both configurations display a high thermal conductivity, which leads to solidification of the steel [7].

### Purge Plug Portfolio

A wide variety of plug designs and characteristics is available (Table I) [8, 9, 10]. This is necessary as the required gas flow rates for different applications can vary from above 80 Nm<sup>3</sup>/h to soft bubbling with approx. 1.5 Nm<sup>3</sup>/h [10, 11].

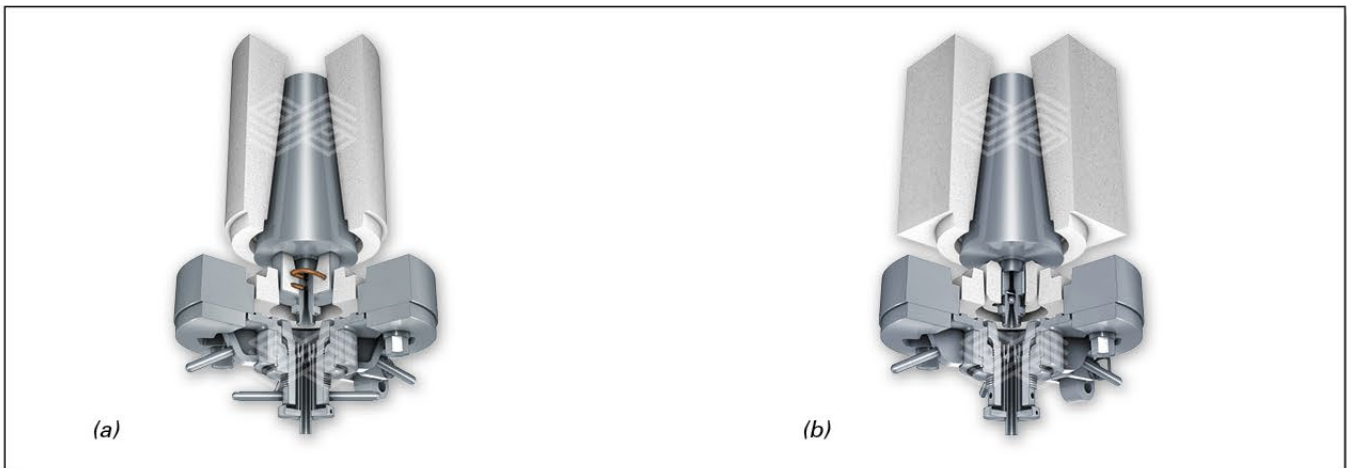


Figure 10. SOC-H with (a) exchangeable safety pad with copperspiral and (b) non return valve.

Purging plug types				
Porous plug	Single component plugs		Multi component plugs	
	Slot plug	Star plug	Segment plug	Hybrid plug
Random pore structure	Direct pore structure		Random and direct pore structure	
High porosity	Separate slots	Continuous slots	High porosity and planar parallel slots	High porosity and surrounding slots
Pressed	Cast		Pressed and cast	

Table I. Different purging plug designs.

The divergent requirements of both high and extremely low gas flow rates are a very challenging task, however a hybrid plug [12] will provide an ideal compromise to cover a wide range of flow rates.

## Conclusions

This paper provides a general overview of the main parameters for achieving top availability of gas purging in secondary metallurgy.

CFD analysis demonstrates opportunities to reduce the homogenization time in steel treatment ladles and to optimize the interaction of steel with the slag for desulphurization. Purging instrumentation is a key success factor for secondary metallurgical facilities. Automatic gas coupling equipment is a prerequisite for operational safety. However, a regular preventive maintenance is mandatory to avoid malfunction leading to deep steel infiltrations into the purging plugs. PFD is the key for standardized plug maintenance

to achieve high purging availability and minimizes the influence of the single operator during plug cleaning. The impact of steel plant logistics on purging efficiency should not be underestimated. Logistic planning models are useful tools for continuous improvement. The SOC-H as a safety closing system provides reliability and confidence in a critical area due to its high safety level. It is clear that the proper selection of the most suitable plug is also a key factor for high purging availability and performance. By determining, recording and keeping all relevant purging data available, condition monitoring of the process equipment is possible. This data may also be used for steel quality prognosis [13]. Efficient ladle purging for steel teeming ladles is achievable only if all related partners are working together for continuous improvements in purging ceramics, equipment for gas purging, maintenance practice, and influences from the steel making production. A holistic approach is needed to generate a sustainable high quality steel production [14].

## References

- [1] Viertauer, A. and Schröter, H. Steel Teeming Ladle- Applications, Wear Mechanism and Failures, *VDEh Steel Academy*, Seminar for Refractory Technology, Handout, April 24<sup>th</sup> – 27<sup>th</sup> 2016, Cologne, Germany.
- [2] Hackl, G., Köhler, S., Fellner, W., Marschall, U., Trummer, B. and Hanna, A. Characterization and improvement of steelmaking process steps influenced by refractory products using modelling and simulation tools. *AISTech.2016*, Proceedings, Pittsburgh, USA.
- [3] Ehrenguber, R. Excellence in Inert Gas Control Systems for the Steel Industry. *RHI Bulletin* 2015 No. 1, 7–15.
- [4] Cotchen, J. K. and Eggert, R. R. Automatic gas coupling systems for ladle metallurgy. *MPT International* 5/2012, 54–59.
- [5] Görnerup, M. The Forgotten Process Area- How to Manage Ladles in Metals Production for Increased Safety and Production Stability. White Paper Presented by Metsol, Homepage [www.metsol.se](http://www.metsol.se)
- [6] Görnerup, M. Lean and Mean?- How to Standardize Production in Liquid Metals Production. White Paper Presented by Metsol, Homepage [www.metsol.se](http://www.metsol.se)
- [7] Trummer, B., Kneis, L., Pellegrino, M., Klikovich, M. and Kreslado, M. SOC-H System- the new standard solution for ladle gas purging. *RHI Bulletin* 2013 No. 1, 45–50.
- [8] Hammerer, W., Raidl, G. and Barthel, H. Gas Purging Plugs for Steel Ladles. *RadexRundschau* 1992 No. 4, 217–226.
- [9] Kneis, L., Trummer, B. and Knabl, B. The Hybrid Plug – An Innovative Purging Plug for Steel Ladles. *RHI Bulletin* 2004 No. 1, 34–38.
- [10] Trummer, B., Fellner, W., Viertauer, A., Kneis, L. and Hackl, G. A Water Modeling Comparison of Hybrid Plug, Slot Plug and Porous Plug Designs. *RHI Bulletin* 2016 No. 1, 35–38.
- [11] Pellegrino, M.S., Trummer, B., Viertauer, A. and Hackl, G. Advances in Soft Bubbling Technology, *AISTech Proceedings* 2016.
- [12] Patent applications and patents pending.
- [13] Kurka, G. and Hohenbichler, G. TPQC- Through-Process Quality Control. 9<sup>th</sup> China International Steel Congress CISA 2016, May 15-18, Beijing, China.
- [14] Razza, P., Yaseen, A., Lammer, G. Rom, A. and Hanna, A. Statistical Data Analysis for Process Improvements at Emirates Steel. *AISTech 2015*, Proceedings, Cleveland, Ohio, USA.

## Authors:

Andreas Viertauer, RHI Magnesita, Steel Division, Vienna, Austria.  
 Bernd Trummer, RHI Magnesita, Steel Division, Vienna, Austria.  
 Leopold Kneis, RHI Magnesita, Steel Division, Vienna, Austria.  
 Bernhard Spiess, RHI Magnesita, Steel Division, Vienna, Austria.  
 Michael S. Pellegrino, RHI Magnesita, Steel Division, Munster, USA.  
 Reinhard Ehrenguber, Stopinc AG, Hünenberg, Switzerland.  
 Gernot Hackl, RHI Magnesita, Technology Center, Leoben, Austria.

**Corresponding author:** Andreas Viertauer, [andreas.viertauer@rhimagnesita.com](mailto:andreas.viertauer@rhimagnesita.com)



# Open Eye Formation: Influences of Plug Design and Size Investigated in a Water Modelling Comparison of Hybrid, Porous, and Slot Purging Plugs

Water modelling has shown that gas bubble formation characteristics such as the number of bubbles and bubble size differ significantly according to the purging plug design (i.e., hybrid, porous, or slot) as well as the specific flow rate. In contrast, the width of an open eye, which can form at the fluid surface as a result of gas purging, is controlled by the size of the gas injection area and the flow rate only. Regardless of the plug design, an increase in flow rate always increases the open eye whereas an increase of the size of the gas injection area always retards and shifts its formation to higher flow rates. The growth of the open eye follows a root function law depending on the flow rate. For optimum soft bubbling this has consequences regarding plug selection. The best results can be achieved with plugs having maximum sized gas injection areas generating a large number of small bubbles at a given flow rate like specially designed “clean steel” hybrid or porous plugs.

## Introduction

Soft bubbling at low flow rates with inert gases is the final process step in steel secondary metallurgy in order to achieve maximum steel cleanliness. During soft bubbling nonmetallic inclusions (NMIs) are floated up by inert gas bubbles from the steel bath into the slag layer. As an important precondition the opening of the slag layer – the so called open eye formation – has to be avoided in order to prevent slag entrainment into the melt and reactions of the melt with air. Finely distributed gas bubbles are desired. A brief introduction to this topic with further references is available in the literature [1–4].

Mathematical and experimental modelling of the processes taking place at the steel/slag interface during argon bubbling, which also consider open eye formation in the slag, have been published [5, 6]. It was shown that the opening behaviour and the opening width of the slag were influenced by both the flow rate and by the number of gas inlets that were investigated (i.e., 1 or 2 gas inlets). However, no investigation was carried out regarding the influence of the plug design and the plug size on the slag opening behaviour.

A large number of different purging plug types is available on the market and there is a comprehensive overview of






Purging plug types				
Single component plugs			Multi component plugs	
Porous plug	Slot plug	Star plug	Segment plug	Hybrid plug
				
Random pore structure	Direct pore structure		Random and direct pore structure	
High porosity	Separate slots	Continuous slots	High porosity and planar parallel slots	High porosity and surrounding slots
Pressed	Cast		Pressed and cast	

Table I. Different purging plug designs.

this topic [7]. These plugs differ significantly in design and properties and not all of these plugs are optimized for soft bubbling performance. In order to evaluate the influence of plug design and plug size on soft purging behaviour, water modelling comparisons were carried out at the Technology Center Leoben (Austria). The first results regarding the bubble number, size, and size distributions generated from a hybrid versus a porous and a slot design have been published [1]. It was demonstrated that at a given flow rate the number of bubbles released from a hybrid and a porous plug significantly exceeded those generated by a slot plug. Consequently, the predominant bubble size produced by a hybrid [8] and a porous plug was considerably smaller than from a slot plug. In addition, the bubble size distribution was extremely narrow for the hybrid and the porous plug while the slot plug showed a much broader size distribution. Based on these observations it can be concluded that during soft bubbling the hybrid and the porous plug would be beneficial for floating NMIs up into the slag layer.

This paper describes an extension of these water modelling studies, focusing on the influence of plug design (i.e., hybrid, porous, and slot), plug size and flow rate on a modelled slag layer and open eye formation (Table I). In metallurgy the open eye is required for the addition of alloying elements, which can otherwise end up in the slag instead of the steel bath. However, its formation should be avoided when soft bubbling is carried out because it can negatively influence the steel cleanliness. NMIs may be entrained from the slag layer and steel can pick-up oxygen leading to higher Al fading resulting in additional NMI formation and increased nitrogen contents.

### Theoretical Background

Gas purging into water results in the formation of a gas jet consisting of many gas bubbles ascending from the plug surface. The bubbles generate a column of lower density compared to the surrounding water. The resulting buoyancy effect lifts this column and a buoyant plume forms [9]. Surrounding water in the tank flows back downstream to the plug surface and bath circulation begins in the water model. When the ascending column reaches the surface of the water layer it forms a small hump or spout that protrudes the flat water surface, as can be seen in Figure 1 [10]. During their

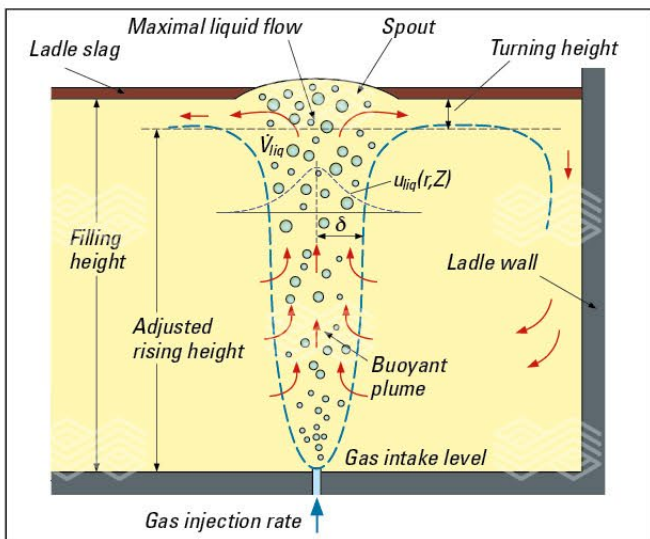


Figure 1. Schematic of the buoyancy plume flow pattern generated by gas purging in a ladle [9].

ascend the bubbles continuously expand due to the decreasing hydrostatic pressure. This increases the buoyancy effect and speeds up the circulation. The gas bubbles are released from the water, resulting in a density increase in the water. As long as the buoyant plume is intact, the degassed water flows off the raised area back into circulation.

When a layer of oil is added onto the water surface this general behaviour remains. The lifting column intrudes into the oil layer and forms a spout. Degassed water flows off the protrusion and recirculates. Depending on the thickness of the oil layer placed on the water and the viscosity of the oil, at a certain flow level the buoyant plume completely penetrates the oil layer forming an open eye. When the gas supply is switched off the remaining gas is released from the water, and the lifting effect as well as the associated bath circulation stops. The spout sinks down and the open eye closes again.

### Experimental Procedure

Investigations were carried out in two steps. In a first step the influence of the plug design was investigated by testing a hybrid plug, a porous plug, and a standard slot plug with gas injection areas of the same magnitude in the water model. Details of these plugs are given in Table II.

In a second step the influence of the plug size was investigated by testing three sizes of porous plugs with increasing gas injection areas. Details of these plugs are given in Table III.

The basin of the water model had a water volume of 1000 litres and a height of 1000 mm. Sufficient height of the basin

	Hybrid plug	Porous plug	Slot plug
Slot number	–	–	24
Slot dimensions (mm)	–	–	16 x 0.25
Open porosity (vol.%)	27	27	12
Bulk density (g/cm <sup>3</sup> )	2.7	2.6	3.1
Gas injection area (mm <sup>2</sup> )	3600	11300	7200

Table II. Geometric and physical characteristics of the hybrid, porous, and slot plugs examined in the water modelling investigation.

	Porous plug small	Porous plug medium	Porous plug large
Open porosity (vol.%)	27	27	27
Bulk density (g/cm <sup>3</sup> )	2.7	2.6	2.7
Gas injection area (mm <sup>2</sup> )	3600	11300	35000

Table III. Geometric and physical characteristics of porous plugs with increasing gas injection area examined in the water modelling investigation.

	Viscosity (kg/ms)	Density (kg/m <sup>3</sup> )
Water (20 °C)	0.001	998.2
Oil (Paraffinum liquidum, 20 °C)	0.032	846
Steel (liquid)	0.006	7020
Slag (liquid)	0.2664	3500

Table IV. Fluid properties of water, oil, steel, and slag.

was necessary in order to observe the behaviour of the gas permeating through the water.

The water was covered with a 20 mm thick layer of coloured oil to simulate a slag layer. This rather thin oil layer was selected in order to be able to investigate the formation of an open eye at very low flow rates. The thickness of the oil layer was kept constant for all plug types and flow rates.

A summary of the fluid properties of the water/oil system [5, 11] and the steel/slag system [5] are given in Table IV.

As the viscosity ratio of water to oil (0.031) is within the same order of magnitude as the viscosity ratio of steel to slag (0.023) the water/oil system is considered to be suitable to model a steel/slag surface [5]. Due to the difference in the density ratio water to oil (1.18) compared to steel to slag (2.00) influences on the flow behaviour can be expected. As a result of the buoyancy difference the open eye in the water model will form earlier and will grow faster compared to real slag covering a steel bath [13].

The plugs were fed with compressed air at ambient temperature with a mass flow controller (range 0–10 NL/min), which allowed precise adjustment and a constant gas flow in the range of 0 NL/min up to 10 NL/min [11]. The basin was illuminated from the bottom on the left and right sides. A digital camera was used to take images of the water surface at a rate of 30 frames/second to observe open eye formation.

Digital image processing was carried out the gain data on the geometrical extensions of the forming open eyes. A surface view of the water model is given in Figure 2 showing the formation of an open eye at a flow rate of 5 NL/min in the dark oil floating on top of the water.

### Water Modelling Results

Water modelling was carried out in two steps. First plugs with different designs but similar sized gas injection areas were investigated. In a second step plugs with identical design but increasing size of gas injection areas were tested.

#### Comparison of Plugs With Different Plug Designs

##### Hybrid Plug

At extremely low flow rates (e.g., 0.5 NL/min) the oil layer remained intact and purging gas bubbles penetrated the oil layer without opening it. However, at 1 NL/min first tiny openings in the dark oil layer were observed. A further increase of the flow rate resulted in a rapid opening of the oil layer and the formation of an open eye. A continuous increase of the flow rates resulted in a further growth of the

open eye size. Figure 3 shows the development of the open eye at flow rates of 0.5 NL/min, 1 NL/min, 5 NL/min, and 10 NL/min.

##### Porous Plug

The porous plug behaved in a similar manner to the hybrid plug. Again at very low flow rates the oil layer remained intact and with increasing flow rates the formation of an

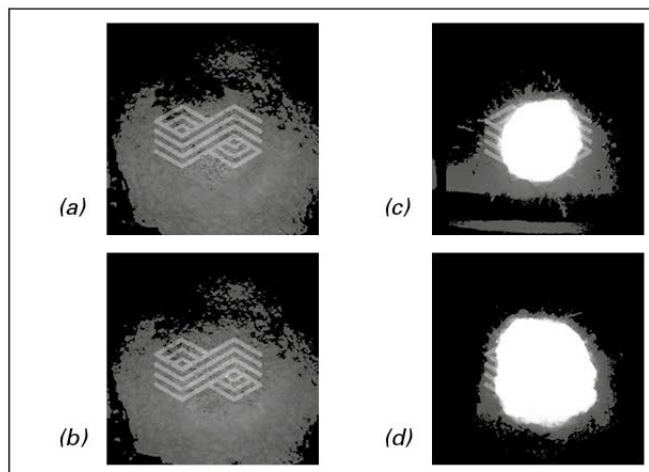


Figure 3. Open eye formation with a hybrid plug at flow rates of (a) 0.5, (b) 1, (c) 5, and (d) 10 NL/min.

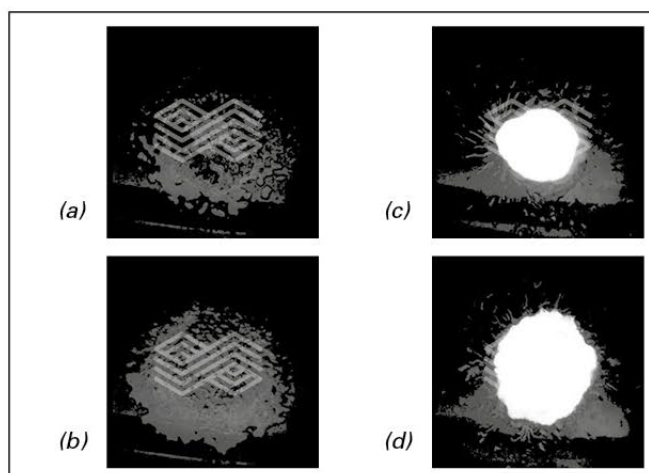


Figure 4. Open eye formation with a porous plug at flow rates of (a) 0.5, (b) 1, (c) 5, and (d) 10 NL/min.

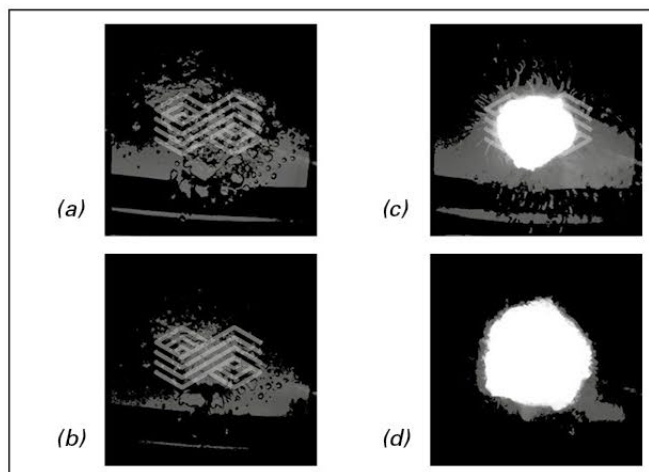


Figure 5. Open eye formation with a slot plug at flow rates of (a) 0.5, (b) 1, (c) 5, and (d) 10 NL/min.

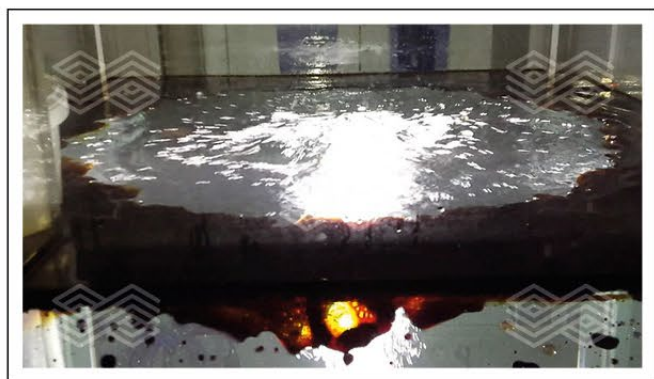


Figure 2. Open eye formation in the dark oil layer covering the water (flow rate: 5 NL/min).

open eye was observed. Increasing flow rates resulted in a continuous growth of the open eye (Figure 4).

**Slot Plug**

Again at very low flow rates the oil layer stayed intact and the purging gas penetrated the oil layer without opening it. Increasing the flow rates resulted in the opening of the oil layer and the formation of an open eye. Rising flow rates resulted in a continuous growth of the open eye (Figure 5).

**Comparison of Plugs With Increasing Gas Injection Areas**

Three porous plugs with increasing hot face diameters, i.e., increasing gas injection areas were investigated in the water model.

**Small Sized Porous Plug**

Results have been presented in Figure 3 demonstrating the effect of different plug designs. In this comparison the

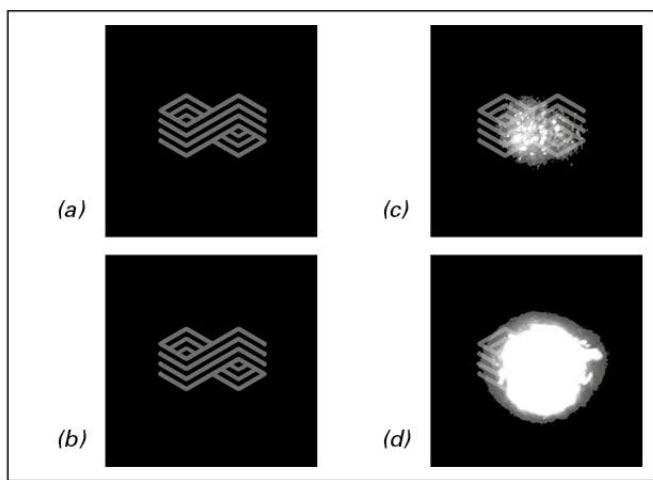


Figure 6. Open eye formation with a large porous plug at flow rates of (a) 0.5, (b) 1, (c) 5, and (d) 10 NL/min.

porous element of the hybrid plug was taken as smallest porous plug. First open eye formation was observed at flow rates as low as approximately 0.8 NL/min.

**Medium Sized Porous Plug**

Results have been presented in Figure 4 demonstrating the effect of different plug designs. The gas injection area of this plug was about 3 times larger than the small sized porous plug. Compared to the porous plug with smaller gas injection area higher flow rates were necessary to open the oil layer. At 0.5 NL/min and 1 NL/min the oil layer stayed intact, first open eye formation was observed at a flow rate of 1.9 NL/min. With increasing flow rates the open eye grew continuously (Figure 4).

**Large Sized Porous Plug**

The gas injection area of this plug was about 10 times larger than the small sized plug and about 3 times larger than the medium sized plug. Compared to smaller plugs of similar design significantly higher flow rates were required to open the oil layer covering the water model. Up to 5 NL/min the oil layer stayed completely intact. Starting with 5 NL/min the oil layer was thinning out and first small spots started to open. A further increase of the flow rates resulted in a full opening and subsequent expansion of the open eye (Figure 6).

**Comparison of Open Eye Development and Flow Rate**

In order to enable a quantitative evaluation of the water modelling results a compilation of images was prepared covering a 30 minute period where the flow rate was continuously increased from 0 to 10 NL/min. Every 0.03 seconds images of the oil layer were taken and the open eye formation was observed. The diameters of open eye and surrounding oil were determined and projected into the compilation image. By applying this diagram the size of the open eye can be determined at every given flow rate.

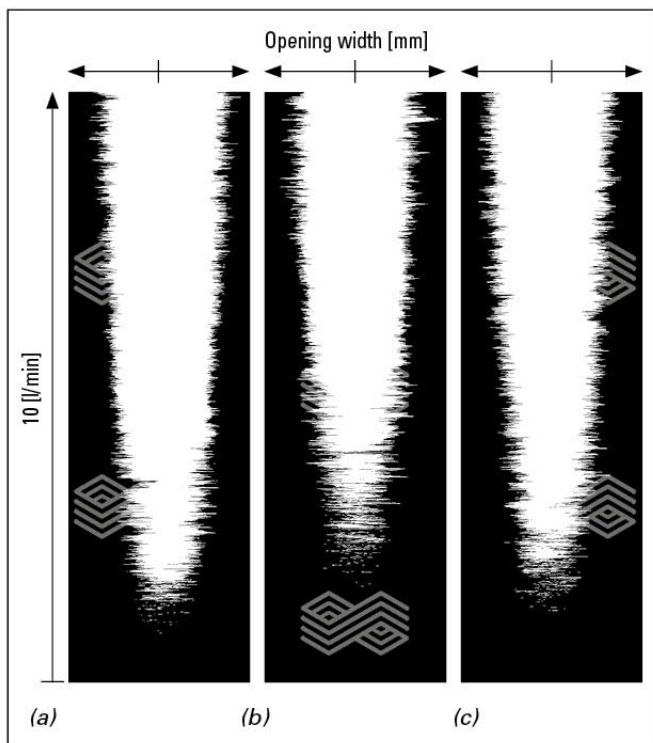


Figure 7. Development of the open eye diameter versus flow rate for the (a) hybrid plug, (b) porous plug, and (c) slot plug.

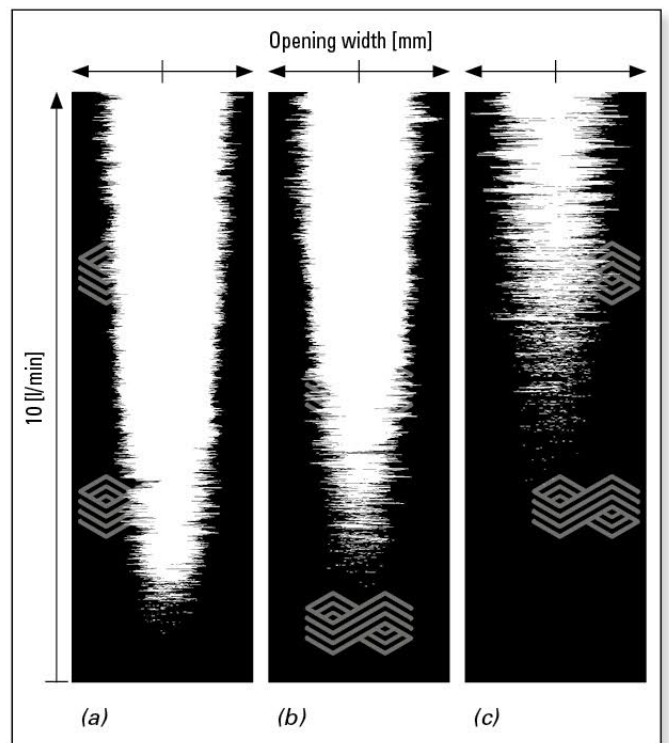


Figure 8. Development of the open eye diameter versus flow rate for the (a) small sized, (b) medium sized, and (c) large sized porous plug.



**Plugs With Different Designs but Similar Gas Injection Areas**

The development of the open eye for a hybrid, porous, and slot plug with similar sized gas injection areas is shown in Figure 7. The bottom line of each picture represented a flow rate of 0 NL/min, the top line 10 NL/min.

The compiled images for hybrid plug, porous plug, and slot plug were quite similar regarding size and opening velocity of the oil layer. A central bright zone representing the full open eye was surrounded by a shaded area representing a zone with a fluctuating oil layer and a black outermost area representing the intact oil layer.

The total width of the open eye grew with increasing flow rates. A detailed comparison of the diagrams revealed some minor differences among the three plug types: The hybrid plug (7a) and the slot plug (7c) opened the oil layer a little earlier at lower flow rates compared to the porous plug (7b).

Concluding from these observations the plug design seems to have only minor influence on the opening of the oil layer.

**Porous Plugs With Increasing Gas Injection Areas**

The development of the open eye formation for porous plugs with increasing size of gas injection areas is shown in Figure 8. Again the bottom line of each picture represented a flow rate of 0 NL/min, the top line 10 NL/min.

Contrary to the plug design a clear linear dependence of the oil layer opening upon the size of the gas injection area (plug size) and the flow rates was observed. Whereas the small sized porous plug started to open the oil layer at flow rates as low as 0.8 NL/min, the medium sized and the large sized porous plugs preserved the oil layer up to 1.9 NL/min and 5.5 NL/min, respectively. Figure 9 shows the dependence between size of gas injection area and the flow rate required for opening the oil layer.

For the given experimental configuration the following relation was found:

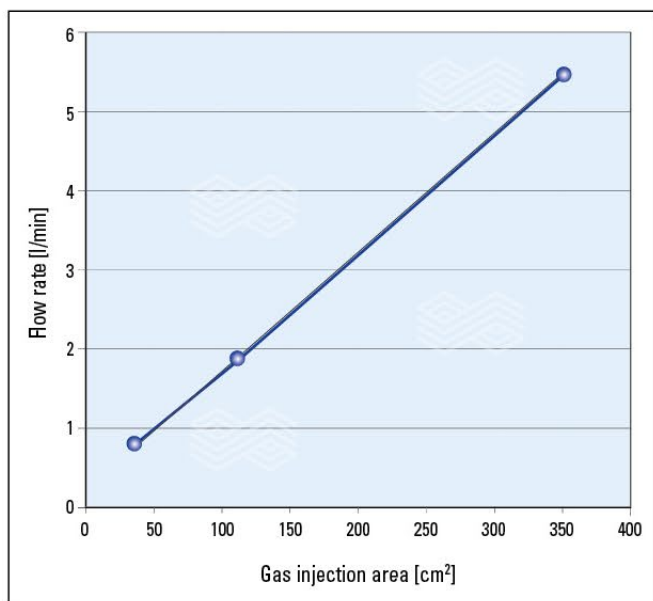


**Figure 9.** Flow rates required to open the oil layer and form an open eye versus effective gas injection area.

$$Q = 2 * 10^{-3} * A + 0.235 \tag{1}$$

where  $Q$  is the flow rate in NL/min and  $A$  is the size of the gas injection area in mm². The confidence interval R2 for this linear regression has been found to be 0.9999.

**Summary and Discussion**

As shown above the open eye formation clearly depended on the size of the gas injection area and the flow rate. There seemed to be a linear correlation between these parameters. When increasing the size of the gas injection areas higher flow rates were necessary to open the oil layer, or in other words: Plugs with larger gas injection areas allowed higher flow rates before the oil layer opened.

At a given size of the gas injection area the size of the open eye grew following a root function law depending on the flow rate. The opening width of the open eye could be described by the following equation:

$$R(Q) = 3.4 * Q^{0.2} \tag{2}$$

Where  $R$  is the radius of the open eye (cm) and  $Q$  is the flow rate (NL/min). This correlation is illustrated for hybrid, porous, and slot plugs in Figure 10.

Good accordance to [12] was found where the relationship is described by:

$$R = 0.38 * Q^{0.15} * H^{0.62} \tag{3}$$

where  $H$  is the bath height. Since the bath height was kept constant in all investigations, the equation can be simplified to:

$$R \sim k * Q^{0.15} \tag{4}$$

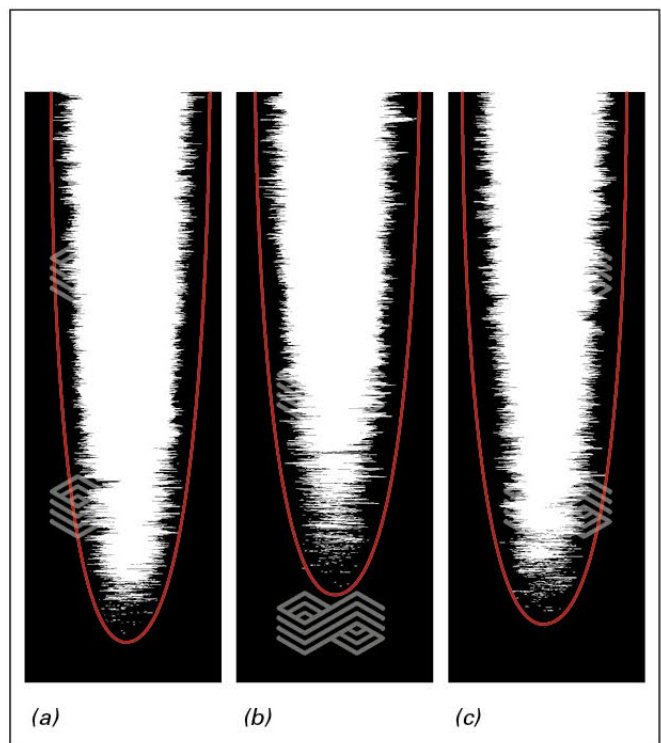


**Figure 10.** Mathematical modelling of the open eye formation for the (a) hybrid plug, (b) porous, and (c) slot plug.

The results found were in good accordance with this relationship.

Contrary to the beneficial effect of hybrid and porous plug design upon bubble size and amount of bubbles no correlation was found between plug design and open eye formation. Hybrid, porous and slot plug generated open eyes of the same size at a given flow rate, provided that the gas injection areas which were in contact with the water were of the same size.

## Conclusion

Soft bubbling is a process step carried out to remove NMIs from the melt. The interaction of the slag with the steel bath during purging has a substantial influence on the finished steel quality. An opening of the slag layer has to be avoided in this process step in order to prevent reoxidation or nitrogen pick-up of the steel from the surrounding air as well as an entrainment of slag into the steel bath. Low flow rates in combination with a high number of bubbles and large bubble surfaces are beneficial for this process [13]. Constant low flow rates will prevent the formation of such an open eye, namely opening of the slag layer.

The water model investigations have shown that the geometry of the purging plug has considerable influence on the formation of an open eye. By increasing the gas injection area the opening of the slag layer can be retarded and shifted to higher flow rates. Plugs with larger purging surface or plugs especially designed with larger gas injection areas should be considered for this purpose. The plug type itself had no direct influence on the opening of the slag layer. However, in order to achieve best NMI flotation as many small bubbles as possible are required. Considering previous water modelling results [1] and combining them with the results of this study best results are to be expected with hybrid plugs, possibly also with porous plugs with maximized gas injection areas. Optimum NMI removal is an ongoing technological challenge. Such special plugs in combination with a gas control system designed for precise, low gas flows [14, 15] provide the current optimum solution for NMI removal by soft purging. Considering ongoing developments in plug and flow control equipment as well as research in steel plant operations substantial improvements in future NMI removal may be expected. Based on the results of this study for optimum NMI removal the whole ladle bottom should be considered as gas interface.

## References

- [1] Trummer, B., Fellner, W., Viertauer, A., Kneis, L. and Hackl, G. A Water Modelling Comparison of Hybrid Plug, Slot Plug and Porous Plug Designs. RHI Bulletin. 2016, No. 1, 35-38.
- [2] Pochmarski, L. and Deutsch, H. Herstellung hochreiner Stähle für Langprodukte (Production of Ultra-Clean Steel Grades for Long Products). BHM. 1995, 140, 463-469.
- [3] Simpson, I., Moore, L., Lee, M. and Jahanshahi, S. Implementation of a Thermodynamic Model for Inclusion Engineering. Iron & Steelmaker. 2002, 29, 53-59.
- [4] Egger, M.W., Pissenberger, E., Pissenberger, A., Winkler, W. and Gantner, A. Reinheitsgraduntersuchungen zur Klärung von Clogging-Phänomenen bei höherfestem Baustahl (Investigation of Steel Cleanliness for the Identification of Clogging Phenomena in High-Strength Construction Steels). BHM. 2009, 154, 523-528.
- [5] Llanos, C.A., Garcia-Hernandez, S., Ramos-Banderas, J.A., Barreto, J.J. and Solorio-Diaz, G. Multiphase Modeling of the Fluidynamics of Bottom Argon Bubbling during Ladle Operations. ISIJ International. 2010, 50, 396-402.
- [6] Mishra, R., Nandwana, A. and Chaudhary, R. Revisiting Slag Eye in Molten Steel. Proc. AISTech 2015. 2015, 2308-2317.
- [7] Kneis, L., Trummer, B. and Knabl, B. The Hybrid Plug – An Innovative Purging Plug for Steel Ladles. RHI Bulletin. 2004, No. 1, 34-38.
- [8] Patent applications and patents pending.
- [9] Ebner, G. and Pluschkell, W. Dimensional Analysis of the Vertical Heterogenous Buoyant Plume. Steel Research. 1985, No. 56, 513-518.
- [10] Pluschkell, W. Angewandte Strömungsmechanik. Presented at Stahlinstituts VDEh Seminar Sekundärmetallurgische Prozesstechnik, Krefeld, Germany, Jan., 28-30, 2013; p. 25.
- [11] Technical Datasheet Paraffinum liquidum
- [12] Krishnapisharodiy, K. and Irons, G.A. Modeling of Slag Eye Formation over a Metal Bath Due to Gas Bubbling. Metallurgical and Materials Transactions B. 2006, 37B, 763-772.
- [13] Lindenberg, H.U. Beiträge der metallurgischen Forschung zur Qualitätsverbesserung. (Contributions of Metallurgical Research to Quality Enhancement). Stahl und Eisen. 1999, No. 5, 79-85.
- [14] Ehrenguber, R. Excellence in Inert Gas Control Systems for the Steel Industry. Proc. 8<sup>th</sup> European Continuous Casting Conference. 2014, 1080-1091.
- [15] Pellegrino, M.S., Trummer, B., Viertauer, A. and Hackl, G. Advances in Soft Bubbling Technology. Proc. AISTech 2016. 2016, 1277-1285.

*Originally presented at the 15<sup>th</sup> Biennial Worldwide Congress, UNITCR 2017. Reprinted with permission from the Latin American Association of Refractory Producers (ALAFAR).*

## Authors:

Bernd Trummer, RHI Magnesita, Steel Division, Vienna, Austria.

Andreas Viertauer, RHI Magnesita, Steel Division, Vienna, Austria.

Wolfgang Fellner, RHI Magnesita, Technology Center, Leoben, Austria.

Leopold Kneis, RHI Magnesita, Steel Division, Vienna, Austria.

Gernot Hackl, RHI Magnesita, Technology Center, Leoben, Austria.

**Corresponding author:** Bernd Trummer, bernd.trummer@rhimagnesita.com



Martin Geith, Susanne Jörg and Roland Krischanitz

# Influence of Flexibilisers on Basic Cement Rotary Kiln Brick Properties

Basic refractories for cement rotary kiln applications contain in addition to magnesia (MgO) a flexibiliser to optimize thermomechanical behaviour. In order to allow a direct comparison of cement rotary kiln bricks based on different flexibilisers, lab trial bricks with hercynite, MA spinel and pleonaste have been produced in laboratory scale and investigated regarding their most important properties considering linear elastic, crack propagation, thermomechanical, and corrosion behaviour. According to the test results hercynite is the most efficient flexibiliser leading to superior performance in application in cement rotary kilns.

## Requirements on Basic Refractory Material in Operation of Cement Rotary Kilns

For the lining of cement rotary kilns the base refractory material is selected considering temperature profile and chemical load, with respect to the chemical characteristic of the kiln feed. Figure 1 provides an overview of available refractory oxides. Due to the high refractoriness with a melting point of ~2800 °C and the low chemical reaction potential with the highly basic cement clinker, magnesia (MgO) is the most appropriate base raw material for areas of high thermal load in cement rotary kilns.

However MgO is also characterized by physical properties such as high thermal expansion which leads to a low thermal shock resistance and brittle behaviour. Under the unique operating conditions of a rotating kiln, the thermomechanical properties, especially high flexibility, are essential for the performance of refractories. In refractory product development the term flexibility is used to evaluate the ability of a material to prevent spontaneous cracking under mechanical stresses. Different additives are in use to increase the brick flexibility and reduce brittleness in cement rotary kiln bricks [1].

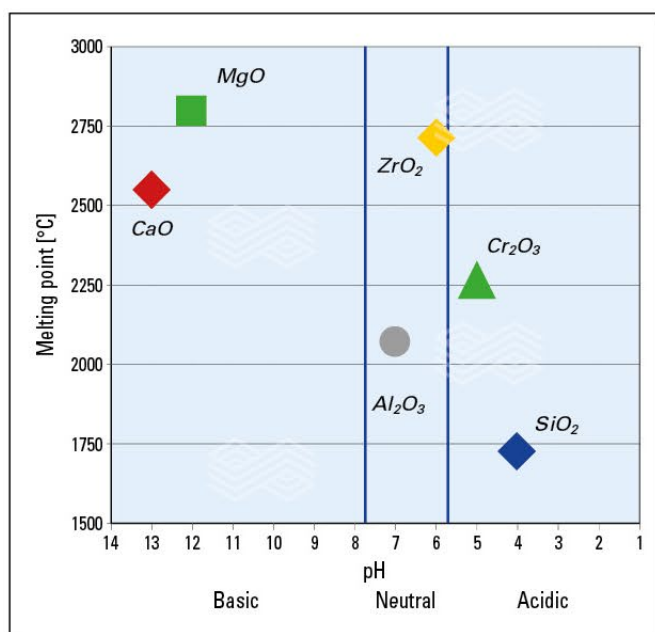


Figure 1. Overview: refractory oxides – melting temperature and chemical characterization.

## Additives Influencing the Flexibility of Cement Rotary Kiln Bricks

While magnesia seems to be an ideal material in the operation of cement rotary kilns from a refractoriness and chemical point of view, there is a requirement for additives to increase the flexibility. Historically chrome ore was the first additive that was used to increase the flexibility of cement rotary kiln bricks.

When chrome became environmentally questionable it was replaced by synthetic magnesium aluminate spinel (MA spinel, MgO·Al<sub>2</sub>O<sub>3</sub>). Chrome free magnesia spinel bricks still are an environmental friendly solution for the lining of cement rotary kilns.

In the last years alternative fused, synthetic spinels were developed for the application in refractory products for the cement industry. The most important are hercynite, a Fe-Al spinel, galaxite, a Mn-Al spinel and most recently pleonaste, a Mg-Fe-Al spinel.

The main effect resulting in flexibilisation, known as “thermal misfit”, is quite similar for all types of spinels. The principle of thermal misfit is based on a lower thermal expansion of the flexibiliser compared to the surrounding magnesia (MgO) fines matrix, which is shown in Figure 2. During cooling of the brick firing, the matrix shrinks more than the flexibiliser grains. This leads to the formation of stress centers and microcracks in the surrounding of the flexibiliser grains [2]. These stress centers and microcracks do not harm the brick structure, but ensure flexibility [1]. In addition to the thermal misfit (the difference in thermal expansion between flexibiliser and magnesia) the grain size of the flexibiliser also has an influence on the intensity of the stress centers.

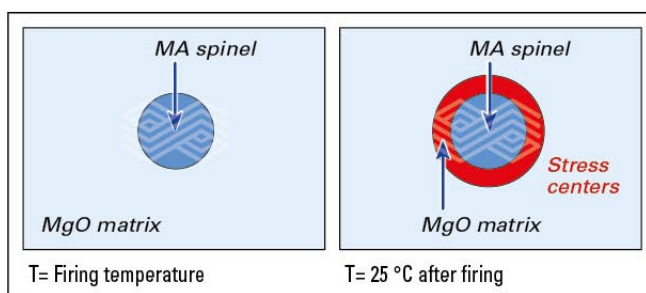


Figure 2. Flexibilisation effect of thermal misfit.

The use of a high iron containing flexibiliser such as hercynite or pleonaste has an additional effect, namely a diffusion process, shown in Figure 3, superimposes the thermal misfit. The high iron content of the flexibiliser compared to the magnesia fines matrix and the high mobility of iron at firing temperatures results in a densified diffusion zone. This zone strengthens the stress center region, leading to an additional increase of flexibility. With increasing difference in Fe content between flexibiliser grains and the MgO matrix this effect intensifies.

### Evaluation of Brick Flexibility

To evaluate the influence of different flexibilising additives on the flexibility of basic cement rotary kiln bricks, two different stages of the brick deformation process have to be distinguished: A linear elastic behaviour and a crack propagation behaviour.

#### Linear Elastic Behaviour

The first stage of strain on a material is the so called linear elastic stage. In this stage stresses of a mechanical or thermo-mechanical origin occur within the brick, but no crack formation is observed. All deformations and stresses are within the linear elastic material behaviour and totally reversible. In this stage the Young's modulus is the relevant material property. A typical material behaviour is shown in Figure 4. While a material with a high Young's modulus (e.g., a pure magnesia brick) shows a high stress level with a certain deformation, the stress level is reduced significantly with addition of a flexibilising additive.

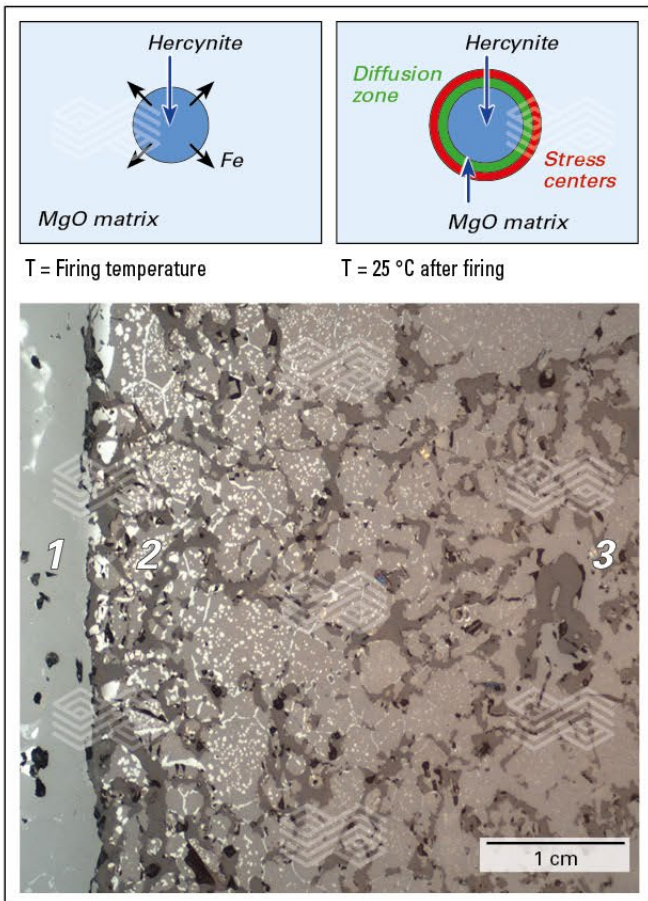


**Figure 3.** Flexibilisation effect of thermal misfit superimposed by a diffusion zone of iron oxides. The micro image shows a detail of a hercynite grain (1) with a Fe oxide rich diffusion zone (2) and the surrounding magnesia matrix (3).

The most simple test method is the indirect measurement of the Young's modulus with the ultrasonic method. This value is called dynamic Young's modulus and calculated as

$$E = \rho \cdot v^2 \text{ [GPa]} \tag{1}$$

where  $\rho$  = density [kg/m<sup>3</sup>] and  $v$  = ultrasonic speed [m/s]. The main advantage of the dynamic test method is the ability to obtain temperature dependent Young's modulus behaviour in a short time period with a single measurement cycle. This is of importance because the Young's modulus is dependent on temperature.

Figure 5 shows the typical behaviour of a magnesia brick without flexibiliser (green line) and a magnesia brick containing a flexibiliser (red line). While a pure magnesia brick shows an almost constant Young's modulus progression at a high level, with the inclusion of a flexibiliser, the Young's modulus starts at a low level, increases slightly during heating and shows strong increase in the first stage of cooling to ~1000 °C. The flexibilisation effect occurs during cooling at temperatures below 1000 °C, lowering the Young's modulus significantly. The Young's modulus level provides an indication of the ability of an additive to flexibilise a magnesia brick.

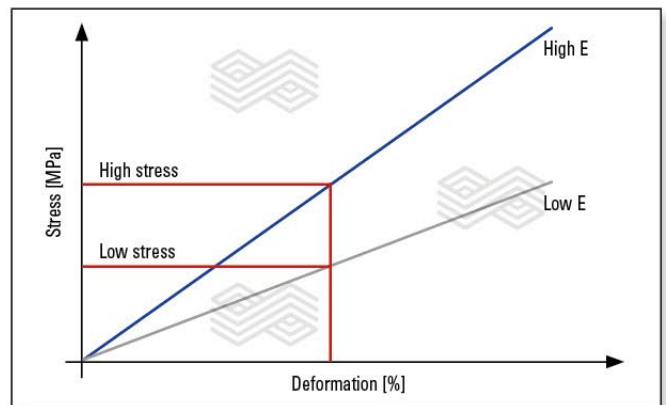


**Figure 4.** Comparison of materials with different Young's moduli.

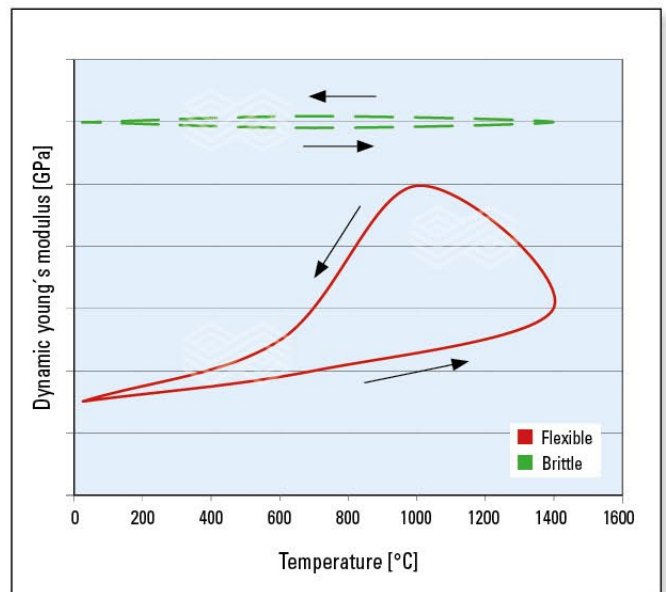


**Figure 5.** Typical Young's modulus progression of a pure magnesia brick (green) and a magnesia brick containing a flexibilising additive (red).

### Crack Propagation Behaviour

If the maximum stresses in the lining exceed the material strength, the state of linear elastic material behavior is exceeded and cracks will form. After initiation the crack propagates through the sample until destruction. The crack propagation behavior of refractory material can be measured using the wedge splitting test. Based on results of the Young's modulus determination a test temperature of 1100 °C was chosen because at this temperature level the lowest material flexibility is expected. In the wedge splitting test the specimen is split with aid of a ceramic alumina wedge. The specific crack initiation energy  $G_C$  and the specific fracture energy  $G_F$  are measured [3]. The specific crack initiation energy (in J/m<sup>2</sup>) can be explained as stored elastic energy until the crack is initiated while the specific fracture energy (in J/m<sup>2</sup>) is the total energy required for the destruction of the sample.

A high value of  $G_F$  indicates a greater requirement of energy for destruction of the material while high absolute values of  $G_C$  indicate that at the moment of crack initiation a high level of elastic energy is stored, resulting in the spontaneous destruction of the specimen. In product development it can be assumed that materials show the highest flexibility if they have a high specific fracture energy  $G_F$  combined with a high  $G_F/G_C$  ratio (slow crack propagation). Figure 6 shows a comparison of a brittle material (blue curve) with a flexible (ductile) material (magenta curve). While a brittle material shows a crack initiation at a high level resulting in the release of the stored high elastic energy  $G_C$  at crack initiation, followed by rapid crack propagation, in a flexible material, crack initiation occurs at a low stress level (low  $G_C$ ) followed by a slow crack propagation and a high specific fracture energy  $G_F$ .

### Evaluation of the Flexibilising Effect of Different Additives

To evaluate the flexibilising effect of different additives, bricks with addition of 5% of MA spinel, hercynite and pleonaste have been produced in laboratory scale. In order to

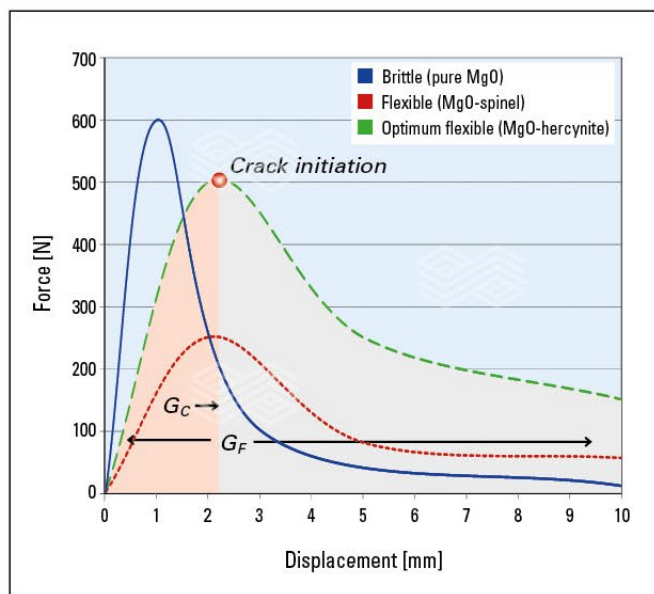


Figure 6. Wedge splitting test curve for a brittle and a flexible material.

ensure comparability the bricks are based on the same type of magnesia and flexibiliser grain size distribution and have been produced under the same firing conditions. The bricks were investigated with regards to the physical properties. Furthermore alternatives with 15% MA spinel and pleonaste were produced. The dynamic Young's modulus and the wedge splitting test behaviour were investigated to evaluate the flexibilisation behaviour relative to additive type and amount.

### Linear Elastic Behaviour

In the production of basic cement rotary kiln bricks, flexibilisation occurs during cooling from highest firing temperature through thermal misfit. This procedure can be determined by dynamic Young's modulus. Figure 7 shows that with an addition of 5% hercynite, a Young's modulus level of 26 GPa can be achieved, while an addition of 5% MA spinel or pleonaste results a Young's modulus of 51 and 37 GPa, respectively.

To obtain the required flexibilisation effect with MA spinel and pleonaste the amount had to be increased to 15%. With this addition, the Young's modulus could be decreased to 25 GPa which is a similar to the level that can be reached with 5% hercynite.

### Crack Propagation Behaviour

To evaluate the crack propagation behavior wedge splitting tests at 1100 °C were carried out, test curves and data are shown in Figure 8 and Figure 9.

A comparison of the 5% alternatives shows that regarding the consumed specific fracture energy  $G_F$ , hercynite shows the highest level, followed by pleonaste and MA spinel. With an increase of the flexibiliser amount to 15%, the  $G_F$  of the MA spinel and pleonaste alternatives can be increased, however for pleonaste  $G_F$  is still lower than for 5% hercynite. Nevertheless, even with 15% of MA spinel and pleonaste the wedge splitting test curve shows a faster decrease than that of 5% hercynite leading to a lower  $G_F/G_C$  ratio.

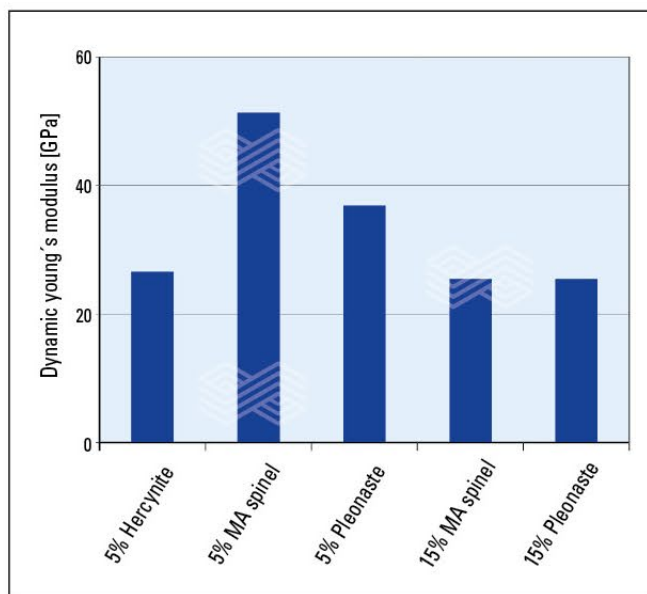


Figure 7. Linear elastic flexibilisation effect: influence of different flexibilisers and their content on the dynamic Young's modulus.

This means faster crack propagation through the brick and consequently a lower flexibility.

The crack propagation behaviour of a brick containing 5% hercynite is superior due to the most appropriate combination of specific fracture energy  $G_F$  and  $G_F/G_C$  ratio. When the flexibiliser is increased to 15%, bricks containing pleonaste have a comparable specific fracture energy  $G_F$  but a lower ratio  $G_F/G_C$ , while MA spinel containing bricks typically have a lower  $G_F$  value, but high  $G_F/G_C$  ratio.

An overall evaluation of the thermo-mechanical behaviour is shown in Figure 10. A summary of the discussed properties indicates that magnesia-hercynite bricks show a superior behaviour, followed by magnesia-pleonaste and magnesia-spinel bricks.

### Chemothermal Load

An evaluation of post mortem investigations has shown that the most common wear factor for basic bricks in cement rotary kilns is the infiltration by alkali salts. In around 58% of all post mortem investigations alkali salt infiltration was identified as the dominant wear factor, followed by clinker melt infiltration with 20%. A study of the chemical environment shows that in the basic section of cement rotary kilns predominantly acidic or neutral compounds (49% of 280 post mortem investigations from all over the world) are present, while alkali surplus is only of minor importance.

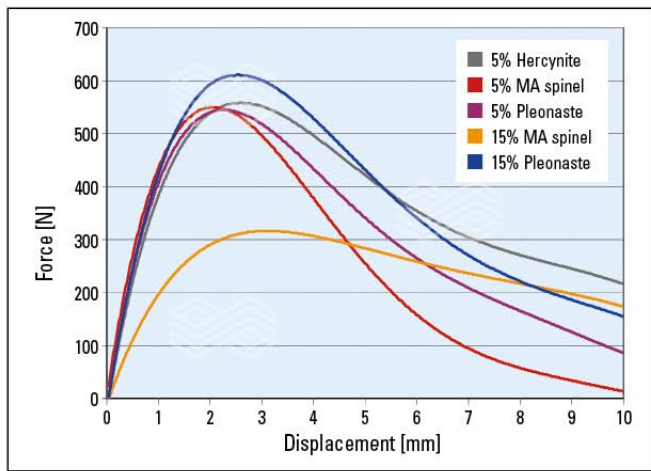


Figure 8. Wedge splitting test curves (fit data) of the test alternatives at 1100 °C.

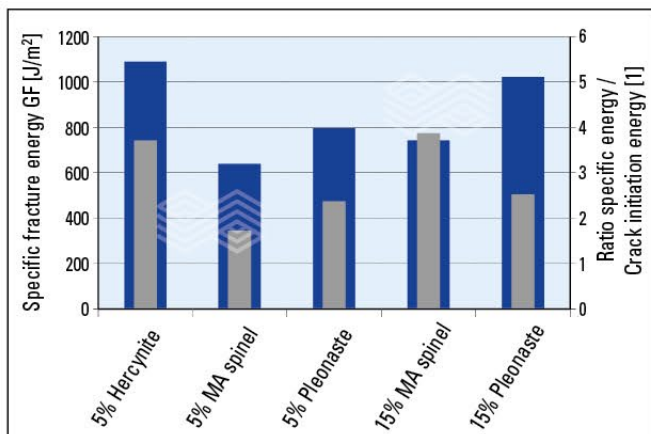


Figure 9. Crack propagation - flexibilisation effect: influence of different flexibilisers and their content on wedge splitting test values.

From a theoretical point of view a chemical reaction of the flexibiliser grains (MA spinel, hercynite, and pleonaste) with infiltrating alkalis is possible only in case of a particular strong alkali surplus in the kiln, but very rarely observed in real cement kiln operations. This reaction has been observed to a significant extent in laboratory scale crucible tests, independent of the type of flexibiliser used.

Consequently the main influence to reduce corrosion reactions is provided by the type of sintered magnesia and the strength of ceramisation. In practice the flexibiliser has only a very limited influence on the corrosion behavior in case of alkali salt attack.

### Clinker Melt Infiltration

For the production of cement clinker a certain amount of liquid phase is needed in the production process. The average amount of liquid phase is ~25% and consists mainly of Ca aluminates and Ca ferrites. If the process temperature exceeds the standard level "overheating" or in case of an unfavourable composition of the raw meal, the amount of liquid phase increases and the clinker melt easily penetrates deep into the brick.

The corrosive attack of the supplied clinker melt initially affects the flexibiliser grains, independent of their type, by dissolution of the alumina and iron components. As a result the total amount of soluble components is of major importance regarding the severity of the effects of clinker melt attack. Consequently it is advantageous to minimize the amount of flexibiliser. Table I provides an overview of the

	Hercynite	Pleonaste	MA spinel
Al <sub>2</sub> O <sub>3</sub> (%)	49.5	51.0	66.5
Fe <sub>2</sub> O <sub>3</sub> (%)	47.0	23.0	0.2
MgO (%)	1.9	24.0	33.0
CaO (%)	0.2	0.5	0.2
SiO <sub>2</sub> (%)	0.1	0.2	0.1
Amount flexibiliser (%)	5.0	15.0	15.0
Al <sub>2</sub> O <sub>3</sub> sum. (%)	2.5	7.7	10.0
Fe <sub>2</sub> O <sub>3</sub> sum. (%)	2.4	3.5	0.0
Oxides melt sum. (%)	4.8	11.1	10.0

Table I. Overview: major oxides in flexibilisers that contribute to liquid phases depending on the flexibiliser amount.

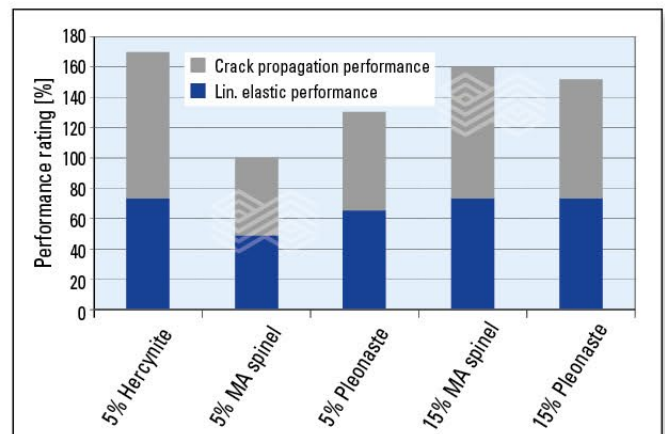


Figure 10. Thermo-mechanical behaviour of bricks containing different flexibilisers and their content, reference is a brick containing 5% MA spinel.

amount of oxides from the flexibilising additives that can form liquid phases. Therefore hercynite is superior to other flexibilisers due to the lower required amount and therefore the lower total amount of oxides contributing to liquid melt formation.

## Thermal Load

In order to obtain information about the influence of different flexibilising additives on the thermal performance of the bricks, hot modulus of rupture (HMOR) tests according to DIN EN993-7 were performed. HMOR test values at 1400 °C are shown in Table II. With a standard addition of 5% flexibiliser, bricks containing common MA spinel show the highest HMOR at 1400 °C. The HMOR of bricks with iron containing spinels, hercynite, and pleonaste are on a lower, but similar level. As it is necessary to increase the amount of MA spinel and pleonaste in order to achieve the required flexibilising properties, a decrease in HMOR was observed.

In addition to the hot modulus of rupture, the refractoriness under load according to DIN EN ISO 1893 was evaluated. Comparing the refractoriness  $T_0$  and  $T_{0.5}$  values for bricks with 5% flexibiliser, MA spinel shows the highest values. Considering that a higher amount of flexibiliser is required for MA spinel and pleonaste to achieve similar flexibility levels as with hercynite, a drop in refractoriness was also observed. This is reflected in the refractoriness values for bricks with 15% MA spinel or pleonaste.

## Conclusion

Flexibilisation of the basic brick structure is the main purpose for adding different types of spinels, wherefore particular attention has been paid to thermo-mechanical properties. Additionally other influencing parameters taking place during operation in cement rotary kilns such as chemical attack by alkali salts and clinker melt as well as thermal stresses have been considered.

The general performance level of different types of basic cement rotary kiln bricks is shown in Figure 11. The test series has shown that hercynite is the most efficient flexibiliser to increase brick flexibility, while if pleonaste or MA spinel is used a high percentage of flexibiliser is required to

achieve comparable brick flexibility. Based on numerous post mortem investigations the chemical resistance in cases of alkali salt and clinker melt attack should be considered equal. The disadvantages of corrosion effects observed in all types of flexibilisers can be reduced in case of hercynite due to the lower percentage needed to achieve required flexibility level. This lower amount has also an additional positive influence on refractoriness.

The performed investigations identified hercynite as the most suitable flexibilising additive. This is also confirmed through experiences over the past 20 years.

	5%			15%	
	Hercynite	MA spinel	Pleonaste	MA spinel	Pleonaste
RUL $T_0$ (°C)	1635	1685	1637	1538	1586
RUL $T_{0.5}$ (°C)	> 1700	> 1700	> 1700	> 1700	> 1700
HMOR 1200 (MPa)	3.1	4.3	3.2	2.7	2.4

**Table II.** Hot properties – refractoriness under load according to DIN EN ISO 1893, HMOR according  $T_0$ , DIN EN 993-7.

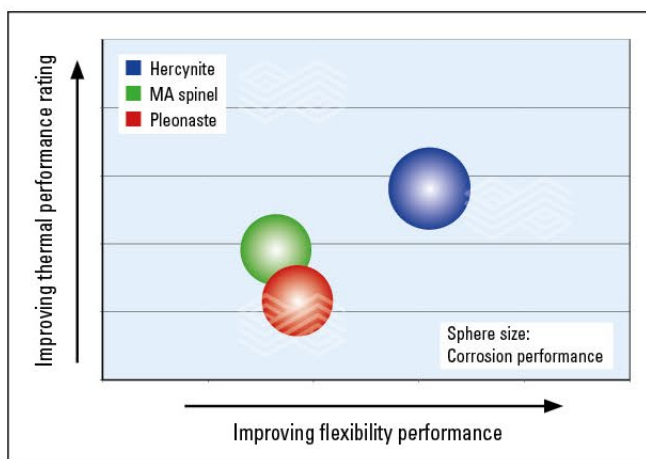


**Figure 11.** Qualitative overall performance of different flexibilisers based on their performance level, x-axis: flexibility performance, y-axis: thermal performance, sphere size: corrosion resistance performance.

## References

- [1] Harmuth, H. and Tschegg, E. A Fracture Mechanics Approach for the Development Of Refractory Materials With Reduced Brittleness, *Fatig Fract Eng Mater Struct*, (1997) Vol 20, No.11, 1585–1603.
- [2] Fasching, C., Gruber, D. and Harmuth, H. Simulation of micro-crack formation in a magnesia spinel refractory during the production process. *J. Eur. Ceram. Soc.*, (2015) Vol. 35, No. 16, 4593–4601.
- [3] Jin, S., Gruber, D. and Harmuth, H. Determination of Young's modulus, fracture energy and tensile strength of refractories by inverse estimation of a wedge splitting procedure. *Eng Fract Mech*, (2014), Vol. 116, 228–236.

Originally presented at the 15<sup>th</sup> Biennial Worldwide Congress, UNITCR 2017. Reprinted with permission from the Latin American Association of Refractory Producers (ALAFAR).

## Authors

Martin Geith, RHI Magnesita, Technology Center, Leoben, Austria.  
 Susanne Jörg, RHI Magnesita, Technology Center, Leoben, Austria.  
 Roland Krischanitz, RHI Magnesita, Industrial Division, Vienna, Austria.  
**Corresponding author:** Martin Geith, martin.geith@rhimagnesita.com





RHI MAGNESITA

Introducing RHI Magnesita

# Taking innovation to 1200 °C and beyond

Refractory products withstand extreme temperatures, enabling the production of steel, cement, glass and many more materials essential to daily life.

Discover more innovation  
under extreme conditions at  
[rhimagnesita.com](http://rhimagnesita.com)



# Characterization and Improvement of Steelmaking Process Steps Influenced by Refractory Products Using Modelling and Simulation Tools

## Introduction

In the steelmaking process, there are several crucial steps where refractory products are involved, e.g., the tap hole during transfer of steel from one vessel to another or purging plugs during the refining process. With the increasing demand on steel quality on the one hand and an optimum cost to performance ratio on the other hand, each process step and product selection must be carefully evaluated. In that context simulation methods provide an excellent framework to evaluate the impact of refractory products on the process. The results of such modelling projects provide insight into physical phenomena that take place in the steelmaking process and provide the basis for design improvements and developments. Modelling tools such as computational fluid dynamics (CFD) and physical modelling through a water model are very powerful to study transport phenomena in metal processing. These phenomena include turbulent flow of liquid metal and slag, the transport of bubbles and inclusions, multi-phase flow phenomena in addition to the effect of heat transfer. finite element analysis (FEA) is used to assess the thermo-mechanical load of refractory components or complete lining installations during the process. Problematic areas can be identified and possible solutions can be derived from the results. Considerable effort is constantly undertaken by RHI to further improve the functionality of refractory products for the steelmaking process to meet the growing demands from the steel industry. In the following sections, different examples of how the simulation methods are applied to characterize the benefit of smart refractory products will be shown and discussed.

## Tapping Systems

The taphole is an important element of both, the electric arc furnace (EAF) and the basic oxygen furnace (BOF), having a considerable influence on the vessel availability and secondary metallurgy. To reduce taphole repair and maintenance, constant developments of high-performance taphole brands with respect to the raw material composition and production technology has been undertaken for both segmented and isostatically pressed sleeves [1]. An example of an EAF and BOF taphole is shown in figure 1.

In addition to the material selection, the design of the channel is of significant importance because it plays a substantial role in the process. For example, the amount of carry over slag is of interest for producing clean steel, as it is a possible source for reoxidation due to the FeO and MnO content [2]. Turbulence created in the tap channel is also a critical parameter, due to the effect on stream stability and the associated melt to air interface, which determines the potential of oxygen pick-up during the tapping process.

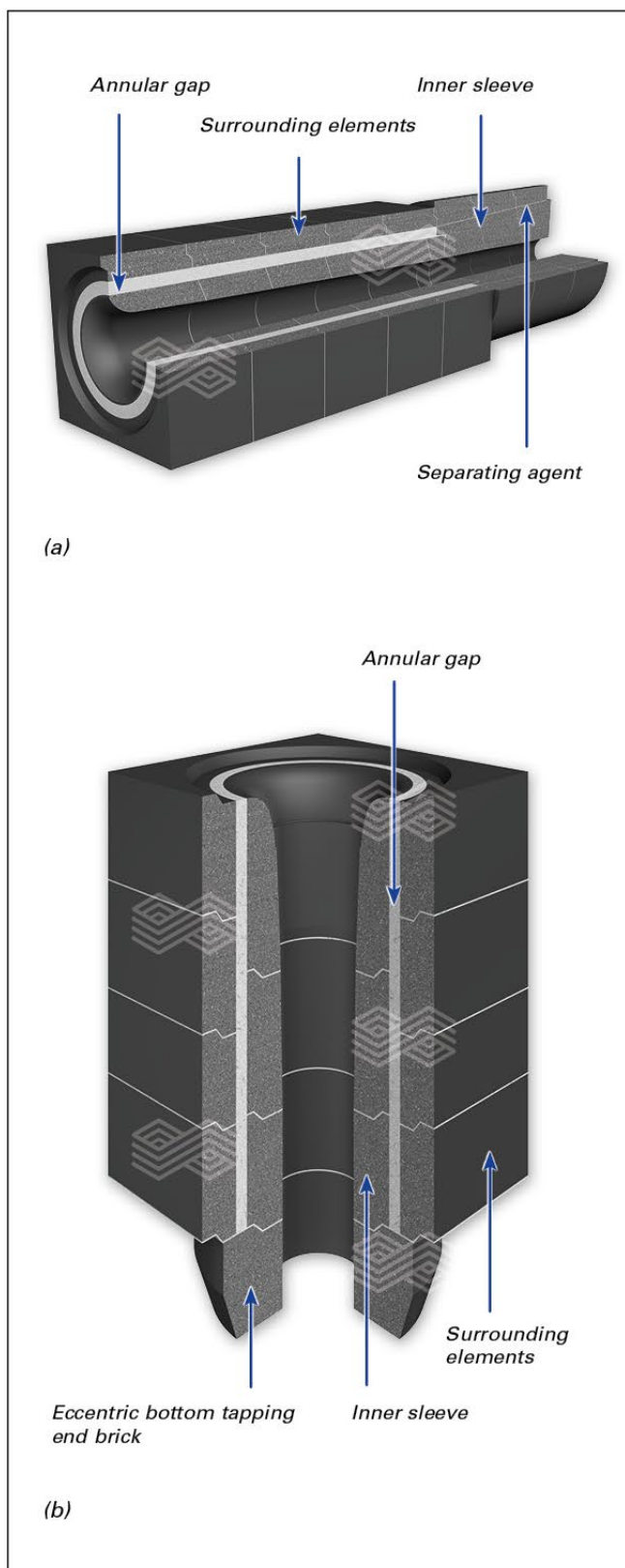
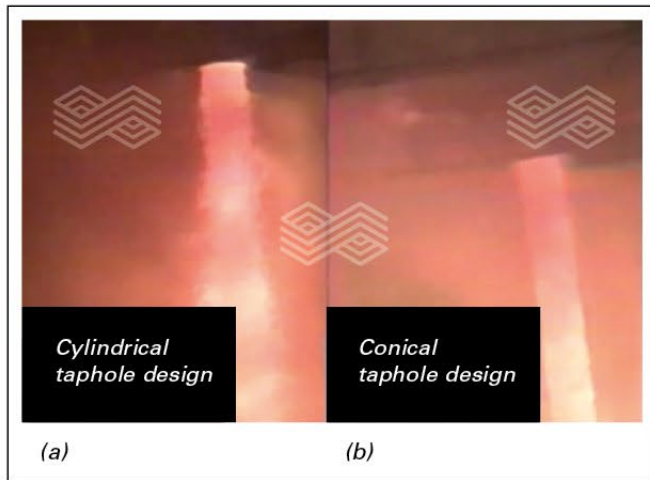


Figure 1. Showing (a) BOF tap hole and (b) EAF tap hole.

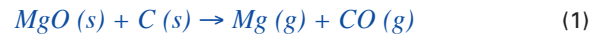
Figure 2 shows the reduced turbulence with varying taphole design.

As a further parameter, the pressure inside the tap channel has been identified. Depending on the geometry, an under-pressure may be generated.



**Figure 2.** Turbulence of the tapping stream using (a) standard cylindrical and (b) a CFD optimized taphole design [2].

It is well known, that  $MgO$  can be reduced to gaseous  $Mg$  at steelmaking temperatures when it is in direct contact with carbon, see reaction 1.



In addition to temperature, which is determined by the process, the local pressure conditions are of importance. A lower pressure will enhance the reaction and as a consequence the disintegration of the refractory material.

#### CFD Simulation

In order to characterize the performance of tapholes extensive CFD simulations were performed. Initially the flow conditions including turbulence and the pressure distribution inside the channel were compared between a conventional cylindrical geometry and the CFD optimized design, shown in Figure 3. It was shown that the flow characteristics were improved. Due to the avoidance of stream constriction in the inlet zone, the flow was less turbulent, the zone of underpressure was avoided and as a consequence a higher throughput could be achieved while maintaining the same diameter of the end brick for the optimized design. Alternatively, if the tapping time should be maintained a smaller end brick diameter can be selected.

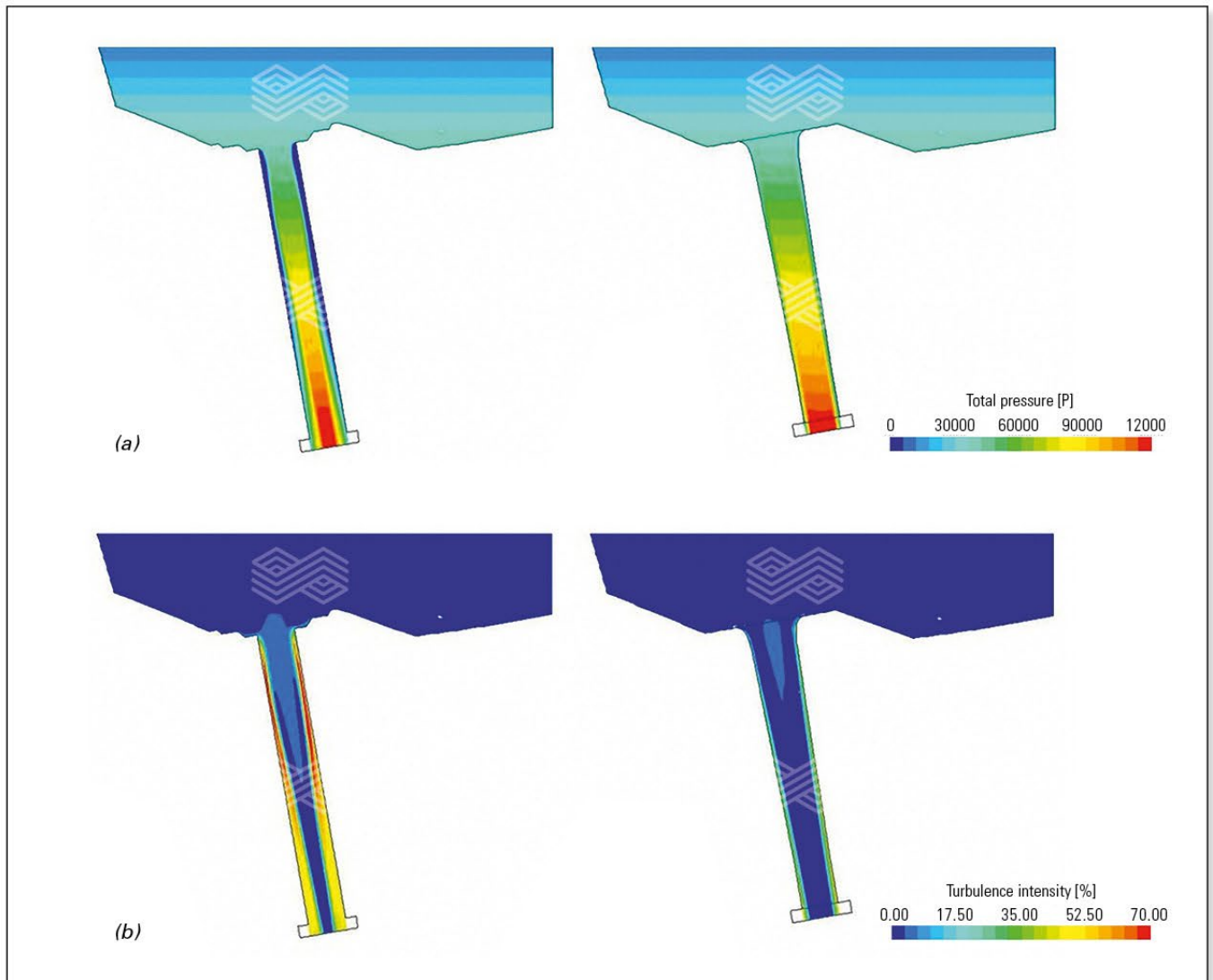


**Figure 3.** (a) Pressure distribution and (b) turbulence intensity in the tap hole for standard cylindrical (left) and CFD optimized design (right).

In addition to the measurement of pressure and throughput, the potential for slag entrainment was also characterized. For that purpose light plastic beads were placed on top of the water surface. An optical sensor was developed and used to detect particles and/or air that were entrained into the tap hole. What the potential for slag carry over by vortex formation is concerned, the CFD optimized design shows a superior behavior over the standard design. The vortex onset was initiated at a lower level, hence yield can be optimized. In Figure 4 (a) a snap shot taken during the experiments shows the area above the tap hole, when a strong vortex has been established. The measured residual bath height in the vessel are shown in Figure 4 (b).

## Design Evaluation of BOF Linings

The increasing requirements for higher productivity, the targeting of longer BOF lifetimes and the aging steel shells of the BOF vessels required an evaluation of common BOF lining designs. Even though there are differing (regional)

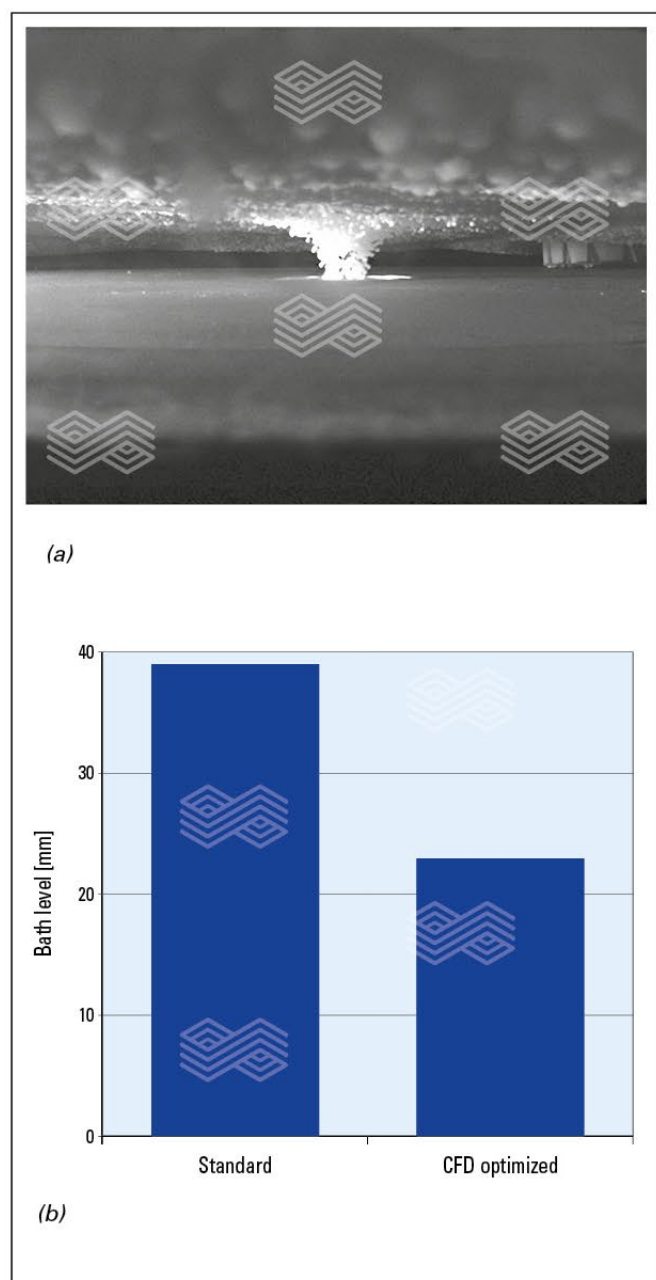


**Figure 4.** (a) Strong vortex formation directly above the tap hole and (b) measured residual level at which particle entrainment occurs.

operating conditions with different maintenance philosophies the main foundation for high availability and the achievability of lifetime targets is the quality and design of the lining. However the diversity of vessel shapes and sizes, the different production program of the shop, the varying metallurgical process parameters, and opposing trends in maintenance philosophy prevent customers and refractory suppliers from developing a perfect one-fits-all BOF lining concept. The success of a concept is influenced by several parameters. Examples of such differences in concepts are: the preheating procedure, the selection of material including the type of bonding (carbon vs. resin bonded) and the design of the lining in different areas. All these topics are thermo-mechanical aspects, hence the simulation method finite element analysis (FEA) was ideal to address these aspects.

In contrast to steel ladles the preheating of the BOF is mainly to stabilize the lining before tilting for charging (thermal expansion) and to reduce thermal shock. However, for this investigation the main point was to avoid the burn out of residual carbon of the refractory. Therefore the lining is heated to 1100–1200 °C (2000–2200 °F) on the hot face (measured using a thermocouple in the taphole). Limiting the preheating time to four hours and using an excess of coke (or natural gas) during preheating avoided the burn out of the residual carbon from the refractories. The thermo-mechanical aspect of material selection with focus on the bonding type has been discussed in [3] highlighting the influence of the bonding type on the stresses in the steel shell. Based on the higher flexibility of the carbon bonded bricks, this type of lining resulted in reduced stresses in the steel shell.

One of the areas in which the design of the lining is of interest is the transition area between the bottom and cylinder. This area has always been a major prewear area. Complex solutions for bottom joints like filler bricks and end arches, cover bricks and labyrinth joints are used. With the invention of the radial bottom, the bottom joint vanishes or in case of removable bottoms turns into a defined smooth easy to ram gap. Best preconditions for obtaining the highest lifetimes without excessive maintenance are the unique selling point of the radial solution for the fixed bottom [4].

An example of the application of the simulation method finite element analysis to thermo-mechanical questions in the refractory industry and the evaluation of this area is discussed here. Three dimensional finite element models as discussed in [3] have been created and subjected to a finite element analysis (FEA). The stresses calculated by the analyses were used to compare the different designs in a qualitative way. The three different BOF designs compared here are: a) a bottom joint filled with a ramming material, b) a cut bottom joint and c) the domed bottom without joint.

Based on requirements to obtain simulation results within reasonable timeframes, the models are based on a 1.2° section through the BOF. In combination with suitable boundary conditions this simplified modelling approach is capable to represent a full BOF lining design including horizontal and vertical joints between the bricks with an acceptable computational effort but it neglects the influence of BOF sections not covered the full circumference such as the trunnion, the taphole or the scrap impact pad.

The thermo-mechanical comparison of the three different designs is shown in Figure 5 using the largest tensile stress in the brick lining, the maximum principal stress in the bricks, to represent those areas with a high risk of the formation of cracks. Those areas are shown in red.

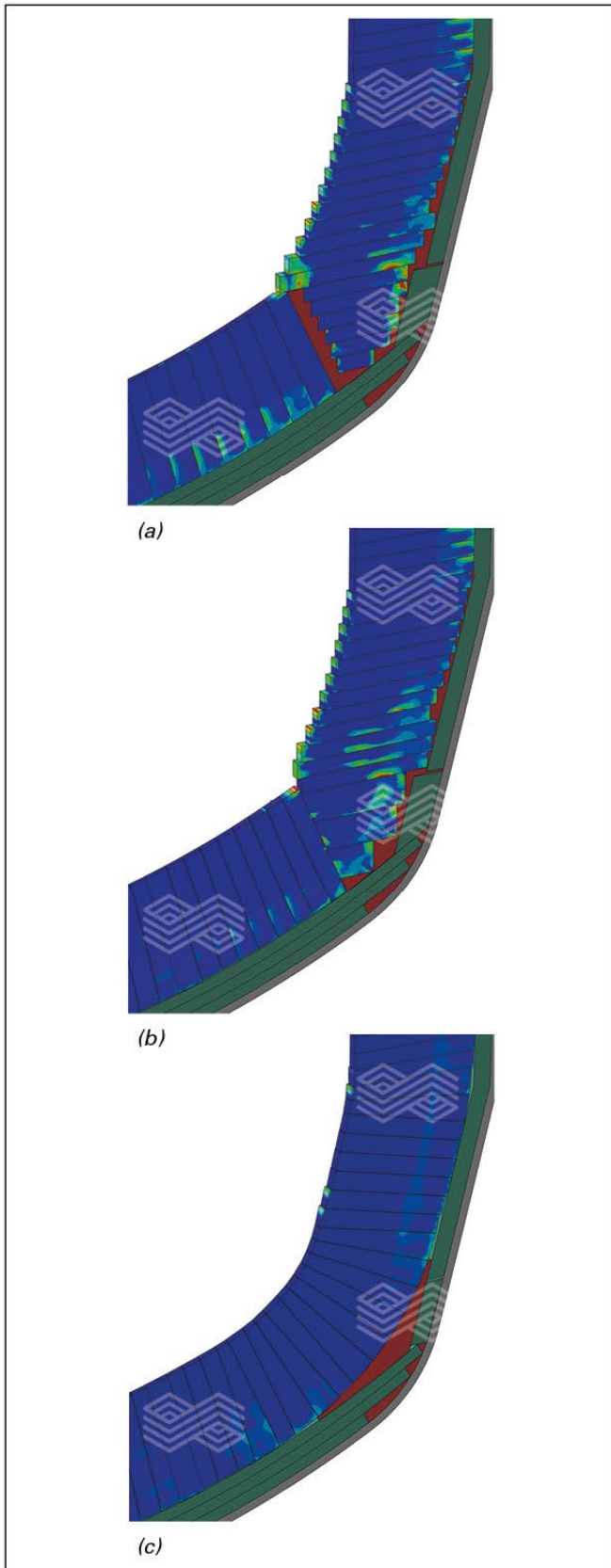


**Figure 5.** Maximum principal stresses in the three lining designs from left to right: a) BOF with bottom joint filled with ramming material, b) BOF with cut bricks in the bottom joint and c) BOF with a domed bottom without joint. Red colours indicate a high risk of cracking.

It is evident from the comparison of these stress patterns, that the lining in the BOF with the domed bottom is subjected to almost no tensile stresses while the other designs are suffering from significant tensile stresses in critical regions.

## Ladle Purging Systems

Inert gas purging in the ladle is an important step in the steelmaking process. Major tasks are the homogenization of temperature and chemical composition. Additionally, ladle stirring is essential for the removal of nonmetallic particles, as natural flotation of small diameter particles (e.g.,  $< 20 \mu\text{m}$ ) is not effective. All phenomena are linked to the fluid dynamics in the ladle. Therefore, knowledge thereof and the interaction between molten metal, slag and the purging gas are of great interest to increase the understanding of the process. Factors influencing the efficiency of the process are the number and position of purging plugs, the type of purging plug and the control unit to provide accurate flow rates and maximize the availability of the system, as described in [5].

### Type of Purging Plug

The “soft bubbling” practice is currently a common process step in secondary metallurgy for the production of several high-grade steels, especially to fulfill steel cleanliness requirements. Several types of purging plugs are available on the market and a comprehensive overview has been published [6]. However, not all plugs are optimal for soft bubbling, due to the induced flow characteristics. In a water model experiment two types, namely a hybrid and a slot plug design, Figure 6, were investigated and compared with respect to the pressure vs. flow rate characteristics and the formation and uniformity of bubbles released from the plug. In Figure 6 (a) the relationship between flow rate and back pressure is shown. Both show a linear relationship in the low flow test regime. However, the hybrid plug shows a significantly lower gradient to the curve. From these measurements it can be concluded, that the hybrid plug provides a better and more accurate adjustment of flow rates. In terms of metallurgical efficiency the specific surface of gas injected into the melt is a characteristic parameter, the higher the specific surface the higher the flotation potential. Using a video-optical method the number of bubbles directly above the plugs were counted for a defined control volume, utilizing the same flow rate regime as the previous experiments. In Figure 6 (b), the result for the two plug types is shown. At the same flow rate, the hybrid plug produces many more and as a consequence finer bubbles compared to the slot plug.

### Number and Position of Purging Plugs

The number and position of purging plugs installed in a ladle have an influence on the mixing energy and therefore describe the efficiency for thermal and composition homogenization. Depending on the size of the ladle, one or more plugs at different positions are installed. With the aid of CFD simulations, predictions regarding mixing, the presence of dead or stagnant areas, the interaction between steel and slag, e.g., open eye formation, and occurring shear stresses at the refractory wall, have been described in [7, 8, 9]. The mixing efficiency can be characterized by the obtained average velocity and turbulence in the melt or by the determination of mixing time of a tracer, where the concentration gradient is measured at different locations. Complete mixing is achieved, when each control point reaches the same value.

The result of such kind of benchmark study for a 100 to ladle assuming a flow rate of 30 l/min and 100 l/min, comparing a one and two plug set up is shown in Figure 7. Due to the generation of a higher average velocity field the mixing time can be significantly decreased. Depending on the plug positions not only mixing is affected, but also the velocity in the vicinity of the ladle lining. When the distance between the plug and the side wall is close, high velocities and corresponding shear forces occur. Evaluation of the situations can indicate possible problem areas regarding preliminary wear caused by erosion. In Figure 8 the location of maximum wall shear forces in the circumference of a ladle with asymmetric plug installation is shown.

To diminish the problem of too close plug positions, a possible countermeasure through an inclined purging plug installations was investigated. To that purpose a water model study with a hybrid plug was conducted with (a) standard installation and (b) with a 10° inclination angle. Different flow rates ranging from 10 to 100 l/min were taken into account. Video recording of the different plug types was carried out. To account for the plume shape, the time averaged bubble intensity was calculated using the entire video sequence. To characterize the differences in the plume location a multi channel picture was generated, Figure 9. Left (blue channel) represents the time averaged bubble concentration for vertical installation and right (red channel) the 10° installation. The middle picture is an

overlay of both channels. When the colour magenta is present, gas from both installation types was present. The colour remains blue or red only when the gas of one plug is recorded. Analyzing the overlay picture shows that an inclined installation does not have a positive effect on the gas distribution, the plume position and shape. The momentum energy of the incoming gas is not significant enough to entrain the melt perceptibly. In contrast, it will immediately rise and does not induce a higher stirring energy.

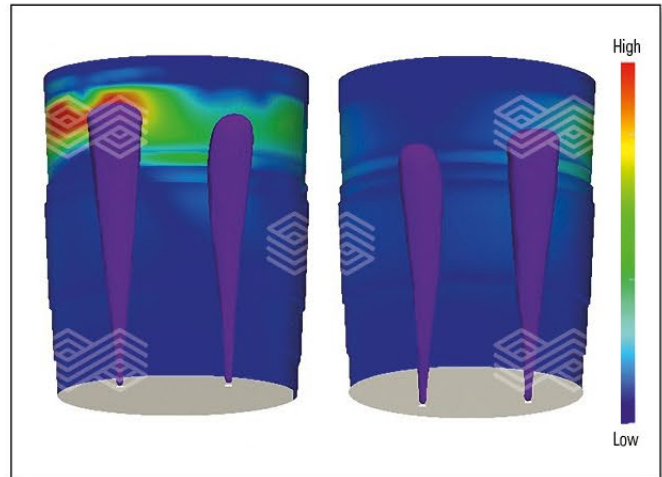


Figure 8. Contour plot of wall shear stress at the refractory lining for a ladle with two purging plugs.

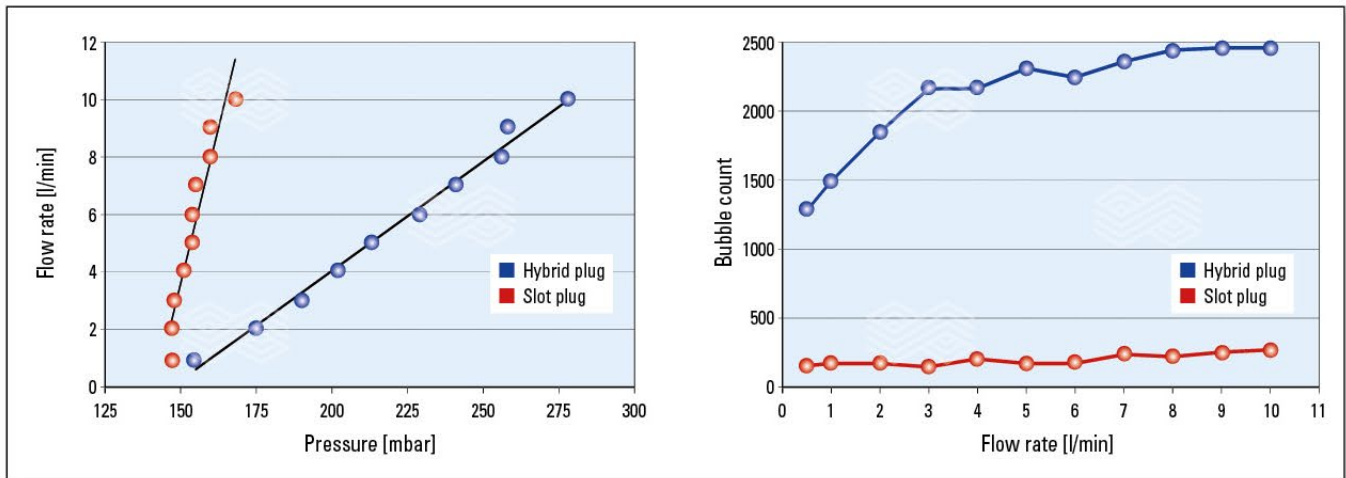


Figure 6. (a) Flow rate vs. pressure diagram and (b) amount of bubbles vs. flow rate diagram.

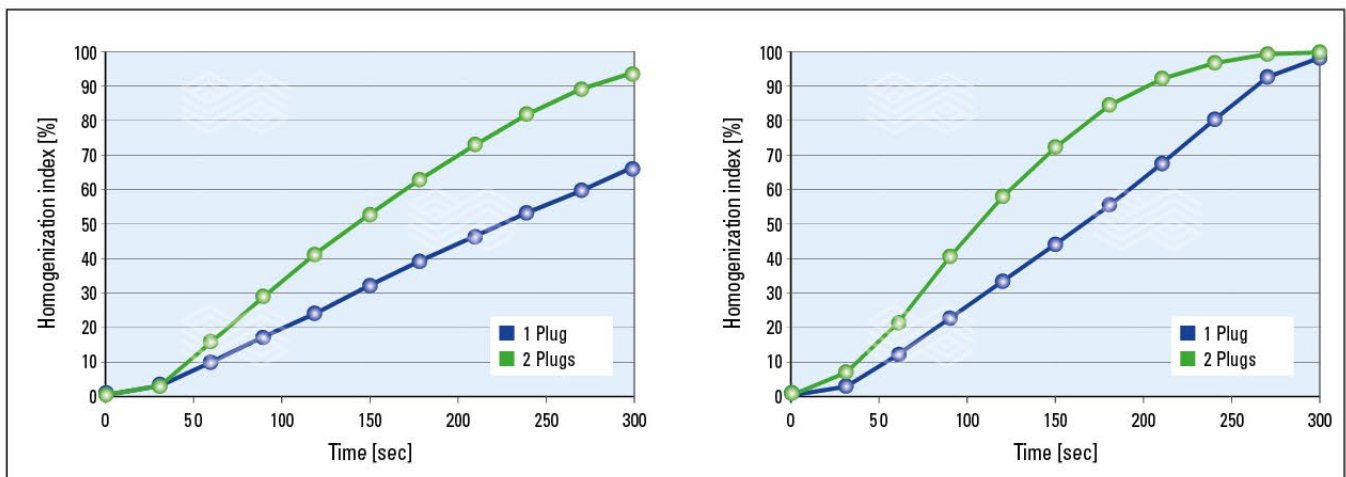
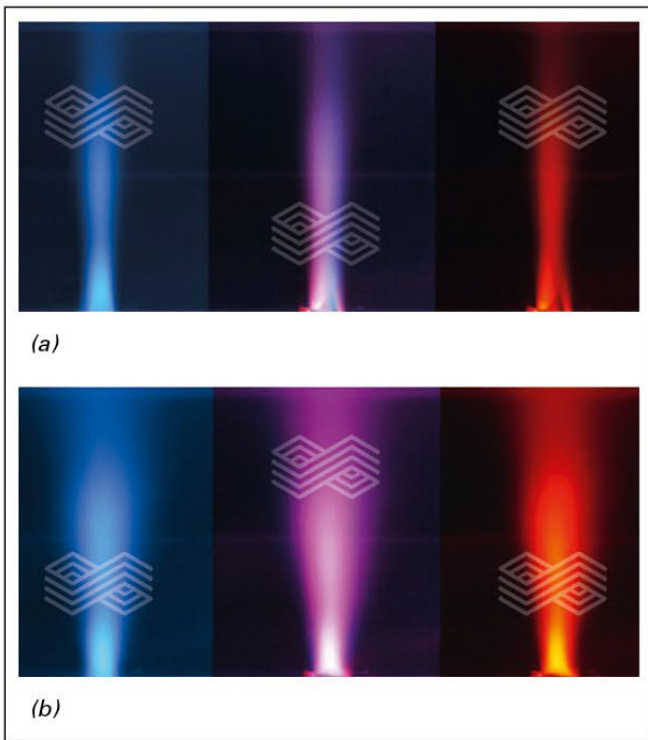


Figure 7. Calculated mixing time for (a) 30 l/min and (b) 100 l/min.



**Figure 9.** Comparison of plume shape for vertical (blue) and inclined (red) plug installation obtained with (a) 10 l/min and (b) 100 l/min.

Based on the water model result an inhomogeneous gas distribution was observed, when the purging rate is low and in both cases a narrow plume occurs because of the smaller projected surface. Due to the fact, that there was no obvious benefit and the installation would require significant effort, such a plug positioning is not recommended.

## Conclusions

Technology in the steel industry is continuously developing and topics such as clean steel are becoming ever more important as well as the increasing necessity of higher productivity at optimized costs. As a global partner for the steel industry, RHI is always striving to offer the best customer solutions based on individual conditions and requirements. One important aspect is the use of modelling and simulation tools to predict the behaviour of refractory components and its influence on the steelmaking process. Several examples, showing the potential of those tools were presented in this paper.

## References

- [1] Bellgardt, B., Köhler, S., Neubauer, B. and Pungerssek, R. Taphole Developments for Specific Steel Industry Demands, *RHI Bulletin*, No.1, 2015, pp 30—36.
- [2] Badr, K., Tomas, M., Kirschen, M. and McIlveney, G. Refractory Solutions to Improve Steel Cleanliness, *RHI Bulletin*, No. 1, 2011, pp 43—50.
- [3] Marschall, U. and Jandl, C. Design Evaluation of BOF-linings with the Aid of Thermomechanical Simulation, *Proc. AISTech*, 2011, Indianapolis.
- [4] Okita, K., Ishikawa, R., Sasaki, K. and Sennou, Y. The Efficiency of Round Corner Linings on BOF Bottom, *Journal of the Technical Association of Refractories*, Japan, 29 [2], 2009, pp 93—99.
- [5] Ehrenguber, R. Excellence in Inert Gas Control Systems for the Steel Industry, *RHI Bulletin*, No.1, 2015, pp 7—15.
- [6] Kneis, L., Trummer, B. and Knabl, B. The Hybrid Plug – An Innovative Purging Plug for Steel Ladles, *RHI Bulletin*, No. 1, 2014, pp 34—38.
- [7] Shivaram, P. K. CFD Modeling to Simulate Gas Stirring Process Using Bottom Plugs in a Steel Ladle, *Proc. AISTech*, 2015, Cleveland.
- [8] Goldschmit, M. B. and Coppola Owen, A. H. Numerical Modelling of Gas Stirred Ladles, *Ironmaking and Steelmaking*, Vol. 28, No. 4, 2001.
- [9] Llanos, C. A., Garcia-Hernandez, S., Ramos-Banderas, J. A., Barreto, J. de J. and Solorio-Diaz, G. Multiphase Modeling of the Fluid Dynamics of Bottom Argon Bubbling during Ladle Operations, *ISIJ International*, Vol. 50, No. 3, 2010, pp 396—402.

Originally presented at AISTECH 2016; 16–19 May; David L. Lawrence Convention Center, Pittsburgh, Pennsylvania, USA. Reprinted with permission from the Association for Iron and Steel Technology (AIST).

## Authors

Gernot Hackl, RHI Magnesita, Technology Center, Leoben, Austria.  
 Sarah Köhler, RHI Magnesita, Technology Center, Leoben, Austria.  
 Wolfgang Fellner, RHI Magnesita, Technology Center, Leoben, Austria.  
 Ulrich Marschall, RHI Magnesita, Technology Center, Leoben, Austria.  
 Bernd Trummer, RHI Magnesita, Steel Division, Vienna, Austria.  
 Ashraf Hanna, RHI Magnesita, Steel Division, Burlington, Canada.

**Corresponding author:** Gernot Hackl, gernot.hackl@rhimaginesita.com



Goran Vukovic, Bojan Zivanovic, Klaus Gamweger, Bernhard Handle and Bob Drew

# Continuous Online Temperature Measurement System

Reaction bath temperature is a major factor in processing liquid metals and in many applications where a balance between process duration and temperature has to be found to run a procedure efficiently. Also extremes of temperature can decrease the output of a process if too cold or even make it impossible, conversely overheating can be detrimental to both the product and furnace integrity. With the help of the new online temperature measurement system very accurate monitoring of the process is possible in contrast to the current routine practice where the temperature is measured periodically with dip thermocouples. The system works with a digital, fibre optic pyrometer, which is embedded in a refractory housing. Installation in the lining is possible below liquid level as nitrogen is blown to keep the system open and to ensure continuous sight from the optical head of the pyrometer to the molten metal through the tuyere. This permanent temperature measurement gives optimal process control with the potential of taking appropriate actions at an early stage enabling proactive process control. Therefore energy savings and even process endpoint detections can be realized.

## Introduction

During the production of metals and metallic components the single most important quantifiable parameter is temperature, making accurate measurement critical. However the current industry standard techniques of using thermocouples or pyrometers only provide intermittent data of questionable accuracy. A system that can provide accurate real time measurement on a long term basis is now required to meet the demands of modern metals production.

Today's demand for high product quality at reduced costs poses an ever increasing challenge to metal producers, therefore strict adherence to production parameters is becoming even more critical to achieving these targets. Additionally to comply with quality assurance, industrial consumers demand that the manufacturer supply documentation of production parameters upon delivery of the goods and the producer must be able to provide adequate records of the manufacturing process requiring them to continuously monitor and document the variables which are relevant to quality.

The disadvantages of the temperature measured by repeatedly and manually immersing a thermocouple into the metallurgical furnaces are:

- >> Exposing operators to a hazardous environment.
- >> High operational costs of consumable thermocouples.
- >> Temperatures are only measured sporadically and discontinuously; continuous monitoring and recording of temperatures is not possible.
- >> The accuracy of the readings will vary, depending on the precision with which the operator of the instrument takes the measurement, such as the position and depth of the immersion.

Continuous pyrometric measurement from above the bath surface may also be employed, but is known to give poor

results because of emissivity variations, interference from gases and particulate matter in the intervening atmosphere, and dust accumulation on the optics.

Due to the problems arising from the immersion thermocouples method and continuous pyrometric measurement from above the bath surface, a noncontact temperature measurement system has been developed using a pyrometer tuyere in a submerged position. The pyrometer detects the infrared radiation emitted by the molten metal and converts it into a signal which is proportional to the temperature.

## Historical Overview of the Tuyere Pyrometer

In the early 1980's the Horne Smelter first introduced the concept of temperature measurement through the tuyere [1, 2]. It was concluded that reliable bath temperature measurement was imperative to produce fluid slag and reduce the incidence of foaming. In a very short time, based predominantly on this work, over 40 units were installed in smelters worldwide.

The initial concept of the tuyere pyrometer is shown in Figure 1 [3]. It is comprised of electronic enclosures located in a safe area and connected to the tuyere mounted periscope by a shielded fibre optic cable. The required strict regimen of routine inspections and maintenance of the tuyere mounted periscope was justified considering the benefits of timely and precise converter bath temperature control. However, by the mid 1990's only a few of the Noranda tuyere pyrometers commissioned were still in operation [3].

Even during the initial installation and field trials problems in the tuyere pyrometer set functionality were detected [3]. It was required from the operators, most critically in the early stages of operation, to ensure uninterrupted operation of the pyrometer. Frequent breakdowns did result in equipment and systems being abandoned along with the challenges of implementing strict maintenance regimens.

For those operators who had success in maintaining the operation of the pyrometers, temperature calibration was problematic. Temperature calibration changes occurred with the reaction involved as well as with the oxygen enrichment of the tuyere gas. The periscope being hit by a punch bar when in the sighting position or in other words extended inside the tuyere. This was an expensive repair as the periscope, and in most cases, also the fibre optic cable, required replacing. There was a combination of causes that often led to the periscope being stuck inside the tuyere, this has been described in detail in a prior study [3]. Either the actuators facilitating periscope's up and down movement failed due to temperature changes or particles/dust adhered to the oily surface of the periscope pipe both leading to restriction of periscope movement. If the periscope was in the sighting position, a failsafe feature was installed that would disable the puncher's punching cylinder when it approached the pyrometer tuyere. This was based on limit switches, and if the switches failed or were disabled, the failsafe system was inoperable. A red/green light station in clear view of the operator was also used to indicate if it was safe to punch. These safety devices only worked if they were operational and not ignored by operators.

Since almost all tuyere pyrometer failures were due to mechanical failures associated with the periscope, a new design was considered. This resulted in the development of a dedicated pyrometer tuyere, the Smart Cylinder tuyere pyrometer [3, 4]. This involved the integration of the periscope into the "smart" cylinder (Figure 2b). In the new design, the dual small diameter actuators cylinders (Figure 2a) were replaced with one larger diameter cylinder which would not be affected by the high temperature, and due to the greater cylinder surface area when compared to the two small actuators, more force was available for periscope movement. The main component of the new cylinder was the piston which also serves as the periscope. As cylinder forces are balanced around the axis of the piston/periscope they are directly and more efficiently applied to the movement of the periscope, eliminating the possibility of jamming due to only one actuator being operational as in the original design. Incorporation of the periscope inside cylinder provides additional protection from temperature variations. A new floating gland assembly was installed to prevent blowback particles from wedging between the periscope and bushing. This floating gland is split to facilitate easy removal of the periscope without disassembling the cylinder from the tuyere.

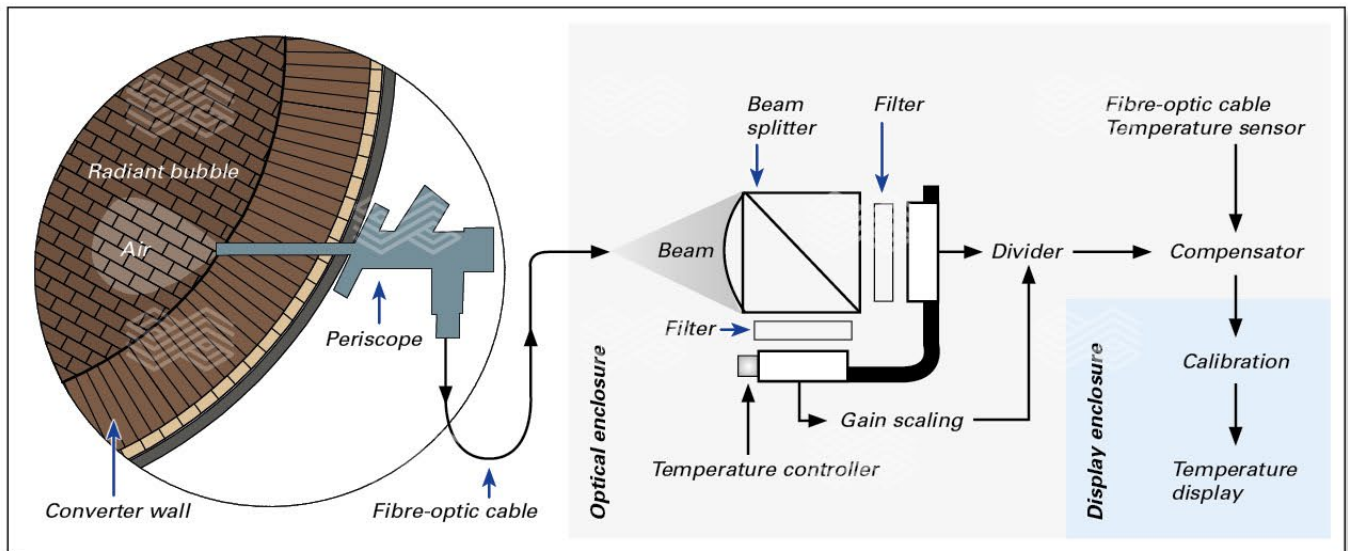


Figure 1. Original schematic of the tuyere pyrometer. [3]

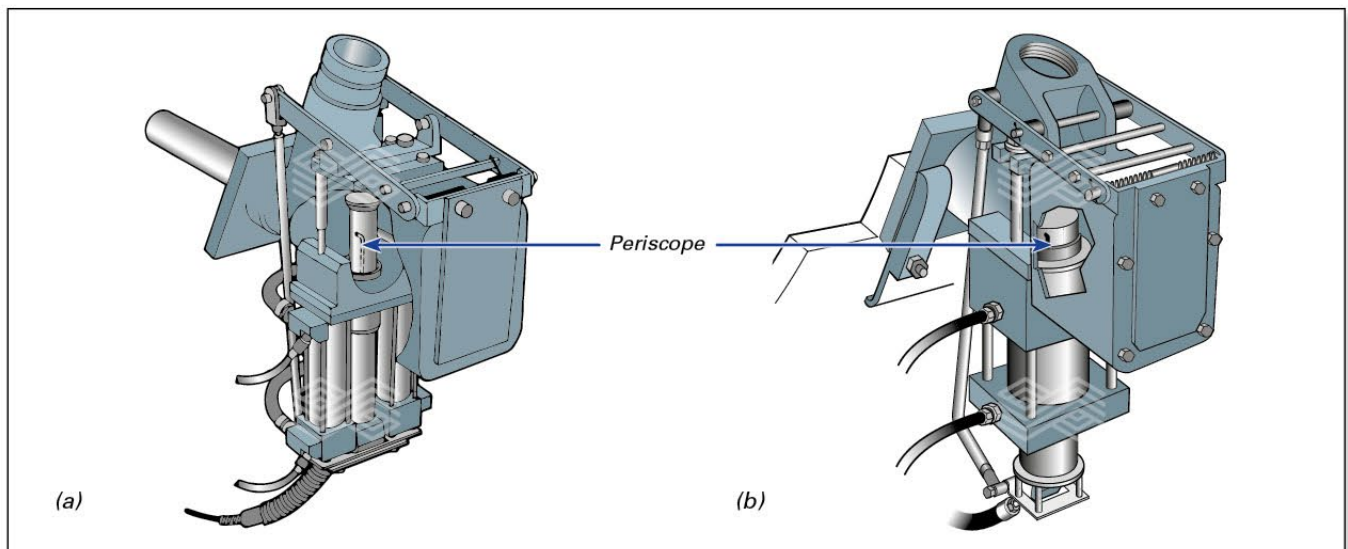


Figure 2. (a) Original periscope with dual outboard cylinders. (b) New generation with periscope integrated into the smart cylinder [3].



The latest reference list from the company Heath & Sherwood (1964) Ltd. [5] indicates that currently there are approximately 20 smelters using tuyere pyrometers. Improved temperature controls along the tuyere line allow them to approach extended campaigns on continuous converters. It is a high maintenance item and often abandoned, however it is considered critical to the operation of continuous vessels. This is why typical installations include two pyrometers, one in operation and one on standby to ensure constant availability of temperature control.

### A New Design of the Pyrometer Tuyere

The previously presented concepts mostly considered pyrometer installation direct at the process gas tuyere of a converter which is normally used for feeding air (or reactants) into the bath of the furnace. The typical converting operation involves lateral purging of air/oxygen enriched air into molten matte through a bank of tuyeres. This blowing operation occurs at low air pressure from the blowers, and the induced bubbling regime is considered inefficient from both a process and an energy utilization perspective [6]. Inherent drawbacks include recurrent tuyere blockage and inevitable tuyere punching to clear airways. To overcome these difficulties significant work has been carried out on the development and implementation of the sonic injection tuyere in the metallurgical industry [7].

The presented concept of the pyrometer tuyere shows in general some disadvantages. Often pyrometer tuyere blockage leads to a lack of temperature measurements and requires punching, establishing a possibility of mechanical damage to the pyrometer tuyere. Pyrometer installation on the process tuyere enables measurements when the tuyeres line is below the bath level, however there are no temperature measurements of the process in the furnace when the tuyeres line is above the bath level.

A new integrated, infrared, digital, fibre optic pyrometer, located at the rear side of the injection pyrometer tuyere was developed. It allows continuous noncontact temperature measurements of the melt in a submerged position (Figure 3). The diameter of the tuyere pipe is 10 mm with nitrogen flow ensuring the pyrometer tuyere is always free of blockage without punching action as well as keeping the

optical head and the integrated lens, free of dust. The pyrometer tuyere is independent of the process tuyere and can be installed in the side walls or the end walls of the furnace, ensuring it is always below metal bath level for the duration of the process. The developed system can also provide temperature feedback when the process tuyeres are above bath level and additionally can be used in metallurgical furnaces that do not normally employ submerged process tuyeres (TSL, Flash, induction and secondary vessels). The optical head is permanently installed during the operating state and no supporting devices such as actuators are required ensuring the whole arrangement is very robust even in the most inhospitable environment.

### Non Consumable Optic Components of the System

The integrated pyrometer is a highly accurate digital infrared measuring instrument with fibre optic for non contact temperature measurements of the melt in a submerged position. Non consumable components of the pyrometer tuyere are shown in the Figure 4. The instrument is equipped with an exchangeable optical head and a fibre. The fibre cable and optical head are unaffected by electromagnetic interfaces (e.g., induction) and can be used in high ambient temperatures up to 250 °C.

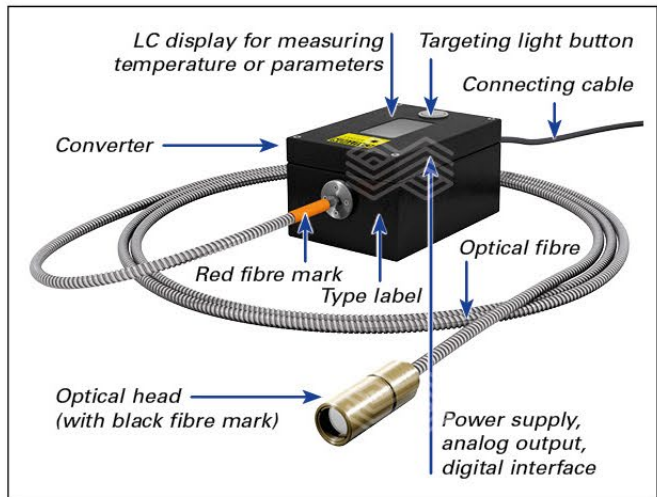


Figure 4. Nonconsumable optic components of the system.

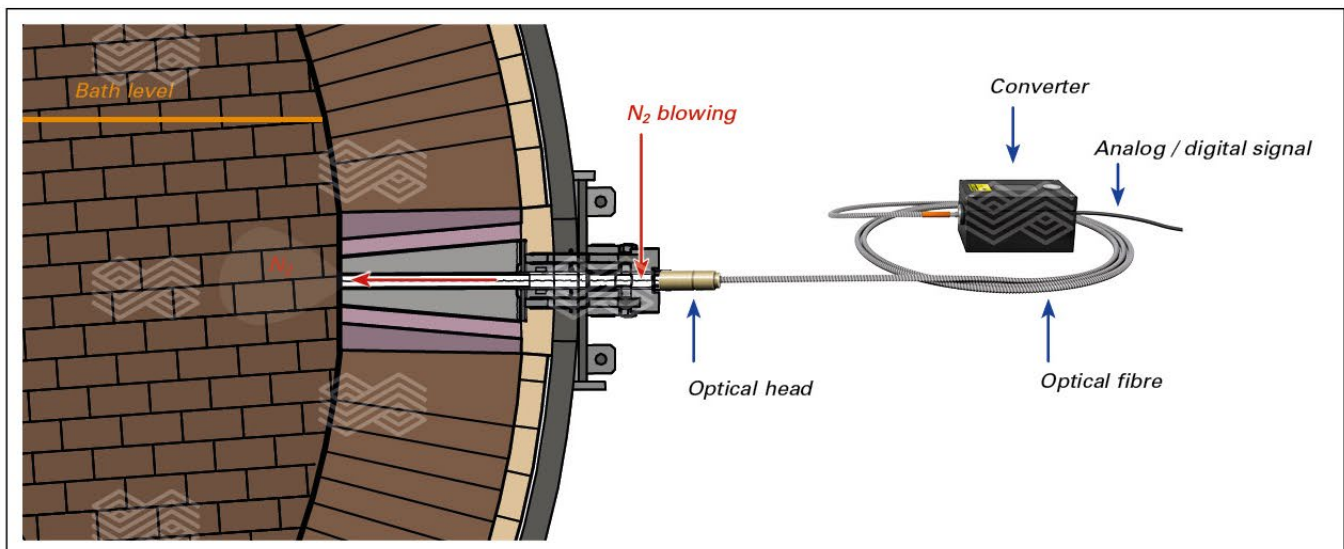


Figure 3. Online pyrometer tuyere arrangement.

The transmission between optical head and converter is done via 0.2 mm mono fibre with a stainless steel protection hose. The optical head contains only the lens and the sensor with the electronics located in the remote converter. The very short response time of below 1 ms facilitates the measurement of the most rapid heating process, enabling a real-time monitoring of temperatures and processes. Additionally, all parameters can be read if they are changed via the integrated keys at the instrument. The temperature can be displayed and stored via serial interface and via operating and analyzing software. In addition to allowing parameter adjustments via PC, the software also provides temperature indication, data logging, and measurement analysis features. The only regular maintenance required is periodic inspection of the external window for build up of foreign particles that if allowed to build up, can reduce the thermal radiation received by the instrument.

### Refractory Components of the System

Refractory components of the system and the changeable arrangement is shown in Figure 5. It consists of the pyrometer tuyere, surrounded by an insert and a well block.

The pyrometer tuyere is comprised of pressed and high fired alumina chrome with a maximum length of 450 mm. It is enclosed in a stainless steel casing including a wear indicator (thermocouple). The insert between the pyrometer tuyere and the well block serves to protect the well block when the pyrometer tuyere is changed. The well block and the insert are both produced from a highly refractory material to guarantee long lifetime and compatibility with the rest of the lining.

The interchangeable pyrometer tuyere is positioned with a uniquely designed closing system (Figure 6). The periphery devices (COP LOCK and COP PULL) were developed to endure a safe and efficient pyrometer tuyere changing operation in hot conditions with reduced physical efforts. With these devices the average changing time per pyrometer tuyere component is no longer than 40 minutes. During the pyrometer tuyere replacement, burners in the furnace are maintained at switch on mode preventing the exposure of the refractory lining to the thermal shocks. Downtime is also reduced as complete emptying of the furnace during pyrometer tuyere replacement is not required.

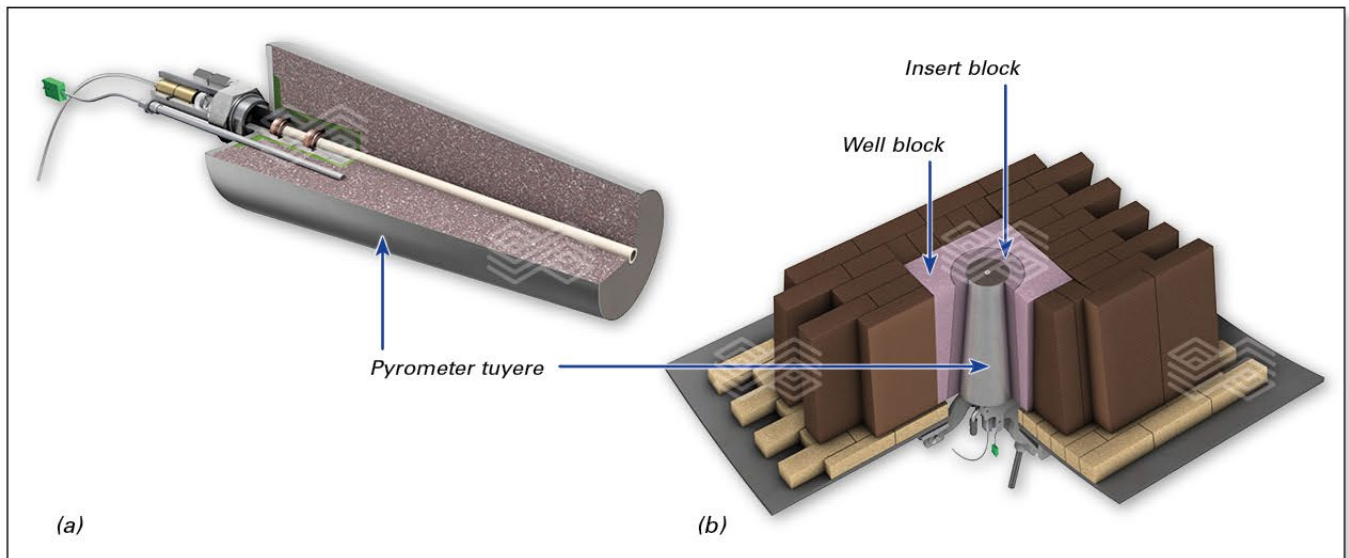


Figure 5. Refractory components of the system.

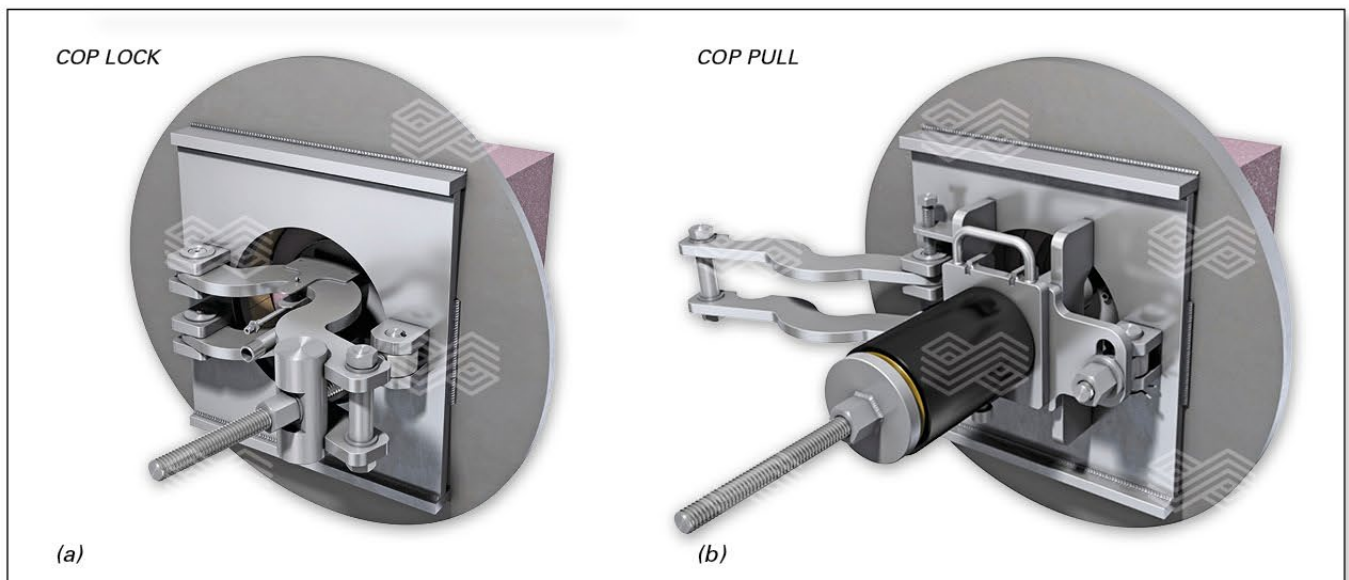


Figure 6. Peripheral devices of the pyrometer tuyere: showing (a) COP LOCK and (b) COP PULL.

## Application, Objectives, and Benefits

The very robust and flexible arrangement of the pyrometer tuyere, especially the refractory components, well block, and insert block, enables installation in a wide variety of metallurgical furnaces, such as:

- >> Anode furnace (rotary, tilting, stationary),
- >> Converters,
- >> Slag cleaning furnace,
- >> Rotary holding furnace,
- >> Refining ladles (e.g., BBOC), and
- >> Flash furnace

It is essential to select an appropriate position for the pyrometer tuyere in the furnace to enable the operator an overview of all the process steps. The integrity of the vessel and safety in operation must be carefully observed when selecting the most appropriate location within the vessel.

Objectives of using pyrometer tuyere in metallurgical furnaces are to ensure the bath temperature control through an automatic burner regulation, and detection of the end-point of the processes in the furnace.

The major benefits of using pyrometer tuyere are:

- >> reduced refractory wear,
- >> reduced energy consumption (burner fuel),
- >> reduced off-gas volume,
- >> constant casting temperature,
- >> improved metal quality,
- >> reduced production costs.

## Conclusions

The ability to accurately and reliably measure the bath temperature constantly is important to achieving optimized process uniformity, product quality, environment protection, and to reduced production costs. Without continuous temperature measurement operators of the furnaces have a little opportunity to optimize the process in the metallurgical vessels. Successful laboratory testing at the RHI Technical Center have demonstrated that the new design of the pyrometer tuyere is now ready for field trials. The results of which will be published in a later article.

*Reproduced with permission from the Canadian Institute of Mining, Metallurgy and Petroleum.*

## References

- [1] Pelletier, A., Lucas, J.M., Mackey, P.J. The Noranda Tuyere Pyrometer, A New Approach to Furnace Temperature Measurement. *Pyrometallurgy of Copper, Volume IV Copper 87-Cobre 87*, 1987, Santiago, Chile. pp. 489–508.
- [2] Lucas, J.M., Kitzinger, F., Labuc, V.M., Peacey, J.G., Pelletier, A., Wint, G.A. Tuyere Pyrometer. US Patent No. 4,619,533. 1986.
- [3] Marinigh, M.J. Technology and Operational Improvements in Tuyere punching, silencing, pyrometry and refractory drilling equipment. International Peirce-Smith Converting Centennial, 2009, San Francisco, USA, *Minerals, Metals & Materials Society* pp. 199–215.
- [4] Heath & Sherwood (1964) Ltd., Smart Cylinder – Tuyere Pyrometer, Retrieved on April 28, 2015, from <http://heathandsherwood64.com/assets/pdf/Tuyere/SMRTCYL3.pdf>
- [5] Heath & Sherwood (1964) Ltd., (2013). Tuyere Pyrometer User's List, Retrieved on April 28, 2015, from [http://heathandsherwood64.com/assets/pdf/References/Tuyere\\_Pyrometer.pdf](http://heathandsherwood64.com/assets/pdf/References/Tuyere_Pyrometer.pdf)
- [6] Chibwe, D.K., Akdogan, G., Bezuidenhout, G.A., Kapusta, J.P.T., Bradshaw, S., Eksteen, J.J. Sonic injection into a PGM Pierce-Smith converter: CFD modelling and industrial trials. *The Southern African Institute of Mining and Metallurgy Pyrometallurgical Modelling*. 2014, Johannesburg, South Africa pp. 99–108. <http://www.saimm.co.za/Conferences/PyroModelling/099-Chibwe.pdf>
- [7] Kapusta, J.P. Sonic injection in bath smelting and converting: myths, facts and dreams. *Ralph Lloyd Harris Memorial Symposium*, October 27-31, 2013. Montreal, Canada, pp. 267–317.

*Reproduced with permission from the Canadian Institute of Mining, Metallurgy and Petroleum. Cited from COM2015, Paper No 9186.*

## Authors

Goran Vukovic, RHI Magnesita, Industrial Division, Vienna, Austria.  
 Bojan Zivanovic, RHI Magnesita, Industrial Division, Vienna, Austria.  
 Klaus Gamweger, RHI Magnesita, Industrial Division, Leoben, Austria.  
 Bernhard Handle, RHI Magnesita, Industrial Division, Vienna, Austria.  
 Bob Drew, RHI Magnesita, Industrial Division, Newark, UK.

**Corresponding author:** Goran Vukovic, [goran.vukovic@rhimagnesita.com](mailto:goran.vukovic@rhimagnesita.com)



Gernot Hackl, Wolfgang Fellner, Beat Heinrich and Roland Bühlmann

# New Slide Gate Water Model Facility

## Introduction

The function of a slide gate system is either to control the flow of steel from the ladle to the tundish (ladle gate system) or from the tundish to the mould (tundish gate system). In the case of a ladle slide gate system, the refractory components comprise the well block, the inner nozzle, the upper and lower plate, and the collector nozzle, as shown in Figure 1.

Usually, a ladle shroud is connected to the collector nozzle to prevent air exposure of the liquid steel during the transfer process. At the start of casting, the slide gate is fully opened to achieve maximum possible throughput until the working level in the tundish is reached. Then the flow of steel is reduced by moving the lower, mobile part of the slide gate. The geometry and dimensions of the refractory components determine the flow conditions and throughput characteristics of the system. For the determination of the system analytical approaches can be used. However by far not all phenomena can be properly described in this way. Therefore water models provide excellent tools to gain more insight into the system, identify critical states or areas, and derive measures for improvement. In the following sections several examples, like the influence of refractory design or operational practices will be presented and discussed.

## The Modelling Approach

Physical modelling by means of water modelling is an efficient way to understand steel flow inside metallurgical vessels or systems, such as a slide gate. Fundamental considerations of water modelling require the model system to approximate as closely as possible the conditions in the actual system. To warrant this, certain similarities between the real application and the model must be fulfilled, which includes geometric, dynamic, kinematic and thermal similarity. In general not all of those criteria can be fulfilled simultaneously, however models either full or downscaled are able to provide useful information about general critical relationships and influencing factors and can thus be used to characterize the system.

## The Model Setup

The actual setup guarantees a flexible use of the water model test facility. Depending on the used model scale factor any ladle size can be replicated. Different measurement systems/techniques can be applied for the system investigation, such as multiple pressure probes, located at different vertical and tangential positions. Standard and high speed video recording is applied for the visualization of the flow. A replica of a ladle slide gate system is shown in Figure 2.

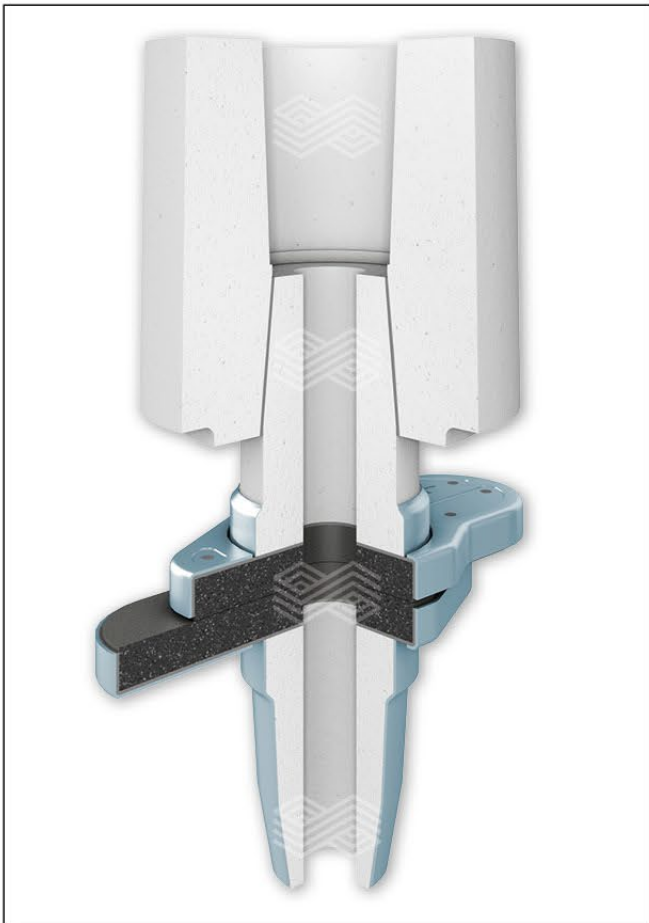


**Figure 1.** Refractory components of a ladle slide gate system.

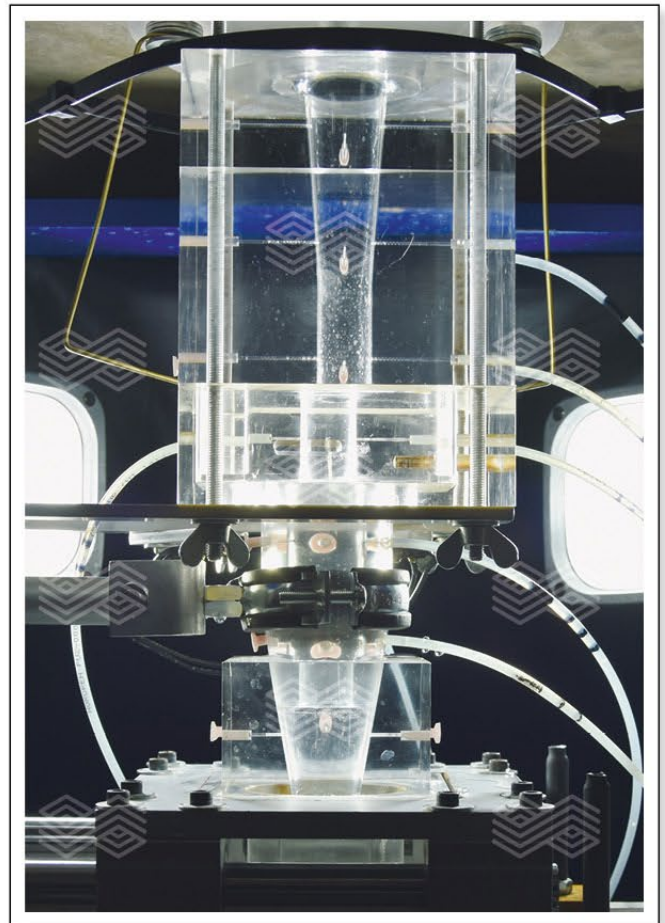


**Figure 2.** Frontal view of casting channel.

### General Pressure Distribution

Determined by fluid dynamics, the slide gate system is subject to the generation of under pressure and subsequent possible air ingress, which could have detrimental effects on the plate life time and cleanliness of the steel. The most critical areas in terms of air ingress are the interfaces of the slide gates and the connection of the ladle shroud to the collector nozzle due to wear, mechanical deformation or a non proper alignment.

In Figure 3 typical pressure characteristics at two different positions as a function of slide gate opening is shown, whereas the first position (P1) is just below the throttling face and the second (P2) is below the contact line of collector nozzle and ladle shroud. The pressure was continuously recorded while the slide gate was moved from the fully opened to the closed position. Starting from fully opened position a more negative pressure is obtained at P2. Due to the strong pressure drop caused by throttling, the pressure at P1 significantly decreases reaching a minimum at approximately 60% slide gate opening, based on the residual surface, which is a typical value during steady state casting. At P2 a different behaviour can be identified. The minimum pressure is obtained when the gate is fully opened and will slightly increase while closing.

These findings confirm the potential risk for air ingress. To minimize this, close attention has to be paid to the system and the operation. Interstop's ladle gate Type S [1] incorporates important features to address the aforementioned problems [2, 3]. Due to the robust and accurate mechanisms, like the automatic system tensioning and self clamping of the plates, human mounting errors have been eliminated. Housing and slider have been optimized by finite element analysis to reduce thermally induced stresses and deformation and the plate design provides maximum refractory overlap in operation. Inert gas purging at the critical areas will minimize the risk of air ingress, such as the opportunity for argon purging between the plates or into a special designed gasket between the connector nozzle and ladle shroud (shielded shroud connection (SSC)) [4], as shown in Figure 4.

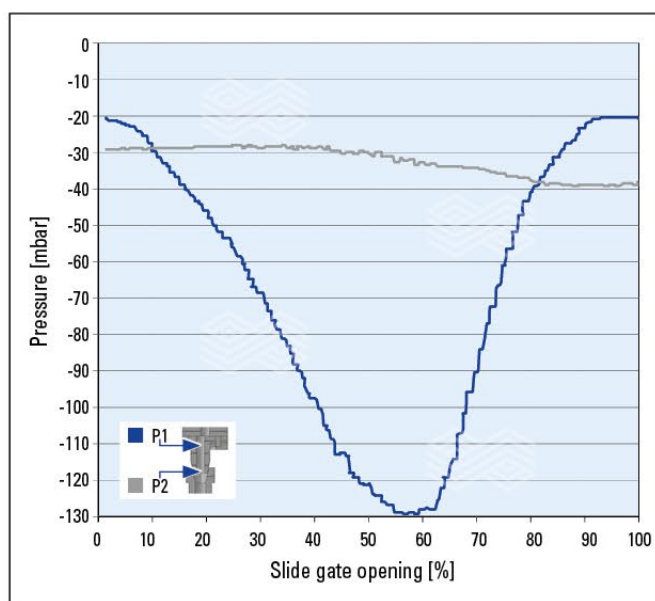


Figure 3. Pressure vs. throttling position at two critical locations.

### Influence of Inner Nozzle Geometry

The calculation of the maximum possible throughput is traditionally calculated by an analytical approach, see Equation 1.

$$\dot{M} = \mu \cdot A \cdot \rho \cdot \sqrt{2gh} \tag{1}$$

Where  $\mu$  is the coefficient of loss [1], A is the cross section [m<sup>2</sup>],  $\rho$  the density of the liquid [kg/m<sup>3</sup>], g the gravitational acceleration [m/s<sup>2</sup>] and h the height of liquid [m].

The influence of geometrical factors on the maximum possible throughput is described by the loss coefficient, which needs to be individually determined. This could be done by numerical simulations or experiments. Subject to this investigation were two different inner nozzle geometries, as shown in Figure 5, a standard cylindrical shape (60 mm diameter) versus a flow optimized shape (55 mm diameter).

The water model was filled to a certain level and a draining experiment without the application of a ladle shroud was carried out. The throughput was continuously recorded. Applying the fundamentals of similarity it is possible to convert the results (e.g., volumetric flow rate) obtained in the water model into the real application. The already converted results are compared against the analytical approach,

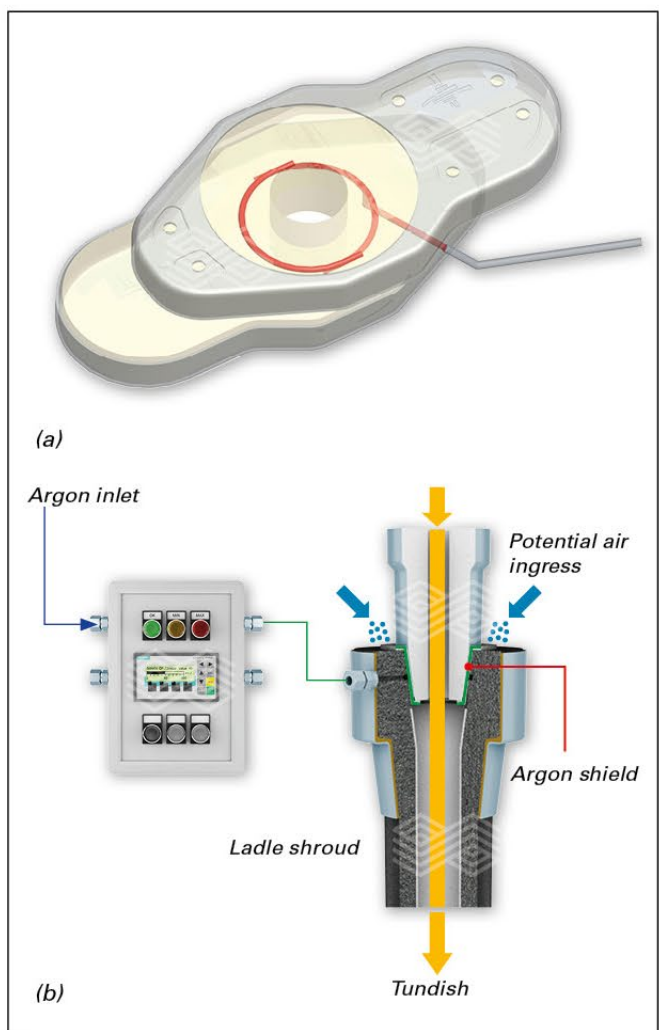


Figure 4. Showing (a) argon purging between the plates and (b) shielded shroud connection.

whereas the loss coefficient was varied until the measured curve matched the theoretical one. This is shown in Figure 6a and 6b.

The loss coefficients were determined as 0.82 for the standard and 0.94 for the optimized nozzle, which provides a theoretical throughput gain of 15% of the optimized design, if the diameters are kept constant.

In addition to the maximum possible throughput, the relationship between throttling position and throughput for both geometries was measured. In Figure 7 the throttling characteristics with and without a ladle shroud are shown. It is evident, that with a ladle shroud a higher possible throughput is obtained. For this situation it can be noticed, that for opening rates greater than ~70%, the throughput for the optimized inner nozzle geometry is even higher than for the standard nozzle, although the diameter is smaller.

The results indicate, that it is possible to tune the throughput to a certain extent by geometrical optimization without changing, e.g., increasing, the casting diameter of the system.

### Vortex Formation During Draining

Slag entrainment caused by vortex formation is a common problem during ladle draining. There are several motivations for minimizing that phenomenon, namely steel cleanliness and productivity (yield). The bath level at which a vortex occurs, known as critical height, is triggered by several factors, such as the throughput and a tangential flow in ladle [4, 5]. Since entrained ladle slag is one possible source for exogenous inclusions, it should be suppressed as much as possible.

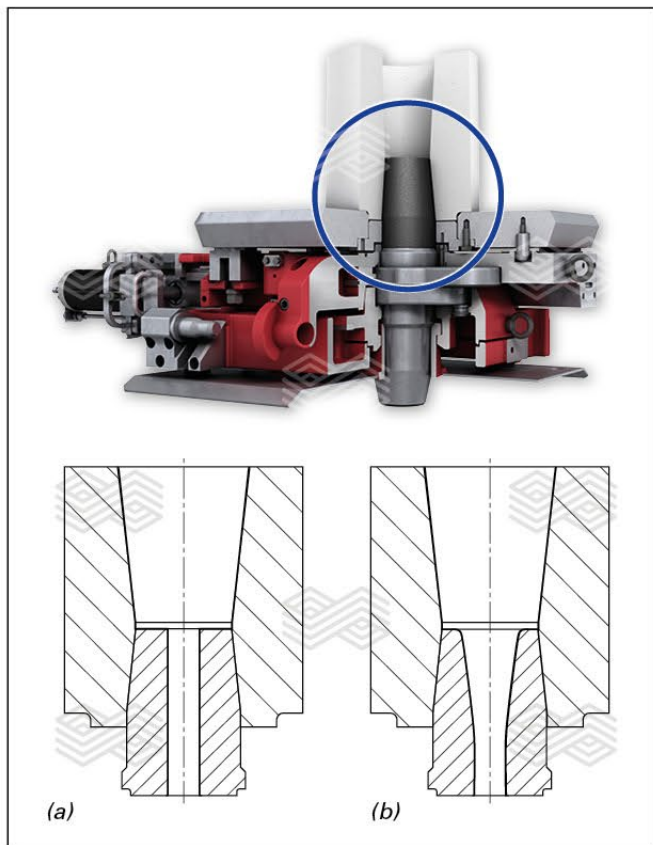


Figure 5. Tested inner nozzles: (a) standard and (b) optimized geometry.

One question included in this topic is the potential to suppress an already existing vortex by closing and re-opening the slide gate. To that purpose the water model was employed to investigate the potential of the aforementioned procedure. Once a fully developed vortex occurs, the gate is closed and reopened again. A close up view showing the

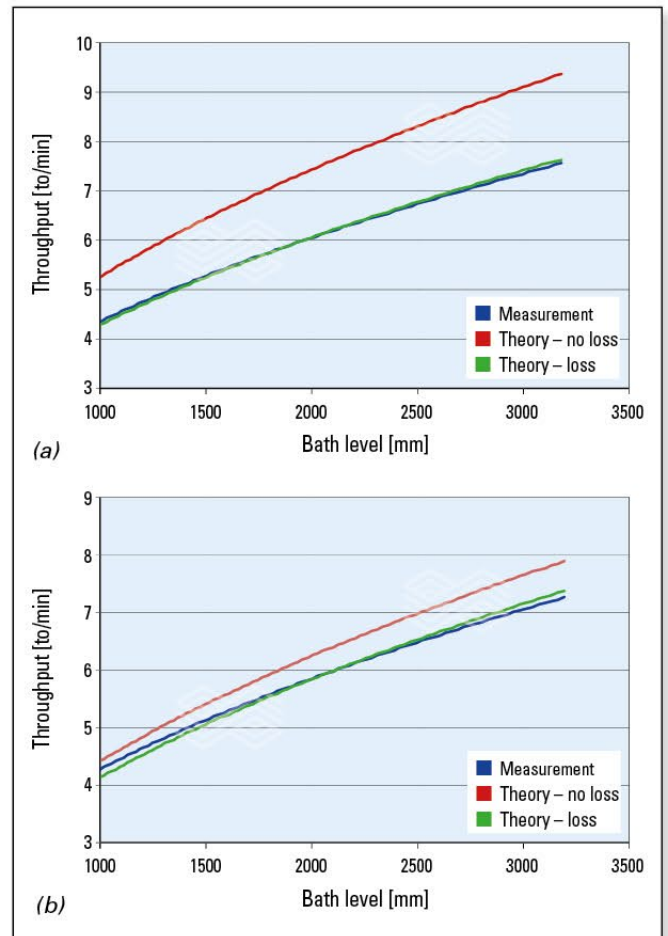


Figure 6. Calculated and measured maximum throughput dependent on the bath level for (a) standard and (b) optimized geometry.

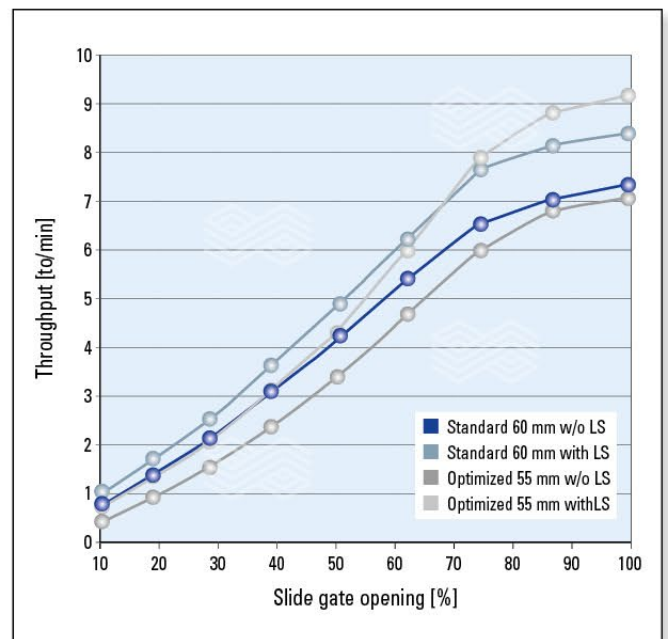


Figure 7. Throughput vs. slide gate opening.

ladle bottom and slide gate system during that complete procedure is shown in the picture sequence of Figure 8.

The picture sequence indicates that the vortex disappears shortly before the complete closing position. However, during the reopening period it quickly appears again. It was found, that throttling positions greater than 20%, based on the open area, do not give the desired effect of suppression. Below that opening rate, the vortex occurred with a certain time delay. Only below a very small opening of approximately 10% was it completely suppressed.

## Summary

Transferring steel from one vessel to the other is a critical step in the steelmaking process. The flow of steel should be precisely controlled, any contamination of steel, e.g., by air ingress, should be avoided as well as the entrainment of slag. To gain a better understanding of the system characteristics a water model of the slide gate system was established. The setup provides a powerful framework for the investigation of process relevant phenomena and helps to further improve the understanding.

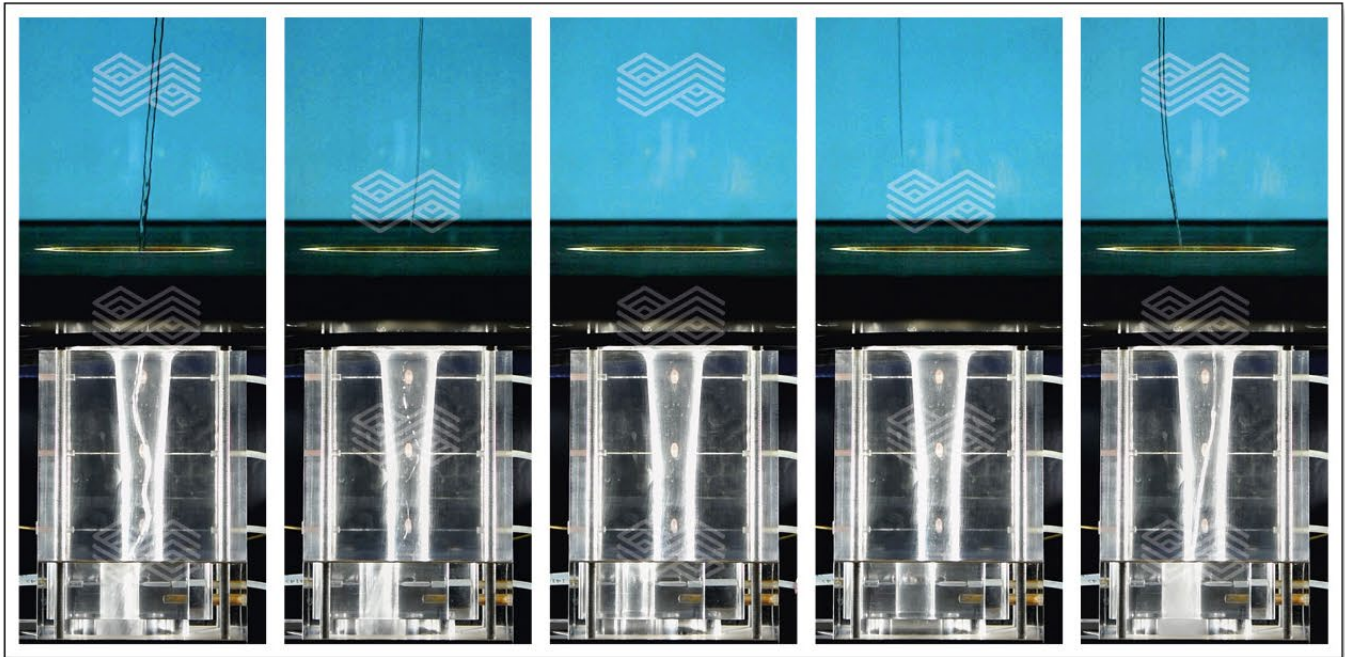


**Figure 8.** Image sequence showing the effect of slide gate closing and reopening on the behaviour of a vortex.

## References

- [1] Patent applications and patents pending.
- [2] Heinrich, B., Hackl, G. and Marschall, U. Advantages of Optimised Flow Control from Ladle to Tundish. *Proc. 2<sup>nd</sup> ESTAD*. 15–19 June, 2015, Düsseldorf.
- [3] Ehrenguber, R. and Bühlmann, R. INTERSTOP Ladle Gate Type S – A new Milestone in Ladle Gate Technology. *RHI Bulletin*, No. 1, 2015, pp 61–66.
- [4] Sankaranarayanan, R. and Guthrie, R. I. L. Slag Entraining Vortexing Funnel Formation During Ladle Teeming: Similarity Criteria and Scale-up Relations, *Ironmaking and Steelmaking*, Vol. 29, No. 2, 2002.
- [5] Morales, R. D. Davila-Maldonado, O., Calderon, I. and Morales-Higa, K. Physical and Mathematical Models of Vortex Flows During The Last Stages of Steel Draining Operations from a Ladle. *ISIJ International*. Vol. 53, No. 5, 2013, pp. 782–791.

## Authors

Gernot Hackl, RHI Magnesita, Technology Center, Leoben, Austria.  
 Wolfgang Fellner, RHI Magnesita, Technology Center, Leoben, Austria.  
 Beat Heinrich, Stopinc AG, Hünenberg, Switzerland.  
 Roland Bühlmann, Stopinc AG, Hünenberg, Switzerland.

**Corresponding author:** Gernot Hackl, gernot.hackl@rhimagnesita.com



Gregor Arth, Daniel Meurer, Yong Tang, Gernot Hackl and Bernd Petritz

# Tundish Technology and Processes: Ladle to Mould Systems and Solutions (Part II)

Ladle-to-mould steel transfer is of critical importance regarding refractory lifetime as well as steel cleanliness. Part II of this publication series deals with the effect of impact pot parameter variations to influence steel fluid flow as well as impact pressure and energy distribution. Impact pot designs in general are known to influence previous mentioned parameters, whereas nearly no literature can be found about the effect of small variations in refractory thickness or gap sizes, nor distance from the ladle shroud exit towards the impact pot bottom. The results of CFD and water modelling tests presented in this publication will reveal potentials to further improve lifetime of refractory products as well as enhanced steel cleanliness, by adjusting only small variables with consequent high impact.

## Introduction

The previous publication Part (I) [1] dealt with an overview of shrouding approaches during the ladle-to-tundish transfer, ensuring low to no re-oxidation and thus guaranteeing a high steel cleanliness level. Continuing the steel production line the next point of interest addresses the impact area below the ladle shroud inside the tundish. Only few works have been published dealing with this topic and when, aligning the ladle shroud perfectly vertical or slightly misaligned is the main varying factor. This article focuses on especially this first section in tundish metallurgy, going into more detail regarding impact pot design and adjustment on casting parameters. A schematic drawing of several ladle-to-mould solutions is presented in Figure 1. Part II of this publication series focuses on the blue edged section, namely the impact area.

A general overview on influencing factors on steel cleanliness and solutions therefore has previously been

published [2]. Tundish metallurgy today generally aims on achieving a homogeneous temperature distribution inside the tundish, steel bulk or plug flow, and a high residence time to enhance non-metallic inclusion (NMI) flotation. The casting start of a sequence as well as the ladle change practice should also be optimized to avoid and/or reduce steel splashing. Especially as each ladle change creates a disturbance of the steel flow and with changing grades during a casting sequence, the mixing should also be minimized to reduce product downgrades. This can be ensured by correct selection and installation of a suitable impact pot.

During casting itself, open eye formation and high surface turbulences can also be sources for re-oxidation and reduced steel cleanliness. The following chapters provide an insight into design and material selection potentials to ensure the previously mentioned beneficial casting conditions.

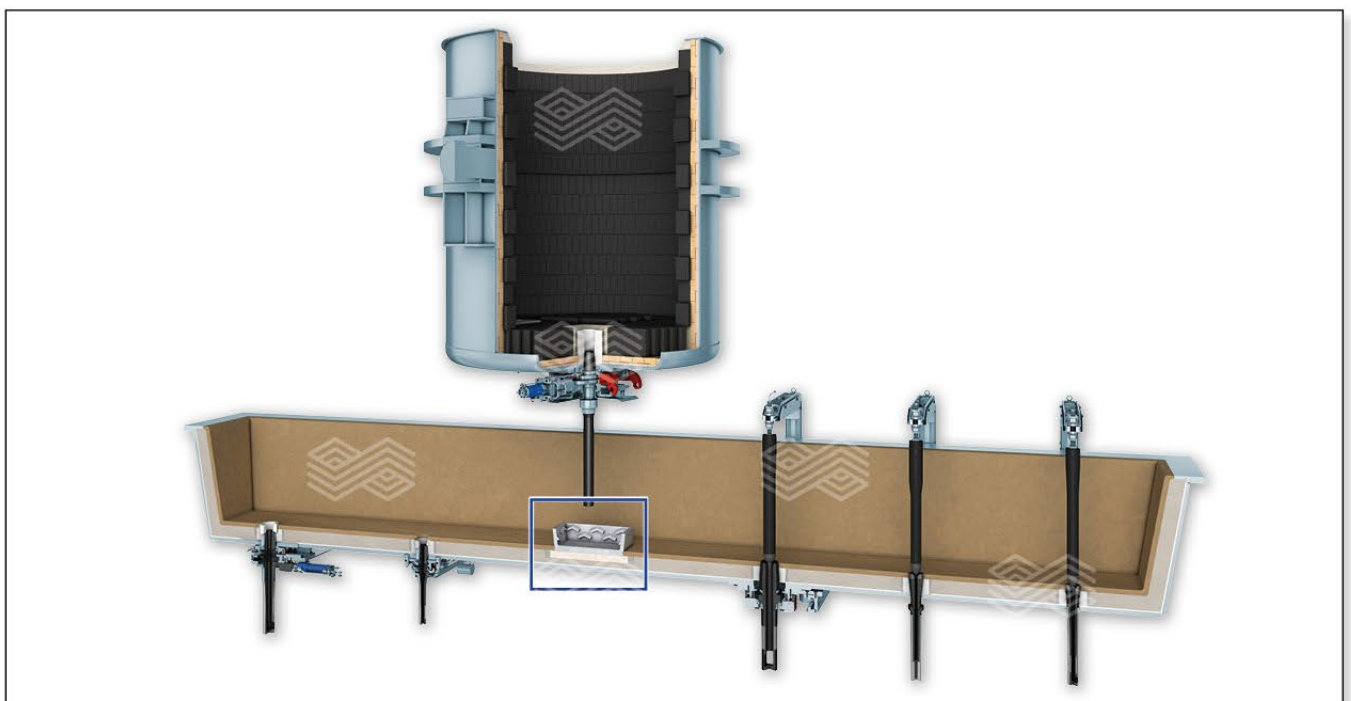


Figure 1. Ladle to mould systems and solutions.



**Variation of Impact Pot Design**

Figure 2 shows representative snapshots for the characterisation of surface turbulence and “open eye” formation obtained by a water model benchmark. Three different impact pot designs assuming a perfect vertically aligned ladle shroud (LS) (a, b, c) as well as an 1.5° inclined LS (d, e, f), that may occur during casting due to a distorted ladle bottom or steel splashes onto the collector nozzle, were compared. The installation of RHI’s FLOWERPOT [3] design leads to a significant decrease of the open or red eye compared to a conventional lipped impact pot design, for vertical as well as inclined LS installation. Using the TUNFLOW CHEVRON [3] design, the surface turbulence can be further reduced, and as a consequence the open eye formation can be almost completely avoided for a perfect aligned LS (Figure 2, c). Even if there still is an open eye formation with the CHEVRON design with a misaligned shroud (Figure 2, f), the superior performance compared to the other cases (Figure 2, d and e) is obvious. Details to similar simulations with misaligned ladle shrouds can be found in [4, 5].

**Variation of Impact Pot Design Details**

**Thickness of CHEVRONS**

A milestone regarding impact energy reduction inside the tundish was achieved by the patented RHI impact pot

design TUNFLOW CHEVRON. The CHEVRON design was found to be the key to calm the incoming steel stream from the ladle. The next step regarding further optimization was the variation of the CHEVRON thickness. CFD simulation results of varying CHEVRON thickness (Figure 3) are presented in Figure 4. The results of the varying thickness show a clear reduction of the surface turbulence with increasing CHEVRON size. Furthermore it was found that with increasing inner volume of the impact pot, the greater the importance of elevated chevron thickness to calm down the up-stream.

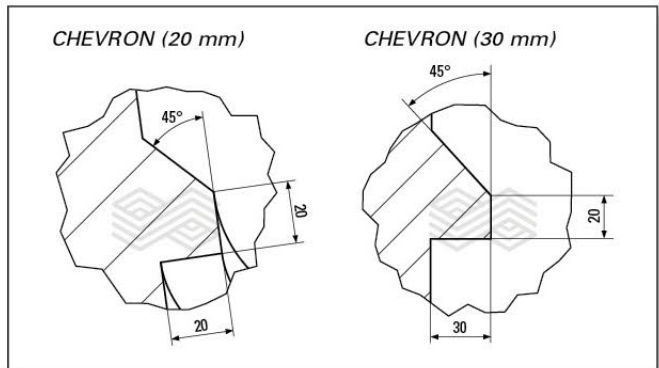


Figure 3. Schematic of various CHEVRON design thicknesses.

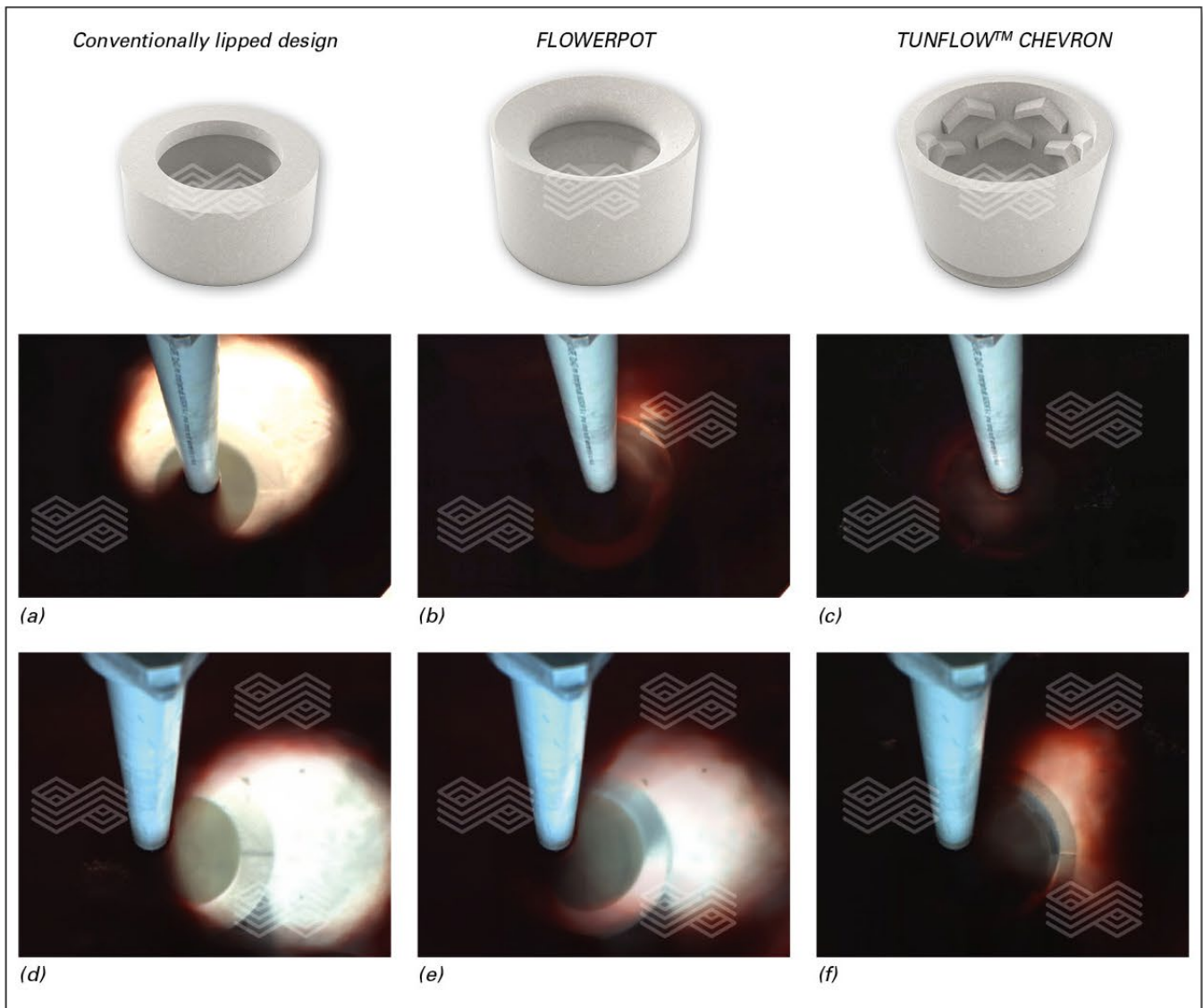


Figure 2. Impact pot performance respective open eye formation.

These results clearly highlight the need to select tundish furniture as well as furniture details according to the customers process, to achieve the most beneficial influence possible on steel production and casting process.

As CFD simulation boundary conditions the tundish steel throughput was set 3.6 t/min, the bath level was defined as 1043 mm and the LS immersion depth held constant at 339 mm. These boundary conditions are constant over the whole results presented in this publication.

### Opening Dimensions and Orientation of the Progressive Slot

The next example below depicts CFD simulation results regarding the orientation of the TUNFLOW progressive slot. In a typical one strand slab tundish layout the progressive slot is generally aligned towards the outlet, whereas in the second simulation case the impact pot is turned 180°. The progressive slot is then orientated towards the tundish wall. Another simulation parameter was the progressive slot size variation in 5 mm steps between 15 and 40 mm. The results revealed, that with varying slot width near the bottom itself only an eventual increase in the steel jet length results thereof. Due to the low differences between these results, only the ones of the 30 mm progressive slot are presented in Figure 6 representatively. Nevertheless it should be stated, that these results are only valid for the selected boundary conditions, and the results may vary for increased steel throughput and/or impact pot volume as well as slot direction.

The corresponding residence time distribution (RTD) data provided evidence of the improved TUNFLOW performance, if the progressive slot is directed towards the tundish wall (Figure 5). The minimum residence time ( $t_{\min}$ ), the average residence time ( $t_{\text{mean}}$ ), and the plug flow volume ( $V_p$ ) are increased, whereas the dead volume ( $V_d$ ) and the mixing volume ( $V_m$ ) are reduced. The RTD parameters were calculated according to the model of Sahai and Emi, considering the dispersed plug flow volume [6]. Additional information about RTD curves can be taken out of [7]. The most important parameters to ensure high steel cleanliness inside the tundish are as follows:

- >> Dead volume fraction should be small;
- >> Too small  $t_{\min}$  means short circuit exists in the tundish, and should be avoided
- >> Large  $t_{\text{mean}}$  and  $V_p$  is good for inclusions floating up and separation

It is important to mention that the progressive slot has the advantage to slightly force the steel in a certain direction, helping to achieve a more homogeneous plug flow and temperature distribution inside the tundish. Nevertheless the flow energy is only small compared to the energy of the steel stream directed back towards the steel surface by the impact pot, as long as the ladle shroud is vertically aligned. Inclined ladle shrouds can have a tremendous influence on the steel flow performance, especially on steel flow through the progressive slot, eliminating the beneficial effects. Thus the vertical alignment is of greatest importance to ensure correct casting parameters.

Figure 7 presents velocity and temperature contour plots of the CFD simulations. The results indicate a beneficial influence of the backwards orientated progressive slot towards the wall regarding all parameters calculated by the simulation. Nevertheless it should be considered, that temperature differences inside the tundish can lead to NMI generation and decreased steel cleanliness. While the temperature is increased in the space between wall and the impact pot, and thus the dead volume is reduced, the area between the impact pot and the outlet contains a much lower temperature distribution near the tundish bottom than in the typical arrangement.

Additionally, if the ladle shroud is not aligned vertical, a slightly inclined steel stream towards the progressive slot intensifies energy through the slot, which may cause increased wear of the working lining at the tundish wall.

It is now clear, that not only impact pot design and details like CHEVRON size or slot size can have an influence, but also the arrangement of the impact pot itself can be a key to increase tundish performance regarding steel cleanliness.

### Variation of Tundish Bath Level

Shroud immersion depth [6], ladle slag carry over and impact pot selection have a significant influence on the metallurgical performance of the tundish, and hence the product quality. Nevertheless a so called piston streaming or plug flow in the tundish is also desired. Again CFD simulations were carried out for a progressive slot design with previously mentioned boundary conditions. The distance of the ladle shroud outlet to the impact pot was in addition varied to determine changes regarding tundish surface turbulence and stresses applied to the impact pots. Tundish bath levels of 550, 650, 750, 850, 950, 1050, and 1150 mm were set as boundary conditions during these simulations.

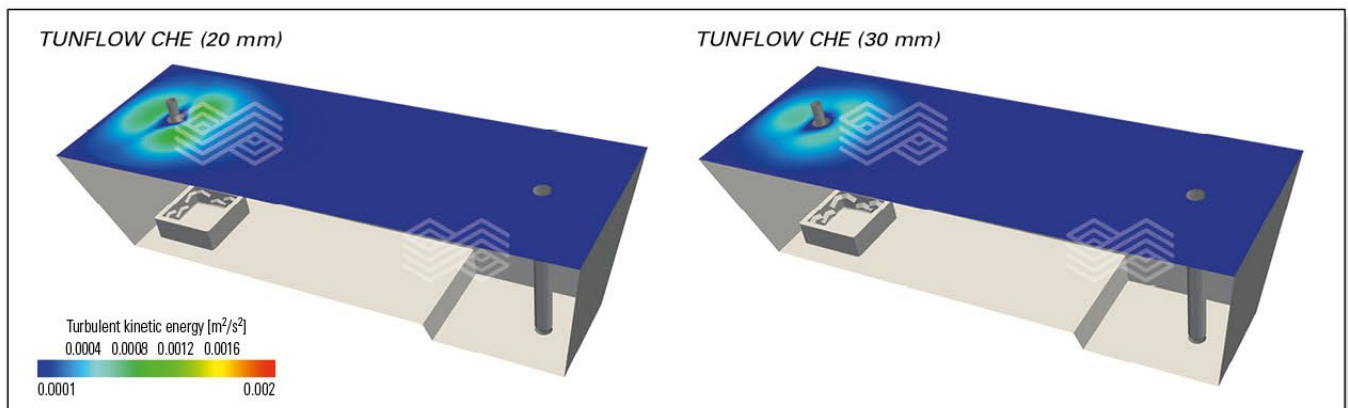


Figure 4. Turbulent kinetic surface energy distribution on the tundish surface at varying CHEVRON thickness.

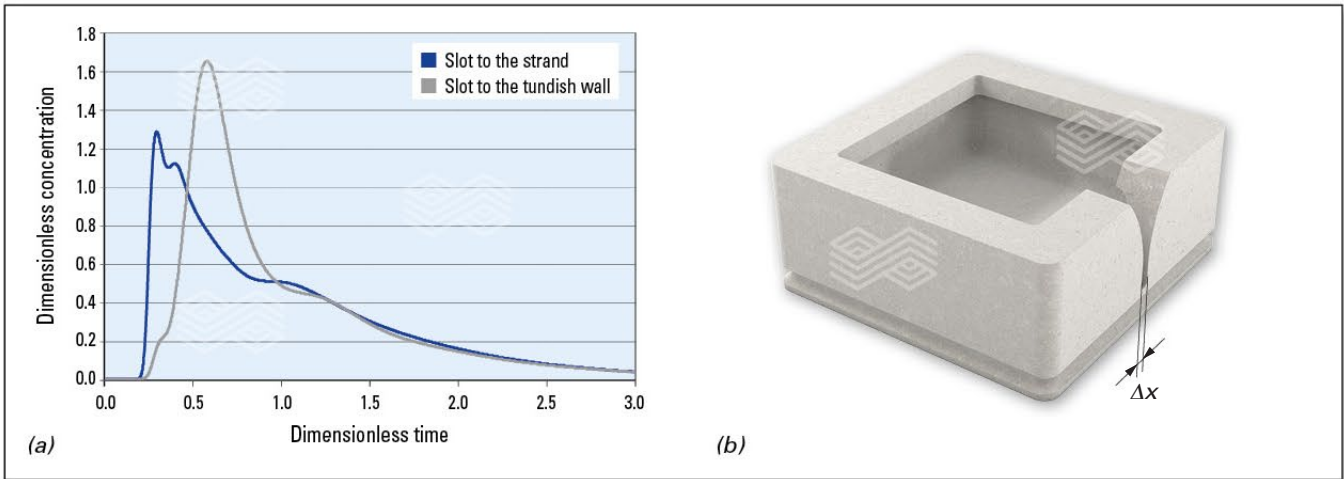


Figure 5. Showing (a) RTD results of TUNFLOW arrangement (outlet vs. wall) and (b) slot size variations tested.

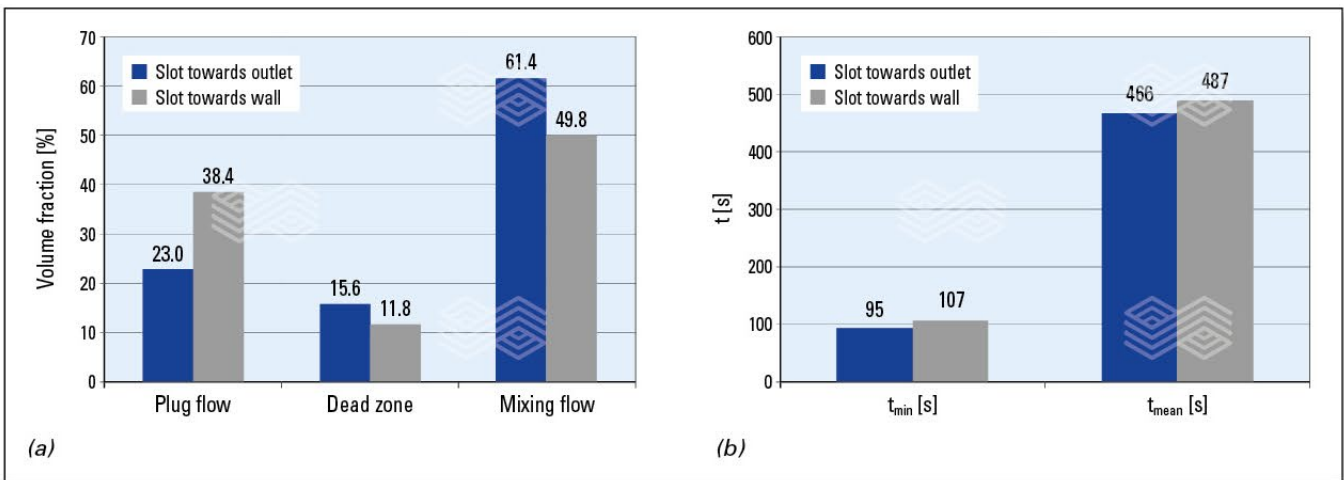


Figure 6. Showing (a) the influence of TUNFLOW arrangement on plug flow volume (PFV), dead zone volume (DZV) and mixing flow volume (MFV; outlet vs. wall) and (b) influence on minimum and mean residence time.

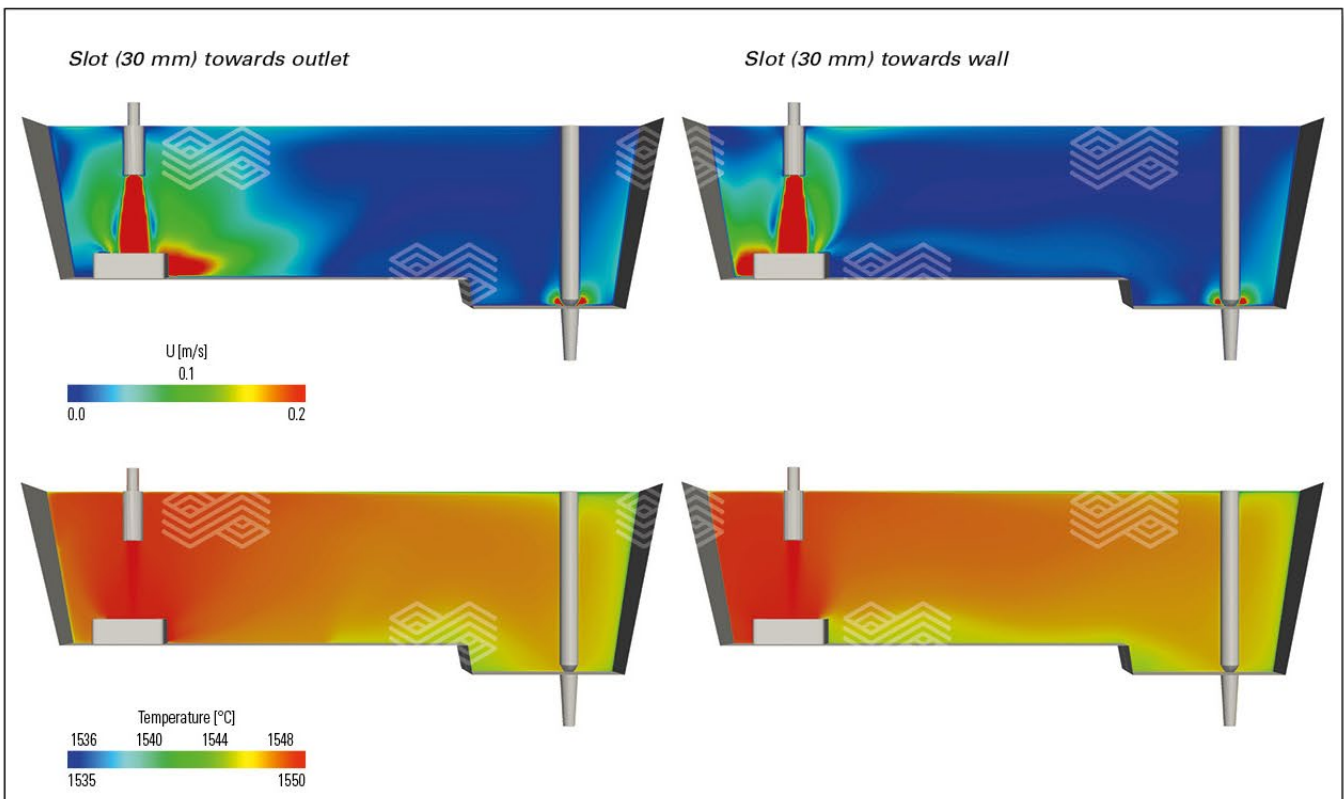


Figure 7. Velocity and temperature contour plot of a progressive slot design with varying direction of the progressive slot.

Figure 8 shows the average wall shear stress over the whole impact pot area and the average turbulent kinetic energy over the whole tundish top surface at different tundish bath levels. The immersion depth of the ladle shroud in the bath was kept the same for all cases. The distance from the ladle shroud tip to the impact pot bottom was varied. It is very clear from Figure 8 that the higher the bath level (the longer distance of the LS outlet to impact pot bottom), the less averaged wall shear stress on the whole impact pot area, the less averaged turbulence kinetic energy on the total tundish top surface.

The calculated wall shear stress distributions are depicted in Figure 9 for two significant different ladle shroud distances. The main stress area is focused at the bottom where the incoming steel stream is redirected and calmed back to the tundish surface. Using the previously mentioned boundary

conditions, the results reveal a reduced influence of the steel stream on the impact pot bottom, above a shroud tip distance of more than 800 mm. A clear explanation of the weighting of these stress values regarding impact pot material behaviour cannot be provided currently. The influence of different material grades in more and less stressed areas of the impact pot will be part of a separate publication. However it is clear that increased tundish performance regarding steel cleanliness will go hand in hand with enhanced impact pot lifetime, which makes material selection more and more a key value on performance in addition to impact pot design.

Figure 10 contains the results of CFD analysis regarding the tundish surface turbulence kinetic energy distribution at the bath level of 650 mm and 750 mm. It was also found that as the bath level is more than 850 mm, dispersed plug flow is decreased and transition time is increased significantly.

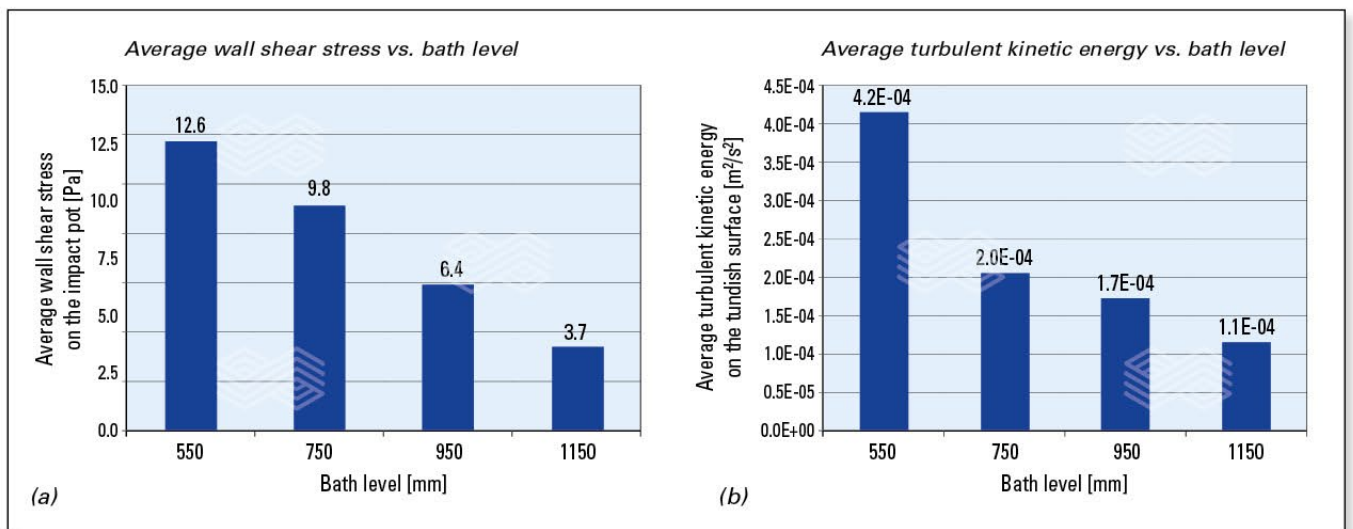


Figure 8. Average wall shear stress and average turbulent kinetic energy at varying distance of the ladle shroud on a slotted TUNFLOW design.

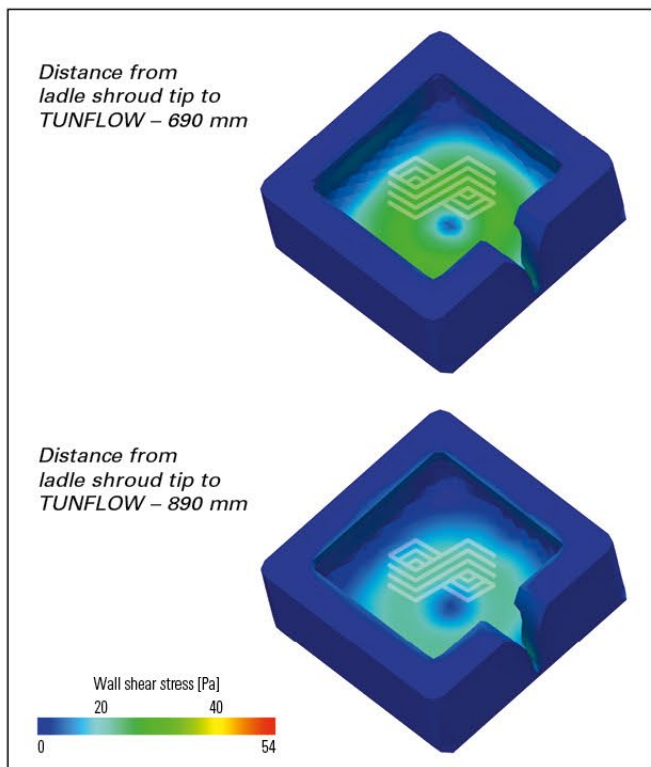


Figure 9. Wall shear stress distribution at varying distance of ladle shroud to impact pot bottom on a slotted design.

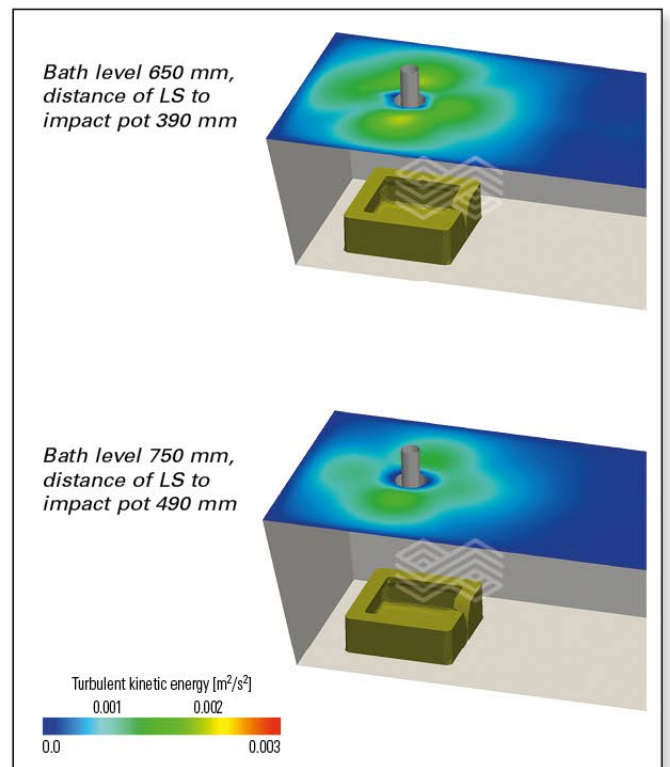


Figure 10. Turbulence kinetic energy distribution on the tundish surface at varying distance from LS to impact bottom.

In addition to these findings it has also to be stated, that these values are not valid for all tundishes due to the high variability of casting parameters like tundish throughput or ladle shroud size. Adding these results to the previous mentioned understandings of impact pot size, design, orientation, and design details on tundish behaviour, the correct selection of also the impact pot material is a key to ensure longer lifetime of the tundish furniture and increase sequence length.

**Potential of Material Selection**

As previously mentioned, the selection of the best material according to the customer’s process is a key to reach casting goals. Optimal performance comes from the selective material concepts and impact pot design, cross-checked with test results under similar process conditions carried out in the RHI Technology Center. One example of such test application is the production of different TUNFLOW materials and testing them against varying ladle and tundish slags in a small induction furnace (Figure 11).

In that way, and during a defined test duration, 4 samples (also called “fingers”) are submerged into the molten slag and put into rotation. After the test, wear patterns can be observed and the samples are analyzed using light-optical microscopy as well as scanning electron microscopy/energy dispersive X-ray spectrometry (SEM/EDS). The parameters that can be adjusted during this test are product quality, slag composition, reaction time, sample rotating speed, testing temperature, and test atmosphere.

In combination with investigations regarding wear due to interaction of tundish and ladle slag on the working lining of the tundish using FactSage, the same procedure can be used to cross-check these laboratory trial results with the thermodynamic ones. This will also be presented in further publications of this series.

**Combination of the Previously Found Parameters**

Based on the previously presented results of simulations as well as experience with field trials, a combination of these findings was the next step regarding performance improvement of the impact pots. Figures 12 and 13 provide schematic drawings of novel TUNFLOW designs.



Figure 12. TUNFLOW concept with material combinations.

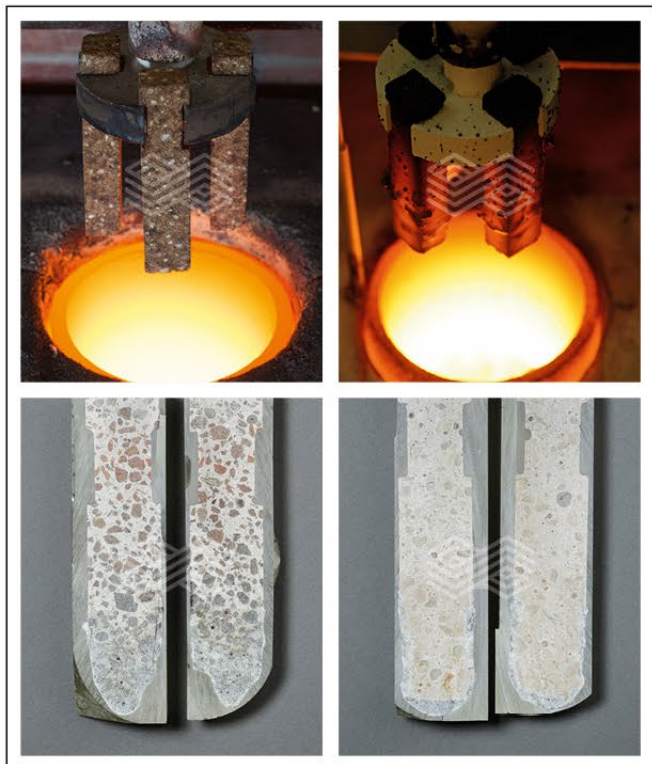


Figure 11. Example of the so called “finger-test” at TCL.

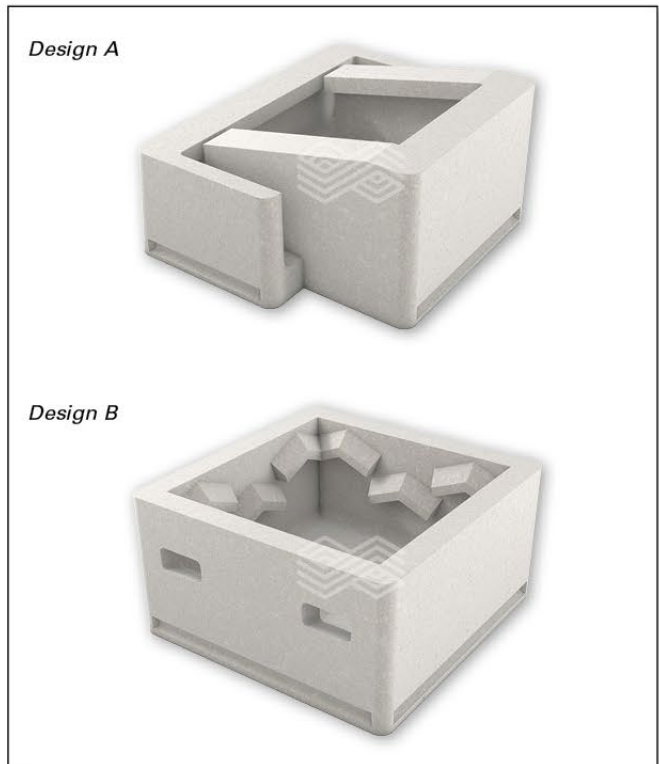


Figure 13. TUNFLOW concept with enhanced designs and design combinations.

As can be seen in the schematic drawings in Figure 13, design A includes one channel at opposite sides redirecting the steel flow backwards to the area between impact pot and tundish wall, aiming to reduce dead volumes between impact pot and tundish wall, thus increasing steel cleanliness. The inclined wall at the back of design A targets creating a more intense plug flow towards the tundish outlet. Design B was created as a combination of the CHEVRON and the progressive slot approach, to force a defined amount of steel in a certain direction while calming turbulence using the CHEVRONS. Several CFD studies as well as water modeling tests were carried out and proved the advanced performance regarding tundish fluid flow.

As previously mentioned, limited information can be found in literature regarding investigations similar to the presented designs. Cloete et al. [8] did research on impact pots with the addition of holes, slightly comparable to design B, in combination with the installation of dams in the tundish, but found no clear improvement in flow properties. These results are in contrast to those found in the present simulations that will be presented in a separate paper of this publication series. The differences can be explained by comparing the simulation boundaries and geometries differing drastically from the ones used in this work.

This example will reveal the importance of customer sized decisions and simulation for correct tundish furniture selection, based on the customer's needs, as well as adequate adjustment regarding material selection.

## Summary and Outlook

The influence of impact pots on tundish performance, based on specific selection of pot design and design details,

pot arrangement inside the tundish, tundish bath level as well as combinations thereof were presented in this article. Water modelling as well as CFD simulation are ideal tools to estimate best fitting impact pots to the customer's needs, as well as help to further improve the material selection of the impact pot.

It was revealed, that certain changes in design details only lead to positive results if these changes are adjusted to the customer's casting conditions. Contemporary selective pushing of the incoming steel stream can lead to increased casting performance, helping to reduce dead areas or increase plug flow inside the tundish.

The correct selection of the impact pot can help to reduce open eye formation by reducing the surface turbulent kinetic energy. Nevertheless it has to be stated that these results are mainly achieved by optimum casting conditions, like a perfectly aligned ladle shroud. Comparable results with inclined shrouds were also presented and proved the obvious beneficial influence of the CHEVRON design. This is also a part of RHI's contribution as refractory solution provider, to offer the customer this service of simulation and experience, to support the aims of higher steel cleanliness and longer casting sequences.

Results of the parameter combinations (design A & B) as well as material selection and material combinations (TUNFLOW HYBRID) [3] thereof on impact pot performance will be part of further publications in this series.

## Acknowledgement

The authors would like to thank Mrs. Patricia Polatschek for her contributions to this article.

## References

- [1] Arth, G., Viertauer, A., Hackl, G., Krumpel, G., Petritz, B. and Meurer, D. Tundish Technology and Processes: Ladle to Mould Systems and Solutions (Part I), *RHI Bulletin*. 2016, No. 1, pp. 38–44.
- [2] Secklehner, B.A., Casado, M.T., Viertauer, A., Wappel, D. and Brosz, B. Tundish Technology and Processes: A New Roadmap, *RHI Bulletin*. 2015, No. 1, pp. 68–77.
- [3] Patent applications and patents pending.
- [4] Hackl, G., Ehrenguber, R. Tomas, M. and Eglsäer, C. Flow control refractory design optimisation by modelling and simulation, *UNITECR 2015 Proceedings*, No. 447 (2015).
- [5] Hackl, G., Wappel, D., Meurer, D., Tomas, M. and Komanecky, R. Product Development and Flow Optimization in the Tundish by Modelling and Simulation, *AISTech 2014 Proceedings* (2014), pp. 1911–1919.
- [6] Sahai, Y. and Emi, T. Melt Flow Characterization in Continuous Casting Tundishes, *ISIJ International* 36 (1996), 6, pp. 667–672.
- [7] The AISE Steel Foundation (Ed.), *The Making, Shaping and Treating of Steel*, 11<sup>th</sup> Edition, Casting Volume: Chapter 13, Tundish Operations, Pittsburgh, Pa, 2003
- [8] Cloete, J.H., Akdogan, G., Bradshaw, S.M., and Chibwe, D.K. Physical and numerical modelling of a four-strand steelmaking tundish using flow analysis of different configurations, *J. South. Afr. Inst. Min. Metall.* 115 (2015), 355-362.

## Authors

Gregor Arth, RHI Magnesita, Steel Division, Leoben, Austria.  
 Daniel Meurer, RHI Magnesita, Steel Division, Leoben, Austria.  
 Yong Tang, RHI Magnesita, Technology Center, Leoben, Austria.  
 Gernot Hackl, RHI Magnesita, Technology Center, Leoben, Austria.  
 Bernd Petritz, RHI Magnesita, Steel Division, Leoben, Austria.

**Corresponding author:** Gregor Arth, gregor.arth@rhimagnesita.com



Marcos Tomás Casado, Gregor Arth, Andrea Giacobbe and Alessandra del Moro,

# New Casting Solutions: Value Innovation for RHI Customers

This article provides an overview of the latest continuous casting solutions offered by RHI as an outcome of the cooperation agreement signed with PROSIMET, a company engaged with development and manufacturing of mould and tundish powders.

## Introduction

During the last few years, steel plants (groups) have been changing the way of addressing the steel market. In a very competitive and global environment the search for differentiation is needed through a wide steel grade portfolio. It reaches from “commodity” steel grades to the high end “clean” steel grades. For the first, the focus is set to optimize the total running cost mainly through longer sequences at the caster – the motto would be “endless casting”. For the latter, the differentiation shall be reached by striving on the technological side, casting special grades and/or creating and casting new qualities that can fulfil existing or new steel applications – the motto would be “fulfil high metallurgical targets to produce clean steel” [1]. In both cases mentioned above the role played by refractory design in combination with tundish covering powders, mould fluxes and innovative solutions is of ultimate importance in order to support the optimization, not only of the metallurgical process, but also of the caster operation itself.

RHI and PROSIMET are able to generate value and innovation while approaching these new challenges together with

the steel producers. Figure 1 shows a schematic overview of the actual ladle-to-mould portfolio.

## What Does it Mean New Value and Innovation?

Most of the refractory suppliers to the steel industry have considered that through optimization of their products and services, the most value can be transferred to the end user, the steel plants. That means actively working on products and services, innovation will automatically lead to the creation of new value. This concept alone has been proven to be incomplete on many occasions. A few suppliers are undertaking what it has been called holistic approach and can be in general defined as: We have all the products needed for a specific production area (e.g., caster) and the service attached, so we are able to provide to you a complete solution.

What RHI, together with PROSIMET, is offering now goes one step further in the area of the continuous casting and extent the product and services definition in RHI’s ladle-to-mould approach. Now, every step creates additional value innovation for both partners, as will be clarified in detail later in this publication.

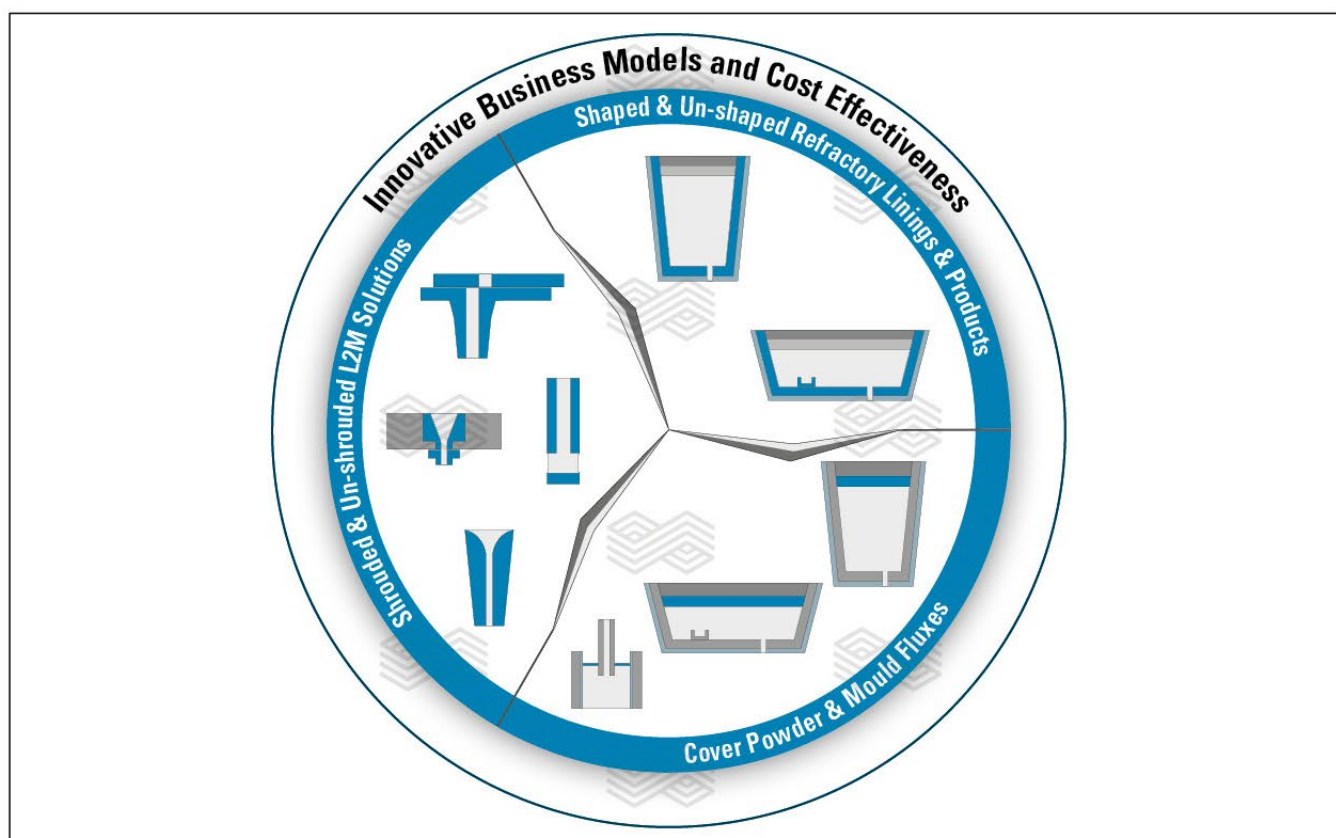


Figure 1. Complete RHI product portfolio now offering also covering powders and mould fluxes.

## How Does it Work in Practice?

### PROIL

PROIL could be taken as a very good example of raising and creating an element the industry has never offered. The product consists of a mixture of synthetic oil and synthetic continuous casting powder, leading to a new product which can easily be defined as a liquid casting powder, pumped at room temperature into the mould [2]. PROIL combines the advantages of a fluid with the properties of a casting powder (Figure 2).

Utility of the system, which includes not only the product itself but the whole pumping and dosing equipment, brings a new value proposition to the steel plant where following phenomena have been observed, as can be seen in Figures 3–6.

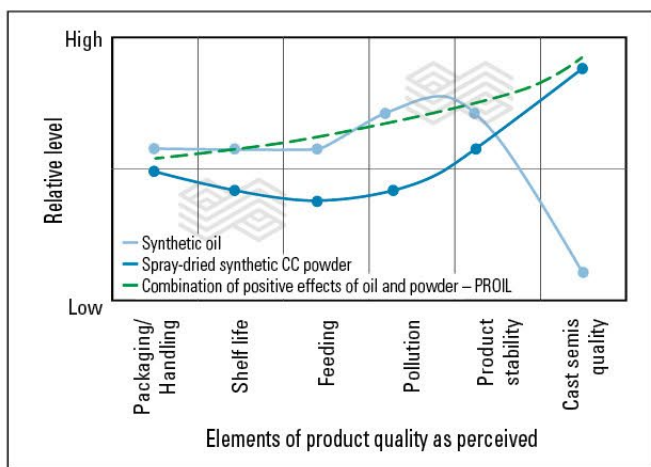


Figure 2. PROIL – The perceived combination of beneficial effects.

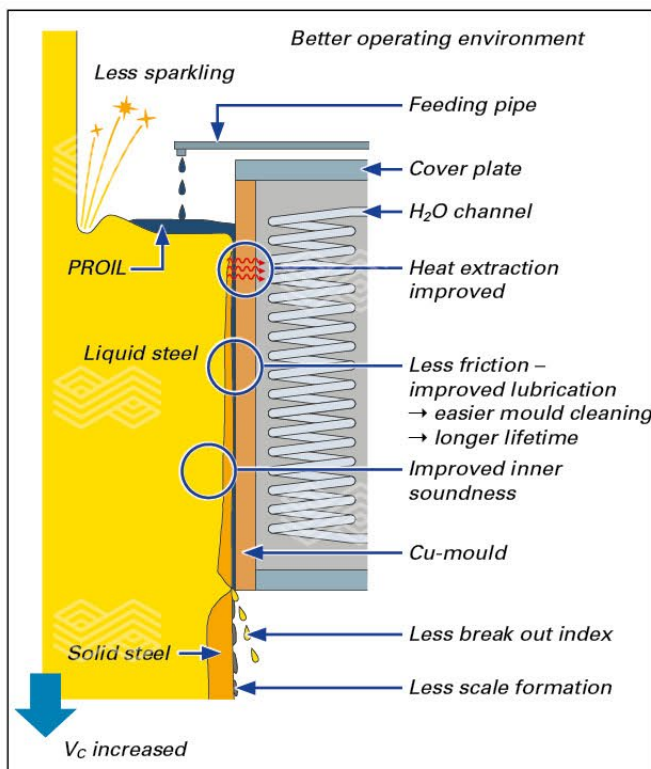


Figure 3. Overview of beneficial effects of the use of PROIL at several industrial billet casters.

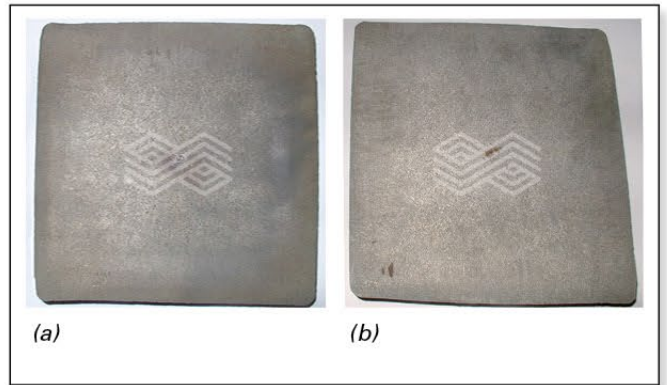


Figure 4. Improved rhomboidity of billets through the use of PROIL, showing (a) quality of billet using PROIL, and (b) using oil.



Figure 5. PROIL – Product appearance on laboratory and industrial scale.

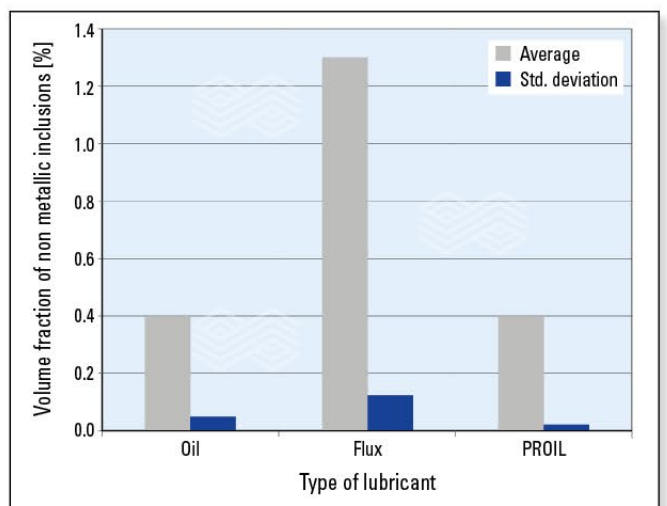


Figure 6. PROIL – Cleanliness compared to the use of mould flux and common oil.



**Casting Solutions—ANKERFILL TCP and DELTEK IF Series**

It is not the intention of this article to present some of the existing products in the ANKERFILL TCP (ladle and tundish covering powder) and DELTEK IF (mould fluxes) series, but to provide some answers to the customer demands when breaking them down to the products:

- >> Has RHI some standard products like the rest of competitors? – **Yes**
- >> Has RHI granulate powders and loose powders? – **Yes**
- >> Can RHI, together with PROSIMET, design a tailor made product for a given customer and application? – **Yes**
- >> Can RHI influence the refractory interaction with slags and covering powders, by offering tailor-made solutions? – **Yes**
- >> Has RHI the raw materials flexibility in order to address any challenge? – **Yes**

**Tailor-Made Ladle-to-Mould Systems Using Laboratory Scale Testing and Thermochemical Modelling**

There is always more than one way to deal with a problem or a situation. RHI has placed the focus on adding value through the solutions offered to the customers, those solutions vary from case to case and from customer to customer. In this way using several tools in order to fulfil the customer’s unique requirements.

Selection of the best materials for the customer process is carried out by conducting a series of thermochemical (Figure 7) as well as computational simulations (Figure 8). These results are crosschecked with laboratory scale test results, carried out under similar process conditions at the Technology Center in Leoben.

**Influence of ANKERFILL TCP on the Performance of Different Wear Lining Mixes**

The laboratory tests are carried out using a similar method to that described in [3] where crucibles are prepared from different tundish mixes, filled with tundish cover powder and fired at 1550 °C for 4 hours. The crucibles are covered at the bottom and the sidewall with coal, but kept open at the top to ensure a reducing atmosphere at the sidewall, while

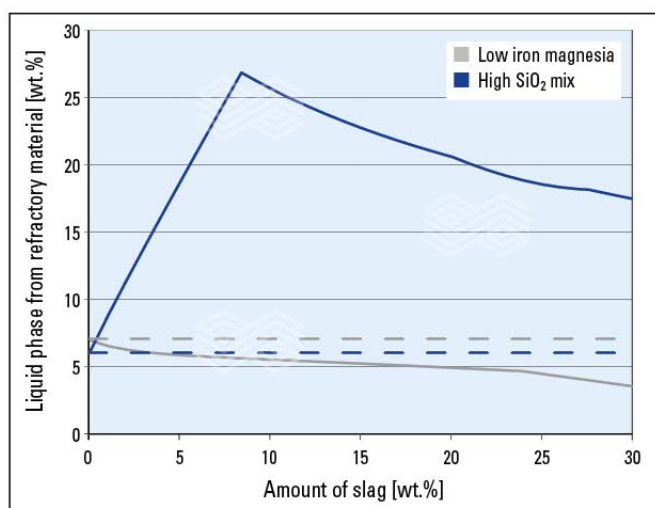


**Figure 7.** Example of FactSage simulation (1550 °C) corresponding to laboratory testing of different wear linings with covering powder. Compare data to images presented in Figure 9.

maintaining an oxidizing atmosphere at the top. After cooling, the crucibles are cut and a mineralogical investigation is performed. Examples of two different mixes in combination with an ANKERFILL TCP powder are presented in Figure 9.

It can be clearly seen, that the interaction between the high SiO<sub>2</sub> containing mix and the cover powder leads to high damage and infiltration of the crucible. The low iron magnesia mix has a lower degree of infiltration and does not show elevated wear, but good corrosion resistance against the slag. The results regarding wear and infiltration are in good accordance with the thermochemical simulation, presented in Figure 7. Dashed lines mark the liquid phase fraction of the mixes with no infiltration, full lines the results from the interaction mix-slag. The simulation predicts a high amount of liquid phase coming from interaction of the high SiO<sub>2</sub> containing mix with the cover powder, whereas no additional liquid phase in interaction with the low iron magnesia is predicted. The decreasing slope of the low iron magnesia predicts a reduced amount of liquid phase by interaction of mix and slag, meaning a stiffening of the mix and thus a decreased wear during casting. Details to these results can also found in [4].

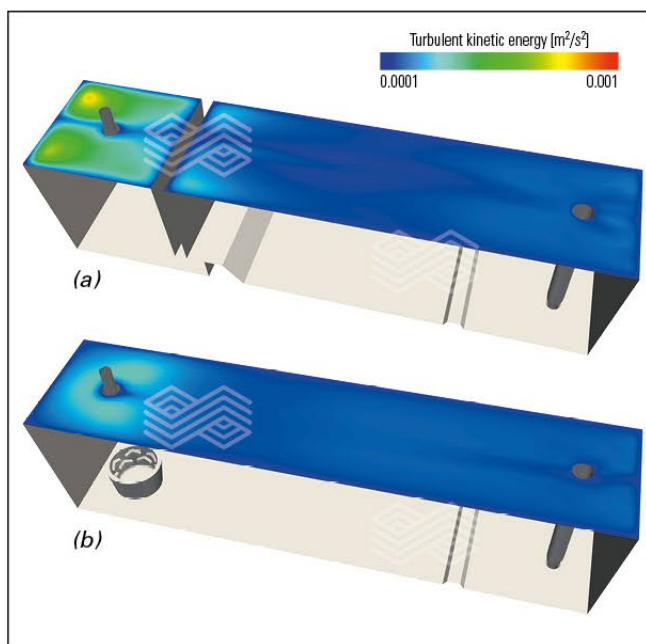


**Figure 8.** Example of a CFD analysis to investigate flow behaviour of the liquid steel, as well as kinetic energy and turbulence showing (a) dam/weir combination and (b) TUNFLOW CHE impact pot.

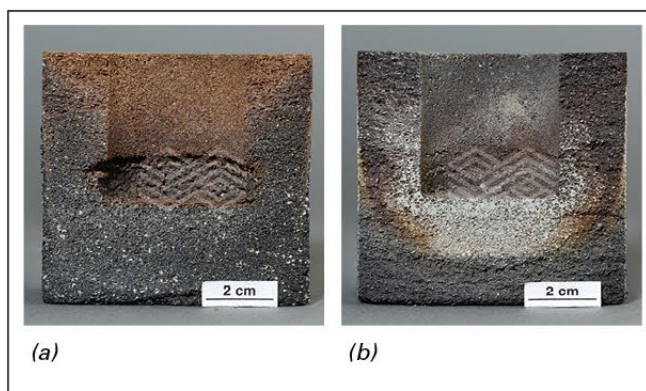


**Figure 9.** Laboratory testing of the interaction between covering powder and different wear lining mixes, showing (a) high SiO<sub>2</sub> mix, and (b) low iron magnesia.

**Influence of DELTEK IF on the Performance of Different SEN Slag Band Materials**

In contrast to the crucible test used for covering powders, materials for isostatically pressed products are also tested under different test conditions. A high amount of mould flux is melted inside a refractory crucible and held at constant temperature under standard atmosphere. The temperature can be selected based on fusion temperature of the flux or aligned to near process conditions, then four so called “fingers” made from different materials (e.g., refractory bricks or isostatically pressed products) are immersed into the liquid slag and kept in rotation at a certain speed. After a defined time the fingers are emerged and cooled to room temperature. A mineralogical investigation is performed after cutting to investigate the microstructure and the wear of the samples.

Images of the emerged unused as well as used fingers after the test are presented in Figure 10. The wear of two different slag line materials of isostatically pressed products is also depicted. The difference regarding the remaining thickness of the samples is a clear indicator for increased wear in contact with the mould flux. As is shown in Figure 11, different qualities of isostatically pressed products can be tested and investigated using this test method.

**Advantages Gained by Extended Services**

Contemporary to completing RHI’s product portfolio by offering now also covering powders and mould fluxes, a new approach towards business models establishes new potentials to increase the customers casting performance and caster equipment. These business models contain customer benefits like variable product prices, premium services or resource releases (Figure 12).

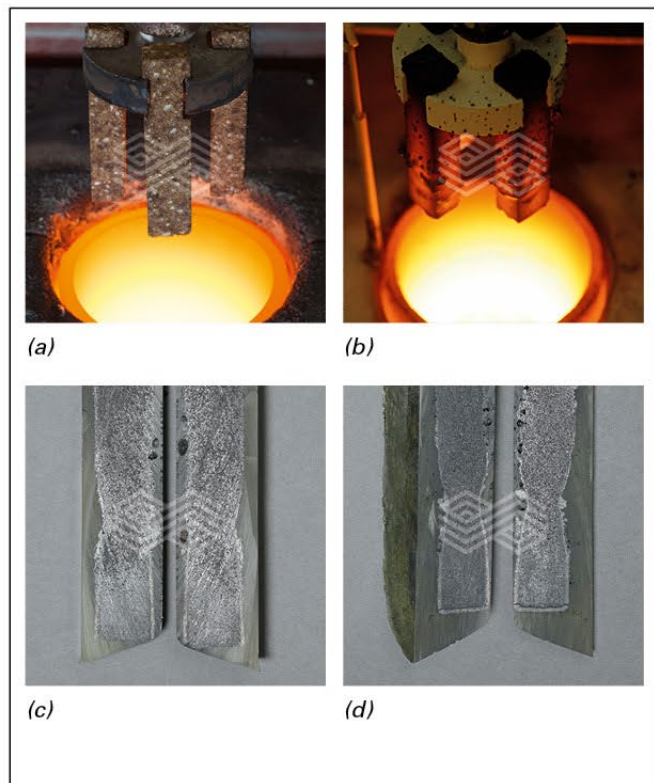


**Figure 10.** Example of finger test and results, showing (a) unused sample, (b) samples lifted above the crucible, (c) ISO slag band material – low wear, and (d) ISO slag band material – increased wear.

- Process consulting—Knowledge exchange
- >> Exchanging information and experiences regarding steel production process,
- >> Working out solutions that are sustainable and innovative,
- >> Active R&D support at the customer,
- >> Incorporate and balance economics vs. solution.

- Clean steel kit
- >> SEM/EDS evaluation of the NMI landscape,
- >> Specific products design and technologies to achieve cleanliness goals,
- >> Cleanliness survey.

- Safety first kit
- >> Specific products design and technologies,
- >> Automation,
- >> AI (avoid-intervention) philosophy.

- On-demand equipment, service and assistance
- >> Expertise multidisciplinary teams to support equipment assistance,
- >> Follow up team for supervision,
- >> Measurement and application equipment.

**Conclusion**

By extending the products and services through the cooperation with PROSIMET, RHI is now, more than ever, able to offer customized products and services to customer process and needs. In this global market environment it is no longer about only having a product to offer, but having the tools to address innovatively what will fit to the customer today, and moreover in the future, when the market situation changes.

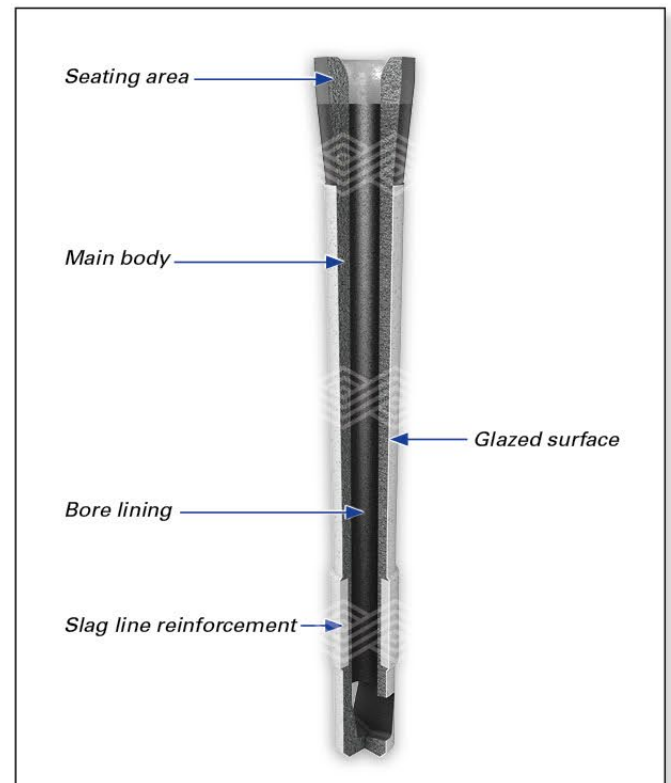


**Figure 11.** Example of qualities of isostatically pressed products that can be tested using the “finger-test”.

Using these new business models, additional service is granted by RHI on the area of responsibility at the customer, if more than singular products, meaning RHI's holistic solutions are purchased in a package.

The target of this cooperation is "value innovation for every single RHI customer; whatever that means to every one of them.

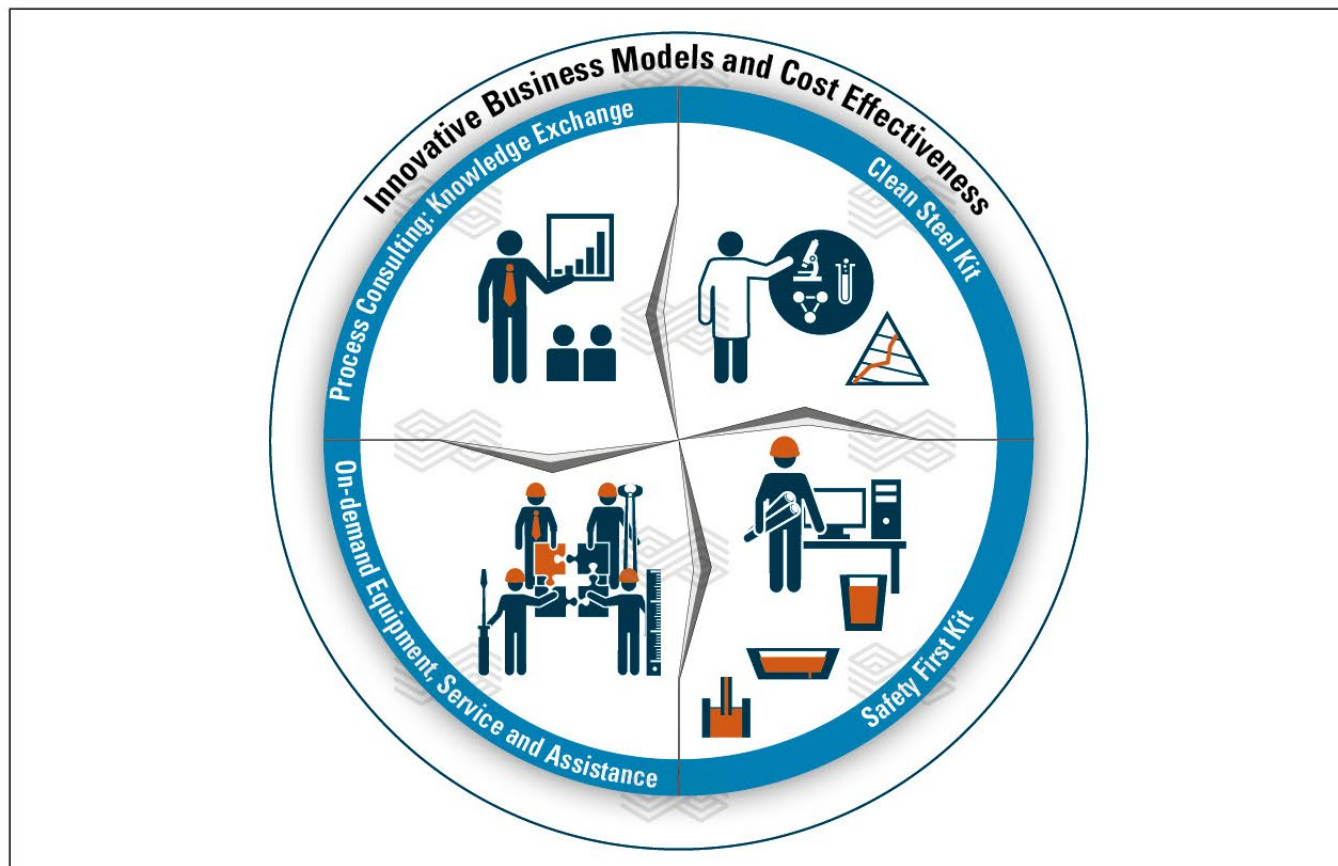


**Figure 12.** Overview of RHI's services to customer using new business models.

## References

- [1] Secklehner, B. A., Tomás Casado, M., Viertauer, A., Wappel, D. and Brosz, B. Tundish Technology and Processes: A New Roadmap *RHI Bulletin*, 2015, No. 1, 68–77
- [2] Nucci, S., Del Moro, A., Carli, R. and Alloni, M. Realizing a Child Dream: Liquid Powder for Continuous Casting. Fact and Figures. Presented at *ESTAD 2015*. Düsseldorf, Germany, June 15–19, 2015.
- [3] Hackl, G., Wappel, D., Meurer, D., Casado, M. T. and Komanecky, R. Product Development and Flow Optimization in the Tundish by Modelling and Simulation, Presented at *AISTech 2014*, Indianapolis, USA, 5–8 May, 2014.
- [4] Wappel, D., Komanecky, R., Petritz, B. and Casado, M. T. New Improvements for Dry Setting Tundish Mixes, Presented at *AISTech 2016*, Pittsburgh, USA, 16–19 May, 2016.

## Disclaimer

The material in this paper is intended for general information only. Any use of this material in relation to any specific application should be based on independent examination and verification of its unrestricted availability for such use and a determination of suitability for the application by professionally qualified personnel. No license under any patents or other proprietary interests is implied by the publication of this paper. Those making use of or relying upon the material assume all risks and liability arising from such use or reliance.

## Authors

Marcos Tomás Casado, RHI Magnesita, Technology Center, Leoben, Austria.

Gregor Arth, RHI Magnesita, Steel Division, Leoben, Austria.

Andrea Giacobbe, RHI Magnesita, Brescia, Italy.

Alessandra del Moro, PROSIMET SpA, Filago, Italy.

**Corresponding author:** Marcos Tomás Casado, marcos.tomas@rhimagnesita.com



Georg Schnalzger, Philip Bundschuh, Roman Rössler, Johannes Schenk and Andreas Viertauer

# Calculation Model to Quantify the Amount of Carry–Over Slag From Primary Metallurgical Plants

Primary metallurgical plants and especially basic oxygen furnaces are usually equipped with slag-retaining systems to control slag carry-over. The amount of carry-over slag is an indicator for the efficiency of these devices. A quantitative evaluation of these systems requires the determination of the mass of carry-over slag. Consequently, in literature several approaches applied in the past have been published. However, their area of application is usually limited to steel grades and production facilities, which were used for the development. Therefore, a new calculation model was developed within a bachelor thesis at Montanuniversitaet Leoben (Chair of Ferrous Metallurgy) in cooperation with RHI and voestalpine Stahl GmbH. This paper gives an overview on the modelling approach and development process. The focus is on the results of an extensive evaluation with industrial process data.

## Introduction

Generally, the separation of steel and slag is insufficient during tapping of primary metallurgical plants. Thus, carry-over slag is unintentionally transferred into the ladle and forms with additives such as lime and magnesia the slag for the subsequent ladle treatments. As reactions in secondary metallurgy usually require reducing conditions, highly oxidizing carry-over slag strongly impairs their efficiency. Especially the high content of SiO<sub>2</sub>, FeO, MnO and P<sub>2</sub>O<sub>5</sub> (Table I) can influence the final product’s quality as well as production costs due to these associated aspects [1,2]:

- >> phosphorus pick-up
- >> silicon pick-up
- >> impact on desulfurization efficiency
- >> steel cleanliness
- >> deoxidation and alloying agent consumption
- >> wear of ladle lining

Therefore, primary metallurgical plants and especially basic oxygen furnaces (BOF) are usually equipped with a slag retaining system, particularly if steel grades limited regarding phosphorus- and silicon contents are produced. To quantify the amount of carry-over slag and consequently to evaluate the tapping performance several methods were used and published in the past [5–11]. In this paper a new calculation model is introduced, which was developed within a bachelor thesis at the Chair of Ferrous Metallurgy at Montanuniversitaet Leoben. An evaluation of the model using process data from voestalpine Stahl GmbH will be presented [3].

## Slag Retaining Systems

Currently, especially BOF are equipped with various slag retaining systems to reach a reproducible steel quality and lowering production costs. The total carry-over slag consists of three characteristic components (Figure 1) [12]:

- >> pre-slag: slag carry-over at tilting begin, due to slag’s lower density compared to steel (30% of total slag carry-over)

	Chemical composition slag [wt. %]						
	FeO	SiO <sub>2</sub>	MnO	CaO	MgO	Al <sub>2</sub> O <sub>3</sub>	P <sub>2</sub> O <sub>5</sub>
BOF	20.7	15.1	7.1	45.5	4.9	3.4	1.65
EAF	32.0	19.0	5.0	28.0	7.0	7.0	0.40

**Table I.** Average chemical composition of primary metallurgical slags (carry-over slags) for low-alloyed steel production with basic oxygen furnace (BOF) and electric arc furnace (EAF) [3,4].

- >> vortex: slag carry-over during tapping steel due to the formation of whirls (30%)
- >> post-slag: slag carry-over at tilting end, due to slag’s lower density compared to steel (40%)

The slag retaining device minimises the amount of post-slag. In addition, some technologies have also been developed for the minimisation of pre-slag. Generally, systems are divided into two groups according to their functional principle [1,10,12]:

- >> floating body systems
- >> mechanical interlocking systems

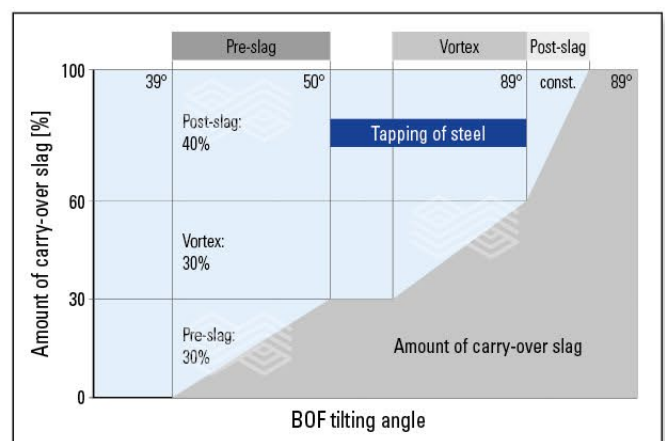


**Figure 1.** Tapping procedure BOF [12].

Within the first group lockers with different shapes, e.g., balls, tetrahedrons or darts have prevailed for BOF. Devices are introduced into the converter during tapping and float on the steel bath but remain under the slag due to their specifically chosen density. Consequently, these bodies seal the tap hole before an extensive amount of post-slag is tapped. [1,12]

In contrast, mechanical interlocking systems are mounted on the vessel's steel shell and thus can retain post-slag as well as pre-slag. At present two technologies are commonly used [10,12]:

- >> pneumatic slag stopper
- >> slide gate system

The core of the first system is a hinged moveable arm with a cast iron nozzle. Gas (e.g., nitrogen) is conveyed through the nozzle at high pressure and the tap hole is sealed by means of a gas jet blowing into the tap hole from the outside [12].

Occasionally slide gate systems, which are more common in electric arc furnaces (EAF) and standard for ladles, are also used for BOF [10].

The visual detection of slag in the tapping stream with the naked eye strongly depends on the skills of the operator. Formation of fumes and gases exacerbate the situation further. To guarantee standardized and reproducible operational conditions, interlocking systems are usually directly triggered by the signal of an automatic slag detection system. Currently, two differentiating properties of steel and slag are utilized for these systems [1,12]:

- >> electromagnetic characteristic
- >> infrared emissivity characteristic

Electromagnetic indication systems consist at least of one current carrying coil, which is located inside the tap hole socket. During tapping the characteristic change of the magnetic field caused by different interferences of steel and slag is monitored. From the signal record, the accurate moment for triggering the slag-retaining system is set [12].

In thermographic slag detection, an infrared sensor measures the surface of the tapping stream. As slag has a higher emissivity than steel in the infrared range, the appearance of slag can be detected. With rising sensitivity of the slag detection system, the remaining steel in the furnace increases. This can negatively influence the steel yield. [2]

The achievable amount of carry-over slag strongly depends on the system (Figure 2) [10].

### Quantification of Carry-Over Slag

In the past, several methods were used for the quantification of carry-over slag. Table II illustrates that the clear majority of published calculation models are based on element mass balances. Usually, details about the models are not mentioned especially regarding the development and evaluation process. In addition, each model is tailor-made for a specific steel grade group and production parameters. Consequently, the models' areas of application are restricted. Thus, a new model, which could be more

universally applicable, was devised for the quantification of carry-over slag [3,5–11].

### Introduction of a New Calculation Model

Following most calculation models in literature, the new model is based on element mass balances. The model was devised with industrial data from voestalpine Stahl GmbH in Microsoft Excel®. Concretely, specific steel mill's process data of heats belonging to one steel grade group were selected and used for the development. Furthermore, a sensitivity analysis was implemented to determine the effect of common measurement inaccuracies on the calculation results occurring during input data acquisition [3].

The provided heats are aluminium killed and pre-alloyed during tapping. To control the amount of carry-over slag, the BOF was equipped with a pneumatic slag stopper triggered by a thermographic slag detection system. The ladle was transferred to a ladle furnace (LF) after a few minutes of argon stirring at a ladle purging station (LPS). At the LF, the steel was desulfurized to very low-level and the chemical composition as well as the temperature are set. Before continuous casting (CC) the heats were degassed at a Ruhrstahl-Heraeus degasser (RH). During several production steps steel- and slag samples were taken. All relevant data concerning alloying and slag forming additions (short: additions), e.g., type, amount, and location of addition, are available and used for the model. In Figure 3, the process steps and specific process data used for the calculation model are summarized graphically.

Calculation model	Quantification principle
Turkdogan [8]	Phosphorus mass balance
Loescher, Pluschke and Scheel [5]	Iron mass balance
Boecher <i>et. al.</i> [10]	Phosphorus mass balance (combination with vanadium- and chromium mass balance)
Jánosfy <i>et. al.</i> [6]	Aluminium mass balance
Jandl [7]	Independent aluminium oxide- and phosphorus mass balance
Reisinger, Pissenberger and Zumba [9]	Correlation of mass increase of ladle and EMLI-signal
Li <i>et. al.</i> [11]	Addition of barium carbonate (BaCO <sub>3</sub> ) and mass balance

Table II. Overview on quantification methods from literature [5–11].

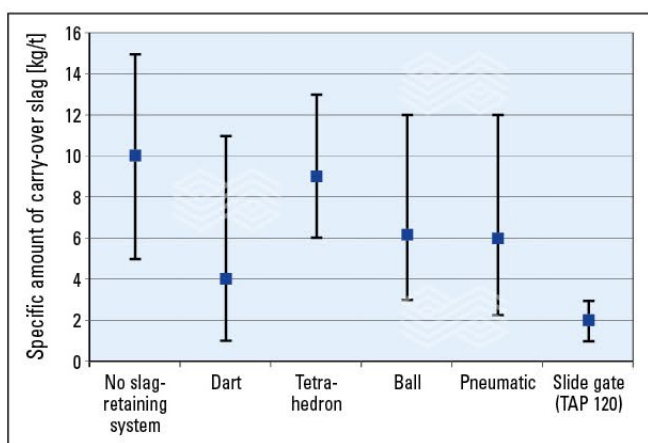


Figure 2. Quantitative comparison of different slag-retaining systems [10].

### Mass Balances

The model provides the opportunity to quantify the mass of carry-over slag from two independent balances, as a phosphorus and an aluminium mass balance is implemented. All necessary input parameters are obtained from the process data in Figure 3.

#### Yield Calculation

For the determination of the mass contribution from additions, which are charged during tapping and secondary metallurgy, a yield calculation is integrated in the model (Figure 3). This section uses information about additions and enables in combination with the weighing result at the ladle turret the calculation of the steel and slag mass at every process step.

#### Phosphorus Mass Balance

For the quantification of carry-over slag based on a phosphorus balance the boundaries marked in Figure 3 are used. Consequently, the amount of carry-over slag is determined from Equation 1. Accordingly, the calculation requires steel and slag samples, which are taken at LPS and LF. In addition, a BOF slag sample, the phosphorus input from additions, as well as the results from the yield calculation are required. All formula symbols of Equation 1 are listed in Table III.

$$m_{COS} = \frac{m_{P, Steel, LF} + m_{P, Slag, LF} - m_{P, Slag, LPS} - m_{P, Input}}{wt.\% P_{Slag, BOF}} \quad (1)$$

A study of five heats produced at voestalpine Stahl GmbH (Figure 3) showed, the term  $m_{P, Slag, LF}$  in Equation 1 is negligible for this steel grade group, as its consideration influences the calculation result only marginally. Therefore, Equation 1 can be simplified to Equation 2 for these heats. However, it must be kept in mind that for the investigated heats the average phosphorus content in the ladle slag was very low (84 ppm) due to the deoxidation with aluminium. Consequently, Equation 2 is not universally applicable. The reason for this is described later [3].

$$m_{COS} = \frac{m_{P, Steel, LF} - m_{P, Slag, LPS} - m_{P, Input}}{wt.\% P_{Slag, BOF}} \quad (2)$$

#### Aluminium Mass Balance

For the quantification of carry-over slag based on aluminium mass balance the boundaries shown in Figure 3 are taken. The amount of carry-over slag is calculated from Equation 3. In contrast to the phosphorus balance, the steel sample from BOF is used instead of the one from LPS, as the aluminium content of crude steel is zero, which guarantees a certain initial condition. Therefore, in Equation 3 the mass of aluminium in crude steel is considered only formally. Beside this information, a steel sample taken at LF, the aluminium inputs from additions, as well as the results of the yield calculation are required. All formula symbols of Equation 3 are shown in Table IV [3].

$$m_{COS} = \frac{m_{Al, Steel, LF} + m_{Al, Slag, LF} - m_{Al, Steel, BOF} - m_{Al, Input}}{wt.\% Al_{Slag, BOF}} \quad (3)$$

According to investigations, in contrast to the phosphorus balance for the provided heats, the slag sample taken at LF must be considered at this point. As the average alumina content of the LF slag is 28.82 wt.% for these heats, Equation 3 cannot be further simplified [3].

Formula symbol	Description
$m_{COS}$	Mass of carry-over slag
$m_{P, Steel, LF}$	Mass of phosphorus in steel at LF
$m_{P, Slag, LF}$	Mass of phosphorus in slag at LF
$m_{P, Slag, LPS}$	Mass of phosphorus in steel at LPS
$m_{P, Input}$	Mass of phosphorus yielded with additions
$wt.\% P_{Slag, BOF}$	Phosphorus content of BOF-slag

Table III. Formula symbols Equation 1.

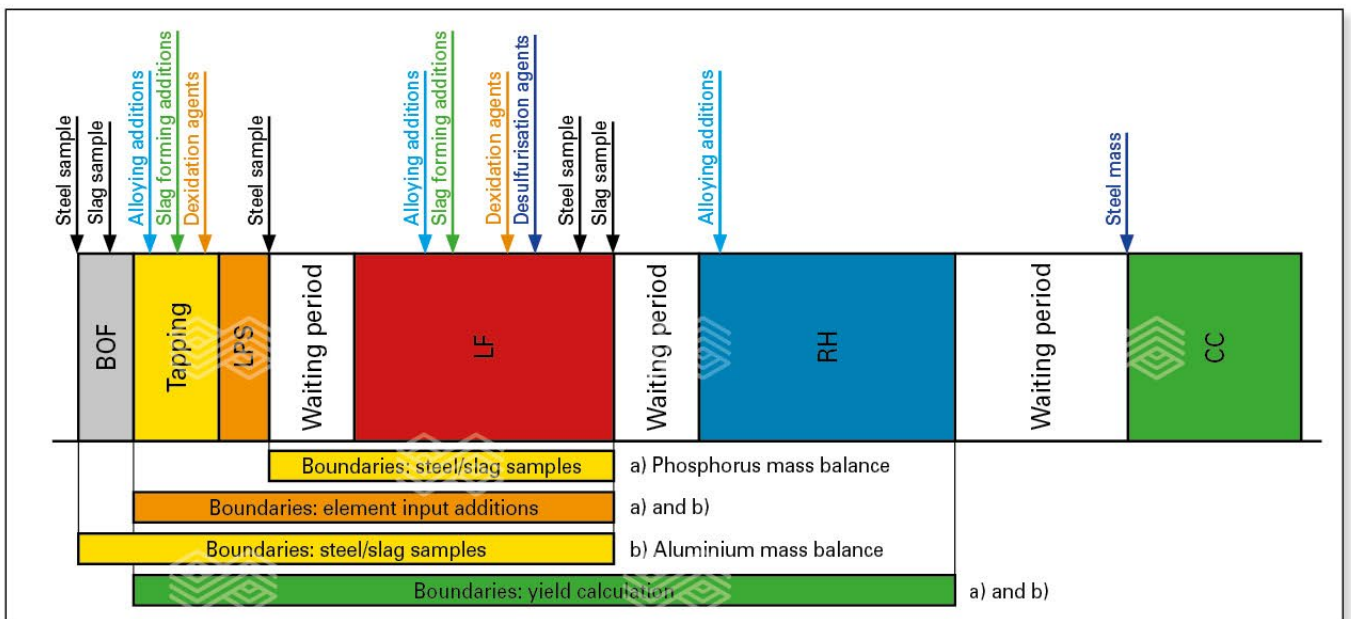


Figure 3. Process steps and actions during operation at steel mill voestalpine Stahl GmbH and (a) balancing zones for phosphorus and (b) aluminium mass balance.

Formula symbol	Description
$m_{COS}$	Mass of carry-over slag
$m_{Al, Steel, LF}$	Mass of aluminium in steel at LF
$m_{Al, Slag, LF}$	Mass of aluminium in slag at LF
$m_{Al, Steel, BOF}$	Mass of aluminium in steel at LPS
$m_{Al, Input}$	Mass of aluminium yielded with additions
$wt.\% Al_{Slag, BOF}$	Aluminium content of BOF-slag

Table IV. Formula symbols Equation 3.

### Sensitivity Analysis

A sensitivity analysis, which considers independently three types of measurement errors (Table V), was implemented for both balances in this model. Therefore, this section enables the determination of the impact of common measurement inaccuracies occurring during input data acquisition on the calculation result [3].

For the provided heats, a study regarding the impact of measurement errors was carried out. According to this, only

Error from	Description
Steel weighing	Scattering of result of steel mass weighing at ladle turret ( $\pm 1\%$ )
Steel sample analysis	Element analysis scattering ( $\pm 3x$ standard deviation for each sample)
Addition analysis	Element analysis scattering ( $\pm 3x$ standard deviation for each sample)

Table V. Types of measurement errors.

the error of the steel sample analysis has a critical effect on both mass balances and restricts the calculation's accuracy. Therefore, all other types are neglected for the following evaluation of the model [3].

### Evaluation

The evaluation of the model was carried out with process data of five heats, which were produced according to the previously mentioned process steps at voestalpine Stahl GmbH. First, the mass of carry-over slag was quantified from both mass balances without consideration of any measurement inaccuracies (average masses of carry-over slag) for all heats. Secondly, the implemented sensitivity analysis was used to determine the resulting scatters caused by the error of steel sample analysis (minimum and maximum masses of carry-over slag).

### Results

In Figure 4 all results obtained from the investigated heats are summarized graphically. For a better illustration, the masses of carry-over slag were correlated with the corresponding total phosphorus pick-up  $\Delta P_{tot}$  during secondary metallurgy. This phosphorus pick-up is calculated from the chemical analyses of two steel samples with Equation 4.

$$\Delta P_{tot} = (wt.\% P_{Steel, Ladle Furnace}) - (wt.\% P_{Steel, Ladle Purging System}) \quad (4)$$

In general, the total phosphorus pick-up consists of two parts:

- >> phosphorus input from charged additions ( $P_{additions}$ )
- >> rephosphorization from carry-over slag ( $P_{carry-over\ slag}$ )

The lines in Figure 4 are determined and extrapolated by means of linear regression of the discretely calculated points. As within the investigated heats the maximum

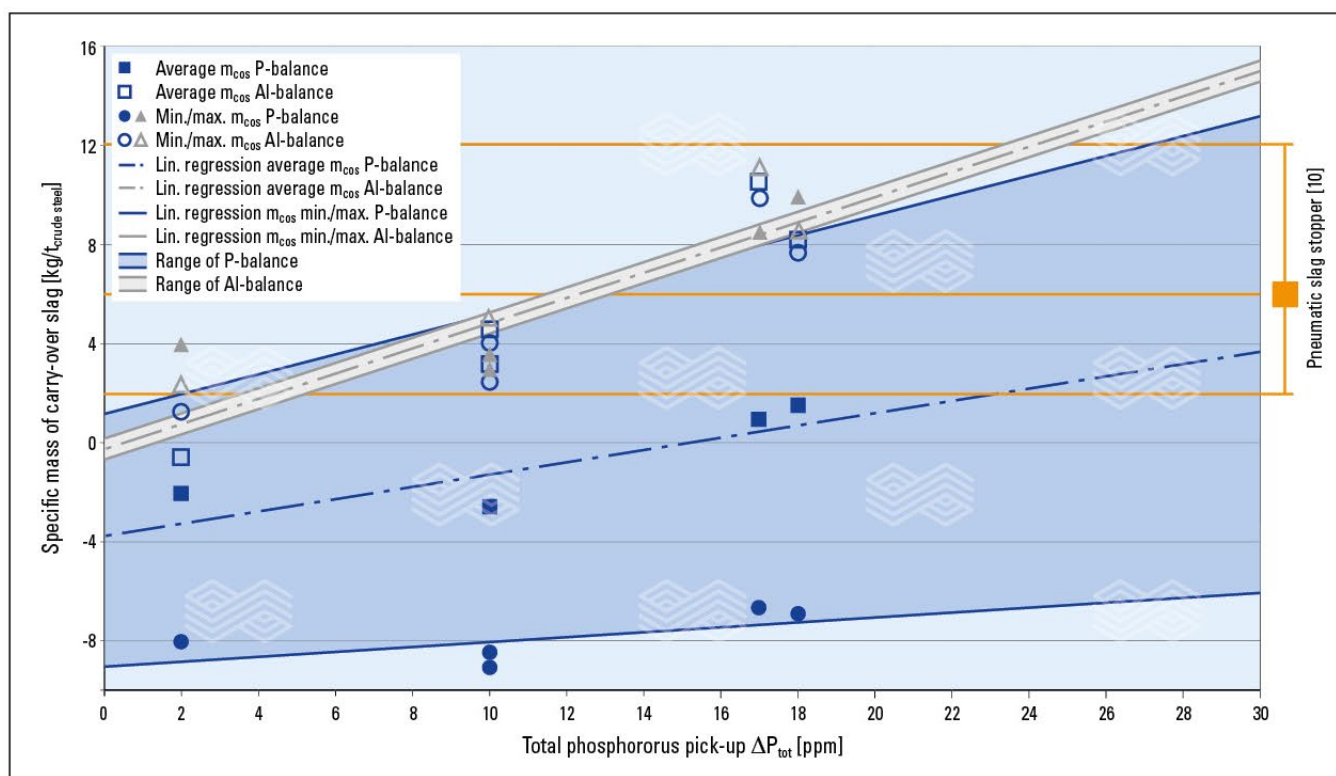


Figure 4. Results of the calculation model for heats from voestalpine Stahl GmbH (diagram only valid for investigated heats) [10].

phosphorus pick-up is 18 ppm, all functions are theoretically only valid up to this value. For a comparison with data from literature the published range for the pneumatic slag stopper is also plotted in the diagram (horizontal lines) [10].

### Discussion

For the investigated heats both mass balances lead to different average values for the mass of carry-over slag. While the results gained from the aluminium balance correlate with data of the pneumatic slag stopper from literature, the phosphorus balance leads to negative masses for most investigated heats [10].

Furthermore, the scatters calculated from the sensitivity analysis are variable. From this point of view, the aluminium balance is less sensitive regarding the considered measurement inaccuracies, as the scatter is clearly narrower. With further investigation two reasons were found for this effect. Firstly, for the quantification of carry-over slag from the aluminium mass balance only one steel sample is required, as the aluminium content in the BOF is zero (Equation 3). In contrast for the phosphorus balance two samples are used (Equation 2). Secondly, the aluminium content measured in the samples is much higher compared to the phosphorus contents, as aluminium is used for deoxidation and phosphorus is an undesired tramp element for the investigated heats. As a result, measured phosphorus contents are far smaller compared to those of aluminium. Consequently, measurement inaccuracies have a greater impact on the phosphorus analysis in relative terms.

Under consideration of the error from the steel sample analysis, the maximum values gained from the phosphorus balance correlate very well with the results of the aluminium balance. Therefore, both balances give an indication for the mass of carry-over slag considering the

measurement accuracy. Nevertheless, the aluminium balance is considered to be more suitable for the quantification of carry-over slag for the investigated heats for two reasons:

- >> less sensitivity to error from the steel sample analysis
- >> correlation with comparable data published by Boecher *et. al.* [10]

The mass balances were not evaluated with further industrial data. In this form they are consequently only applicable for the investigated heats. However, for a more universally applicable indication of carry-over slag the phosphorus mass balance was modified.

### Indication of Carry-Over Slag for Selected Heats From Phosphorus Mass Balance

For the indication of carry-over slag for other selected heats the phosphorus content of the converter slag was varied manually for the provided heats. Furthermore, the phosphorus input from additions was neglected, while all remaining data were left unchanged. Due to this negligence,  $\Delta P_{tot}$  is equivalent to  $P_{carry-over\ slag}$  and consequently all functions only depend on the rephosphorization from carry-over slag. The mass of carry-over slag was determined for all five heats and correlated again with the total phosphorus pick-up  $\Delta P_{tot}$  (Figure 5). All linear slopes are constructed by means of linear regression of the discretely calculated points, which are not shown in Figure 5.

Finally, the full lines in Figure 5 enable the estimation of carry-over slag for melts, which fulfil the following assumptions:

- >> total phosphorus pick-up caused by rephosphorisation from carry-over slag

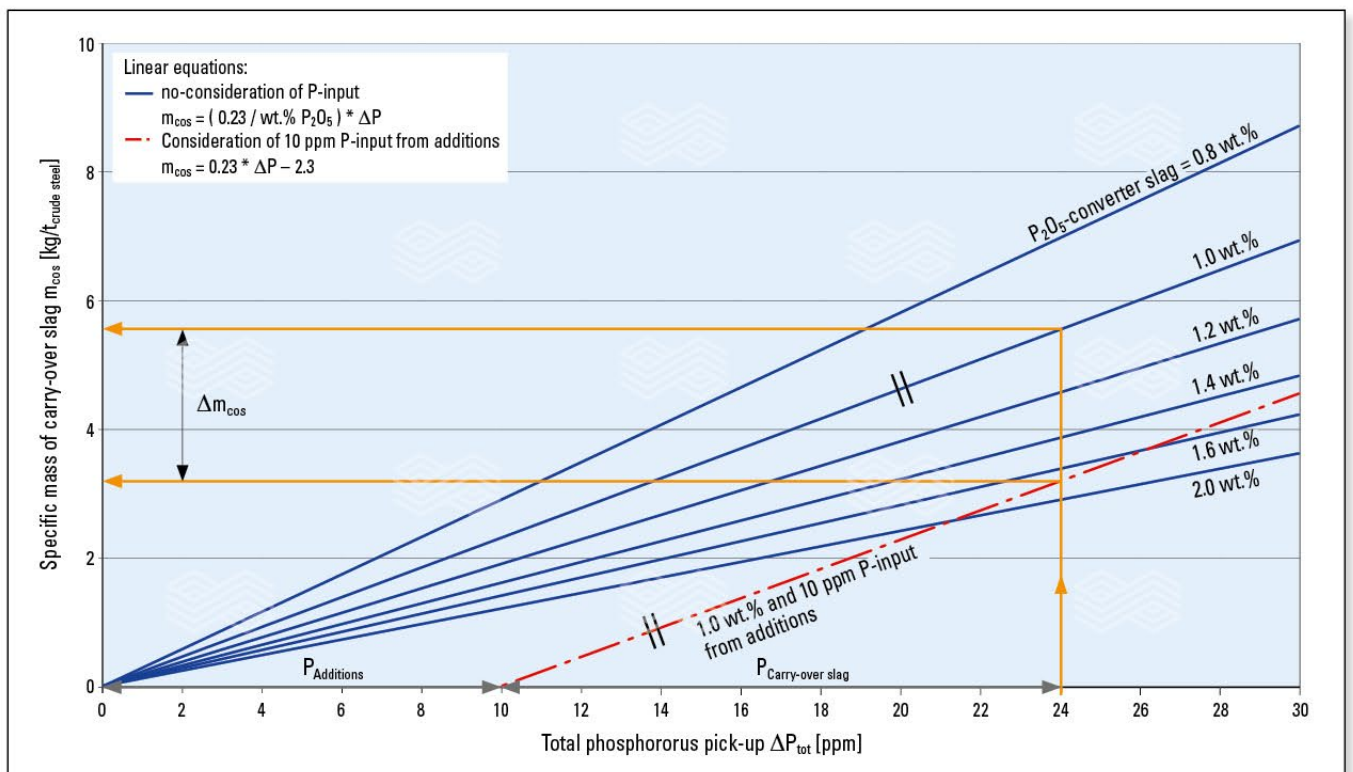


Figure 5. Diagram for the estimation of carry-over slag for selected melts (based on the previous assumptions).



- >> no consideration of phosphorus input from additions
- >> P<sub>2</sub>O<sub>5</sub> content of ladle slag is 0 wt.%

However, it must be kept in mind that the figure only considers average values, as the previously mentioned measurement inaccuracies are neglected.

For a phosphorus content of 1 wt.% in BOF slag and a freely chosen phosphorus input of 10 ppm from additions, the effect of the consideration of phosphorus input from additions is shown as an example in Figure 5 (dashed-dotted line).

For a total phosphorus pick-up of 24 ppm the impact of the phosphorus input from additions is shown in Figure 5. In addition, it is illustrated how to determine both parts of the phosphorus pick-up.

## Conclusion

The present paper describes an approach for a new calculation model to quantify carry-over slag from primary metallurgical plants. This model enables the determination of carry-over slag from a phosphorus and an aluminium mass balance. After developing the model an evaluation with selected industrial data from voestalpine Stahl GmbH was carried out. The following results could be gained from this:

- >> The quantification of carry-over slag without consideration of measurement inaccuracies leads to totally different results for the investigated heats for both element mass balances. Values obtained from the aluminium

mass balance correlate very well with data published [10]. The phosphorus mass balance predominately leads to negative results, which are physically impossible but are considered in the model with the selected heats from voestalpine Stahl GmbH.

- >> Within a sensitivity analysis, it was found that the error from the steel sample analysis has a significant impact on both mass balances. For the aluminium balance the scatter is clearly less compared to the phosphorus balance and results correlate very well with data from literature. However, the maximum values gained from the sensitivity analysis for the phosphorus balance also correlate with results from the aluminium balance. From this point of view, the phosphorus balance is more sensitive regarding the error from the steel sample analysis for the detailed investigated and analysed heats.
- >> The evaluation also showed, that the model is not generally applicable for any heat, as the calculation strongly depends on the alloying concept and process parameters. However, with a few assumptions (e.g., no phosphorus input from additions) a figure was created to obtain an indication of carry-over slag for heats fulfilling the specific assumptions.

Finally, the phosphorus contents (mean value: 80 ppm) and the phosphorus pick-up (mean value: 11 ppm) were very low for the five investigated heats. Consequently, the error from the steel sample analysis has a significant impact and leads even to negative amounts of carry-over slag. A final adjustment of the model and therefore a universal application for any heat of it was not scope of the work.

## References

- [1] Block, F.R. and Piotrowiak, R. Verringerung der Menge an Mitlaufschlacke bei der Stahlherstellung. *Stahl und Eisen* 116. 1996, 2, 95–99.
- [2] Li, J., Zhou, J., Zhong, Z., Li, C. and Kong, X. Application of Thermographic Slag Detection System in Baosteel. Presented at AISTech 2007, Indianapolis, Ind., USA, May 2007, 1-10.
- [3] Schnalzger, G. Bachelorarbeit, Montanuniversitaet Leoben, Austria, 2016.
- [4] European Commission. Best Available Techniques (BAT) reference document for iron and steel production, Seville, Spain, 2013.
- [5] Loescher, W., Pluschkell, W. and Scheel, H. Pfanenschlacken bei der Stahlnachbehandlung. *Koch, K., Janke, D. Schlacken in der Metallurgie*. 1984, 263–280.
- [6] Jánosfy, G., Kónya, S., Karóly, Z. and Károly, G. Metallurgical Aspects of Oxygen Soluble Aluminium Control of Low Carbon Aluminium Killed Silicon Free Converter Steels. Presented at 2<sup>nd</sup> European Oxygen Steelmaking Congress, Taranto, Italy, October 1997, 407–415.
- [7] Jandl, C. Diplomarbeit, Montanuniversitaet Leoben, Austria, 2005.
- [8] Turkdogan, E.T. Fundamentals of steelmaking. London, UK, 2010.
- [9] Reisinger, P., Pissenberger, E. and Zuba, G. Slag Carry-Over A Quantitative Analysis During Tapping. Presented at 19<sup>th</sup> International ATS Steelmaking Days, Paris, France, December 1998, 26–27.
- [10] Boecher, G., Grethe, U., Kempken, J., Schnurrenberger, E., Amsler, H. and Müller, H. Further Improvements on Clean Steel Technology with the Converter Tap Hole Gat TAP 120. Presented at 3<sup>rd</sup> European Oxygen Steelmaking Conference, Birmingham, UK, March 2000, 1–9.
- [11] Li, H., Chen, T., Chen, L. and Guo, D. Research and Application of Control Technology for the Amount of Slag-roughing in Converter Tapping Process. Presented at 5<sup>th</sup> International Conference on Advanced Design and Manufacturing Engineering, Shenzhen, China, September 2015, 1977–1983.
- [12] Enkner, B., Paster, A. and Schwelberger, J. New slag stopping system for oxygen converter steelmaking. *MPT International*. 2001, 3, 40–45.

## Annotation

This paper is an extract of the bachelor thesis from Mr. Schnalzger. The work was carried out under supervision of the co-authors. The thesis was honoured with the INTECO-ASMET Award 2017 Category Bachelor Thesis in May 2017 at Leoben.

## Authors

Georg Schnalzger, Chair of Ferrous Metallurgy, University of Leoben, Austria.

Philip Bundschuh, Chair of Ferrous Metallurgy, University of Leoben, Austria.

Johannes Schenk, Chair of Ferrous Metallurgy, University of Leoben, Austria.

Roman Rössler, voestalpine Steel Division AG, Austria.

Andreas Viertauer, RHI Magnesita, Steel Division, Austria.

**Corresponding author:** Andreas Viertauer, andreas.viertauer@rhimagnesita.com



Christoph Piribauer, Anthony McEaney, Anna Felsner, Erich Feichtenhofer and Gerald Gelbmann

# Investigation of Caustic Calcined Magnesium Oxide Produced From Seawater for Hydrometallurgical Applications in Cobalt and Nickel Extraction Processes

As part of a major diversification project, RHI, through its plant in Drogheda Ireland, has developed a caustic calcined magnesium oxide (CCM) for use in the cobalt (Co) and nickel (Ni) hydrometallurgical extraction industry. In the course of the development, the chemical and physical properties of a number of different magnesia's used in Co and Ni hydrometallurgy applications were investigated. The goal of this study was to determine the important parameters for a special designed CCM quality for hydrometallurgical applications. A number of live plant trials have confirmed the results of this test work. The next step is now to produce this product in commercial quantities at RHI Magnesita, in Drogheda, Ireland. This paper will outline the development work conducted in strong cooperation between the R&D department raw materials and Sales raw materials, and highlight the important chemical and physical properties for a successful Co hydroxide precipitation. Much of the research was conducted at the RHI Technology Center in Leoben, Austria. In addition, a number of external laboratory studies were conducted on behalf of RHI. The result of this work has allowed the company to develop a magnesia product with optimised properties for use in the cobalt and nickel hydrometallurgical extraction process.

## Introduction

RHI Magnesita produces magnesia from seawater at its plant in Drogheda, Ireland. While the main focus is on production of refractory grade dead burned magnesia for the steel industry, the plant also produces a number of different grades of caustic calcined magnesia as well as magnesium hydroxide products. As part of a major project to diversify the company's product base, the use of CCM in the cobalt (Co) and nickel (Ni) hydrometallurgical extraction industry was investigated. One of the company's highly reactive grades of caustic calcined magnesia was found to be particularly suitable for this application. In an effort to understand what makes a successful magnesia for hydrometallurgy the chemical and physical properties of different magnesia's used in Co and Ni hydrometallurgy were investigated. This paper outlines the findings of this process.

Magnesium oxide or magnesia (MgO) is produced commercially by two main processes. By sheer volume based on tonnage, the important production process is by calcination of natural magnesite ( $\text{MgCO}_3$ ). The second important commercial process is based on thermal decomposition of magnesium hydroxide ( $\text{Mg(OH)}_2$ ), which is obtained from seawater or magnesium rich brines. Large deposits of magnesite are found in Austria, Australia, Brazil, Canada, China, Russia, Slovakia, Greece, Turkey, Spain, North Korea, and USA, while the main producers of magnesia from seawater or brines are located in Ireland, The Netherlands, Israel, and USA [1].

The physical properties of the magnesia are determined primarily by the calcination conditions. Depending on the

conditions, caustic calcined magnesia (CCM) or dead burned magnesia (DBM) is obtained. The chemical composition of magnesia is mainly determined by the source. If the MgO comes from calcination of natural magnesite, the chemical composition will reflect the composition of the original mine. In the case of seawater derived magnesium oxide, there is some scope to manipulate the final chemistry of the CCM or DBM products. Caustic calcined magnesia is typically produced by calcination of magnesite or magnesium hydroxide in temperatures up to 1000 °C and dead burned magnesia by temperatures above 1600 °C.

The most important application for magnesium oxide is as dead burned magnesia in the refractory industry, where its high melting point and resistance to hydration make it an ideal refractory material. Caustic calcined magnesia is much more reactive due to the lower production temperatures. This gives it a much wider range of applications including agricultural, industrial, chemical, construction, environmental, pharmaceutical and others. The chemical purity and reactivity largely determine the end application.

In recent years a new and important application for caustic calcined magnesia has emerged in hydrometallurgical circuits, specifically in the cobalt, nickel, uranium and rare earth metal processing industries, where it's used to precipitate the metal hydroxide. Magnesia offers a number of advantages over the more common and cheaper calcium based alkali sources, such as lime, in hydrometallurgical processes. The first major advantage with magnesia is that in a sulphate circuit insoluble gypsum (calcium sulphate,  $\text{CaSO}_4$ ) is not produced. A second important benefit is that

it produces a precipitate that's more easily processed in the subsequent thickening, filtration and washing steps. This is due to the slower precipitation rate from magnesia resulting in a metal hydroxide morphology with larger, heavier crystals [3].

Looking more specifically at the use of magnesia in cobalt hydrometallurgical processes, Miller described the process as following [3]:

At the wetted magnesia surface, magnesia reacts with water



Magnesium hydroxide precipitates at the magnesia surface.



The outer layer of the magnesium hydroxide surface re-dissolves in the bulk solution



The important parts of the process are the delivery of water molecules to the magnesia surface and dissolution of the magnesium hydroxide skin to expose a fresh magnesia reaction surface.

Metal hydroxide precipitation process is described as follows



Higher pH levels are required for precipitating cobalt than for other metal hydroxides such as copper. It must be noted, however, that at higher pH levels the driving force for dissolution of the alkali reagent is reduced. This is relevant for magnesium hydroxide, whose solubility limit is closer to that of cobalt and manganese [3]

The reactivity of the magnesia is important in two main aspects. Firstly it must yield a metal precipitate with the correct morphology for settling and further processing. Secondly, the magnesia must be readily available to react with the dissolved metal to precipitate the metal hydroxide. Unreacted magnesia will remain as an impurity. It is then unavailable for further reaction, requiring the operator to add more magnesia to allow the reaction to continue. This leads to poor magnesia utilization and possible overdosing of magnesia, thus adding to increased operating costs [3].

## Experimental Procedure

Various physical and chemical properties of nine different caustic calcined magnesia's were examined and compared. Some of the CCM products examined were derived from magnesite and others from seawater or brine. The primary objective of the testwork was to compare the RHI Magnesita caustic calcined magnesia product PREMIER TM45, made from seawater, with other commercially available caustic calcined magnesia, some of which are used in hydrometallurgical applications. Samples from some plant trials conducted at RHI Magnesita were also included in the testwork. A secondary objective of the study was to define an optimum set of physical properties for caustic calcined

magnesia for hydrometallurgical applications, specifically for cobalt and nickel processing. Details of the various samples tested are shown in Table I.

Sample	Source
Sample 1	Brine
Sample 2	Magnesite
Sample 3	Magnesite
Sample 4	Magnesite
Sample 5	Brine
Sample 6	Seawater
Sample 7	Seawater
TM45-1	Seawater
TM45-2	Seawater

**Table I.** Caustic calcined magnesia samples tested and their source.

Physical properties examined include reactivity by citric acid activity, specific surface area measured by the B.E.T. method (DIN ISO9277) and particle size distribution with a Sympatec laser diffraction HELOS instrument. In addition, certain chemical parameters like loss on ignition (LOI) measured at 1025 °C for 30 minutes (according ISO 26845), MgO content and various impurity levels such as CaO, SiO<sub>2</sub> and Fe<sub>2</sub>O<sub>3</sub> (measured by X-ray fluorescence, according ISO 26845) were examined. Additional testwork conducted by an external consultant on behalf of RHI is also presented and discussed.

Citric acid reactivity (CAR) is a standard industry test for assessing the reactivity of different types of magnesia. The time taken for the magnesium oxide to neutralise the citric acid solution is measured. Neutralisation is detected by the colour change from white to pink due to phenolphthalein indicator mixed with the citric acid solution. In addition the total change in pH over the time is recorded. Values less than 60 seconds are considered by industry to be indicative of highly reactive magnesia [5].

Specific surface area was measured by a technique based on the DIN ISO 9277 standard, which describes measurement of specific surface area in porous solids by gas adsorption technique based on the B.E.T. theory developed by Brunauer, Emmett and Teller [2]. The instrument used was a Micromeritics Flow Sorb III 2305.

The particle size distribution of the test magnesia samples was analysed by a Sympatec laser diffraction HELOS instrument. Laser diffraction for particle size measurement uses the diffraction of the laser light with the particles being measured to determine particle size. The analyser utilises the Fraunhofer or Mie theories and is specifically useful for analysis of dry powders. The test used for loss on ignition (LOI) is a standard laboratory test, where the weight loss of a sample is measured after ignition in an oven or furnace at 1025 °C for 30 minutes.

## Results and Discussion

The results of the various tests are presented in the following tables and figures.

The results in Table II are shown graphically in Figure 1. Samples 2, 3, 4 and 5 are all presently used in the cobalt industry. Given that CAR values less than 60 seconds are considered to be indicative of high reactivity magnesia [5] then the results for the TM45 samples are very positive as they are well within the range considered to be important for hydrometallurgy use.

Figure 2 displays the change of the pH over time. The TM45 samples show a fast reaction from the beginning and are in the range of similar products already used in hydrometallurgical applications.

The citric acid reactivity as shown in Table II and Figures 1 and 2 represents a useful method for initial screening of different magnesia products to determine their potential in hydrometallurgical application. It must be noted however, that visual determination of the end point, the colour change from white to pink, can be very subjective. In the end, the representation of the data as shown in Figure 2 presents a less subjective interpretation of the end-point and is possibly a more accurate assessment of the usefulness of any particular magnesia.

Based on several laboratory trials a CAR less than 50 seconds is considered to be optimal for magnesia for hydrometallurgical application.

High reactivity is a very important requirement for a successful magnesia for hydrometallurgical application. High reactivity ensures a high level of utilization of the MgO and

minimum carry over into the metal hydroxide, where it would exist as an impurity. Like CAR, specific surface area is another measure of reactivity – a high specific surface area is desired. Increasing calcination temperature combined with longer residence time in the furnace leads to lower specific surface area as internal pores in the MgO crystallite structure close leading to densification, resulting in a lower surface area and less reactive magnesia. The specific surface areas can be found in Table III and Figure 3.

A highly reactive CCM requires specific surface areas above 50 m<sup>2</sup>/g, preferable above 70 m<sup>2</sup>/g. To achieve these values calcination at lower temperatures than usually employed in production of caustic calcined magnesia for dead burned magnesia production is required. Typical calcination temperatures for dead burned magnesia production are in the region of 1000 °C whereas for production of caustic calcined magnesia they are below 1000 °C.

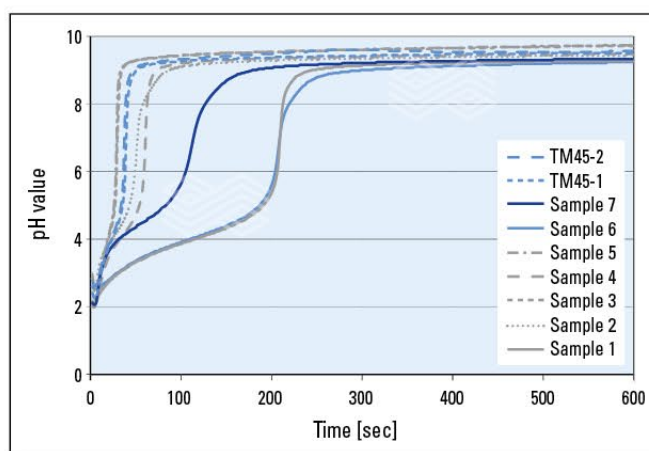


Figure 2. Citric acid reactivity diagram.

Sample	1	2	3	4	5	6	7	TM45-1	TM45-2
CAR (sec)	236.0	68.0	31.0	64.0	29.0	218.0	144.0	39.0	42.0

Table II. Citric acid reactivity (CAR)

Sample	1	2	3	4	5	6	7	TM45-1	TM45-2
BET (m <sup>2</sup> /g)	11.8	86.8	90.5	36.0	86.1	10.3	104.3	90.5	61.0

Table III. Specific surface area (BET).

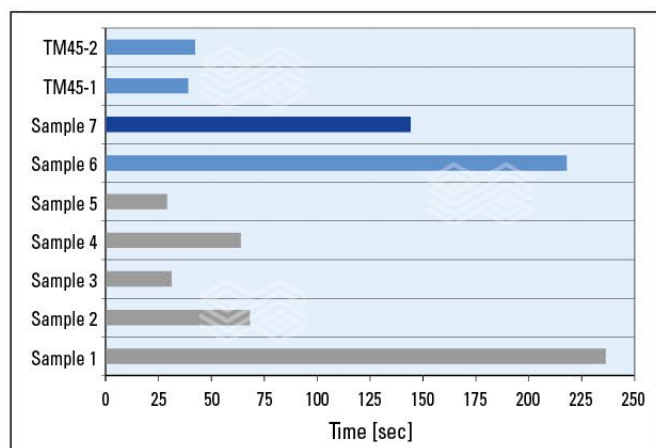


Figure 1. Citric acid reactivity of test caustic calcined magnesia samples.

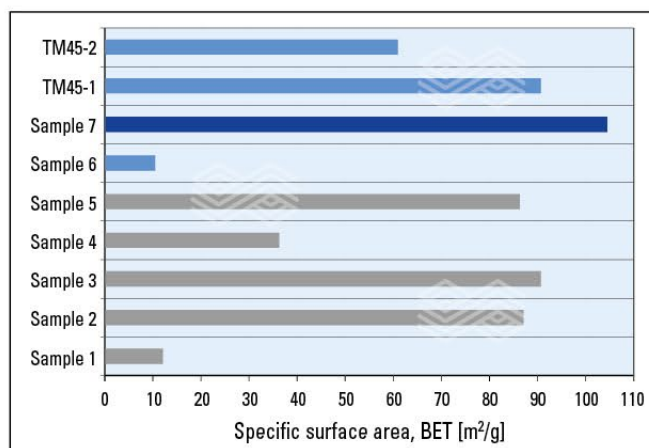


Figure 3. Specific surface area measurement.

Table IV and Figure 4 present the particle size distribution, specifically the  $D_{90}$  values, of the various samples studied in this testwork as analysed on a Sympatec laser diffraction HELOS instrument.

The role of particle size distribution is not as clear from the study as the  $D_{90}$  values don't correlate with the specific surface area values as would be expected. This is suggesting that something else, possibly product morphology, is a stronger determinant of surface area. From the study, the optimal  $D_{90}$  value should be as fine as possible.

Looking at role of loss on ignition as an indicator of suitability for hydrometallurgical application, conventional belief suggests that low loss on ignition, possibly less than 5%, is necessary. This research has shown that higher LOI up to a limit does not impede performance of magnesia in hydrometallurgical circuits. The LOI values, measured at 1025 °C for 30 minutes, of the samples in this study are shown in Table V and present graphically in Figure 5. Overall, the results show a high degree of variability in LOI between different magnesia types.

It's generally believed that higher LOI leads to a loss of reactivity of the magnesia, probably due to the presence of unreactive chemical species, the composition of which will depend on the original source of the magnesia. This unreactive species may be unburned carbonate from the original thermal decomposition of magnesite or brucite formed by exposure to high levels of moisture. Research reported by Miller, at the Alta 2016 Conference, suggests that the presence of additional

moisture up to a limit of about 12% does not impede the performance of the magnesia in a simulated cobalt precipitated circuit [3].

Miller concluded that the conditions more likely to adversely affect magnesia utilization include low temperature, overdosing, poor dispersion and extended magnesia hydration time. His research suggests that overall, these parameters could account for up to 50% magnesia wastage [3].

The following table (Table VI) and graph (Figure 6) show the magnesium oxide content, as delivered, of the different test magnesia samples.

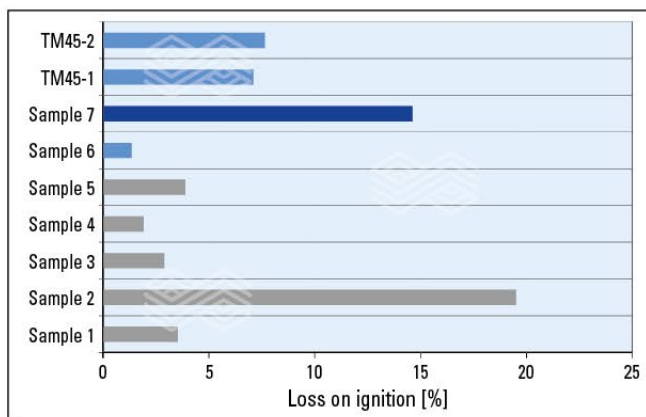


Figure 5. Loss on ignition analysis measured at 1025 °C x 30 minutes.

Sample	1	2	3	4	5	6	7	TM45-1	TM45-2
$D_{90}$ (µm)	60.2	18.8	16.5	15.0	20.8	9.5	11.3	5.8	12.2

Table IV. Particle size distribution.

Sample	1	2	3	4	5	6	7	TM45-1	TM45-2
LOI (%)	3.5	19.5	2.9	2.0	3.9	1.4	14.6	7.7	7.1

Table V. Loss on ignition (1025 °C x 30 minutes).

Sample	1	2	3	4	5	6	7	TM45-1	TM45-2
MgO (%)	94.6	78.8	94.6	92.1	93.7	94.7	82.4	88.3	88.8

Table VI. Magnesium oxide content (as delivered).

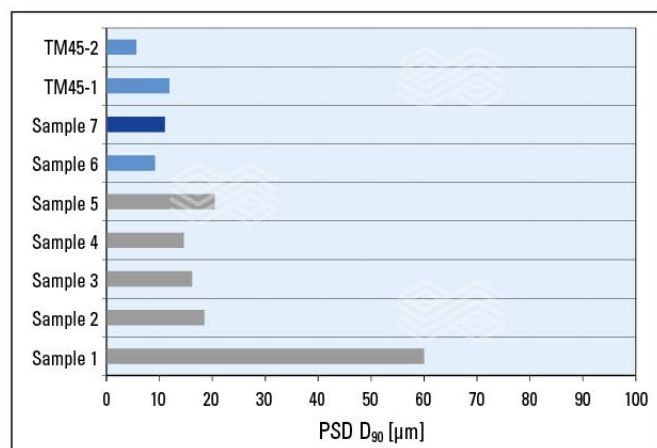


Figure 4. Particle Size Distribution analysis.

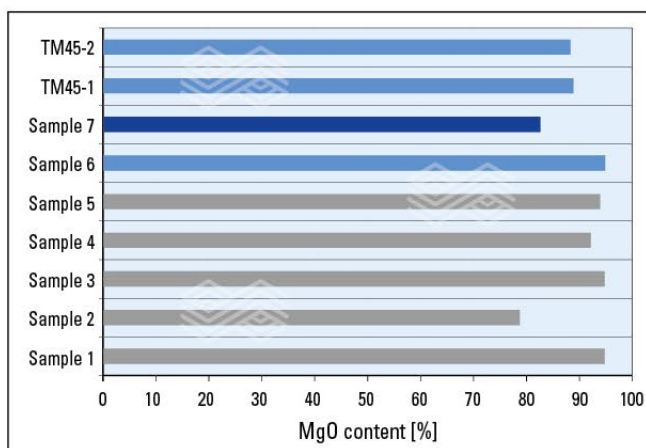


Figure 6. MgO content as delivered.

Generally, it would be expected that the highest purity magnesia would provide the best performance, i.e. have the highest reactivity. This does not appear to be the case, PREMIER TM45-1 or TM45-2 has a lower MgO content (as delivered) than many of the other samples tested including some already in use in cobalt precipitation circuits. Plant trials with both PREMIER TM45 at active mine sites have clearly demonstrated that this is not the case. Both PREMIER TM45 samples have been shown to perform at least as well, if not better than the leading commercially used caustic calcined magnesia. This suggests that calcination conditions are more important than the chemical purity of the magnesia as what is important is the number of reactive sites available in the magnesia. This determines how reactive it is.

### Conclusions

Following the testwork described in the previous section a list of the important physical and chemical characteristics of an ideal caustic calcined magnesia for use in cobalt and nickel hydrometallurgical precipitation circuits was prepared.

This study has highlighted the role of various parameters, particularly physical one, in the cobalt precipitation process. While it might be believed that chemical purity was the most important factor influencing the performance of caustic calcined magnesia in hydrometallurgical circuits, the testwork has shown that the physical properties of the magnesia are equally, if not more important.

Trials at mine sites have shown that the RHI caustic calcined magnesia perform as well as, if not better, than other commercial magnesia products used in the same application. It is a magnesia with a high reactivity and increased utilisation. This is an important factor, as less magnesia is required in the process due to the increased reactivity of the RHI product.

High reactivity is a very important requirement for a successful magnesia for hydrometallurgical application. High reactivity ensures a high level of use of the MgO with minimum carryover into the metal hydroxide precipitate where it would exist as an impurity.

Citric acid reactivity represents a good initial screening test to determine if a magnesia might work in cobalt or nickel

hydrometallurgical circuits. However, its value is very limited, partly due to the highly subjective nature of determining the end point. A modification of the CAR test may turn out to be more useful but this will require additional work. In his research Miller suggests that a chemical test that mimics process conditions would be a more useful and reliable technique for quantitative evaluation of the magnesia products [3].

High specific surface area is important as it's thought to provide more reactive sites, thus increasing reactivity. Calcination conditions play a very important role in determining the effectiveness of a caustic calcined magnesia. Calcination temperatures below 1000 °C are required to produce a high reactivity CCM but care must be taken not to produce a material with excessively high loss on ignition, which Miller suggests is above 12% [3]. The results of the particle size analysis didn't correlate with surface area as would be expected, suggesting that maybe product morphology has a role to play in the magnesia performance. From this study, it is clear that the  $D_{90}$  must be as fine as possible. Again, this points to the need for careful control of the calcination conditions to ensure the correct particle size. The data recorded from different laboratory trials suggest that above a certain BET value the major factor influencing reactivity is the particle size at it is also shown in Figures 7 and 8.

While all the parameters discussed in this paper are important and all have a role to play in determining the suitability of a magnesia for hydrometallurgical applications, in the end any evaluation of products has to be made in the context of the end use. Hydrometallurgical circuits are very complex which makes it very hard to assess the potential of any magnesia without really going to pilot or plant trials where "real life" conditions are encountered. The parameters discussed here are all indicators to a successful magnesia but they must be carefully controlled to ensure a product with optimised properties is obtained.

Successful on-site trials at working mines have shown that caustic calcined magnesia from RHI Magnesita is an effective magnesia for cobalt hydrometallurgical precipitation circuits. It is a product with well-balanced physical and chemical properties that allow a high performance with a high degree of utilisation and minimum carryover into the metal hydroxide.

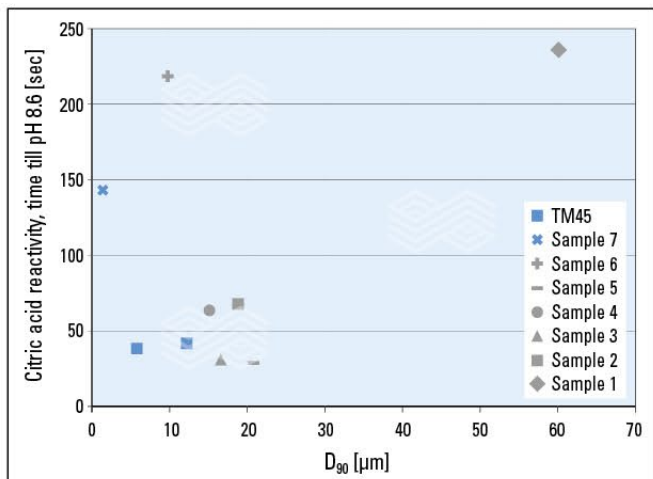


Figure 7. Particle size ( $D_{90}$  value) versus citric acid reactivity.

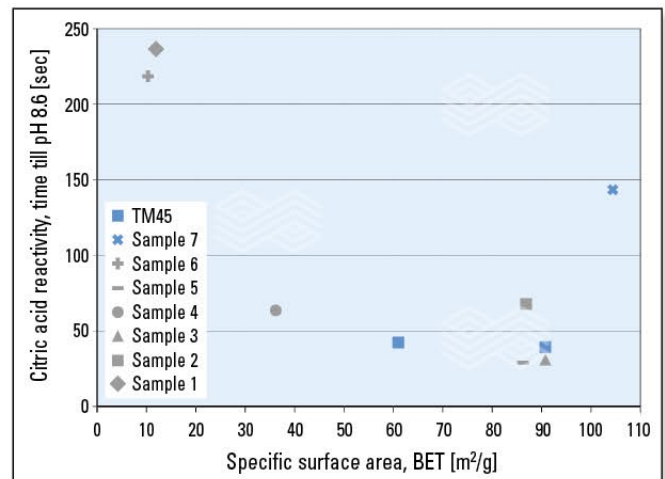


Figure 8. Specific surface area versus citric acid reactivity.

## Acknowledgments

This paper represents a summary of a large volume of work conducted at the RHI Technology Center and by Mike Miller, from Mike Miller Consultancy Services, on behalf of RHI Magnesita, Drogheda. Many other colleagues in RHI Magnesita have also contributed both directly and indirectly through meetings, discussions etc. and their contributions are valued and much appreciated.

## References

- [1] U.S. Geological Survey, 2016, Mineral Commodity Summaries 2016: U.S. Geological Survey, 202, <http://dx.doi.org/10.3133/70140094>
- [2] Atkins, P. W. *Physical Chemistry. 4th edition*; Oxford University Press, Oxford 1990.
- [3] Miller, M., Optimising the Utilisation of Caustic Calcined Magnesia in a Hydrometallurgical Application. *Proceedings of Alta 2016 Nickel – Cobalt – Copper Sessions*, Perth, Australia, 21–28 May, 2016, 128–142.
- [4] Shand, M.A., *The Chemistry and Technology of Magnesia*. John Wiley and Sons, Inc: New Jersey, 2006. ISBN: 9780471656036
- [5] Van der Merwe, E. Hydration of Medium Reactive Industrial Magnesium Oxide with Magnesium Acetate Thermogravimetric Study. *J. Therm. Anal. Calorim.* 2004, 77, 49–56. <https://www.researchgate.net/publication/243956930>

*Reproduced with permission from the Canadian Institute of Mining, Metallurgy and Petroleum. Cited from COM2017, Paper No 9732.*

## Authors

Christoph Piribauer, RHI Magnesita, Technology Center, Leoben, Austria.

Anthony McEaney, RHI Magnesita, Drogheda, Ireland.

Anna Felsner, RHI Magnesita, Technology Center, Leoben, Austria.

Erich Feichtenhofer, RHI Magnesita, Technology Center, Leoben, Austria.

Gerald Gelbmann, RHI Magnesita, Technology Center, Leoben, Austria.

**Corresponding author:** Gerald Gelbmann, [gerald.gelbmann@rhimagnesita.com](mailto:gerald.gelbmann@rhimagnesita.com)



# bulletin

Autumn 2017  
ISSUE 1

